

Versatile Synthetic Strategies Towards the Development of Novel Neuroblastoma Inhibitors and Their Analogues

A thesis submitted in
partial fulfilment of the requirements
for the degree of Doctor of Philosophy.
University of Oxford

Samira Alishahi

St Cross College

Oxford

October 2012

This thesis is dedicated

to my loving parents,

Mansour & Fariba.

Acknowledgement

This dissertation would not have been possible without the guidance and contribution of others, for which I am extremely grateful. First and foremost, my utmost gratitude must go to my supervisor Angela Russell, for her continuous kind support, her patience and encouragement throughout my DPhil study and I am very appreciative of her generosity with her time during the write up of this thesis. She has been an inspiration as I hurdled all the obstacles in the completion of this research work. I could not have imagined having a better supervisor. I would like to thank everyone in Labs 7 and 8, especially Carole Bataille, Camilo Quevedo, Gu Liu, and Jon Williams for their encouragement, insightful comments and for making my stay at Oxford very memorable.

Many additional colleagues provided valuable information and data that helped me with the biological side of this thesis, and I am grateful to all of them for their assistance. In particular, I would like to thank Anna Nadali, for teaching me how to work with biological assays, Oliver King for helping me with the protein purification, and Owen Clark and Dr. Stoker for testing the effect of my compounds on neuroblastoma cell lines.

Lastly, and for whom I owe the most gratitude, my family. I would like to express my sincerest appreciation to my mum and dad for always being there for me and for all their loving support throughout my life. I would have never made it here without them. This thesis is dedicated to them and I hope I have made them proud. I will always be grateful for the little angel in my life, who never fails to put a smile on my face, my sister, Pegah. I cannot wait to celebrate your graduation. I extend heartfelt thanks to my loving husband, Nader. He was and is a solid anchor on which I rely on again and again. Words cannot express how grateful I am to be in his life and how much this work has been made easier by him being in mine.

Declaration

The work described in this thesis is entirely my own, except where I have either acknowledged help from a named person or given reference to a published source or a thesis. Text taken from another source will be enclosed in quotation marks and a reference given.

Samira Alishahi

Trinity Term, 2012

ABSTRACT

The aim of this thesis was to identify and develop anti-neuroblastoma agents *via* two strategies. The first involves a targeted therapy approach towards the synthesis of new drug-like PTP inhibitors (Chapter 2 and 3) and the second involved devising a new versatile synthetic route to the recently established anti-tumour natural-product lead, methyl jasmonates and its analogues (Chapter 4).

From a unique proprietary screening library of 5000 drug-like compounds targeted towards PTPs, three compounds from two distinct chemical series, tetrahydroquinolines **P00104** and **P00341**, and thiobarbituric acid **P00337,** were identified as PTPN22 inhibitors (IC_{50} = 5 μM) with moderate potency *in vitro*. A synthetic route to each chemical series was established and optimised and the procedure was used to synthesize a series of rationally-designed analogues for detailed structure-activity relationship (SAR) studies. The compounds were tested for PTP inhibitory activity against PTPN22 *via* two experimentally optimised protein assays and were tested for cytotoxicity in a number of neuroblastoma cell lines. However, none of the compounds including the resynthesized hits displayed any promising biological activity, and further investigation on these chemical series was abandoned and another strategy for developing anti-neuroblastoma agents was pursued.

During the last decade, many studies have reported the cytotoxic effects of methyl jasmonate, a plant stress hormone, against various tumours both *in vitro* and *in vivo*. As the research on the anti-tumour properties of methyl jasmonate is still at early stages, and also due to the lack of a versatile synthetic procedure for the preparation of its structural derivatives, detailed SAR studies of this compound have not yet been conducted. In the course of this project, a novel versatile synthetic route to methyl jasmonate and its analogues has been developed, which allows substituents to be readily introduced at the α- and β-position of cyclopentenone. This synthetic procedure will facilitate future extensive SAR studies of methyl jasmonate in tumour cells.

The cytotoxic activity of the synthesized methyl jasmonate was confirmed against a range of neuroblastoma cell lines including SK-N-SH, SHSY5Y, LAN5 and the Kelly cells, and a further study on the mechanism by which methyl jasmonate induces neuroblastoma cell death is currently underway.

Abbreviations

Å	Ångström	Ac	Acetyl
Ar	Aromatic group	aq	Aqueous
Bn	Benzyl	Bu	Butyl
n-BuLi	Butyllithium	C	Celsius
cm^{-1}	Wavenumbers	conc.	Concentrated
COSY	Correlation spectroscopy	DBB	4,4'-Di-tert-butylbiphenyl
DBU	1,8-Diazabicyclo[5.4.0]undec-7-ene	DCC	*N*,*N*'-Dicyclohexylcarbodiimide
DET	Diethyl tartrate	DIPT	Diisopropyl tartrate
DMAP	4-(Dimethylamino)pyridine	DMF	N,N-dimethylformamide
dppe	1,2-Bis(diphenylphosphino)ethane		
e.e.	Enantiomeric excess	eq	Equivalents
ESI	Electrospray ionisation	Et	Ethyl
g	Gram(s)	h	Hours(s)
HRMS	High resolution mass spectrometry	Hz	Hertz
IR	Infrared	i-	Iso
J	Coupling constant	LCA	Lithocholic acid
Me	Methyl	min	Minute(s)
MJ	Methyl jasmonate	mol.	Mole
MP	Melting point		
MOM	Methoxymethyl	Ms	Methanesulfonyl
MS	Mass spectrometry / Molecular sieves	m/z	Mass to charge ratio
Nmax	Peak infrared absorption	NMP	N-Methylpyrrolidone
NMR	Nuclear magnetic resonance	NOE	Nuclear Overhauser effect
NOESY	Nuclear Overhauser Effect Spectroscopy	PG	Protecting group
PMB	Para-Methoxybenzyl	ppm	Parts per million
PPTS	Pyridinium p-toluenesulfonate	PolyCyc	Polycyclic structure
Pr	Propyl	R	Generic organic substituent
Rf	Retention factor	ROM	Ring Opening/cross Metathesis
r.t.	Room temperature	SAE	Sharpless Asymmetric Epoxidation
SET	Single electron transfer	SET	Single electron transfer
TBAF	tetra-n-Butylammonium fluoride	t-	Tertiary
TBDPS	tert-Butylphenylsilyl	TBS	tert-Butyldimethylsilyl
TFA	Trifluoroacetic acid	TESCl	Triethylchlorosilane
ThDP	Thiamine dipyrophosphate	TFAA	Trifluoroacetic acid anhydride
THP	Tetrahydropyran	THF	Tetrahydrofuran
TMO	Trimethylamine-N-oxide dihydrate	TLC	Thin layer chromatography
Ts	Para-Toluenesulfonyl	TMS	Trimethylsilyl

Contents

Chapter 1: Introduction **1**

1.1 Cancer 2

1.1.1 Current Cancer Treatment Strategies 4

1.1.2 Targeted Therapies: A New Generation of Cancer Treatment 9

1.1.3 Oncology: Unmet Medical Needs 11

1.2 Neuroblastoma 12

1.2.1 Current Neuroblastoma Therapies 15

1.3 Medicinal Chemistry in Drug Discovery 16

1.4 Natural Products Screening for New anticancer Drugs 17

1.5 Future Directions for Treatment of Neuroblastoma 19

1.6 Aims of the Project 21

1.6.1 Targeted Approach towards Anti-Neuroblastoma Agents 21

1.6.2 Natural Product-Inspired Approach towards Anti-Neuroblastoma Agents 23

1.7 References 25

Chapter 2: Targeting Protein Tyrosine Phosphatases with Drug-Like Small Molecule Inhibitors for Neuroblastoma Drug Discovery I **29**

2.1 Introduction 30

2.1.1 Characteristics of the PTP Family 30

2.1.2 PTPs in Cancer 34

2.1.3 PTPs in Neuroblastoma 36

2.1.4 PTPs as Drug Targets: Strategies and Challenges of Inhibitor Development 38

2.2 Hit Identification: Thiobarbituric Acid P00337 as a Potential Inhibitor of PTPN22 41

2.2.1 Thiobarbituric Acid 42

2.2.2 Retrosynthesis of Thiobarbituric Acid P00337 and SAR Analysis 43

2.2.3 Resynthesis of Thiobarbituric Acid Compound P00337 44

2.2.4 Synthesis of P00337 Analogues and Further Optimisation of the Synthetic Procedure 47

2.3 Biological Testing 50

2.3.1 Enzyme Purification 50

2.3.2 Biological Assay Development and Optimization 51
2.3.3 p-Nitrophenyl phosphate Assay 52
2.3.4 Malachite Green Assay 54
2.4 Results and Discussion 59
2.4.1 Thiobarbituric Acid Analogues: Malachite Green Assay 59
2.4.2 Thiobarbituric Acid Analogues: p-Nitrophenyl Phosphate Assay 63
2.4.3 Neuroblastoma cell line assays 68
2.5 Conclusion and Future Work 71
2.6 References 72

Chapter 3: Targeting Protein Tyrosine Phosphatases with Drug-Like Small Molecule Inhibitors for Neuroblastoma Drug Discovery II 77
3.1 Hit Identification: Tetrahydroquinoline Compounds P00104 and P00341 78
3.1.1 Tetrahydroquinolines 79
3.1.2 Retrosynthesis and SAR Strategies 79
3.2 Initial Investigations and Resynthesis of Tetrahydroquinolines P00104 and P00341 81
3.3 Optimisation of Synthetic Route and Analogue Synthesis 84
3.4 Triflic Acid as Catalyst in Synthesis of Furanoquinolines 88
3.5 Synthesis of Carboxylic Acid Bioisosteres of Tetrohydroquinoline P00341 93
3.5.1 Planar Acidic Heterocycle-Based Isosteres 96
3.5.1.1 Synthesis of Tetrazole Bioisostere 96
3.5.1.2 Synthesis of 1,2,4-Oxadiazole and Oxo-Oxadiazole Bioisosteres 98
3.5.2 Synthesis of Phosphonic acid Bioisosteres 100
3.5.3 Synthesis of Sulfate Bioisostere 102
3.6 Conclusion and Future Work 107
3.7 References 108

Chapter 4: Synthesis of Methyl Jasmonate 111
4.1 Introduction 112

4.1.1 Biosynthesis 113
4.1.2 Methyl Jasmonate in Cancer 114
4.1.3 Mechanism of Action of Jasmonates 119
4.1.3.1 The Bio-energetic Mechanism 122
4.1.3.2 The Re-Differentiation Mechanism 124
4.1.3.3 The Reactive Oxygen Species (ROS) – Mediated Apoptosis 125
4.2 Cytotoxic Effect of Methyl Jasmonate on Human Neuroblastoma Cell Lines 127
4.3 Previous Synthesis of Methyl Jasmonate 130
4.3.1 Use of Acyclic Compounds as Precursors 131
4.3.2 Conjugate Addition to Cyclopentenone 133
4.3.3 Ene-Based Methodology 134
4.4 Results and Discussion 136
4.4.1 Via a Tandem Conjugate Addition and Enolate Trapping 136
4.4.2 Via Cascade Organocatalysis Strategy 142
4.4.3 α-Alkylation of Cyclopentanone 151
4.4.4 Via α-Substituted Cyclopentenone 159
4.4.5 Via a Protected α-Halocyclopentenol 164
4.6 Conclusion and Future Work 174
4.7 References 176

Chapter 5: Experimental 181

CHAPTER 1

Introduction

1.1 Cancer

Cancer, medically known as malignant neoplasm, is a group of more than two hundred different and distinctive diseases, characterized by an abnormal growth of cells which tend to proliferate in an uncontrolled manner. It is the primary cause of death in developed countries and the second major cause of death in developing countries, accounting for around 13% of all mortalities worldwide in 2008.[1] Cancer arises from the multistep transformation of a single normal cell into a malignant cell as a result of interactions between genetic and environmental factors. Subsequently, the cancer cells then continues to proliferate and differentiate into a new, abnormal tissue which in most cases results in a malignant tumour.

The environmental factors influencing cancer are subdivided into three categories: physical carcinogens such as ionizing and ultraviolet radiations; chemical carcinogens such as elements of tobacco smoke, asbestos and arsenic; and biological carcinogens such as infections from certain viruses (e.g. hepatitis B and C), bacteria or parasites. Another fundamental factor for development of cancer is ageing, and with the advances in public health and the medical field, more people reach the age where they are likely to develop this pathology.[2]

The most common cancer types in adults are skin, lung, colon, rectal, breast, endometrial, ovarian and prostate cancer. Although cancer is generally age dependent, some children are also prone to developing this condition. The types of cancers that develop in children vary from that in adults. In children, malignancies arise as inherited disorders from DNA changes that occur very early in life or even before birth and is independent of lifestyle or environmental factors. Although childhood cancer accounts for only 1% of all cancers diagnosed each year, it is still the second leading cause of death in children under the age of 15, after accidents. The most common cancers in children are neuroblastoma, leukaemia,

brain and other nervous system tumours, Wilms' tumour, lymphoma, retinoblastoma and bone cancer.

In adults, the malignant transformation of a normal cell is due to one or more mutations in its DNA, which is either inherited or acquired (Figure 1.1). The complex multistage process of cancer development depends on genetic changes as well as epigenetic factors, such as hormonal factors, and co-carcinogens that are not cancerous on their own but may increase the chance of the genetic change(s) to lead to cancer.[3,4]

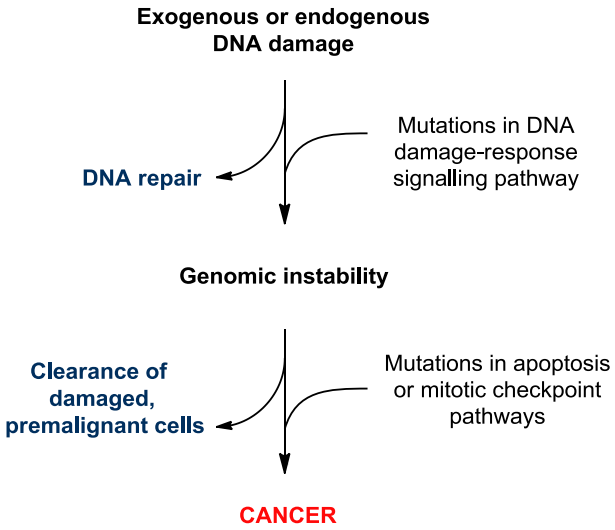


Figure 1.1: A view of the progression of cancer.

The two main classes of genetic changes resulting in cancer are the conversion of proto-oncogenes that are responsible for controlling cell division, differentiation and apoptosis into oncogenes, and the inactivation of tumour suppressor genes such as *p53* and *Rb1* that have the ability to suppress malignant changes. The environmental factors mentioned above cause these genetic changes through point mutations, gene amplification or chromosomal translocation. So far approximately one hundred dominant oncogenes and thirty tumour suppressor genes have been identified.[3]

Six crucial alterations in cell physiology, termed The Hallmarks of Cancer, were proposed by Hanahan and Weinberg to be responsible for the idiopathic and complex nature of almost all types of cancer. Collectively they were thought to direct malignant growth. These alterations, which occur through different mechanisms, include independent activation of growth signals, insensitivity to antigrowth signals, lack of sensitivity to apoptotic factors, limitless potential of proliferation, continuous angiogenesis, and the ability to invade and metastasise.[5] Conceptual progress in the last decade has added two more hallmarks, which includes abnormal metabolic pathways and evading immune destruction.[6] The malignant transformation of a number of these components is a prerequisite for cancer development, and therefore could be the reason for the infrequent occurrence of this disease during an average human lifetime.

Despite many common features, the nature of the molecular defect(s) of different cancers varies considerably, with varying rates of growth and responsiveness towards different types of treatments. Consequently, each type of cancer requires a particular type of therapeutic strategy.

1.1.1 Current Cancer Treatment Strategies

Before 1950, surgical removal of a tumour was the most preferred form of cancer treatment and after 1960, radiation therapy was used to control and kill localized malignant cells. It was soon realized that metastatic cancer could not be treated effectively by each treatment alone or by the combination of both and research focus was turned to antineoplastic agents that can target all tumour cells.[7] The treatment of cancer using a standardized regimen of one or a combination of antineoplastic drugs is referred to as chemotherapy.

The goal of chemotherapy is to kill malignant cells at a dose that is least harmful to normal healthy cells as the "Therapeutic window" of chemotherapeutic agents is often small (Figure 1.2). The main traits of most cancer cells are their abnormal high rate of proliferation relative to normal cells and having independent cell division regulatory processes compared to normal healthy cells. The former characteristic is the target of most common chemotherapy agents, which is apparent when considering the side effect profile of these drugs. Cells of hair follicles, the lining of gastrointestinal tract, cells of bone marrow and the skin, all divide rapidly relative to other types of body cells and therefore they are also targeted and killed by cytotoxic drugs, resulting in hair loss, mucositis and diarrhoea, myelosuppression and rashes, respectively.[8]

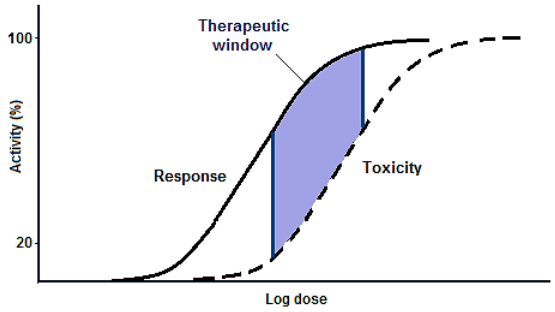


Figure 1.2: Dose-response curves for the efficacy and toxicity of inhaled corticosteroids (ICS). The two vertical lines indicate how the therapeutic index for any ICS narrows as the dose increases.

Chemotherapeutic agents are categorised according to the phase of the cell cycle in which they are active. The cell cycle is a sequence of five phases that takes place in a cell, which results in the duplication of its genome and subsequent division into two cells. G1 represents a growth phase in which protein synthesis is most active. DNA replication takes place in the S phase after which the cell goes through another growth phase called G2. At this point cell begins to prepare for division and mitosis which occurs at the M phase. G0 is the resting

phase where the cell is temporarily out of proliferative cycle and once stimulated, cell would move into G1 phase and the cell cycle begins again. Many chemotherapy drugs are active at the G1/2, S and M phases whereas none is active during the resting phase (G0) of the cell cycle (Figure 1.3).[8,9]

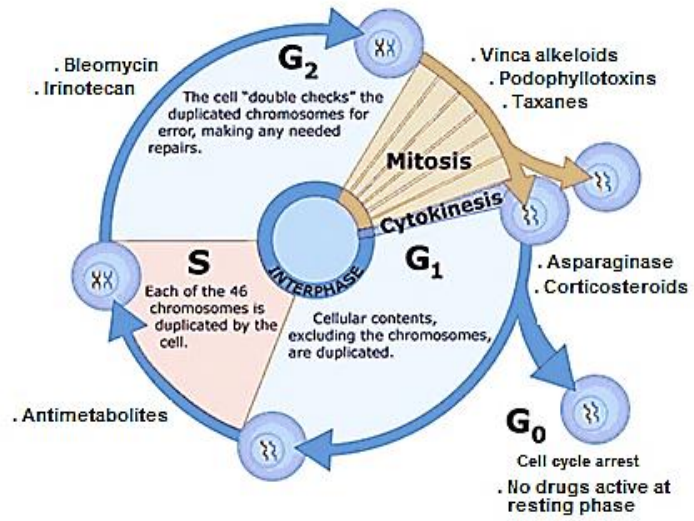


Figure 1.3: Cell cycle and chemotherapeutic agents active in each phase.[10]

The chemotherapy drugs that kill cancer cells during a specific phase are termed cell-cycle specific drugs, and those that are able to kill malignant cells during any phase of the cycle are known as cell-cycle nonspecific drugs.

The major anticancer drugs can be classified into hormones, most importantly steroids, and cytotoxic drugs which include alkylating agents, antimetabolites, and natural product derivatives such as antitumour antibiotics, anthracyclines, plant alkaloids and taxanes.[11] The more recently developed anticancer drugs which are targeted to specific lesions within the tumours do not fall under the cytotoxic category (discussed later in chapter 2).[7]

Alkylating agents are one of the first and most widely used anticancer drugs. Amongst these drugs are active and latent nitrogen mustards, which were compounds originally used as chemical warfare agents during World War I.[12,13] Alkylating agents are cell cycle non-specific and have reactive electrophilic intermediates that act by attaching an alkyl group to a nucleophilic site in the DNA such as on the nitrogen at the 7-position of guanine (Figure 1.4). This leads to cross-linking of DNA strands, DNA strand breaks or irregular base pairing, resulting in prevention of cell division and consequently cell death. Since cancer cells proliferate faster and with less error-correcting than healthy cells, they are more sensitive to DNA damage induced by these drugs.[14,15]

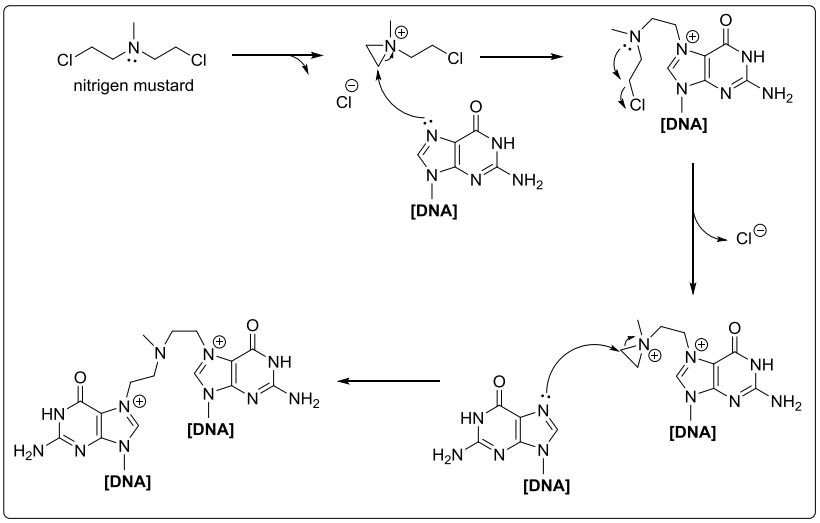


Figure 1.4: Proposed mechanism of action of mustards, alkylating agents that cross-link DNA strands.[16]

Antimetabolites are structural analogues of the naturally occurring molecules involved in DNA and RNA synthesis. These drugs act by competing with normal cell metabolites for the active sites of key enzymes or by mimicking and substituting building blocks of DNA such as purine and pyrimidine during the S phase, thereby preventing development and division of cancer cells.[11]

Many of the currently effective anticancer drugs have been developed from natural products such as plants, bacteria and fungi.[17-19] In addition, some of the semi-synthetic and synthetic analogues of these natural products also have anticancer properties. The majority of antitumour antibiotics are isolated from fungi and they mainly function by applying direct action on DNA. For example, bleomycin intercalates DNA at certain sequences, resulting in the spontaneous oxidation of its ferrous iron and generation of free oxygen radicals that can fragment preformed DNA within cancer cells.[20] Anthracyclines have a similar mode of binding to DNA as bleomycin, thereby preventing DNA and RNA synthesis. They also inhibit topoisomerases I and II, the enzymes involved in unwinding the DNA double helix for repair, replication and transcription.[21]

Plant alkaloids are derived from the periwinkle plant *Vinca rosea*.[19] Their mode of action involves binding to tubulin and thus block polymerization of microtubules in the S phase resulting in disruption of mitosis in the M phase.[22] Taxanes also block mitosis; however they do so by stabilising microtubules instead, effectively 'freezing' them in the polymerized state.[23]

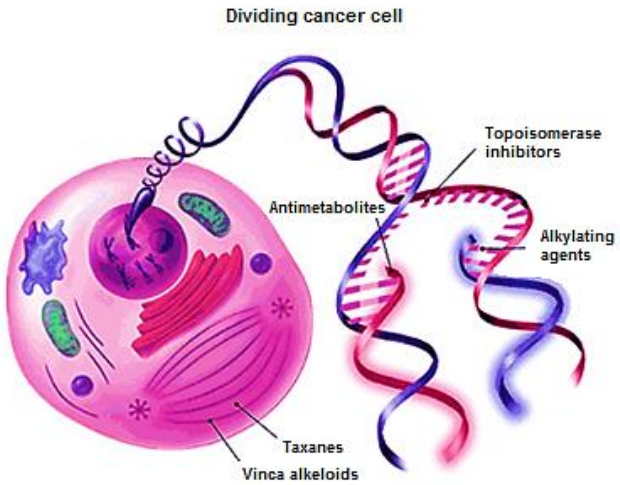


Figure 1.5: Mechanisms of traditional cancer chemotherapy.[24]

For cancer chemotherapy to be effective, it is necessary to have an in-depth understanding of the molecular biology of the tumour, pharmacology, cellular kinetics, and drug resistance. The practice of cancer treatment has changed dramatically since 1949 when the first chemotherapeutic agent, nitrogen mustard, was used to treat Hodgkin's lymphoma.[25] This drug improved patient care but caused severe side effects which required hospitalization. The chemotherapy agents discovered since then, combined with more effective side-effect management, has led to curative therapy for several previously fatal malignancies such as leukaemia, lymphomas, and testicular cancer. Adjuvant chemotherapy and hormonal therapy are now used to extend life expectancy and prevent disease recurrence following surgical removal of localized breast, colorectal, and lung cancers. Chemotherapy is also employed in multimodal treatment of locally advanced malignancies of head and neck, breast, lung, and oesophageal, pediatric solid tumours, and soft-tissue sarcomas, thus permitting for more limited surgery and even cure of these formerly incurable pathologies.

Currently, almost 20% of all new cases of cancer are cured through chemotherapy alone.[8] The research for more effective cancer treatments with reduced toxicity profiles continues to grow. The long-term goal of this intense research is to improve the clinical outcome of cancer patients undergoing treatment.

1.1.2 Targeted Therapies: A New Generation of Cancer Treatment

Traditional chemotherapy works primarily by killing rapidly proliferating cells in a non-selective manner and consequently causes a number of severe side effects. The adverse effects of an anticancer drug can be reduced by increasing its selectivity towards malignant tissue and reducing the dose that reaches and affects normal cells.

Alteration in oncogenes or tumour suppressors leads to upregulation of multiple signalling pathways in cancer cells, which then promotes tumour-cell proliferation.[7] Signals from the

microenviroment of tumours can also have a positive or negative effect on cancer cell proliferation.[26] An improved understanding of the molecular anatomy of these events and molecular fingerprinting of each type of cancer will help to develop drugs that have selective cytotoxicity towards cancer cells, *i.e.* targeted therapy.

In the past decade, a new generation of cancer drugs has been developed that target tumour-specific proteins that are believed to have critical roles in development or progression of malignant tissue.[7,24] The two main categories of targeted therapy are monoclonal antibodies and small molecule inhibitors. Monoclonal antibodies are directed at extracellular molecules such as antigens, ligands and receptor binding domains that are unique to, overexpressed or mutated in cancer cells. Subsequently, an immunological response against the targeted malignant cells is induced, resulting in their death. On the other hand, the small molecule inhibitors can enter cells and interfere with receptor signalling and downstream intracellular molecules, the most common target being kinases.[7,24]

Although cytotoxic chemotherapy is still the main choice of treatment for many types of cancer, targeted therapies are being used successfully as one of the treatments for breast, colorectal, lung, leukaemia, lymphoma, and pancreatic cancer.[24] From the new anticancer drugs approved in 2000 by Food and Drug Administration (FDA), fifteen were targeted therapies and only five were chemotherapeutic agents.[27]

Many researchers are currently focusing on identifying targets or signalling pathways that are either overexpressed or activation of which leads to accelerated tumour growth. However, one recent advance in the field of targeted therapy exploits the opposite concept by targeting a weakness of specific tumours, a concept termed synthetic lethality. A commonly exploited phenomenon in this field targets many tumour cells' compromised ability to repair damaged DNA.[28-31] For example, the impaired ability to repair double strand breaks in DNA in certain

tumour cells is a consequence of mutations in tumour-suppressor genes *BRCA1* and *BRCA2*. The treatment takes advantage of the synthetic lethality of the combination of BRCA mutations (blocks repair of double-strand breaks) and poly (ADP-ribose) polymerase inhibitors (PARP) (blocks repair of single-strand breaks), to attack tumour cells whilst sparing healthy ones with intact DNA repair pathways. This novel strategy uses PARP inhibitors to 'flood' the tumour cell with single-strand breaks, which are subsequently converted into double-stranded breaks in the cells. Consequently, the increase of double-strand breaks kills the tumour cells.[32] Recent clinical trials have shown that the novel PARP inhibitors olaparib or iniparib can be used to control cancers caused by mutations that abolish BRCA activity (certain types of breast and ovarian cancers).[33]

With the triumph of targeted therapy being evident in the past few years, it is clear that the era of a new cancer-therapy strategy has arrived.

1.1.3 Oncology: Unmet Medical Needs

Significant advances in the chemotherapeutic management of cancer have been made since the 1950s. However, currently more than 50% of all cancer patients either are non-responsive to initial therapy or experience recurrence of cancer after treatment, ultimately dying from progressive metastatic malignancies. Even with the discovery of many new cytotoxic drugs that are used to treat cancer, this life-threatening disease continues to cause approximately 7 million deaths every year worldwide with this number still growing.[34] As a result, the continuing obligation of designing and discovering novel cancer therapies remains crucial. The design of new therapeutic agents should also address the problems associated with current chemotherapy agents such as poor selectivity for malignant cells, severe side effect profiles and acquired drug resistance.

The survival rate and treatment response between different tumours varies greatly. Amongst the tumours that confer poor prognosis and are associated with high mortality rate is neuroblastoma.

1.2 Neuroblastoma

Neuroblastoma is among the most clinically heterogeneous of cancers, and has been the focus of intensive ongoing research for many decades.[35,36] This neuroendocrine tumour arises from the neural crest precursor cells of the sympathetic nervous system during foetal or early postnatal life.[37,38] The embryonic tumour can originate in one of the adrenal glands or the nerve tissues of the abdomen, chest, neck and pelvis.[39]

Neuroblastoma is the most common extracranial tumour in children, which peaks in infancy.[40] It accounts for around 8% of cancers in patients younger than 15 years and approximately 15% of all oncology deaths in paediatric patients.[36] The hallmark of neuroblastoma is its clinical heterogeneity, known by a widely varying tumour progressions according to age and stage of disease at diagnosis.[41] Patients are stratified into different prognostic categories: low, intermediate, and high risk groups. In general, for tumours in the low-risk group, the infants, undergo spontaneous regression or are curable with minimal therapy, even if the tumour has metastasized. However, older children who are categorized into a high-risk group, frequently have a very aggressive, metastatic tumour that progress despite any intensive multimodal therapy, with the majority of cases leading to death.[37,40]

The aetiology of neuroblastoma remains unknown; however evidence suggests it is unlikely that environmental factors can impact disease occurrence.[42] Neuroblastoma, like other cancers, occurs when multiple mutations in critical genes controlling cell growth, proliferation and differentiation, cause cells to divide uncontrollably and form tumours. The

clinical diversity of this pathology correlates closely with the complex combinations of acquired genetic aberrations discovered thus far. In most cases, neuroblastoma occurs sporadically through somatic mutations, and only 1% of patients are associated with mutations that are inherited, *i.e.* familial neuroblastoma.[38,43] Mutation in the *PHOX2B*[44] and anaplastic lymphoma kinase (*ALK*) genes[45] have been shown to increase the risk of developing sporadic and familial neuroblastoma. *PHOX2B* is associated with differentiation of the sympathetic nervous system and *ALK* encodes a transmembrane receptor tyrosine kinase, important in cell proliferation.

The first discovered genetic defect in neuroblastoma was the *MycN* proto-oncogene amplification (Figure 1.6).[35] This gene is a member of the *MYC* family of transcription factors[32] which encodes a nuclear phosphoprotein.[46] This protein controls a broad range of regulatory networks involved in cell cycle, DNA damage response, differentiation and apoptosis.[35] *MycN* amplification occurs in 25% of patients and strongly correlates with the severity of the disease and treatment failure.[47] However, it is not yet known how the regulatory pathways controlled by the corresponding gene product, MYCN contributes to neuroblastoma pathogenesis.[48]

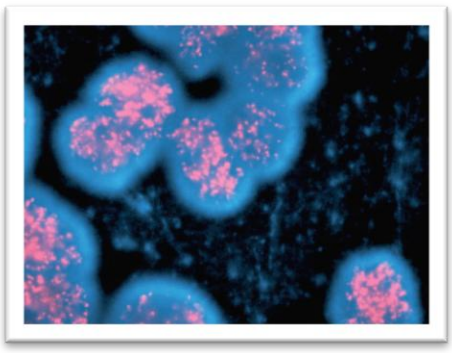


Figure 1.6: *MycN* amplification demonstrated by fluorescence in situ hybridisation (FISH). The presence of multiple copies of *MycN* can be readily detected in tumour cells using a labelled *MycN* probe.[37]

The other common genetic aberrations include ploidy changes, deletion or allelic losses of chromosome arm 1p, 3p, 2q, 7q, 11q, 14q and 19q implicating putative tumour suppressor genes, and gain of chromosome arm 1q, 5q, 7q, 18q and most frequently 17q, presumably affecting growth control genes.[49-51] Despite intensive research, the fundamental biological role of these changes, most importantly of the 1p loss, 17q gain and *MycN* amplification, leading to neuroblastoma remains to be understood. In contrast, great progress has been made in understanding the relation between genetic abnormalities and tumour behaviour and clinical outcome. The predictive value of these biological factors is important not only for the clinical oncologist when considering appropriate chemotherapy, but also for the surgeon when considering the timing and extent of an operative procedure for a child with neuroblastoma.[36] Recently, it has been reported that genes encoding the metabolic enzymes isocitrate dehydrogenase IDH1 (cytoplasmic) and IDH2 (mitochondrial), integral to cellular respiration and metabolism, are recurrently mutated in cancers of colon, nervous tissue tumours and leukaemia.[52,53] The *IDH1* and *IDH2* genes are significant in the citrate cycle in mitochondria, which has a substantial role in apoptosis (Figure 1.7).[54] The mutations cause over abundance of the oncometabolite 2-hydroxyglutarate (2-HG), which then alters a number of downstream cellular activities potentially contributing to lack of apoptosis in cancer cells. In addition, changes in glycolysis metabolism in some malignant cells lead to hypoxia which triggers angiogenesis, another characteristic feature of neoplastic growth.[54]

Otto Warberg first proposed that dysregulated metabolism was the origin of cancer in the 1920s and since then it has been a commonly observed hallmark of tumours including neuroblastomas.[55] As these oncometabolites formed from mutant *IDH1* and *IDH2* have been found to contribute to the pathogenesis of cancer, they provide attractive targets for therapy.

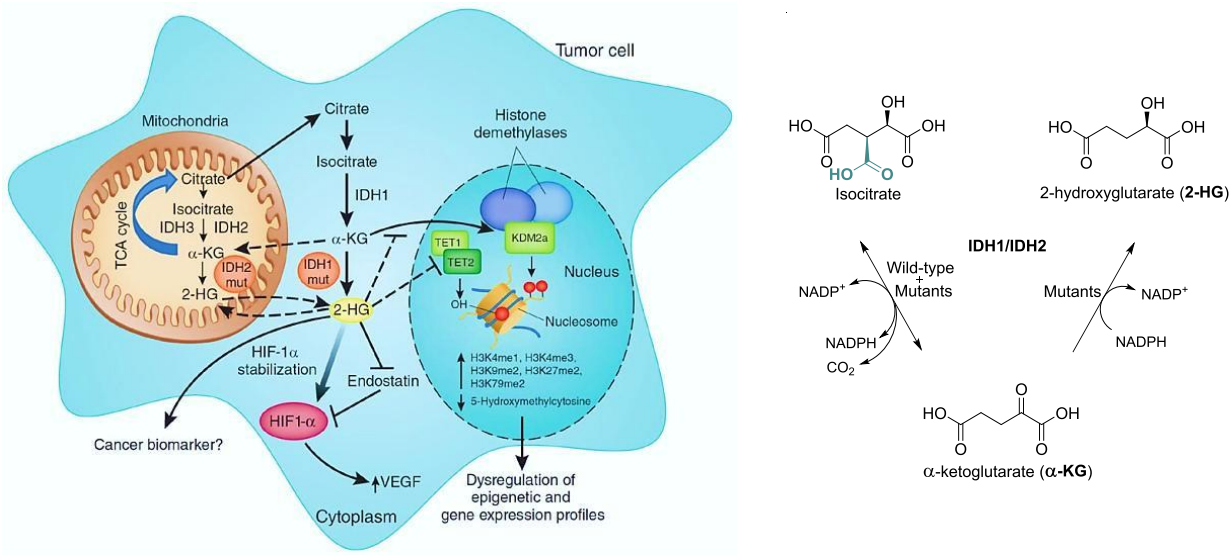


Figure 1.7: Mutant IDH1 (cytoplasmic) and IDH2 (mitochondrial) enzymes show a neomorphic enzymatic capacity to convert α-KG into 2-HG, a small oncometabolite.[52]

1.2.1 Current Neuroblastoma Therapies

Neuroblastoma has been more extensively studied than any other childhood solid-tumour cancer and a complex variety of tumour genetic and many biological factors have been shown to play vital roles in tumour development.[50] Currently, the treatment of most neuroblastomas follows the conventional therapeutic approaches, including surgery, external beam radiation therapy and cytotoxic chemotherapy.[37] Patients are stratified into different prognostic categories: low, intermediate, and high risk groups. Surgery alone or surgery with modest-dose chemotherapy, currently effectively treats patients with low and intermediate risk disease. However, even with the steady improvement in therapy over the past 20 years, only 45% of patients with high-risk, metastatic disease experience an event-free survival.[56]

Molecular profiling of neuroblastoma has led to targeted therapy research focusing on development of new drugs designed to induce differentiation in cancer cells, revive silenced apoptosis pathways, inhibit angiogenesis and target oncometabolites. A novel synthetic retinoid called fenretinide have been shown to induce neuroblastoma apoptosis, and is

currently undergoing clinical trials.[57] Another therapy under study involves the use of a molecule called *meta*-iodobenzylguanidine (MIBG) that is actively taken up by neuroblastoma cells, and when combined with radiolabeled iodine, can be used to kill these cancer cells.[58] Immunotherapy of neuroblastoma using selective antibodies is also increasingly gaining popularity, a number of which have been tested in clinical trials.[59] The combination of these targeted therapies with the traditional therapeutic treatments for neuroblastoma signifies an important advance toward improving cure rates.

1.3 Medicinal Chemistry in Drug Discovery

The process of drug discovery involves disease target identification and validation, pharmacological screening, and establishing hit and lead compounds. Once a hit compound shows activity towards the disease target, it is put through lead optimisation, the process of drug discovery. This is then followed by preclinical and clinical evaluation and finally industrial development (Figure 1.8). Medicinal chemistry is involved in the discovery of hit and lead compounds and in the lead identification and optimisation stage leading to identification of drug candidates.

The most common strategies for hit and lead identification include knowledge-based rational design of compounds based on detailed information derived from endogenous ligands, target or other biostructures or based on literature- and patent-derived molecular entities. These compounds can also be derived from purely serendipitous brute-force approaches such as high throughput screening and combinatorial chemistry or through the screening of bioactive natural products (see next section).[60] The labour intensive lead identification and optimisation phase also requires the skill of medicinal chemists to refine the physicochemical properties of the active molecules to the level required for clinical use. This is generally done by parallel

synthesis of a series of analogues of the hit or lead compound and setting up models for conducting structure-activity relationship studies. The information obtained is then used to design compounds with higher potency, selectivity and improved pharmacokinetic profiles making, them suitable for therapeutic use.

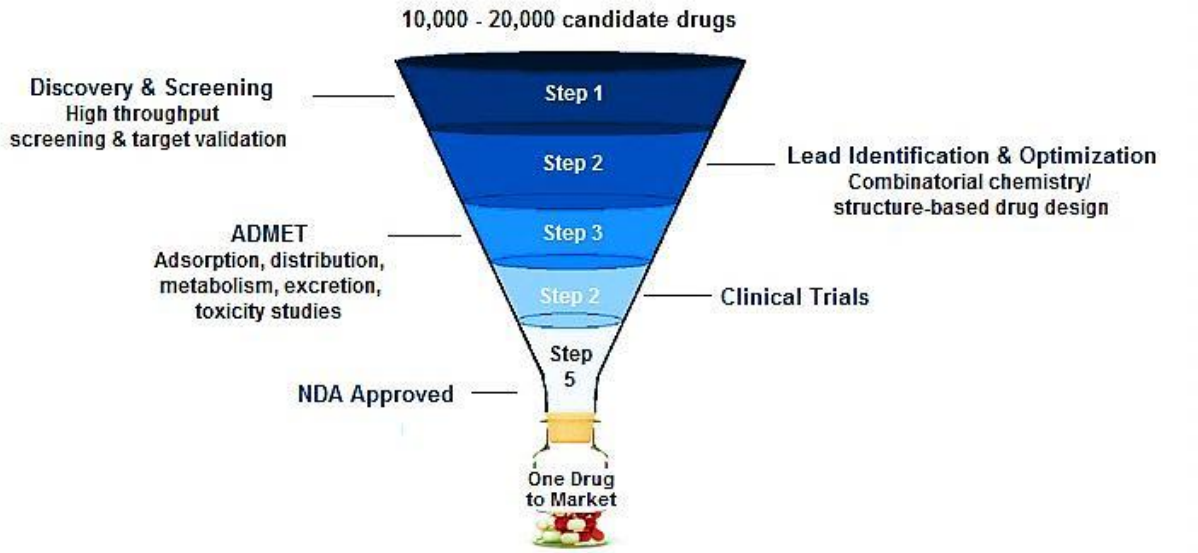


Figure 1.8: A simplified outline of the drug discovery process.

1.4 Natural Products Screening for New anticancer Drugs

Natural products have played an invaluable role in the discovery and development of drugs, especially for the treatment of cancer and infectious diseases. Drugs derived from natural products have been categorized into original natural products, semisynthetic natural products, or synthetic drugs designed from natural product models.[61] More than 60% of the anticancer drugs currently available are reported to be natural products[11] and the continuous search for improved cytotoxic drugs has manifested many more as lead compounds of anticancer drugs.[19,62] Combinatorial chemistry and medicinal chemistry techniques are then generally used to produce a library of analogues of the natural lead compound to uncover the structure-

activity relationship (SAR).[63] This will lead to the preparation of more potent and selective drugs with better pharmacokinetic parameters.[64] In addition, the new leads discovered can be used to improve our understanding of cancer cell biology by subjecting them to biochemical and pharmacology studies.

One example of the natural product lead found was the toxin extracted from Mayapple plant, podophyllotoxin **1**, which has antiviral and antitumour properties (Figure 1.9). The SAR studies conducted on this compound led to the clinically approved anticancer drugs etoposide **2**, its prodrugs teniposide **3** and etopophos **4**. These drugs are effective in the treatment of Wilms' and Ewing's sarcoma, leukaemia, lung, colon and testicular cancer.[65]

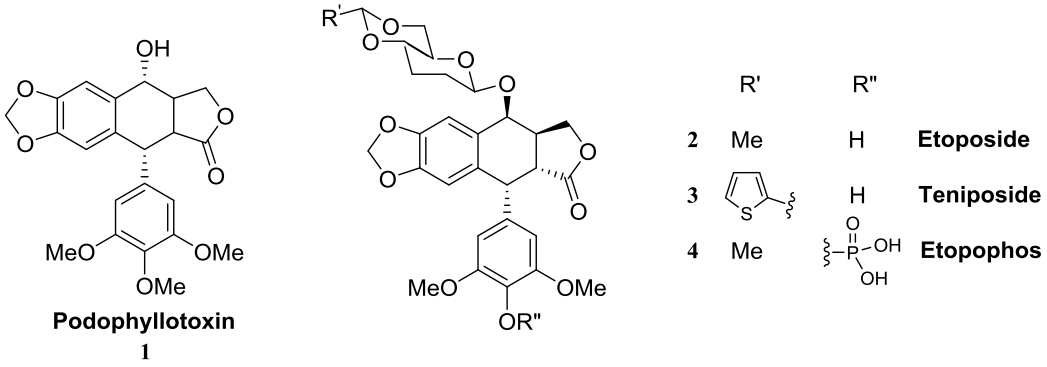


Figure 1.9: Structures of podophyllotoxin derivatives.

Methyl jasmonate is a plant hormone that has been reported to induce apoptosis in a number of neuroblastoma cell lines.[66,67] One of the target molecules of methyl jasmonate in cancer cell mitochondria was discovered to be hexokinase (HK), the initial enzyme in the glycolytic pathway (Figure 1.10).[68] Hexokinase is frequently overexpressed in human cancers and its two isoforms HK1 and HK2 are more tightly bound to outer mitochondrial membranes in cancer cells than in non-malignant cells. Methyl jasmonate detaches hexokinase from

mitochondria via direct interaction, thereby triggering mitochondrial apoptosis. Consequently, targeting the aberrant metabolism of cancer malignancies by methyl jasmonate may provide a new means to treat neuroblastoma.

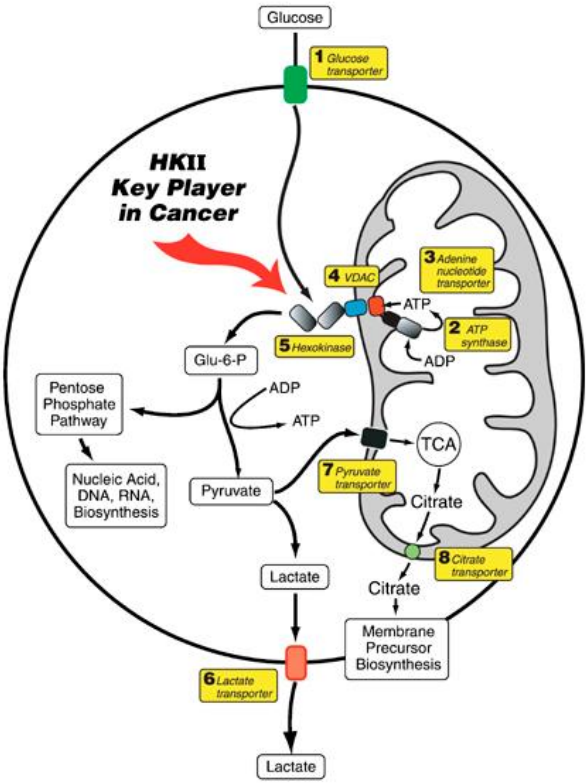


Figure 1.10: Delivery of glucose and ATP to hexokinase (HK) II bound to the outer mitochondrial membrane within a malignant cell and metabolic fates of the glucose-6-phosphate (G-6-P) formed.[68]

1.5 Future Directions for Treatment of Neuroblastoma

As the genes, proteins and signalling pathways that have crucial roles in the pathogenesis of neuroblastomas are identified and characterized, it is expected that this information will provide insights into designing more biologically targeted therapies.[37] These therapies will possibly target pathways that are shared by most types of cancer, as well as targets that are exclusive to neuroblastoma. The most exciting prospects of these therapies would be to

improve the therapeutic index, to have greater specificity and lower toxicity, overcoming tumour resistance to therapy, as well as increasing cure rates.[39]

Molecular profiling of neuroblastoma has led to targeted therapy research focusing on developing new drugs designed to induce differentiation in cancer cells, activate silenced apoptosis pathways, inhibit angiogenesis and target oncometabolites.[37] Many of the new targeted therapy drugs discovered are now undergoing phase I and II clinical trials.

In depth analyses of high-resolution array chromosomal comparative genomic hybridization (aCGH) analyses have further contributed to the molecular portrait of neuroblastoma. Stallings *et al.* have used this technique to identify probable somatically acquired alterations including genes involved in development of tumour, apoptosis, or differentiation of neural cells. The microdeletion of the tyrosine phosphatase PTPRD gene with potential tumour suppressor function was most frequently observed.[26] In addition, a number of protein tyrosine phosphatases (PTPs) have been shown to be implicated in oncogenesis and tumour progression, and Stoker *et al.* have also reported the role of PTPs in neuroblastoma initiation and progression. Thereby, the PTP family also provide a novel target for neuroblastoma treatment.[69]

Furthermore, new anticancer drugs derived from research on plant natural products will certainly continue to grow. New leads can be further developed or modified to yield useful drugs or be subjected to biochemical and pharmacological studies to increase understanding of neuroblastoma cell biology.

Targeting specific mutations in neuroblastoma marks a new step toward personalized therapy for neuroblastoma. Further clinical development of targeted treatments offers new hope for children suffering from this disease.[70]

1.6 Aims of the Project

Neuroblastoma is the most common extracranial solid cancer in childhood and the most frequently diagnosed neoplasm during infancy. In the past few decades, substantial improvements have been made in treatment of patients with low and intermediate risk neuroblastoma, resulting in excellent prognosis with cure rates of 70-90%. However, nearly half of all patients are diagnosed with the high-risk tumour phenotype and have an overall survival rate of less than 40% despite all intensive multimodal therapies. Therefore, the discovery and development of novel and effective drugs for treatment of neuroblastoma remains crucial.[39]

The aim of this thesis is to identify and develop anti-neuroblastoma agents *via* two strategies. The first involves a targeted therapy approach towards the synthesis of new drug-like PTP inhibitors (Chapters 2 and 3) and the second involves devising a new versatile synthetic route to the recently established anticancer natural-product lead, methyl jasmonate and its analogues (Chapter 4).

1.6.1 Targeted Approach towards Anti-Neuroblastoma Agents

More than 30% of the protein tyrosine phosphatases family are said to promote cell-survival signalling in tumour cells. At least 14 oncogenic PTP genes have been reported to be overexpressed in various neuroblastoma cell lines and therefore can be considered as potential therapeutic targets.[69] Development of selective, drug-like inhibitors targeting the specific PTPs overexpressed in neuroblastoma cells may provide a novel therapeutic route for effective treatment of this pathological condition.

The Structural Genomic Consortium has determined the structure of more than 20 human PTPs, including PTPN22 associated with cancer, rheumatoid arthritis and diabetes, providing

a comprehensive coverage of the 'PTPome'. Previous studies by Russell *et al.* have revealed a few distinct structural features of PTPN22 relative to other PTPs, such as an atypical conformation of the catalytically important 'WPD' loop, making these enzymes a suitable target candidate for designing selective drug-like PTP inhibitors.[71] In addition, analysis of the surrounding regions of the active site suggested that, similar to PTP1B, it has the potential of interacting with dually phosphorylated substrates; one via the active site and second via a secondary phosphotyrosine binding pocket.[72] This finding is also of great significance for inhibitor development, since the secondary site can be targeted to increase specificity and affinity, as has previously been achieved for PTP1B. Therefore, PTPN22 has been chosen as the target for identification of new selective PTP inhibitors.

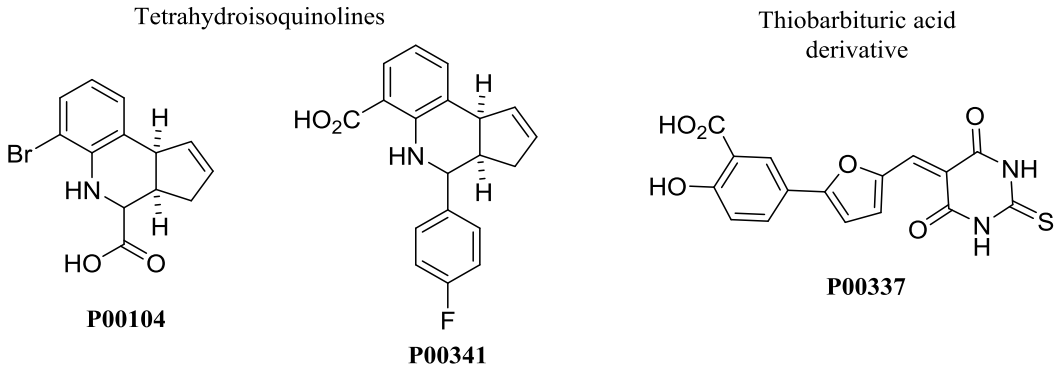


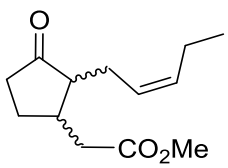
Figure 1.11: Structures of PTPN22 inhibitors identified.

It should be noted that despite the progress in the field of PTP inhibitor development, there are still no clinically approved PTP inhibitors in market, due to many reasons including the lack of drug-like properties of active compounds (discussed in Chapter 2). In an effort to bypass this problem, Russell *et al.* assembled a unique proprietary screening library of 5000 drug-like compounds targeted towards PTPs through a pharmacophore-modelling approach.[71] Initial screening of this library identified two distinct chemical series, tetrahydroisoquinolines **P00104** and **P00341**, and thiobarbituric acid **P00337** as PTPN22 inhibitors (IC_{50} values < 10

μM) with moderate potency *in vitro* (Figure 1.11). Therefore, the first aim of the project was to investigate and optimise a synthetic route towards these compounds and to further prepare a series of rationally-designed analogues for detailed structure-activity relationship (SAR) studies of these compounds against optimised biological PTP assays, in an overall effort to enhance potency, selectivity and physicochemical properties of active compounds (Chapters 2 and 3).

1.6.2 Natural Product-Inspired Approach towards Anti-Neuroblastoma Agents

Natural products play a substantial role in the development of drugs, especially for the treatment of cancer. More than 60% of currently available anticancer drugs are derived from natural compounds.[18,64] Within the past decade, several groups have reported that specific members of the plant stress hormone family, namely methyl jasmonate **5**, exhibit significant selective anticancer activity *in vitro* and *in vivo*, against a wide spectrum of malignancies including neuroblastomas.[67,73] In addition, the poor prognosis of patients with high-risk neuroblastomas is mainly is caused by resistance developed by tumour cells to chemotherapy. Fortunately, a recent study has reported that jasmonates can induce non-apoptotic death in certain high-resistance mutant p53-expressing tumour cells. This provides a stronger rationale for development of jasmonate-derived therapy for late-stage neuroblastoma, as these compounds can induce cell death *via* pathways that bypass the normal resistance developing mechanisms of tumour cells.[74]



Methyl jasmonate
5

Figure 1.12: Structures of naturally occurring methyl jasmonate.

Due to the importance of jasmonates in the perfumery industry, many synthetic routes to these compounds have been developed in the past. However, the majority of these procedures involve complex procedures and precursors and in general lack amenability to diversification and rapid synthesis of analogues. Therefore, a novel route for the versatile synthesis of methyl jasmonate and its analogues will be developed. It is intended that this synthetic procedure would be versatile enough to allow the preparation of a wide range of derivatives through minor changes. This would then provide a platform for future detailed SAR studies of these compounds against different tumour cell lines, aiding a faster movement of optimised compounds into clinical research. Finally, the selective cytotoxicity of methyl jasmonate will be reconfirmed against a series of neuroblastoma cell lines.

1.7 References

1. Jemal, A.; Bray, F.; Center, M. M.; Ferlay, J.; Ward, E.; Forman, D. *Ca-Cancer J. Clin.* **2011**, *61*, 69-90.

2. Andersen, J. N.; Mortensen, O. H.; Peters, G. H.; Drake, P. G.; Iversen, L. F.; Olsen, O. H.; Jansen, P. G.; Andersen, H. S.; Tonks, N. K.; Moller, N. P. H. *Mol. Cell. Biol.* **2001**, *21*, 7117-7136.

3. Barr, A. J. *Future Med. Chem.* **2010**, *2*, 1563-1576.

4. Duesberg, P.; Li, R. *Cell cycle* **2003**, *2*, 202-210.

5. Hanahan, D.; Weinberg, R. A. *Cell* **2000**, *100*, 57-70.

6. Hanahan, D.; Weinberg, R. A. *Cell* **2011**, *144*, 646-674.

7. Sawyers, C. *Nature* **2004**, *432*, 294-297.

8. McKnight, J. A. *Clin. Tech. Small Anim. Pract.* **2003**, *18*, 67-72.

9. Takada, S. *Clin. Tech. Small Anim. Pract.* **2003**, *18*, 73-74.

10. www.scientopia.org.

11. Scott, R. B. *Br. Med. J.* **1970**, *4*, 259-265.

12. Goodman, L.; Wintrobe, M. M.; Dameshek, W.; Goodman, M. J.; Gilman, A.; Mclennan, M. T. *JAMA, J. Am. Med. Assoc.* **1946**, *132*, 126-132.

13. Sanderson, B. J. S.; Shield, A. *Mutat. Res.* **1996**, *355*, 41-57.

14. Lawley, P. D.; Brookes, P. *J. Mol. Biol.* **1967**, *25*, 143-160.

15. Steele, W. J. *Proc. Amer. Assoc. Cancer Res.* **1962**, *3*, 364-364.

16. Bowdon, B. J.; Wheeler, G. P.; Hain, R. *P. Am. Assoc. Canc. Res.* **1984**, *25*, 288-288.

17. Bartlett, D. W.; Clough, J. M.; Godwin, J. R.; Hall, A. A.; Hamer, M.; Parr-Dobrzanski, B. *Pest Manag. Sci.* **2002**, *58*, 649-662.

18. da Rocha, A. B.; Lopes, R. M.; Schwartsmann, G. *Curr. Opin. Pharmacol.* **2001**, *1*, 364-369.

19. Pezzuto, J. M. *Biochem. Pharmacol.* **1997**, *53*, 121-133.

20. Twentyman, P. R. *Pharmacol. Ther.* **1983**, *23*, 417-441.

21. Pommier, Y.; Pourquier, P.; Fan, Y.; Strumberg, D. *Biochim. Biophys. Acta, Gene Struct. Expression* **1998**, *1400*, 83-106.

22. Parness, J.; Horwitz, S. B. *J. Cell Biol.* **1981**, *91*, 479-487.

23. Jordan, M. A.; Wilson, L. *Nat. Rev. Cancer* **2004**, *4*, 253-265.

24. Gerber, D. E. *Am. Fam. Physician* **2008**, *77*, 311-319.

25. Maxwell, M.; Wintrobe, M. M. *Ann. Intern. Med.* **1947**, *27*, 529-540.

26. Stallings, R. L.; Nair, P.; Maris, J. M.; Catchpoole, D.; McDermott, M.; O'Meara, A.; Breatnach, F. *Cancer Res.* **2006**, *66*, 3673-3680.

27. www.centerwatch.com/drug-information/fda-approvals.

28. Bryant, H. E.; Schultz, N.; Thomas, H. D.; Parker, K. M.; Flower, D.; Lopez, E.; Kyle, S.; Meuth, M.; Curtin, N. J.; Helleday, T. *Nature* **2005**, *434*, 913-917.

29. Farmer, H.; McCabe, N.; Lord, C. J.; Tutt, A. N. J.; Johnson, D. A.; Richardson, T. B.; Santarosa, M.; Dillon, K. J.; Hickson, I.; Knights, C.; Martin, N. M. B.; Jackson, S. P.; Smith, G. C. M.; Ashworth, A. *Nature* **2005**, *434*, 917-921.

30. Griffin, R. J.; Pemberton, L. C.; Rhodes, D.; Bleasdale, C.; Bowman, K.; Calvert, A. H.; Curtin, N. J.; Durkacz, B. W.; Newell, D. R.; Porteous, J. K.; Golding, B. T. *Anti-Cancer Drug Des.* **1995**, *10*, 507-514.

31. White, A. W.; Curtin, N. J.; Eastman, B. W.; Golding, B. T.; Hostomsky, Z.; Kyle, S.; Li, J.; Maegley, K. A.; Skalitzky, D. J.; Webber, S. E.; Yu, X.-H.; Griffin, R. J. *Bioorg. Med. Chem. Lett.* **2004**, *14*, 2433-2437.

32. Underhill, C.; Toulmonde, M.; Bonnefoi, H. *Ann. Oncol.* **2011**, *22*, 268-279.

33. Fong, P. C.; Boss, D. S.; Yap, T. A.; Tutt, A.; Wu, P.; Mergui-Roelvink, M.; Mortimer, P.; Swaisland, H.; Lau, A.; O'Connor, M. J.; Ashworth, A.; Carmichael, J.; Kaye, S. B.; Schellens, J. H. M.; de Bono, J. S. *N. Engl. J. Med.* **2009**, *361*, 123-134.

34. Jemal, A.; Bray, F.; Center, M. M.; Ferlay, J.; Ward, E.; Forman, D. *Ca-Cancer J. Clin.* **2011**, *61*, 69-90.

35. Speleman, F.; De Preter, K.; Vandesompele, J. *Semin. Cancer Biol.* **2011**, *21*, 238-244.

36. Maris, J. M.; Hogarty, M. D.; Bagatell, R.; Cohn, S. L. *Lancet* **2007**, *369*, 2106-2120.

37. Brodeur, G. M. *Nat. Rev. Cancer* **2003**, *3*, 203-216.

38. Ora, I.; Eggert, A. *Semin. Cancer Biol.* **2011**, *21*, 217-228.

39. Brodeur, G. M.; Castleberry, R. P. *Neuroblastoma, Principles and Practice of Peditric Oncology*; P. A. Pizzo and D. G. Poplack: Philadelphia, Lippincott-Raven, **1997**, 761-797.

40. Maris, J. M.; Matthay, K. K. *J. Clin. Oncol.* **1999**, *17*, 2264-2279.

41. Maris, J. M. *Curr. Opin. Pediatr.* **2005**, *17*, 7-13.

42. Bunin, G. R.; Ward, E.; Kramer, S.; Rhee, C. A.; Meadows, A. T. *Am. J. Epidemiol.* **1990**, *131*, 776-780.

43. Altura, R. A.; Maris, J. M.; Li, H.; Boyett, J. M.; Brodeur, G. M.; Look, A. T. *Genes, Chromosomes Cancer* **1997**, *19*, 176-184.

44. Trochet, D.; Brien, L. M. O.; Gozal, D.; Trang, H.; Nordenskjold, A.; Laudier, B.; Svensson, P. J.; Uhrig, S.; Cole, T.; Niemann, S.; Munnich, A.; Gaultier, C.; Lyonnet, S.; Amiel, J. *Am. J. Hum. Genet.* **2005**, *76*, 715-715.

45. Mosse, Y. P.; Laudenslager, M.; Longo, L.; Cole, K. A.; Wood, A.; Attiyeh, E. F.; Laquaglia, M. J.; Sennett, R.; Lynch, J. E.; Perri, P.; Laureys, G.; Speleman, F.; Kim, C.; Hou, C. P.; Hakonarson, H.; Torkamani, A.; Schork, N. J.; Brodeur, G. M.; Tonini, G. P.; Rappaport, E.; Devoto, M.; Maris, J. M. *Nature* **2008**, *455*, 930-U922.

46. Castel, V.; Grau, E.; Noguera, R.; Martinez, F. *Clin. Transl. Oncol.* **2007**, *9*, 478-483.

47. Seeger, R. C.; Brodeur, G. M.; Sather, H.; Dalton, A.; Siegel, S. E.; Wong, K. Y.; Hammond, D. *N. Engl. J. Med.* **1985**, *313*, 1111-1116.

48. Yoshimoto, M.; de Toledo, S. R. C.; Caran, E. M. M.; de Seixas, M. T.; Lee, M. L. D.; Abib, S. D. V.; Vianna, S. M. R.; Schettini, S. T.; Andrade, J. A. D. *Am. J. Pathol.* **1999**, *155*, 1439-1443.

49. Look, A. T.; Hayes, F. A.; Shuster, J. J.; Douglas, E. C.; Castleberry, R. P.; Bowman, L. C.; Smith, E. I.; Brodeur, G. M. *J. Clin. Oncol.* **1991**, *9*, 581-591.

50. Bown, N. *J. Clin. Pathol.* **2001**, *54*, 897-910.

51. Mora, J.; Gerald, W. L.; Qin, J.; Cheung, N. K. V. *Oncologist* **2001**, *6*, 263-268.

52. Yen, K. E.; Bittinger, M. A.; Su, S. M.; Fantin, V. R. *Oncogene* **2010**, *29*, 6409-6417.

53. Prensner, J. R.; Chinnaiyan, A. M. *Nat. Med.* **2011**, *17*, 291-293.

54. Reitman, Z. J.; Yan, H. *J. Natl. Cancer Inst.* **2010**, *102*, 932-941.

55. Levy, A. G.; Zage, P. E.; Akers, L. J.; Ghisoli, M. L.; Chen, Z.; Fang, W.; Kannan, S.; Graham, T.; Zeng, L. Z.; Franklin, A. R.; Huang, P.; Zweidler-McKay, P. A. *Invest. New Drugs* **2012**, *30*, 191-199.

56. Seeger, R. C. *Semin. Cancer Biol.* **2011**, *21*, 229-237.

57. Lovat, P. E.; Ranalli, M.; Annichiarrico-Petruzzelli, M.; Bernassola, F.; Piacentini, M.; Malcolm, A. J.; Pearson, A. D. J.; Melino, G.; Redfern, C. P. F. *Exp. Cell Res.* **2000**, *260*, 50-60.

58. Dekraker, J.; Hoefnagel, C. A.; Caron, H.; Olmos, R. A. V.; Zsiros, J.; Heij, H. A.; Voute, P. A. *Eur. J. Cancer* **1995**, *31A*, 600-602.

59. Cheung, N. K. V.; Kushner, B. H.; Yeh, S. D. J.; Larson, S. M. *Int. J. Oncol.* **1998**, *12*, 1299-1306.

60. Bleicher, K. H.; Bohm, H.-J.; Muller, K.; Alanine, A. I. *Nat. Rev. Drug Discovery* **2003**, *2*, 369-378.

61. Butler, M. S. *Nat. Prod. Rep.* **2005**, *22*, 162-195.

62. Mukherjee, A. K.; Basu, S.; Sarkar, N.; Ghosh, A. C. *Curr. Med. Chem.* **2001**, *8*, 1467-1486.

63. Xiang, X. D.; Sun, X. D.; Briceno, G.; Lou, Y. L.; Wang, K. A.; Chang, H. Y.; Wallacefreedman, W. G.; Chen, S. W.; Schultz, P. G. *Science* **1995**, *268*, 1738-1740.

64. Gordaliza, M. *Clin. Transl. Oncol.* **2007**, *9*, 767-776.

65. Hande, K. R. *Eur. J. Cancer* **1998**, *34*, 1514-1521.

66. Tong, Q.; Jiang, G.; Zheng, L.; Tang, S.; Cai, J.; Liu, Y.; Zeng, F.; Dong, J. *Anticancer Drugs* **2008**, *19*, 573-581.

67. Tong, Q.; Jiang, G.; Zheng, L.; Tang, S.; Cai, J.; Liu, Y.; Zeng, F.; Dong, J. *Acta Pharmacol. Sin.* **2008**, *29*, 861-869.

68. Goldin, N.; Arzoine, L.; Heyfets, A.; Israelson, A.; Zaslavsky, Z.; Bravman, T.; Bronner, V.; Notcovich, A.; Shoshan-Barmatz, V.; Flescher, E. *Oncogene* **2008**, *27*, 4636-4643.

69. Clark, O. PhD Thesis, University College London, **2011**.

70. Matthay, K. K.; George, R. E.; Yu, A. L. *Clin. Cancer Res.* **2012**, *18*, 2740-2753.

71. Russell, A. DPhil Thesis, University of Oxford, **2004**.

72. Wiesmann, C.; Barr, K. J.; Kung, J.; Zhu, J.; Erlanson, D. A.; Shen, W.; Fahr, B. J.; Zhong, M.; Taylor, L.; Randal, M.; McDowell, R. S.; Hansen, S. K. *Nat. Struct. Mol. Biol.* **2004**, *11*, 730-737.

73. Flescher, E. *Anticancer Drugs* **2005**, *16*, 911-916.

74. Fingrut, O.; Reischer, D.; Rotem, R.; Goldin, N.; Altboum, I.; Zan-Bar, I.; Flescher, E. *Br. J. Pharmacol.* **2005**, *146*, 800-808.

CHAPTER 2

Targeting Protein Tyrosine Phosphatases with Small Molecule Inhibitors for Neuroblastoma Drug Discovery (I)

2.1 Introduction

The protein tyrosine phosphatases (PTPs) constitute a superfamily of closely related key regulatory enzymes that catalyse the removal of phosphate groups from phosphorylated tyrosine residues on intracellular proteins. Discovered three decades ago, PTPs are now recognized to be the key players in cellular signal transduction pathways that underlie a broad range of fundamental physiological processes.[1] Malfunction in PTP activity is being associated with rapidly increasing numbers of inherited and acquired human diseases including cancer.[2] Consequently, substantial research effort of both academia and the pharmaceutical industry is devoted to defining the function of these phosphatases in normal physiology and in pathological conditions.

With at least 30 PTPs being identified as cancer targets,[3] designing small molecule inhibitors specific for individual or even subsets of PTP molecules to treat cancer has become a topic of considerable interest in the past few years. Although progress has been made, this field of research is still in its early stages. There are a number of significant challenges for producing PTP inhibitors, and major efforts are required to overcome these for the successful development of the first PTP inhibitor as a novel therapeutic drug.

2.1.1 Characteristics of the PTP Family

Protein tyrosine phosphorylation and dephosphorylation is considered to play the most important role in the regulation of cellular signalling pathways involved in proliferation, differentiation, survival, and migration. The reversible phosphorylation of tyrosine residues on proteins is controlled reciprocally by protein tyrosine phosphatases (PTPs) which remove the phosphate group, and protein tyrosine kinases (PTKs) that catalyse the transfer of a phosphate group from ATP to the protein's hydroxyl group (Figure 2.1).[4]

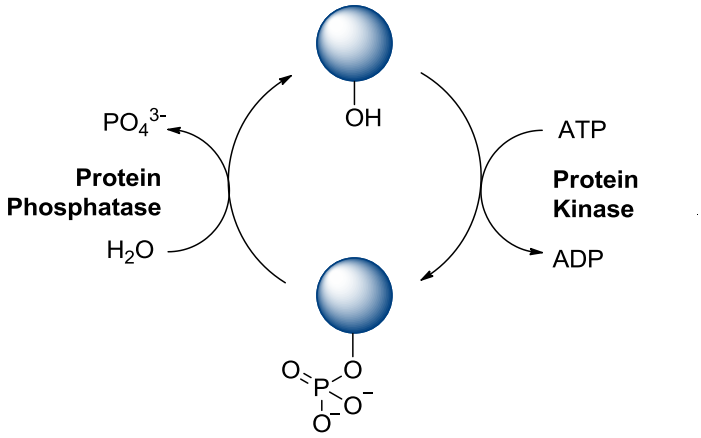


Figure 2.1: Reversible protein phosphorylation by protein phosphatases and protein kinases.

Perturbation of PTK and PTP activities results in aberrant tyrosine phosphorylation, and has been associated with the aetiology of a number of pathologies including cancer.[5] Surprisingly, even though PTPs were discovered only ten years after PTKs, substantial amount of research has been focused on PTKs and research and knowledge of PTPs has lagged behind. Indeed, protein kinases have now become the second most important group of drug targets, after G-protein-coupled receptors,[6] and a number of PTK inhibitors such as imatinib and gefitinib, are now routinely being used for cancer treatment.[7] However, in recent years there has been a considerable increase in PTP studies. From these studies it has emerged that protein phosphatases can no longer be viewed as housekeeping enzyme in intracellular processes, and that PTPs exert remarkably tight control of signal transduction in a positive and negative manner.[1] Consequently, PTPs can coordinate with or antagonise the functions of PTKs depending on the downstream effectors.[8] For example, tyrosine phosphatase PTPN2, induces apoptosis in human tumour cell lines by activating p53,[9] whereas PTP1B dephosphorylates insulin receptor kinase, thereby regulating insulin signalling in a negative manner.[10]

A number of studies have demonstrated that dephosphorylation by PTPs occurs with a high degree of specificity. Zhang *et al.* have shown >1000 fold difference in K_m values for PTPs

targeting different synthetic phosphotyrosine-containing peptides.[11] Studies by Kovalenko *et al.* have also demonstrated that certain subsets of phosphorylated tyrosines are preferentially dephosphorylated by PTPs on proteins that have multiple phosphorylation sites.[12] In addition, the distinct but complementary functions of PTP and PTK enzymes have been highlighted by recent studies, which revealed that phosphatases are important in controlling the rate and duration of the signalling response, whereas kinases often control the amplitude.[1]

The superfamily of PTPs is encoded by 107 genes, of which 38 belong to the classical PTP subfamily that show specificity for phosphotyrosine (Figure 2.2), and 65 encode the heterogeneous dual specificity phosphatases that can act upon tyrosine or serine/threonine residues.[13] Further diversity is also introduced into these groups through alternative promoters and mRNA splicing, and post-translational modifications.[1,2] The structural diversity of this family reflects their varied functional importance in cell signalling.

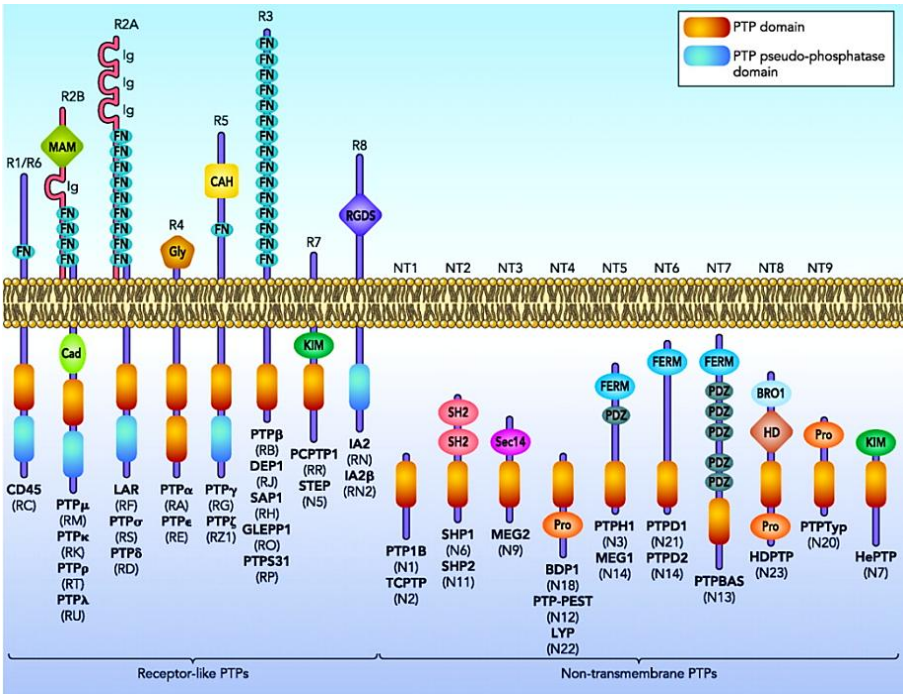


Figure 2.2: The classical protein tyrosine phosphatase superfamily of enzymes is represented schematically, depicting receptor-like and non-transmembrane PTPs. Note the diverse extracellular domains of the receptor-like PTPs and non-catalytic domains of the non-transmembrane PTPs.[13]

The classical PTPs are broadly subdivided into receptor-type PTPs (RPTPs) encoded by 21 of the genes and non-receptor cytoplasmic PTPs encoded by the remaining 17 genes (figure 2.2). The RPTPs are made up of a single transmembrane domain and variable extracellular domains, and are capable of regulating cellular signalling through ligand-controlled protein tyrosine dephosphorylation.[1,14] Most of these RPTPs contain two tandem cytoplasmic PTP domains, a membrane proximal domain (D1) and a membrane distal domain (D2), with the catalytic activity residing in D1 in the majority of PTPs.[15] The extracellular section of most RPTPs includes immunoglobulin-like and fibronectin type III domains, allowing them to function as cellular adhesion molecules in some cases.[16] The cytoplasmic PTPs have substantial structural diversity and are characterized by regulatory sequences that flank the catalytic domain. These sequences control the PTP activity either by targeting them to specific subcellular locations or allowing direct interaction with specific proteins.[17]

The superfamily of PTPs is defined by their highly conserved catalytic active site, which spans approximately 280 amino acid residues. It comprise a consensus signature motif represented by $Cys(X)_5Arg$,[18] encompassed within a core structure domain of four parallel β-strands surrounded on both sides by α-helices (Figure 2.3). In addition, the conserved motif creates a very similar structural motif, termed the PTP loop, which connects a central β-strand to an α-helix at the centre of the catalytic site (Figure 2.3).[19]

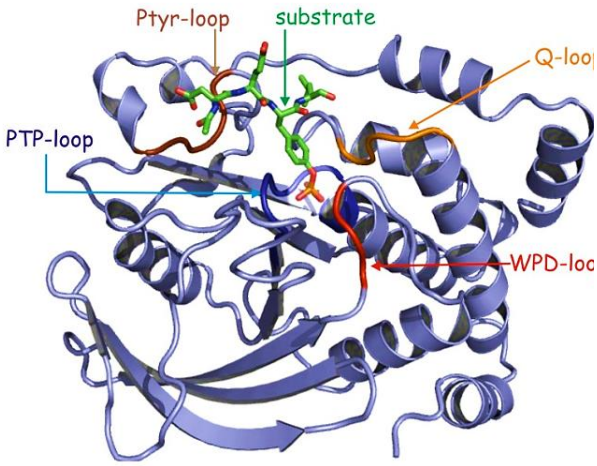


Figure 2.3: The arrangement at the active site of PTP1B. The sides of the catalytic cleft of tyrosine phosphatases are characterized by three motifs: the WPD loop, containing an invariant Asp, the Q-loop, containing an invariant Gln, and the pTyr-loop, containing an invariant Tyr.[20]

Dephosphorylation of phosphotyrosine substrates occurs through a two-step mechanism.[14] First is the nucleophilic attack by the active-site cysteine (Cys215) on the phosphorus atom of the bound substrate that leads to the formation of a covalent PTP-phosphate intermediate, which is subsequently hydrolysed by nucleophilic displacement at phosphorus (Figure 2.4).[19] In this catalytic reaction, the arginine residue is involved in stabilization of the intermediate, as well as assisting substrate binding. The invariant aspartic residue (Asp356) in the WPD (Trp-Pro-Asp) loop has been shown to act as a general acid during the first step and a general base during the second (Figure 2.4).[21]

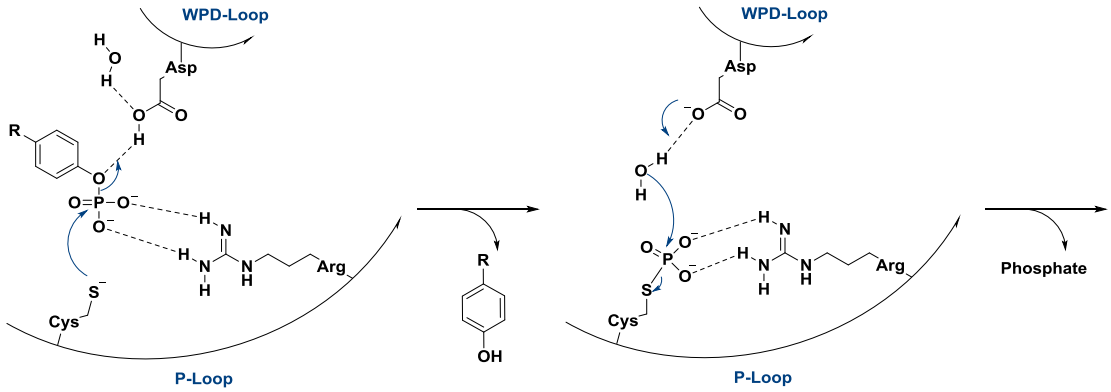


Figure 2.4: Schematic representation of the PTP1B-catalysed hydrolysis of aryl phosphates.

2.1.2 PTPs in Cancer

In contrast to many PTKs that can function as oncoproteins, protein tyrosine phosphatases can have either positive or negative effect on cell proliferation. Due to the antagonistic effect of PTPs on the oncogenic PTKs activities and its downstream targets, they have been intuitive candidates for tumour suppressor genes. However, as they can also activate certain PTKs, as well as being involved in cell differentiation, apoptosis, adhesion and motility, it was also assumed that some PTPs may act as oncogenes. At present, strong experimental evidence

exists to support both tumour-suppressive and oncogenic actions of different PTPs, which result in growth and progression of various types of cancer.

Tumour suppressor genes are characterized by loss of gene function in tumourogenesis, which can occur through methylation-mediated gene silencing, gene deletion, inactivating mutations, and loss of heterozygosity.[22,23] In contrast, oncogenes are characterized by gain of gene function through gene amplification, activating mutations, and translocations, leading to aberrant expression.[23] The following paragraphs provide a few examples of these alterations in expression of PTP genes causing deregulated cellular growth and apoptosis, triggering various types of cancers.

One of the most common and important tumour suppressor genes that is deleted, inactivated or silenced in several major types of neoplasia, including brain, lung, breast and prostate cancers, is *PTEN*.[4,7,24] The corresponding PTEN phosphatase plays a critical role of negatively regulating the phosphoinositide-3-kinase (P13K) PI3K/Akt pathway that has downstream effects on transcription, proliferation, cell survival, invasiveness, and angiogenesis.[25,26] Furthermore, PTEN is linked via several mechanisms to the p53 tumour suppressor, and its mutation leads to genomic instability.[27] As there are no other phosphatases in the superfamily of PTPs that can fully substitute for PTEN function, its inactivation leads to increased cell proliferation and reduced cell death, resulting in neoplastic growth.[24] The widespread misregulation caused by inactivation of this gene poses a tremendous challenge for cancer therapy.

The amplification or gain-of-function mutations in PTPs that have positive influence on growth stimulatory signalling pathways are likely to have oncogenic effects. The first identified PTP proto-oncogene was PTPN11, which encodes the cytoplasmic tyrosine phosphatase SHP2.[28,29] This phosphatase transduces mitogenic and pro-migratory signals

from various receptor types through activation of the Ras/Erk cascade pathway.[30] Germline mutation of PTPN11 causes Noonan syndrome, a complex disease that increases risk of developing juvenile myelomonocytic leukemia.[31] Somatic missense PTPN11 gain-of-function mutations induces aberrant hyperactivation of the Ras/Erk pathway leading to cancers such as leukemias and solid tumours such as neuroblastoma, melanoma, lung adenocarcinomas, and colon cancer.[32] In addition, SHP2 is a key downstream target of other oncogenes;[33,34] consequently, inhibiting SHP2 can provide several new therapeutic avenues for a wide range of cancers.

2.1.3 PTPs in Neuroblastoma

Although research into cancer-related PTP perturbations is still in its early stages, a handful of studies have identified PTPs that are involved in the development and maintenance of neuroblastoma. High-resolution analysis of chromosomal breakpoints and genomic instability were carried out by Stallings *et al.* on 56 neuroblastoma tumours and cell lines to identify genes involved in this disease pathogenesis. The most frequent microdeletion observed involved the 5' untranslated region (5'UTR) of the PTPRD gene, implicating PTPRD to be a possible suppressor of tumourigenesis in neuroblastoma.[35] Ascertaining the possible functional effects that deletions of the 5'UTR might have on either transcription or translation of PTPRD should shed considerable light on the relation between loss of this gene and development of metastatic neuroblastoma.

Another study by the same group showed that eleven noncoding 5'UTR exons in PTPRD are aberrantly spliced in more than 50% of neuroblastoma primary tumours and cell lines, as a consequence of either homozygous genomic deletion, aberrant mRNA splicing or possible aberrant hypermethylation of the promoter region of this gene.[36] In their previous studies

Stallings *et al.* demonstrated that in a matched primary and metastatic tumour sample only the metastatic sample showed microdeletion of PTPRD, and that primary tumours derived from patients with metastatic disease had lower expression of PTPRD relative to loco-regional tumours.[35] This led them to suggest that PTPRD might be acting as a metastasis suppressor, rather than as a tumour suppressor gene.[36] Further evidence suggesting that inactivation of this gene is important for metastasis comes from the fact that PTPRD interacts with a putative metastasis suppressor, MIM, which is a regulator of actin assembly downstream of tyrosine kinase signalling, also implicated in metastasis of cancer cells.[37]

Studies conducted by Shang *et al.* demonstrated that the PTP oncogene, dual-specificity phosphatase 26 (DUSP26), is overexpressed in the majority of neuroblastoma cell lines and tissue specimens.[38] These PTPs dephosphorylate serine, threonine, and tyrosine residues on mitogen-activated protein kinases and are important in regulation of intracellular signalling cascades governing cell growth, differentiation and apoptosis.[39] They found that DUSP26 promotes the resistance of human neuroblastoma to chemotherapeutic doxorubicin which functions by inducing apoptosis. DUSP26 seems to act as a p53 phosphatase and consequently downregulates p53 tumour suppressor function in neuroblastoma cells.

Shang *et al.* elegantly showed that inhibition of DUSP26 expression in a neuroblastoma cell line activated p53 and enhanced doxorubicin induced apoptosis, whereas over-expressing DUSP26 inhibited p53 activation by doxorubicin.[38] DUSP26 can therefore act as a novel therapeutic target for paediatric neuroblastoma malignancy, as inhibition of this phosphatase may increase neuroblastoma chemosensitivity by reactivating cellular apoptosis pathways to promote tumour cell death.[38]

Although some exciting progress has been made, the field of identification of potential PTP targets and development of selective inhibitors to facilitate novel neuroblastoma treatment is still new and requires extensive research.

2.1.4 PTPs as Drug Targets: Strategies and Challenges of Inhibitor Development

The rapidly increasing number of pathologies associated with perturbation of PTP activities has prompted a growing interest in these enzymes as drug targets.[4,7,40-43] The spark that truly ignited the search for PTP inhibitors by scientists in both academia and the pharmaceutical industry, with the promise of great market potential, was the discovery made by Kennedy *et al*. on gene knockout studies carried out in mice.[44] They established that PTP1B knockout is not a fatal deletion, but instead confers protection from obesity and improves insulin sensitivity.[44]

Currently the literature reviews on PTP inhibitors range from natural products and their derivatives,[45-49] nonselective phosphate mimics,[50] phosphotyrosine-like molecules,[51-54] peptidomimetics,[51,52] through to the newer small-molecule inhibitors that have been rationally designed or found through high-throughput screening (Figure 2.6).[55-57] Many potent, and in some cases selective, inhibitors of PTPs such as PTP1B, SHP2, Cdc25 and PRL phosphatases have been reported.[4] However, there are a number of significant technical challenges for designing selective PTP inhibitors, which has led to a relatively slower progression in development of clinically useful compounds.

The major medicinal chemistry challenges of PTP inhibitor development are cell permeability, selectivity and bioavailability. Due to the highly polar nature of the PTP active site, most active-site catalytic PTP inhibitors are highly charged anionic phosphotyrosine mimetics, with poor cell permeability and bioavailability. In addition, as the active site of PTP

enzymes is highly conserved across the superfamily, most therapeutically significant PTPs have a close homolog that will be cross-inhibited, causing unwanted adverse effects.[7,14,58]

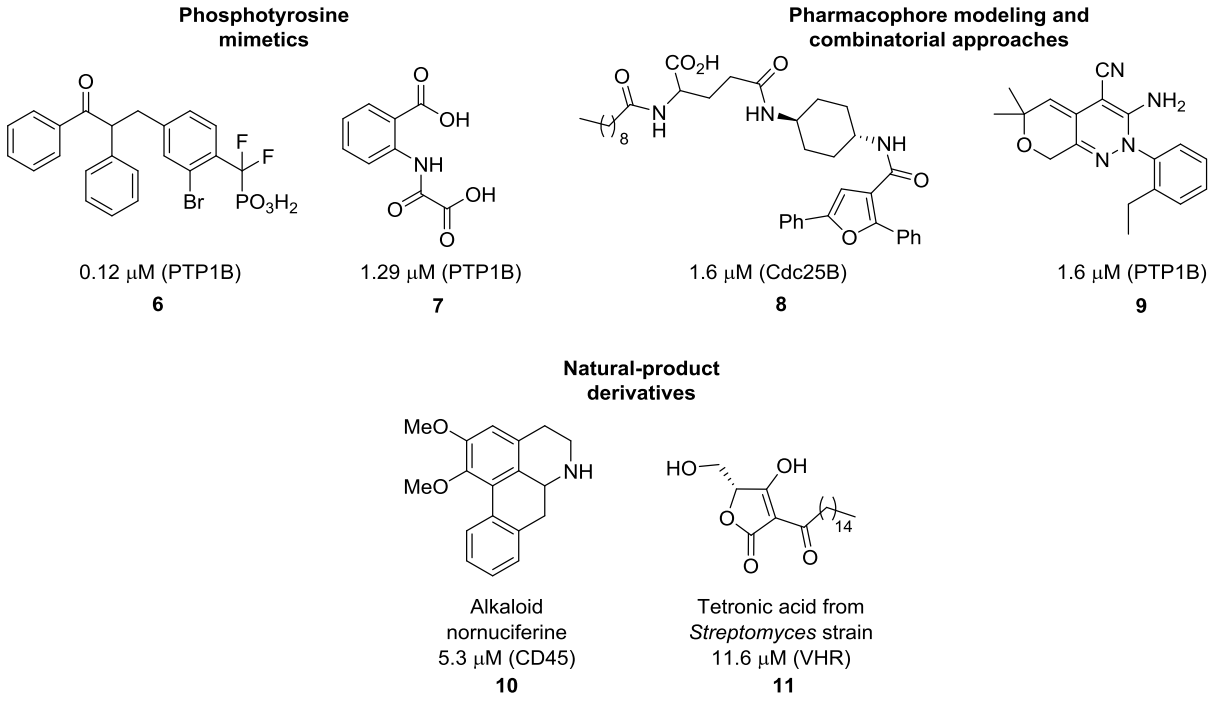


Figure 2.6: PTP inhibitors obtained from diverse approaches; IC_{50} values are given.[45-52]

Another significant challenge encountered is related to the *in vitro* enzymatic assays for PTPs that have a tendency to show a significant incidence of 'false positives', due in large part to the reactivity of the cysteine's sulfur residue at the active site (Figure 2.7). Consequently, the PTPs are prone to inactivation by oxidizing reagents, heavy metals, and alkylating reagents commonly found in various chemical compound collections.[59] For example, some quinone-containing compounds are known to misleadingly inhibit PTPs by these types of active-site modifications, even in the presence of reducing agents like DTT.[58,60-62] These modifications are not likely to yield selective, therapeutically important compounds. Some promiscuous compounds also show false positive results by forming aggregates that sequester the enzymes, rendering them inactive. In addition, the buffer conditions, pH level and salt concentration

have to be cautiously defined to minimise the disruption caused to the ionic interactions in the catalytic active-site. Therefore, it is very important to use a robust assay and kinetic studies should be conducted prior to chemical optimization of the identified hit compound to determine the mechanism of inhibition.[63]

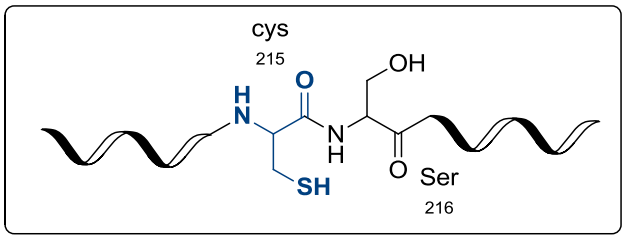


Figure 2.7: Cysteine residue at PTP catalytic site.

Although the catalytic domain of all PTPs is very similar, PTPs have significantly different surface topology and charge distribution in the regulatory domains surrounding the catalytic pocket. These differences reflect the high substrate specificity of PTPs and can be utilised to overcome the challenges of selectivity by designing inhibitors targeting these non-conserved regions, exploiting atypical PTP structural conformations, and developing allosteric inhibitors.[42,58] Furthermore, unlike the hydrophilic and multiply-charged PTP natural substrate mimetics, many cell-permeable lead PTP inhibitors have been reported that can offer improved pharmacological properties.[42] Indeed, a number of PTP inhibitors have progressed to clinical trials, such as ertiprotafib which is a PTPB1 inhibitor, but further development on most of these compounds has been discontinued in phase I and II because of insufficient efficacy and strong unwanted side effects.[64-66]

Despite the progress in the field of PTP inhibitor developments, there have been numerous examples of failed PTP drug discovery programs[67] and the market is still waiting for the first clinically approved selective PTP inhibitor.[68]

2.2 Hit Identification: Thiobarbituric Acid P00337 as a Potential Inhibitor of PTPN22

In an initial effort to identify PTPN22 inhibitors, a proprietary compound collection of over 400 compounds was screened using the *p*-nitrophenyl phosphate (*p*-NPP) enzymatic assay. This compound collection had been 'cherry-picked', from a subset of the Russell group's in-house compound collection of 5000 drug-like small molecules.[69] The 5000-member library is targeted to PTPs, had been assembled using a pharmacophore mapping technique employing common pharmacophores identified from known PTP inhibitors. Thiobarbituric acid compound **P00337** from the library displayed moderate potency *in vitro* against PTPN22 and a set of related phosphatases (Figure 2.8). It was envisaged that this compound could provide a solid starting point for the development of more active drug-like inhibitors of PTPs. In addition, the low molecular weight (mw < 400) of this compound allows further chemical modification to improve pharmacological and physical properties.

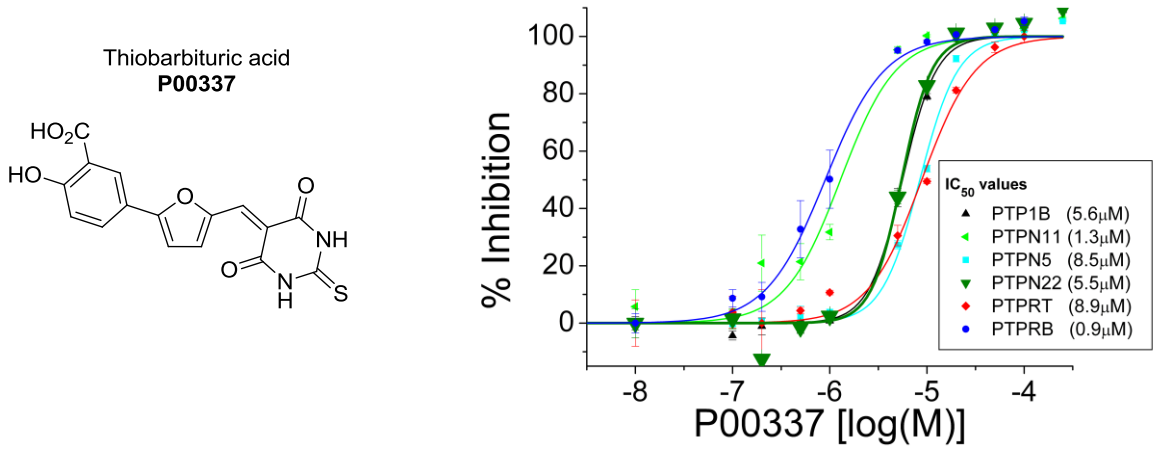
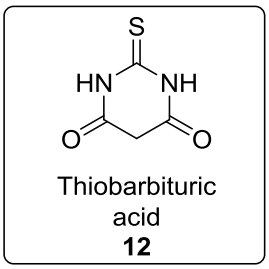


Figure 2.8: IC_{50} values for inhibitor thiobarbituric acid **P00337** against PTP1B, PTPN11, PTPN5, PTPRT and PTPN22.[70]

2.2.1. Thiobarbituric Acid

Thiobarbituric acid derivatives have many medicinal importance, being used as intravenous anaesthetics and showing a wide range of biological activities such as antineoplastic, antifungal, anticonvulsant, antidepressant, antimicrobial and antioxidant properties.[71,72] There has been much more interest in these compounds as platforms in the synthesis of other biologically active compounds.



Thiobarbituric acid
12

Thiobarbituric acid derivatives are useful intermediates in pyrimidine chemistry, since the sulfur substitutent can be easily removed to give ring-fused pyrimidines, or can be displaced by a variety of nucleophilies. The particularly interesting thiobarbituric acid **12** is suitable for nucleophilic attack at C-5 and/or C-2, condensation with aldehydes, synthesis of dyes, as well as condensation with benzoin to give thioxofuro[2,3-*d*]pyrimidines.[71]

Although thiobarbituric acid derivatives have not been reported as frequent hitters (promiscuous compounds) in many biochemical high throughput screens, related compounds with exocyclic, double bonded sulphur atom such as in rhodanines **13** and thiohydantoins **14**, have recently gained a reputation of being unselective false positive compounds or assay-interfering compounds that broadly interact with a plethora of targets (Figure 2.9).[73,74] It has been suggested that the sulphur atom in these compounds has a pronounced propensity to form polar, intermolecular interactions which may cause a promiscuous behaviour at concentrations in the "screening range".[73] However, as these observations appear to be based mostly on anecdotal evidence, and the fact that compounds containing such functionalities show a wide range of useful biological activities, suggests that these compounds should not

be regarded as a general knockout criterion that excludes such screening hits from further development.

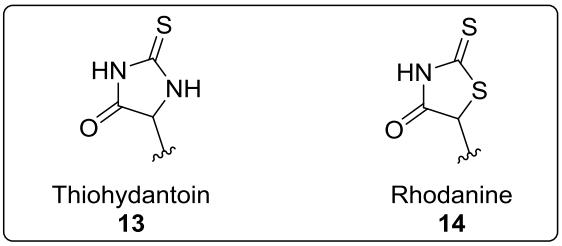
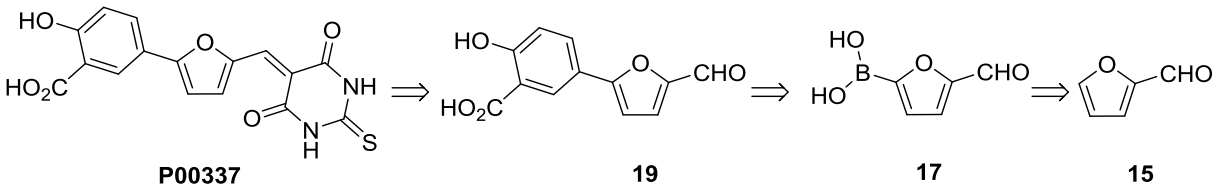


Figure 2.9: Exocyclic, double bonded sulfur atom containing five-membered multiheterocyclic rings that may act as Privileged Scaffolds or Promiscuous Binders.

2.2.2 Retrosynthesis of Thiobarbituric Acid P00337 and SAR Analysis

The Suzuki-Miyaura reaction involving palladium-catalyzed cross-coupling of aryl halides with arylboronic acids represents a straightforward and highly effective method for carbon-carbon bond formation in the synthesis of biaryl compounds.[75-77] It was envisaged that compound **P00337** could be prepared by two main synthetic steps comprising of Suzuki-Miyaura couplings of an aryl halide with 5-formylfuran-2-yl boronic acid **17**, and Knoevenagel condensation of the subsequent 5-arylfuran-2-carbaldehyde **19** with thiobarbituric acid [Scheme 2.1].



Scheme 2.1: Proposed route to the synthesis of **P00337**.

With the new hit compound **P00337** in hand; an extensive SAR study was started. This compound was divided into three regions in order to analyse the specific impact of each of these components on activity against PTPN22 and related PTPs (Figure 2.10). Initially, focus

was turned to the substituents of the phenyl moiety (part A) and synthesizing compounds with thiobarbituric- and barbituric acid moieties (part B). It was thought after the first screening of a panel of analogues of compound P00337 against PTPs, the active compounds identified could then be put through further modifications at the furan ring (part C) to improve the pharmacokinetic profile as well as potency and selectivity.

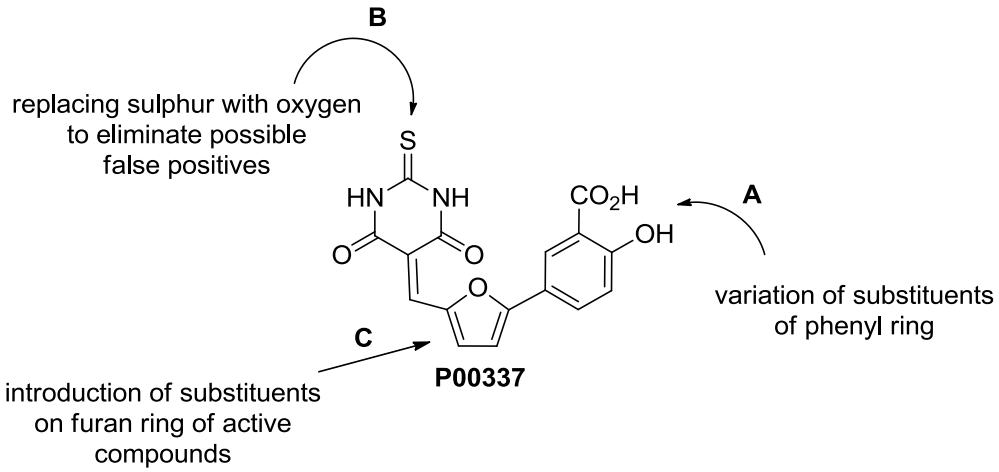


Figure 2.10: Structure-activity relationship study of compound **P00337**.

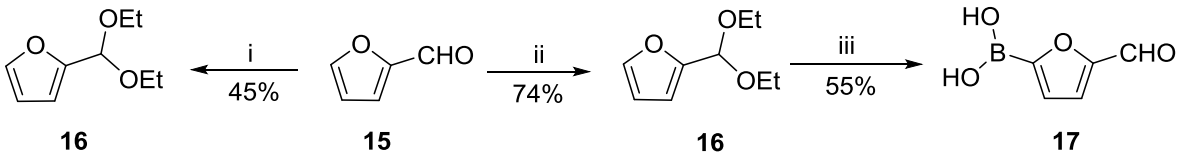
2.2.3 Resynthesis of P00337

The modular design of compound **P00337** makes it an attractive scaffold for the exploration of chemical space and structure-activity relationship (SAR) studies, as units can be synthesized independently and then assembled in a combinatorial process.

For the resynthesis of this hit compound, it was envisaged that a reagent with both boronic acid and aldehyde functionalities should offer great scope for the preparation of π-extended biaryl/heteroaryl systems.[78]

For the synthesis of the boronic acid **17**, furan-2-carbaldehyde (furfural) **15** had to be first protected as the corresponding diethyl acetal. This was initially attempted by refluxing furfural with NH_4Cl and triethyl orthoformate in ethanol.[79] However, this led to the precursor

2-(diethoxymethyl)furan **16** being furnished in poor yield (45%). In an alternative protocol, treatment of furfural with *p*-TSA and triethyl orthoformate[80] afforded **16** in a good yield of 74%. The boronic acid **17** was then prepared as described in the literature,[78] which involved lithiation of acetal **16** using *n*-butyllithium followed by reaction with trimethylborate. Aqueous workup comprising alkaline hydrolysis of the boronic ester and acid-mediated deprotection of the acetal, liberated compound **17** in 55% yield after purification (Scheme 2).

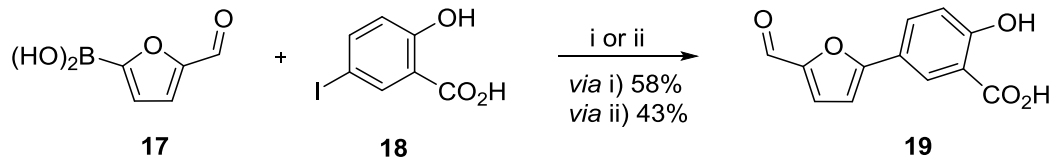


Scheme 2.2: *Reagents and conditions:* i) NH_4Cl, triethyl orthoformate, EtOH, reflux overnight; ii) *p*-TSA (10 mol%), triethyl orthoformate, rt, overnight; iii) *n*BuLi, THF, −78 ºC for 2 h; then $B(OCH_3)_3$, rt overnight; then aq HBr.

Bumagin *et al*. have recently reported a protocol for a ligandless Suzuki-Miyaura coupling reaction of sterically hindered arylboronic acids with aryl halides using palladium acetate as catalyst.[81] These reactions were conducted using neat water as solvent which has clear advantages of being cheap, readily available, and nontoxic. To verify the effectiveness of this procedure for the synthesis of compound **P00337**, boronic acid **17** and 5-iodosalicylic acid **18** were subjected to 0.1 mol% of $Pd(OAc)_2$ and three equivalents of KOH in water under gradual heating from 20 to 75 ºC. In the presence of the base, 5-iodosalicylic acid is converted into the corresponding water soluble carboxylate salt, allowing the reaction to proceed under homogeneous conditions. This protocol afforded the cross-coupling product **19** in 58% yield after 6 hours [Scheme 2.3].

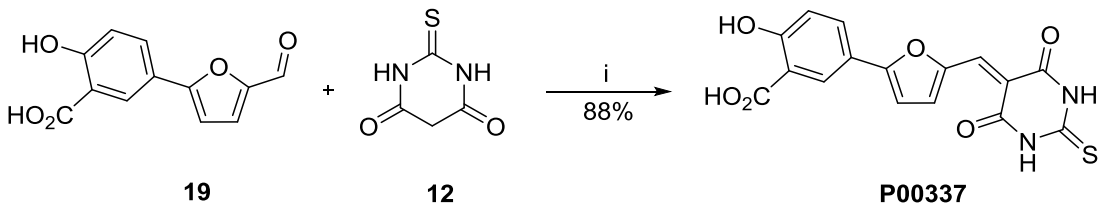
In an attempt to increase the yield of reaction, 5-iodosalicylic acid **18** was subjected to the typical Suzuki reaction, where the reagents were treated with catalytic $PdCl_2(PPh_3)_2$ and 2M

aqueous Na_2CO_3 in DMF/ethanol at 50 ºC for 5 h; however **19** was furnished in only 43% yield after purification [Scheme 2.3].



Scheme 2.3: *Reagents and conditions:* i) $Pd(OAc)_2$ (0.1 mol%), H_2O, KOH, 20 → 75ºC, 6 h; ii) $PdCl_2(PPh_3)_2$, 2M aq. Na_2CO_3, DMF/EtOH, 50 ºC, 5 h.

The last step towards the synthesis of **P00337** was accomplished *via* Knoevenagel condensation of aldehyde **19** with thiobarbituric acid **12** in water at 80 °C [Scheme 2.4]. Sonification was required for the reaction to proceed, which may have been due to the low solubility of the aldehyde in water. Trituration with cold Et_2O furnished the pure compound **P00337** in 88% yield.

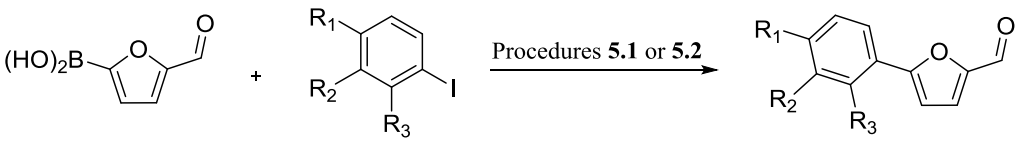


Scheme 2.4: *Reagents and conditions:* i) H_2O, 80 ºC,))).

Thus, thiobarbituric acid **P00337** was prepared according to a modified literature procedure in 69% yield over four steps from furfuraldehyde.

2.2.4 Synthesis of P00337 Analogues and Further Optimisation of the Synthetic Procedure

With a route to hit compound **P00337** established, attention was turned to synthesizing a panel of analogues. Initially, boronic acid **17** was subjected to Suzuki-Miyaura couplings with a series of commercially available aryl iodides (Figure 2.11). The aryl iodides were accordingly selected to investigate SAR *via* systematic variation/removal of functional groups on the arene. With the polar aryl iodides, reactions were performed under the described ligandless Suzuki-Miyaura coupling condition in water (Procedure 5.2).[81] Whereas, the water



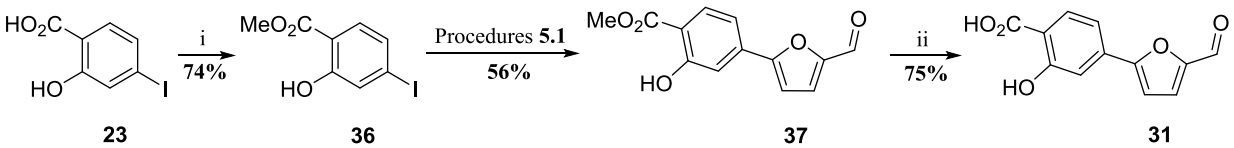
Aryl halide	R_1	R_2	R_3	Procedure	Product	Yield (%)
20	H	H	Me	5.1	**28**	86
21	Me	H	H	5.1	**29**	74
22	CO_2H	H	H	5.2	**30**	52
23	CO_2H	OH	H	5.2	**31**	75
24	H	H	H	5.1	**32**	84
25	OH	H	H	5.1	**33**	88
26	H	CO_2H	H	5.2	**34**	52
27	H	H	CO_2H	5.2	**35**	54

Figure 2.11: Preparation of 5-arylfuran-2-carbaldehydes *via* Suzuki-Miyaura couplings. *Reagents and conditions*: Procedure 5.1 – $Pd(OAc)_2$ (0.3 mol%), TBAI, Na_2CO_3, 50% aq. EtOH, rt; Procedure 5.2 – $Pd(OAc)_2$ (0.1 mol%), H_2O, KOH, 20 to 75ºC.

insoluble and base-labile aryl halides required different reaction conditions and were successfully coupled *via* ligandless Suzuki-Miyaura coupling using a phase-transfer catalyst (Procedure 5.1).[82] The crude products were then purified by flash chromatography to afford compounds **28** to **35** in yields ranging from 52-88%. From mechanistic studies, it has been suggested that the boron reagent possibly first reacts with the base to give the corresponding

boronate, which functions as the nucleophile.[83] Sodium carbonate was selected as the base, to avoid the need for acidification during workup, thereby preventing acid-catalysed polymerisation of products.[84] In this system the aryl halide and the palladium catalyst in the organic phase are partitioned from the boronate salt in the aqueous layer. The phase transfer catalyst, tetrabutylammonium iodide, enables reactions between the anions in the aqueous phase and the organic substrates of the organic phase.[83]

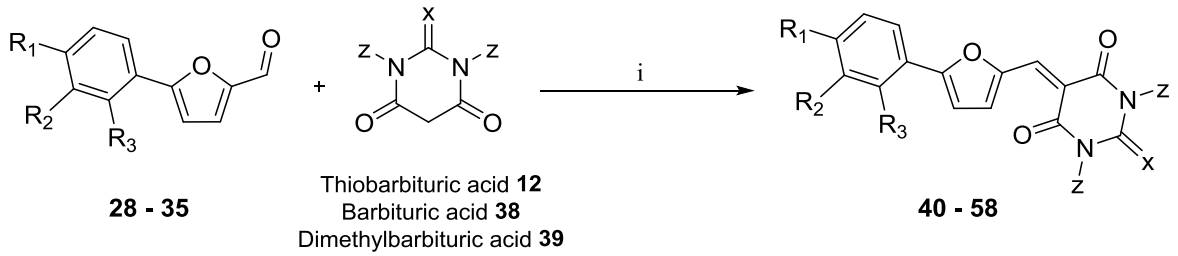
The Suzuki reactions for the non-polar aryl halides were relatively higher yielding than the procedure for the polar reagents. The low yield of polar aryl halides was a result of poor mass return attributed to low solubility of the aryl iodide and possible degradation during the reaction. Therefore, in an effort to increase the yield of compound **31**, it was decided first to synthesize the methyl ester derivative of this compound in order to enhance solubility of the starting material in organic solvent, and then subject it to the second described Suzuki reaction, followed by hydrolysis to return the carboxylate moiety [Scheme 2.4]. Methyl ester **36** was obtained in good yield by treatment of the corresponding carboxylic acid **23** with thionyl chloride and methanol. After the cross-coupling reaction, compound **37** was hydrolysed rapidly at ambient temperature using KOH in methanol;[85] the overall yield of **31** over three steps was 68% [Scheme 2.4].



23 **36** **37** **31**

Scheme 2.4: *Reagents and conditions:* i) thionyl chloride, MeOH, reflux overnight; Procedure 5.1) $Pd(OAc)_2$ (0.3 mol%), TBAI, Na_2CO_3, 50% aq. EtOH, rt; ii) KOH, MeOH, rt.

The last step towards the synthesis of **P00337** analogues involved the Knoevenagel condensation reaction of each aldehyde with barbituric acid, dimethylbarbituric acid and thiobarbituric acid. Barbituric acids were chosen to test the possibility of false positive results that may rise from the thiobarbituric acids, as C=S derivatives can act *via* oxidation pathways. The desired **P00337** analogues **40** to **58** were gained in good to excellent yields (76 to 97%) (Figure 2.12).[86] Trituration with cold Et_2O afforded the pure compounds, which were subsequently evaluated for their inhibitory activity against a panel of PTPs.



No.	R_1	R_2	R_3	X	Z	Yield (%)
P00337	OH	CO_2H	H	S	H	88
40	H	H	Me	S	H	96
41	H	H	Me	O	H	100
42	CO_2H	OH	H	S	H	88
43	CO_2Me	OH	H	S	H	24
44	Me	H	H	O	H	96
45	Me	H	H	O	Me	65
46	Me	H	H	S	H	65
47	H	H	H	O	H	60
48	H	H	H	O	Me	78

No.	R_1	R_2	R_3	X	Z	Yield (%)
49	H	H	H	S	H	88
50	OH	H	H	O	H	96
51	OH	H	H	O	Me	89
52	OH	H	H	S	H	83
53	CO_2H	H	H	O	H	97
54	CO_2H	H	H	O	Me	82
55	CO_2H	H	H	S	H	76
56	H	CO_2H	H	O	H	86
57	H	CO_2H	H	O	Me	95
58	H	CO_2H	H	S	H	92

Figure 2.12: *Reagents and conditions:* i) H_2O, 80 ºC.

2.3 Biological Testing

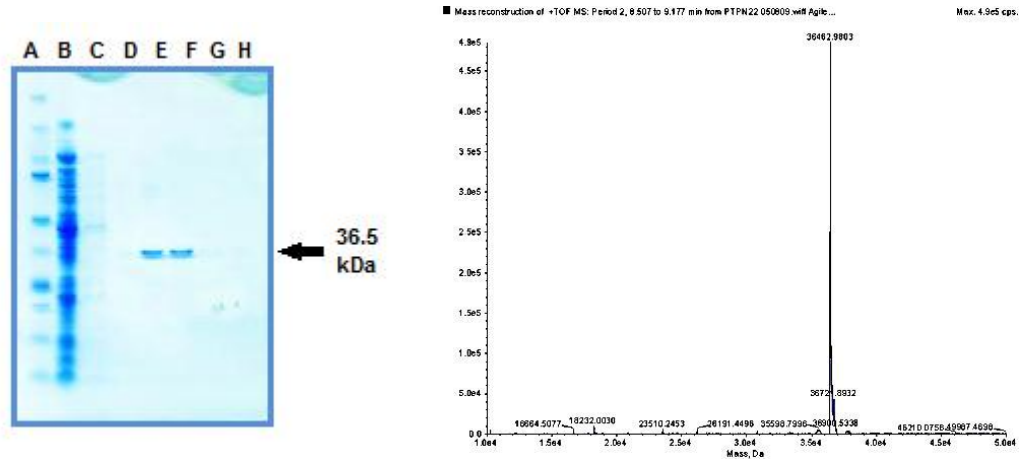
The synthesised compound **P00337** and its analogues were tested for inhibitory activity against tyrosine phosphatase PTPN22 using two PTP assays optimised for this enzyme. The assays employed included the malachite green and the *p*-nitrophenyl phosphate assay. To investigate selectivity, the activity of these compounds was also tested against four other PTPN22-related PTPs (PTP1B, PTPN5, PTPN13 and PTPRT). The latter four proteins were obtained in the purified state from a commercial supplier, whereas recombinant PTPN22 was prepared and purified in house.

2.3.1 Enzyme Purification

The purification of PTPN22 was undertaken at the Structural Genomic Consortium. The PTPase catalytic domain of PTPN22 used in the assays was expressed as a hexa-His-tagged construct in *E. coli rosetta* strains. The cells were grown in the Luria-Bertani growth culture media and homogenized. The *E. coli* cells expressing the PTPase construct were collected by low speed centrifugation and the resulting cell pellet was lysed using a sonicator.

The lysate obtained was purified *via* a standard protocol utilising nickel affinity resins to selectively bind the His-tagged constructs and separate them from other cell lysates.[87] Elution with binding buffers followed by dialysis afforded the recombinant protein.

The protein's purity was evaluated using SDS-PAGE analysis (figure 2a). Coomassie staining and a Western blot probed with an anti-His primary antibody revealed the desired ~37 kDa PTPase construct with only traces of impurities. The protein was further concentrated and rid of any impurities by gel filtration column chromatography and its identity confirmed *via* mass spectrometry (figure 2b, M_r = 36469.2 Da). The concentration of the protein was calculated as 7.46 mg/ml using a Nanodrop spectrophotometer.



a **b**

Figure 2.13: a) SDS-PAGE gel fragment showing the bands of PTPN22 obtained after elution with different buffers. The first band (A) is the standard marker and the second (B) is the flow-through with many impurities. The third (C) and fourth (D) bands are the fractions eluted out with different buffer concentrations. The two dark bands (E + F) signify the presence of PTPN22 in the elution fractions which were washed using elution buffers containing 150mM imidazole and 250mM imidazole, respectively; the last two bands (G + H) are fractions of wash buffer. b) The peak observed in the mass spectrometer corresponding to the molecular weight of PTPN22 PTPase construct (observed mass 36462.9 Da).

2.3.2 Biological Assay Development and Optimization

An assay is defined by a set of reagents that produce a detectable signal allowing a biological process to be quantified. In general, the quality of an assay is defined by the robustness and reproducibility of this signal in the absence of any test compounds or in the presence of inactive compounds. This robustness will depend on the type of signal measured such as absorbance or fluorescence, reagents, reaction conditions and analytical instrumentation employed.

PTPs are defined by their enzymatic activity that catalyses the dephosphorylation of phosphotyrosine residues. Several assays have been developed to detect the hydrolytic

activity of PTPs, determine the rate of dephosphorylation and kinetic constants k_{cat} and K_m. In addition they are used to characterise natural and recombinant PTPs, to elucidate the biological function of PTPs and in both the identification and validation of specific PTP inhibitors. PTPs tend to lose their substrate specificity once they are out of the cellular environment and most assays take advantage of this fact and employ generic synthetic surrogate substrates such as *p*-nitrophenyl phosphate (*p*-NPP),[88] phosphotyrosine,[89] and phosphotyrosyl-containing peptides.[63,90] As a family of enzymes, phosphatases have diverse optimal conditions and the parameters of assays have to be optimised for each PTP. For example, the pH optima of phosphatases are substrate-dependent and there is no one universal buffer systems for the PTP assays.

Two independent protein tyrosine phosphate assays, the malachite green and the *p*-NPP assay protocols, were optimised with recombinant PTPN22 to test the inhibitory activities of the synthesised compounds. Both methods are based on the same principle of measuring the phosphatase enzymatic activity, which involves hydrolysis of a PTP substrate generating a dephosphorylated substrate and free inorganic phosphate. However, they differ in the method of measuring the concentration of the enzymatic products. In the malachite assay, a malachite green reagent forms a green coloured complex with free phosphate that can be quantified by measuring its absorbance at 620 nm, whereas in the *p*-NPP assay absorbance of the dephosphorylated substrate is measured at 405 nm.

The parameters optimised in these assays ranged from the pH to the concentrations of the individual reagents used in each protocol.

2.3.3 *p*-Nitrophenyl phosphate Assay

p-Nitrophenyl phosphate **59** (*p*-NPP) is a chromogenic non-proteinaceous, non-specific substrate for most phophatases. In the presence of the enzyme, the substrate dephosphorylates

to yield colourless *para*-nitrophenol **60**, which forms an intense yellow soluble *p*-nitrophenolate anion **61** under alkaline conditions and can be conveniently quantified at 405 nm on a spectrophotometer (Figure 2.14). This homogeneous "mix-and-measure" assay involves simply adding a single reagent to the phosphatase and measuring the product formation using any absorbance reader.

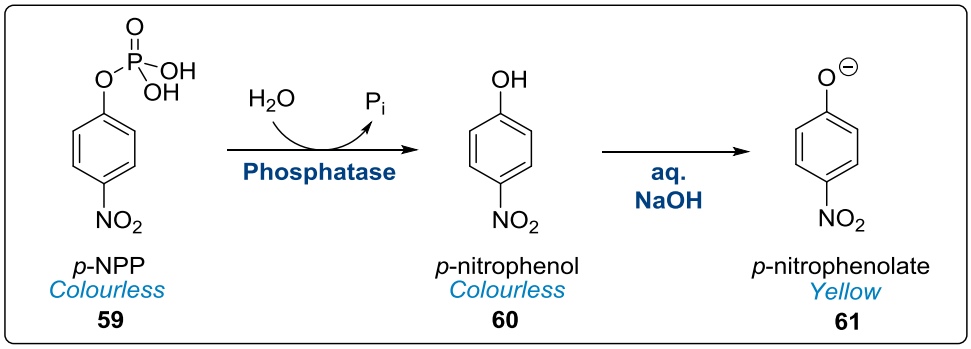


Figure 2.14: Principle of the *p*-nitrophenyl phosphate (*p*-NPP) PTP assay.

A standard *p*-NPP assay had been previously optimised with purified recombinant PTPN22.[91] The assay buffer consisted of 18.2 mM of the buffering agent, HEPES, and 90.9 mM NaCl adjusted to PTPN22 optimal pH of 7.5. The enzyme dilution buffer also contained 5 mM HEPES, 50 mM NaCl and 5 mM of a strong reducing agent, DTT, all dissolved in deionised water. It is critical that the substrate is in excess, so that PTP activity can be measured in the linear range of the assay. Similarly, the concentration of the PTP should be high enough to observe detectable hydrolysis in a reasonable time but is still in a linear range with excess substrate. The ideal substrate and enzyme concentrations have been determined experimentally to be 2 mM and 500 nM, respectively. The compounds tested were dissolved in DMSO to give a final concentration of 50 µM. The protocol required the preparation of reaction premixes in a 96-well plate, which included 16.5 µL of assay buffer, 6 µL of enzyme and 1.5 µL of each compound to be tested for inhibitory activity against the PTPs. The reaction was initiated by the addition of *p*-NPP (6 µL) and allowed to incubate for 60 minutes.

Aqueous sodium hydroxide solution (60 µL of 0.5M) was then added to terminate the reaction. The absorbance of each well was read at 405 nm in a Spectramex plate reader. Absorbance is proportional to free phosphate released, which is dependent on the phosphatase activity. Therefore, decreased phosphatase activity is proportional to increased inhibition.

In addition, it is critical for all PTP assays to include negative and positive controls: negative controls to determine non-specific background activity; and positive to confirm that the assay performed as intended.[92] Both control wells included all contents of the reaction, excluding a synthesised test compound for the positive control and both test compound and the PTP enzyme for the negative. Another reference negative control was obtained *via* the use of the common broad non-specific PTP inhibitor, vanadate.

2.3.4 Malachite Green Assay

The malachite green PTP assay is based on the *in vitro* colorimetric determination of protein tyrosine phosphatase (PTP) activity. Orthophosphate **64**, liberated from a phosphorylated substrate upon cleavage by the phosphatase, forms a bright green complex with ammonium molybdate/malachite green dye in an acidic buffer, absorbing at 620-650 nm (Figure 2.15). Accordingly the amount of released inorganic phosphate can be determined by measuring the absorbance of the molybdate/malachite Green/phosphate complex, thereby quantifying the hydrolysis activity of PTPs.[93]

The malachite green assay first developed by Lanzetta *et al.* was optimised with the purified recombinant PTPN22 and specific conditions were empirically determined.[94] According to this procedure, the substrate used was the synthetic phosphopeptide, tyrosine phosphopeptide-2 DADE(py)LIPQQG, and was diluted with phosphate-free water to give the final assay concentration of 20 µM, and the enzyme (PTPN22) had to be diluted using an enzyme dilution buffer (50 mM HEPES, 1 mM EDTA, 1 mM DTT (pH 7.2)) to give the final assay of

0.13 µM. The protocol required the addition of 10 µL of phosphate-free water, 2 µL of inhibitor, the peptide substrate, 5 µl of assay buffer (100 mM HEPES, 2 mM EDTA, 2 mM DTT at pH 7.2), 0.001% Tween-20 detergent, followed by the enzyme to each well. After an incubation period of 10 min the reaction had to be quenched using 50 µL of the malachite green/ammonium molybdate dye complex, and an absorbance reading taken at the wavelength of 620 nm after another incubation period of 10 min.

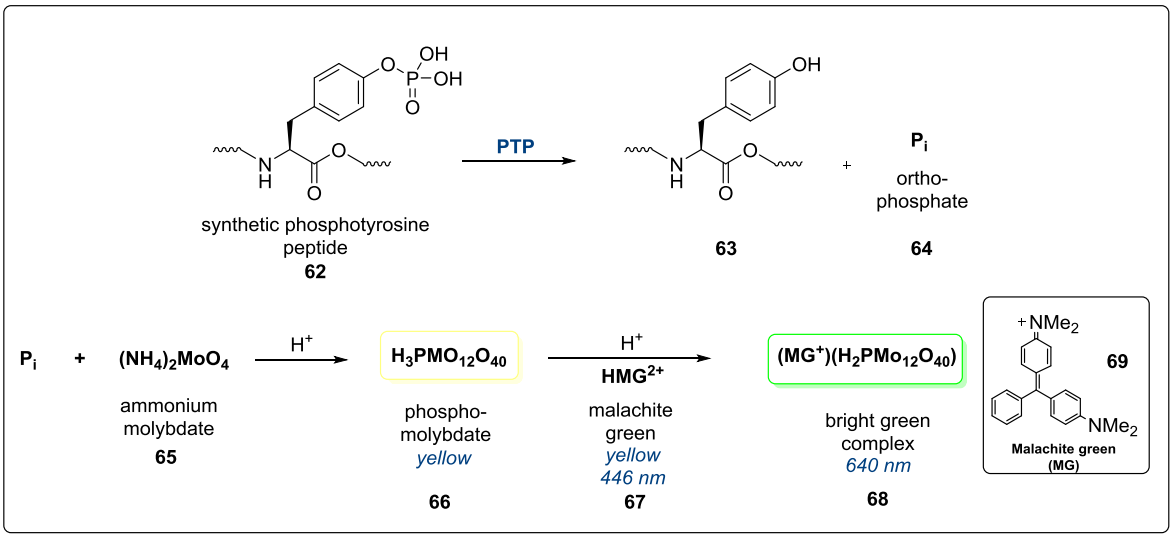


Figure 2.15: Principle of Malachite Green PTP assay.

Free phosphate can be found in a number of laboratory reagents, solvents and glassware. As this highly sensitive assay is based on measuring released inorganic phosphate, any contamination with phosphate will produce high background interference. It was therefore critical that all the reagents and the buffer solutions used were tested to have minimal phosphate contamination. Testing the background noise level of all solvents and buffers (Figure 2.16) revealed that Millipore water had the lowest phosphate contamination compared to solvents A and B and was thus used thereafter for the preparation of all the buffers and substrate dilutions for the assay. The optical density (OD) values of the positive control were in the lower, less sensitive range of the phosphate standard curve and there was only a two-fold difference between the negative and positive controls, which all indicated that the

substrate and enzyme concentration had to be increased to a range that produced a substantially higher signal than the background activity.

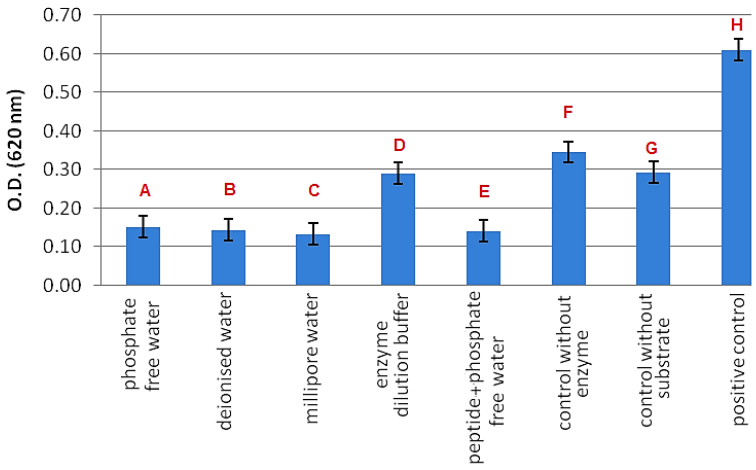


Figure 2.16: Determination of the background phosphatase activity and dynamic range of assay. 50 µL of malachite green ammonium molybdate dye solution (dye) was added to each sample. All controls were in phosphate free water. The data were measured in duplicate and are presented as mean value ± SD, N=1.

To establish the optimal enzyme concentration, a series of the enzyme concentrations were tested (Figure 2.17). The results showed that all concentrations showed very similar activity against a range of substrate concentrations and therefore the lowest enzyme concentration (0.13 µM) was chosen.

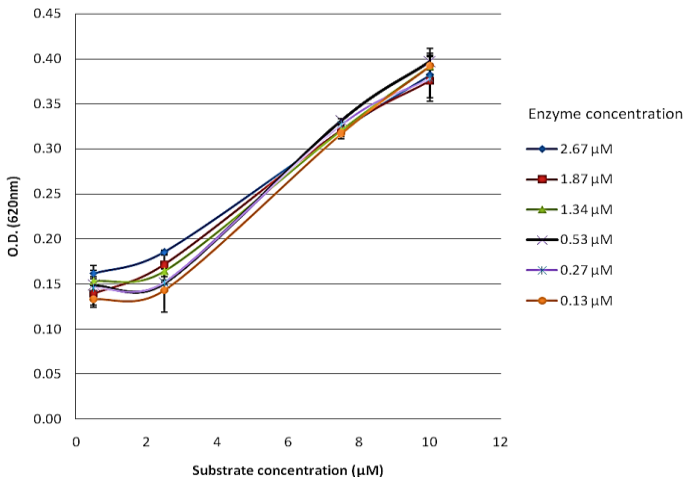


Figure 2.17: Determination of optimal enzyme concentration at pH 7.2. The data are presented as mean value ± SD, N=1.

The optimal substrate concentration using 0.13 µM of PTPN22 at pH 7.2 was determined to be 20 µM. The graph of substrate concentration versus optical density showed that the maximum activity of the enzyme was achieved at a substrate concentration of 50 µM and displayed a bell shaped curve (a classical "Hook" effect) (Figure 2.18 a).[95] The drop off in activity at high substrate concentrations may be attributable to many factors including, for instance, substrate inhibition and protein aggregation. The dose-response curve was used to establish the highest concentration of substrate that can be used before activity decreased (Figure 2.18 b).

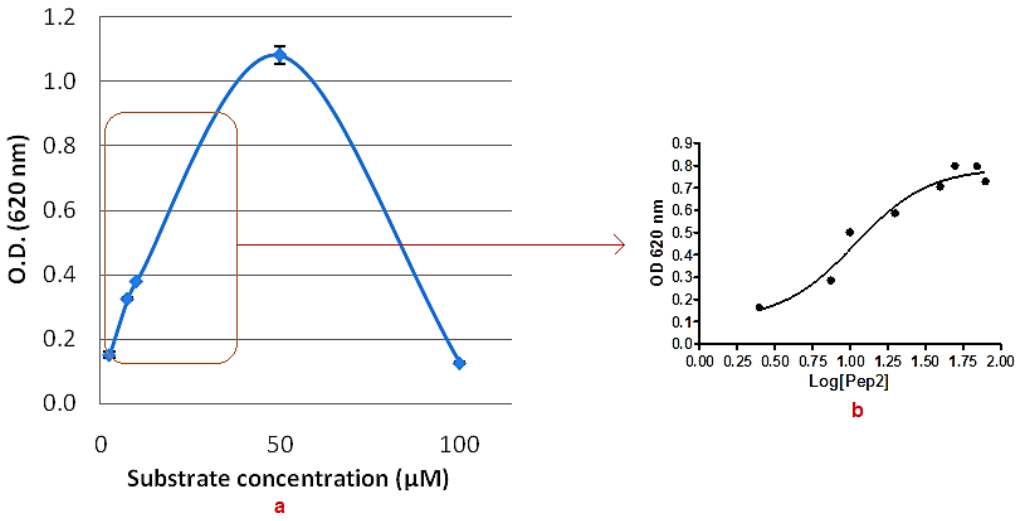


Figure 2.18: a) Determination of optimal substrate concentration using 0.13 µM of PTPN22 at pH 7.2. The data are presented as mean value ± SD, N=1; b) Dose-response curve to establish the upper limit of the substrate concentration before enzymatic activity decreased.

PTPN22 (0.13 µM) was incubated for different time periods with the phosphopeptide substrate (20 µM) to determine the time needed for the enzyme to dephosphorylate all available substrate (Figure 2.19 a). The incubation time required before the reaction was stopped by the dye complex was 30 min. In addition, the effective incubation time required for the maximum level of binding of free phosphates with the ammonium molybdate/malachite green complex was worked out to be 15 min (Figure 2.19 b).

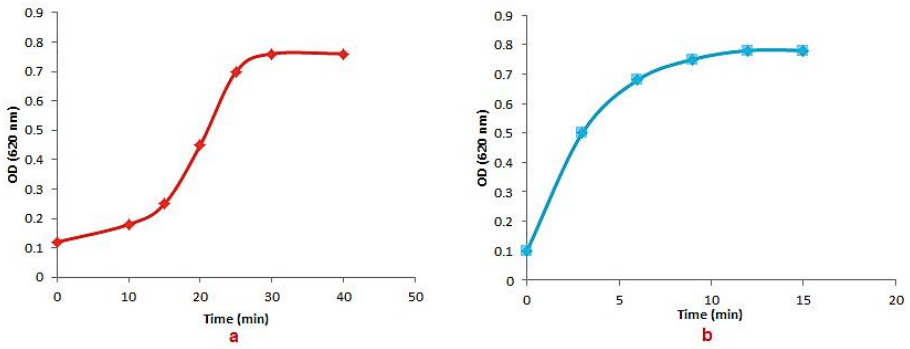


Figure 2.19: a) Time course of PTPN22 (0.13 µM) activity using phosphopeptide substrate (20 µM); b) establishment of the optimal time interval for reading OD after quenching the assay using optimal concentration of enzyme and substrate.

Finally, a standard phosphate curve was then constructed using standard phosphate solutions, by plotting the absorbance at 620 nm against concentration of phosphate. This plot was used to convert the detected OD value of each sample to the amount of phosphate released.

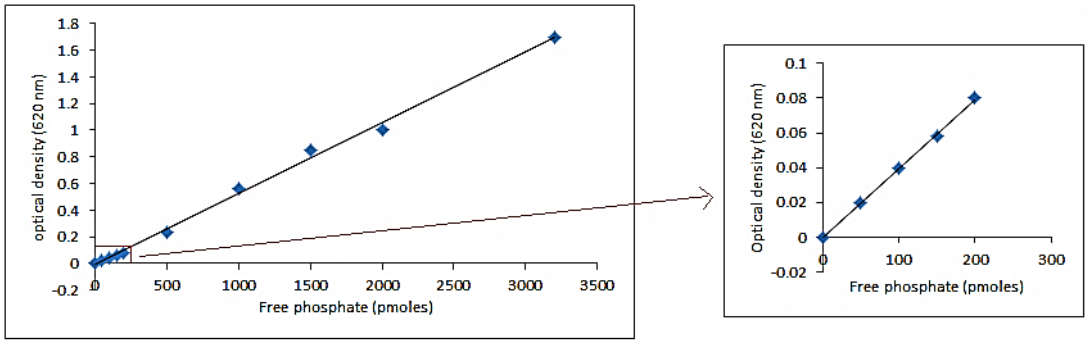


Figure 2.20: Phosphate standard assay curve; the curve was generated using the phosphate standard dilution chart supplied with the PTP assay kit (Promega).

With the two optimised PTP assays in hand, focus was turned to investigating the PTPN22 inhibitory activity of the synthesised compound **P00337** and its analogues.

2.4 Results and Discussion

2.4.1 Thiobarbituric Acid Analogues: Malachite Green Assay

The inhibitory activity of the synthesised thiobarbituric acid library along with some of the synthetic aldehydes and barbiturate precursors were initially tested against PTPN22 using the optimised malachite green protocol. The percentage activity for each of the **P00337** analogues against the PTPN22 enzyme was calculated using the following formula,

$$\textbf{Activity \%} = (A_T / A_C) \times 100$$

where A_T is absorbance of the tested analogue and A_C is the absorbance of the standard control. The results are displayed in Figure 2.21.

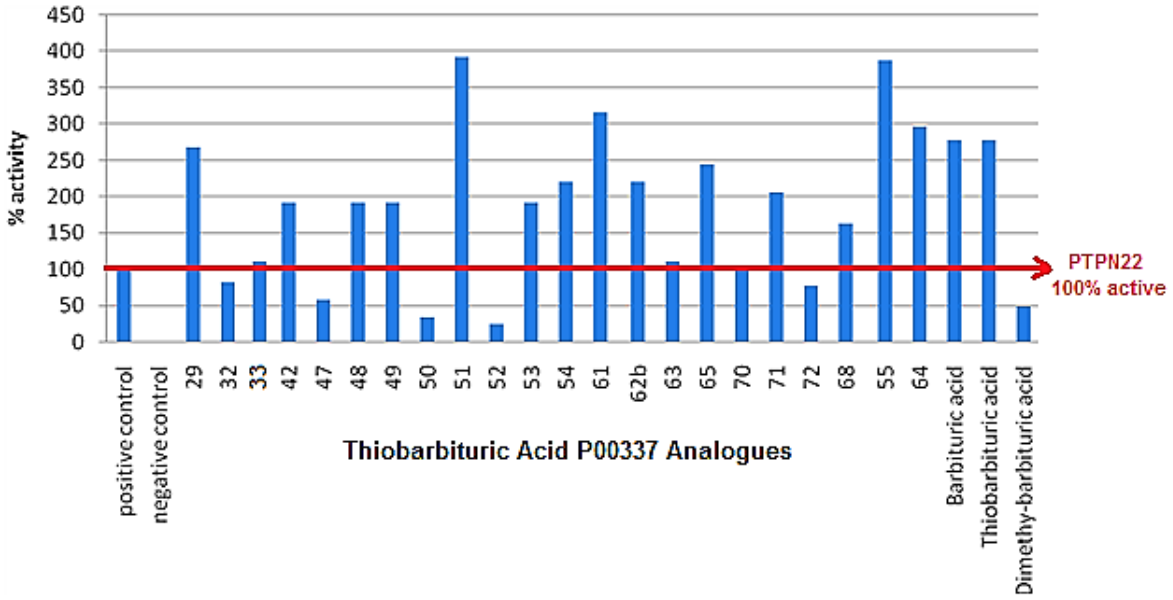


Figure 2.21: The percentage activity of compound **P00337** analogues against PTPN22 (0.13 µM) as determined by the optimised malachite green assay. Compounds tested at single point at 50 µM concentration.

From all of the analogues tested, compounds **47** and **49** displayed significant inhibition against PTPN22, 64% and 74%, respectively (Table 2.1). Both compounds contain the unsubstituted benzyl moiety and both structures only differ by one atom in the barbiturate moiety (C=S *vs* C=O), with relatively similar activity. The dimethyl barbiturate analogue **48** however displays 3-folds higher activity (~ 400%) than the positive control (Table 2.2). The

precursor dimethylbarbituric acid **39** also seems to have caused a decrease in the enzymatic activity of PTPN22 by 50%.

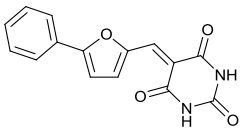
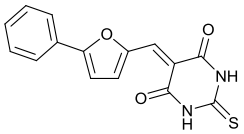
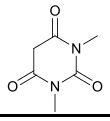
Entry	ID	Structure	% Inhibition of PTPN22
1	**47**		64
2	**49**		74
3	**39**		50

Table 2.1: The percentage inhibition for three of the compound **P00337** analogues against PTPN22 as determined by the malachite green assay.

The highly reactive aldehyde synthetic precursors, the thiobarbituric and the barbituric acid precursors, all displayed an increased activity of up to two-fold more than the positive control (Table 2.2). Although the precursor dimethylbarbituric acid **39** caused 50% inhibition of PTPN22 enzymatic activity, all compounds containing this moiety displayed an increased activity of up to 3-fold relative to the control (Table 2.2).

This observed 'overactivity' can be due to a number of factors; the compounds tested could have inhibited enzyme aggregation and thereby enhanced the dephosphorylation activity of the "free enzyme". This hypothesis should further be tested by disrupting possible enzyme aggregates with different concentrations of a detergent (such as Tween-20 used in this assay) and observing the effect on enzymatic activity in the presence and absence of the test compounds.

Although some compounds are coloured (in particular, yellow), the possibility of the compounds acting as false negatives due to their inherent colour had been ruled out, as there

would be negligible background absorption at the concentrations tested in the assay. This has also been demonstrated independently through measuring absorbance of compounds alone in buffer.[96]

Consequently, in order to determine the reproducibility of the results and to confirm the inhibitory activity of compounds **47** and **49** against enzyme PTPN22, all compounds were subjected to the optimised *p*-NPP assay.

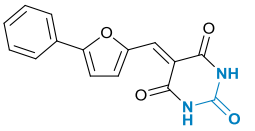
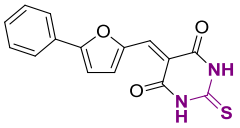
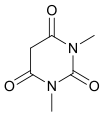
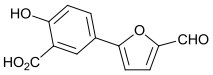
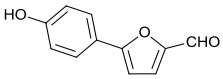
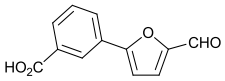
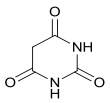
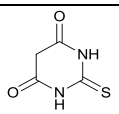
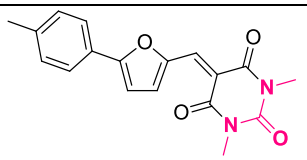
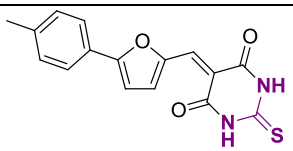
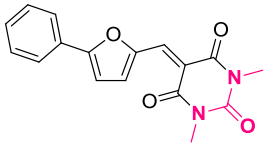
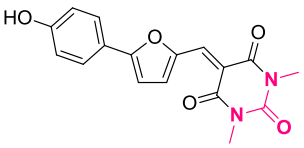
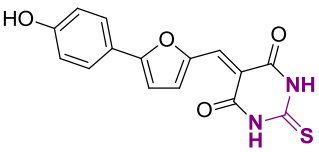
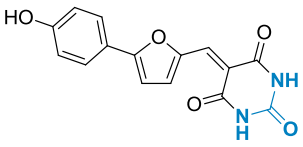
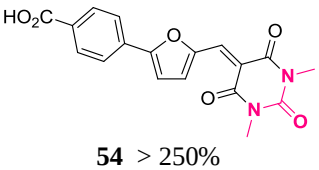
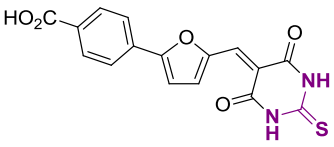
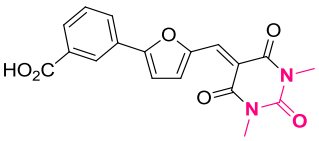
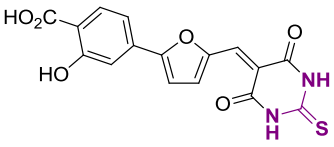
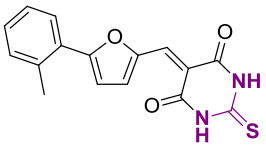
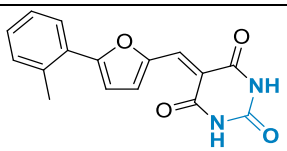
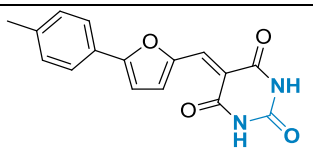
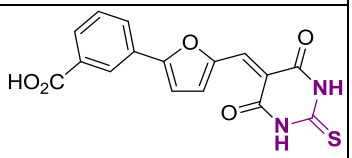
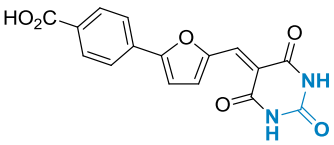
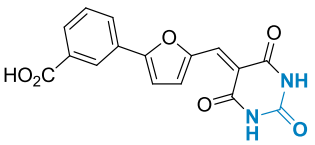
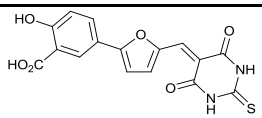
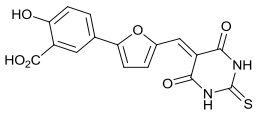
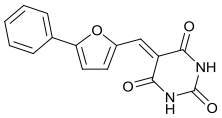
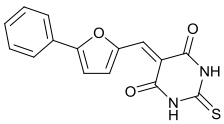
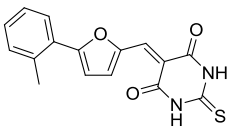
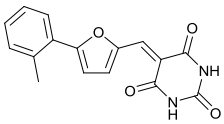
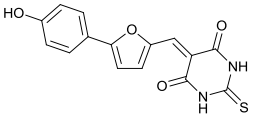
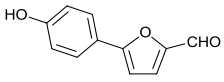
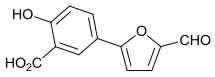
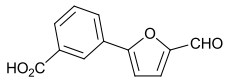
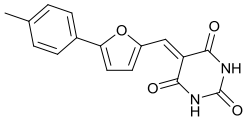
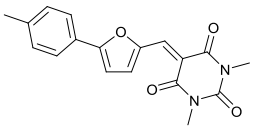
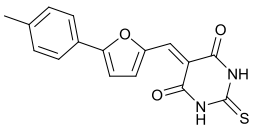
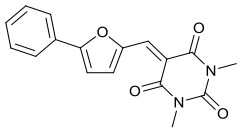
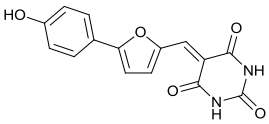
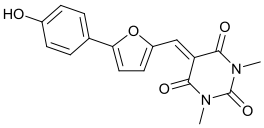
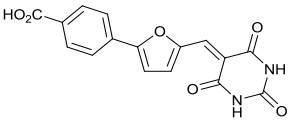
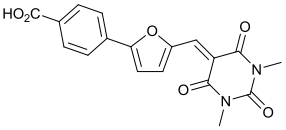
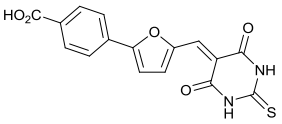
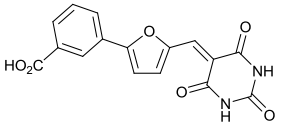
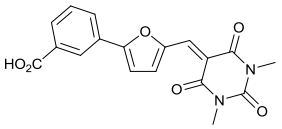
Compounds with significant inhibitory activity	 **47** - 64%  **49** - 74%  **39** - 50%
Synthetic precursors displaying increased activity by one fold or more	 **19** ~ 200%  **33** ~ 300%  **34** ~ 250%  **38** > 250%  **12** > 250%
Analogues that displayed up to three-fold increase in activity relative to the positive control	 **45** ~ 200%  **46** ~ 200%  **48** ~ 400%  **51** ~ 200%  **49** ~ 400%  **50** ~ 200%  **54** > 250%  **55** ~ 250%  **57** ~ 200%  **42** ~ 200%  **40** > 250%
Analogues displaying weak or no inhibitory activity	 **41** ~ 20%  **44** ~ 45%  **58** ~ 20%  **53** no effect  **56** no effect

Table 2.2: The percentage activity of **P00337** analogues tested against PTPN22 using the malachite green assay.

2.4.2 Thiobarbituric Acid Analogues: *p*-Nitrophenyl Phosphate Assay

The inhibitory activity of the synthesised thiobarbituric acid library was further tested against PTPN22 using the optimised *p*-NPP protocol. They were also tested against four other related PTPs (PTPN13, PTPN5, PTP1B and PTPRT) to investigate the selectivity of these compounds. In addition, the IC_{50} values were calculated from direct regression curve analysis for the synthesised analogues and the resynthesized compound **P00337** (Table 2.3).

		IC_{50} (µM)				
ID	**Structure**	**PTPN22**	**PTPN13**	**PTPN5**	**PTP1B**	**PTPRT**
P00337a		5.5	nt	8.5	5.6	8.9
P00337		343	640	Nd	456	483
47		2282	129	294	nd	nd
49		543	309	206	1073	823
40		852	550	262	nd	1501
41		420	114	189	nd	nd
52		438	838	184	799	nd
33		nd	nd	nd	nd	nd

19		nd	nd	nd	nd	nd
34		nd	nd	nd	nd	nd
44		444	229	215	nd	2045
45		344	159	116	584	207
46		nd	191	131	371	569
48		nd	nd	nd	nd	nd
50		220	102	196	886	nd
51		nd	nd	563	nd	nd
53		573	604	nd	nd	1056
54		684	1719	nd	nd	nd
55		305	184	nd	760	757
56		567	365	nd	661	nd
57		1266	1216	nd	nd	nd

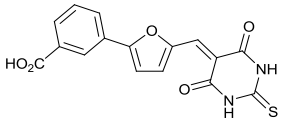
58		363	229	nd	397	718

Table 2.3: IC_{50} values obtained using the *p*-NPP assay for **P00337** analogues tested against PTPN22, PTPN5, PTP1B, PTPN13 and PTPRT. Results which could not be assessed due to high ambiguity have been marked as "nd"= not determinable, values too high.

The first unexpected result observed was the difference in the IC_{50} values of the resynthesized **P00337** against the set of PTPs and the values reported for the original 'hit' compound from the library used in the high-throughput screening (Table 2.3). The IC_{50} value of the resynthesized compound against PTPN22 for example is more than sixty times higher than that reported for the 'hit' compound (343 μM *vs* 5.5 μM). One explanation could be that the commercially sourced molecule **P00337** could have degraded over time and it was the fragmented product that displayed the high inhibitory activity against PTPN22 and its related PTPs. It was thought that the data from the synthetic precursors could clarify this ambiguity; however, these compounds also exhibited no inhibitory effect. Another theory was that the compound was not completely pure and contained a contaminant which was active against the PTPs tested.

Unfortunately, the rest of the data obtained *via* this assay were also not consistent with the data obtained from the malachite protocol. For example, compound **47** showed 64% inhibition of PTPN22 enzymatic activity in the malachite green assay, whereas when tested against the same protein using the *p*-NPP protocol a substantially high IC_{50} of more than 2mM was observed, indicating that the compound is not a very effective inhibitor. Similarly, compound **50** seemed to have almost doubled the PTPN22 enzymatic activity in the malachite assay, but displayed a moderate inhibitory activity (IC_{50} = 220 μM) against the same enzyme in the *p*-NPP assay.

The paradoxical results obtained from the two optimised assays could be due to an inherent discrepancy in the protocols. In addition, both of the assay conditions employed varied in the constitution of the dilution buffers, substrate and the pH at which they were performed, which can certainly cause the enzyme to behave differently. Thus, standardization between the two protocols is of paramount importance and may resolve the inconsistencies observed in the obtained data. This is also reflected in another set of conflicting results from both assays presented in table 2.4. However, for a single assay protocol SAR trends within compound series could be interpreted: the SAR of the resynthesized hit and both of its direct analogues **52** and **58**, were as follows:

- removal of the hydroxyl group from the aryl moiety does not have a significant effect on the inhibitory activity of compound **P00337**;
- the carboxylic acid functionality is preferred for the inhibitory activity of the hit compound, as its removal in compound **52** has resulted in a reduction in inhibition of PTPN22 compared to both **P00337** and **52**;
- elimination of the thiobarbiturate from the hit structure in analogue **19**, abolishes all inhibitory action of this compound, indicating this moiety is responsible for the activity of the hit against PTPN22. N-methylation also ablates inhibitory activity (e.g. **50** *vs* **51**).

Furthermore, it is envisaged that if the test compounds are exerting their inhibitory effects by acting directly on the enzyme, a similar effect would be observed using another assay utilizing the same enzyme (although the degree of inhibitory activity might be different due to, for example, the difference in concentration of the enzyme used). However, although in the *p*-NPP assay both compounds **52** and **58** acted as inhibitors, in the malachite green assay, **52** acts as an inhibitor of enzyme PTPN22, whilst **58** enhanced the enzymatic activity. Consequently, it can be suggested that the compounds could be interfering with the other

constituents of the assay such as the substrate or the malachite dye, thereby affecting the absorbance data recorded by acting as a false positive or negative.

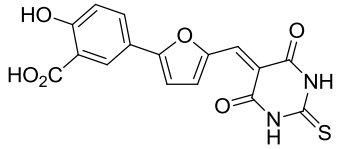
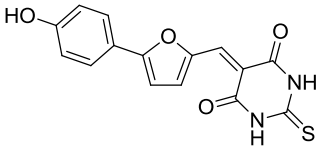
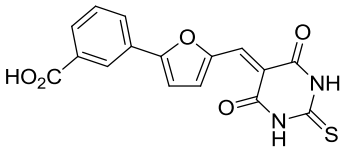
ID	Structure	*p*-NPP assay IC_{50} (μM)	Malachite green assay (% activity relative to positive control)
P00337		343	-
52		438	20
58		363	400

Table 2.4: Conflicting results for compounds **P00337, 52** and **58** from the *p*-NPP and the malachite green assay utilising PTPN22.

Furthermore, the **P00337** analogues similar to the hit compound displayed no significant selectivity against the PTPs tested. The difficulty of achieving selectivity for the PTP of interest is one of the major factors that has led to the failure of many studied PTP inhibitor candidates from reaching the clinic.[60,97]

In conclusion, amongst all the compounds tested in the *p*-NPP assay, only a few exhibited weak inhibitory activity against the enzyme PTPN22 (IC_{50} values ranging between 220 - 363 μM) (Table 2.3) and therefore SAR studies on this class of compounds using PTP assays were abandoned at this point and attention turned to an alternative compound series. However, their anti-tumour activity was further tested using a set of neuroblastoma cell lines (see section 2.4.3).

2.4.3 Neuroblastoma cell line assays

Studies by MacKeigan *et al.* have revealed that as much as 32% of the PTP family promote cell-survival signalling in cancer.[98] Consequently, these oncogenic PTPs are considered as potential therapeutic targets for many different cancers including neuroblastoma.

Stoker *et al.* conducted the first thorough analysis of the difference in the expression of PTP genes between normal nervous system tissues and a range of neuroblastoma cell lines (Figure Figure 2.22).[99] Their results revealed that at least 14 PTPs are overexpressed in one or more neuroblastoma cell lines versus brain, including *PTPRC*, *CDC25c* and *PTPN9* (Figure 2.22).[99]

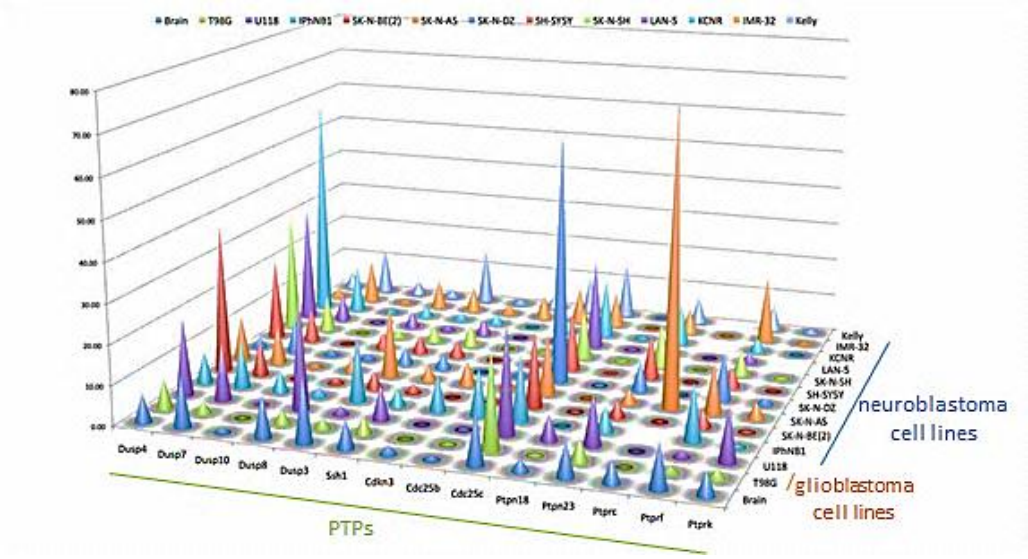


Figure 2.22: Highly expressed PTPs in neuroblastoma cell lines versus non-neoplastic neural tissue.[99]

Further studies by Stoker *et al.* revealed that the broad, non-selective PTP inhibitors vanadate and bis(maltolato)oxovanadium(IV) (BMOV), induce potent but selective apoptosis in significant number of tumour-derived neuroblastoma cell lines (Figure 2.23).[99] Therefore, development of selective, drug-like inhibitors targeting the specific PTPs overexpressed in neuroblastoma cells may provide a novel therapeutic route in treatment of this disease.

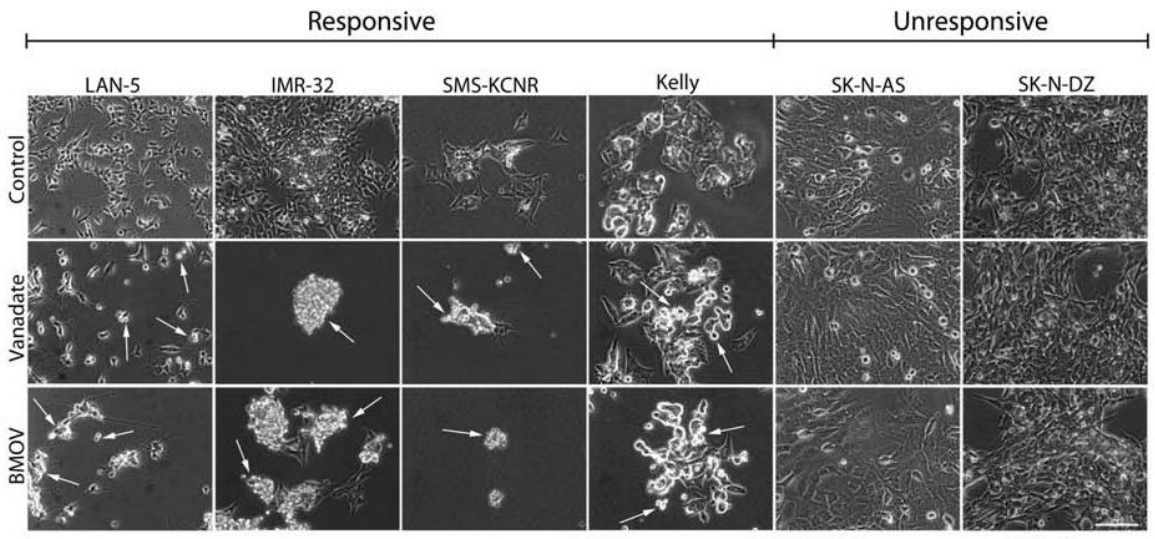


Figure 2.23: VA-induced cytotoxicity is shared with BMOV in distinct neuroblastoma cell lines (IMR-32, KCNR, Kelly), whereas other neuroblastoma cell lines (SK-N-DZ, SK-N-AS) are unresponsive to both inhibitors after the same treatment period (3-6 days)/dosage (10 μM).[99]

Thiobarbituric acid **P00337** was part of a drug-like compound library which was assembled using a pharmacophore mapping technique, employing common pharmacophores identified from known PTP inhibitors. Hence, it was envisaged that although this compound did not show any promising activity against PTPN22, it may inhibit the activity of other PTP oncogenes. The cytotoxicity of compound **P00337** and its analogues was then investigated by Stoker's group using the neuroblastoma cell line SH-N-SY.

2.4.3.1 Neuroblastoma Cell line Results

The effect of each **P00337** analogue was tested against the neuroblastoma cell line SH-N-SY at concentrations ranging from 5 μM to 200 μM, under standard culture conditions (see appendix for protocol). After the treatment period of 6 days, only compounds **P00337**, **52** and **58** caused considerable cell death at different concentrations (Table 2.5).

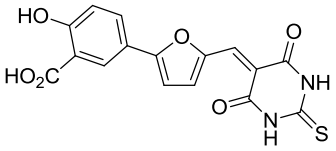
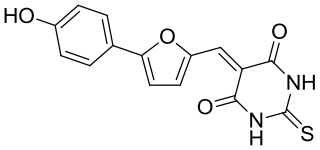
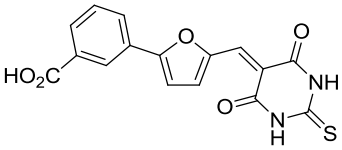
ID	Structure	Minimum Inhibitory Concentration (MIC, μM)	% of cells killed after 6 days @ MIC
P00337		20	100
52		5	90
58		50	40

Table 2.5: The percentage of cell death induced by compounds **P00337, 52** and **58** on SH-N-SY neuroblastoma cell line after the treatment period of 6 days at concentrations stated.

The specificity of the cytotoxic compounds was further investigated using another neuroblastoma cell line, LAN5 and a control cell line, 293T (cell line derived from human embryonic kidney cells) (Figure 2.24).

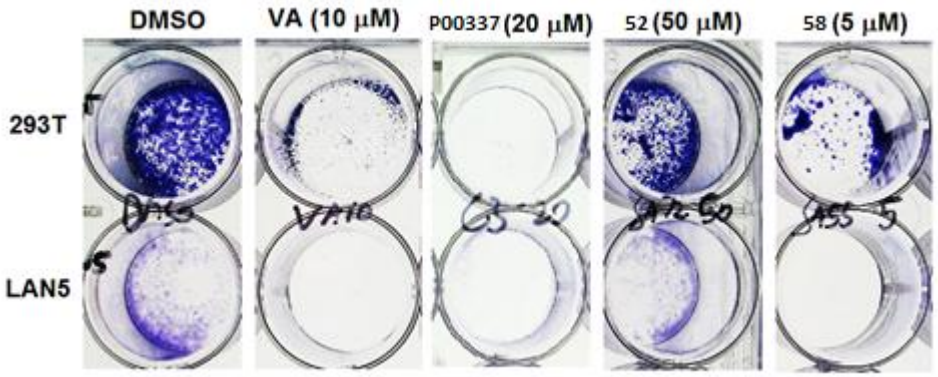


Figure 2.24: Compounds tested at MIC identified with cell line SH-N-SY. Compounds **P00337** (20 μM) and **52** (5 μM) induce cytotoxicity in an unselective manner against neuroblastoma cell LAN5 and the normal cell representative 293T. Compound **58** (50 μM) caused no cell death in either of the cell lines. VA = vanadate (a non-specifc PTP inhibitor used as control); DMSO used as control.

Compounds **P00337** and **52** exhibited no selectivity towards neuroblastoma cells as they displayed high cytotoxicity towards the control cell line 293T. Compound **58** showed no activity towards 293T and LAN5 cell lines, and therefore had moderate selective cytotoxicity in the SH-N-SY cells albeit at a relatively high concentration (50 μM).

Interestingly, PTP inhibitory activity correlated with neuroblastoma cytotoxicity, *i.e.* the three compounds that caused the highest cytotoxicity against SH-N-SY cells (**P00337**, **52** and **58**) were the compounds that caused the highest inhibition of PTPN22 enzymatic activity. However, further investigation is required to find out if the cytotoxicity caused by these compounds on the neuroblastoma cell lines is PTP-dependent.

2.5 Conclusion and Future Work

In conclusion, the weak inhibitory activity observed by the resynthesized compound **P00337** and its analogues against PTPN22, in addition to their display of promiscuous behaviour in different PTP assays confirmed that these compounds cannot qualify for further testing. Those compounds that displayed moderate PTP inhibitory activity also showed cytotoxic effects in neuroblastoma and non-tumour cell lines. Two of the examples showed similar activity in the two tumour cell lines and the non-tumour line tested (compounds **P00337** and **52**), and one showed some signs of selective toxicity towards the tumour cells (**58**).

The lack of success with the thiobarbituric acid **P00337** and its analogues prompted investigation of an alternative family of compounds identified as PTPN22 inhibitors in the original high-throughput screening (see chapter 3 - tetrahydroquinolines).

2.6 References

1. Tonks, N. K. *Nat. Rev. Mol. Cell Biol.* **2006**, *7*, 833-846.

2. Alonso, A.; Sasin, J.; Bottini, N.; Friedberg, I.; Osterman, A.; Godzik, A.; Hunter, T.; Dixon, J.; Mustelin, T. *Cell* **2004**, *117*, 699-711.

3. Andersen, J. N.; Jansen, P. G.; Echwald, S. M.; Mortensen, O. H.; Fukada, T.; Del Vecchio, R.; Tonks, N. K.; Moller, N. P. H. *FASEB J.* **2004**, *18*, 8-30.

4. Jiang, Z.-X.; Zhang, Z.-Y. *Cancer Metastasis Rev.* **2008**, *27*, 263-272.

5. Hunter, T. *Phil. Trans. R. Soc. B* **1998**, *353*, 583-605.

6. Cohen, P. *Nat. Rev. Drug Discovery* **2002**, *1*, 309-315.

7. Scott, L. M.; Lawrence, H. R.; Sebti, S. M.; Lawrence, N. J.; Wu, J. *Curr. Pharm. Des.* **2010**, *16*, 1843-1862.

8. Jacob, S. T.; Motiwala, T. *Cancer Gene Ther.* **2005**, *12*, 665-672.

9. Gupta, S.; Radha, V.; Sudhakar, C.; Swarup, G. *FEBS Lett.* **2002**, *532*, 61-66.

10. Salmeen, A.; Andersen, J. N.; Myers, M. P.; Tonks, N. K.; Barford, D. *Mol. Cell* **2000**, *6*, 1401-1412.

11. Zhang, Z. Y.; Thiemesefler, A. M.; Maclean, D.; McNamara, D. J.; Dobrusin, E. M.; Sawyer, T. K.; Dixon, J. E. *Proc. Natl. Acad. Sci. U. S. A.* **1993**, *90*, 4446-4450.

12. Kovalenko, M.; Denner, K.; Sandstrom, J.; Persson, C.; Gross, S.; Jandt, E.; Vilella, R.; Bohmer, F.; Ostman, A. *J. Biol. Chem.* **2000**, *275*, 16219-16226.

13. Soulsby, M.; Bennett, A. M. *Physiology* **2009**, *24*, 281-289.

14. Ostman, A.; Hellberg, C.; Bohmer, F. D. *Nat. Rev. Cancer* **2006**, *6*, 307-320.

15. Andersen, J. N.; Mortensen, O. H.; Peters, G. H.; Drake, P. G.; Iversen, L. F.; Olsen, O. H.; Jansen, P. G.; Andersen, H. S.; Tonks, N. K.; Moller, N. P. H. *Mol. Cell. Biol.* **2001**, *21*, 7117-7136.

16. Beltran, P. J.; Bixby, J. L. *Front. Biosci.* **2003**, *8*, D87-D99.

17. Mauro, L. J.; Dixon, J. E. *Trends Biochem. Sci.* **1994**, *19*, 151-155.

18. Zhang, M.; Stauffacher, C. V.; Lin, D. Y.; Van Etten, R. L. *J. Biol. Chem.* **1998**, *273*, 21714-21720.

19. Cosentino-Gomes, D.; Meyer-Fernandes, J. R. *Enzyme Inhibition and Bioapplications*; InTech, **2012**, 253-276.

20. Bastien, D. G.; Kramer, I. M.; Tatham, P. E. R. *Signal Transduction*; Academic Press Inc, **2009**, 20.

21. Tiganis, T.; Bennett, A. M. *Biochem. J* **2007**, *402*, 1-15.

22. Ruivenkamp, C. A. L.; van Wezel, T.; Zanon, C.; Stassen, A. P. M.; Vlcek, C.; Csikos, T.; Klous, A. M.; Tripodis, N.; Perrakis, A.; Boerrigter, L.; Groot, P. C.; Lindeman, J.; Mooi, W. J.; Meijjer, G. A.; Scholten, G.; Dauwerse, H.; Paces, V.; van Zandwijk, N.; van Ommen, G. J. B.; Demant, P. *Nat. Genet.* **2002**, *31*, 295-300.

23. Motiwala, T.; Jacob, S. T. *Prog. Nucleic Acid Res. Mol. Biol.* **2006**, *81*, 297-329.

24. Li, L.; Ross, A. H. *J. Cell. Biochem.* **2007**, *102*, 1368-1374.

25. Tamura, M.; Gu, J. G.; Danen, E. H. J.; Takino, T.; Miyamoto, S.; Yamada, K. M. *J. Biol. Chem.* **1999**, *274*, 20693-20703.

26. Hamada, K.; Sasaki, T.; Koni, P. A.; Natsui, M.; Kishimoto, H.; Sasaki, J.; Yajima, N.; Horie, Y.; Hasegawa, G.; Naito, M.; Miyazaki, J.; Suda, T.; Itoh, H.; Nakao, K.; Mak, T. W.; Nakano, T.; Suzuki, A. *Genes Dev.* **2005**, *19*, 2054-2065.

27. Freeman, D. J.; Li, A. G.; Wei, G.; Li, H.-H.; Kertesz, N.; Lesche, R.; Whale, A. D.; Martinez-Diaz, H.; Rozengurt, N.; Cardiff, R. D.; Liu, X.; Wu, H. *Cancer discovery* **2003**, *44*, 1368.

28. Chan, R. J.; Feng, G. S. *Blood* **2007**, *109*, 862-867.

29. Chan, G.; Kalaitzidis, D.; Neel, B. G. *Cancer Metastasis Rev.* **2008**, *27*, 179-192.

30. Neel, B. G.; Gu, H. H.; Pao, L. *Trends Biochem. Sci* **2003**, *28*, 284-293.

31. Tartaglia, M.; Gelb, B. D. *Eur. J. Med. Genet.* **2005**, *48*, 81-96.

32. Hardy, S.; Tremblay, M. L. *Curr. Oncol.* **2008**, *15*, 5-8.

33. Brummer, T.; Schramek, D.; Hayes, V. M.; Bennett, H. L.; Caldon, C. E.; Musgrove, E. A.; Daly, R. J. *J. Biol. Chem.* **2006**, *281*, 626-637.

34. Bentires-Alj, M.; Gil, S. G.; Chan, R.; Wang, Z. G. C.; Wang, Y. P.; Imanaka, N.; Harris, L. N.; Richardson, A.; Neel, B. G.; Gu, H. H. *Nat. Med.* **2006**, *12*, 114-121.

35. Stallings, R. L.; Nair, P.; Maris, J. M.; Catchpoole, D.; McDermott, M.; O'Meara, A.; Breatnach, F. *Cancer Res.* **2006**, *66*, 3673-3680.

36. Nair, P.; De Preter, K.; Vandesompele, J.; Speleman, F.; Stallings, R. L. *Genes Chromosomes Cancer* **2008**, *47*, 1023-1023.

37. Woodings, J. A.; Sharp, S. J.; Machesky, L. M. *Biochem. J* **2003**, *371*, 463-471.

38. Shang, X.; Vasudevan, S. A.; Yu, Y.; Ge, N.; Ludwig, A. D.; Wesson, C. L.; Wang, K.; Burlingame, S. M.; Zhao, Y. j.; Rao, P. H.; Lu, X.; Russell, H. V.; Okcu, M. F.; Hicks, M. J.; Shohet, J. M.; Donehower, L. A.; Nuchtern, J. G.; Yang, J. *Oncogene* **2010**, *29*, 4938-4946.

39. Jeffrey, K. L.; Camps, M.; Rommel, C.; Mackay, C. R. *Nat. Rev. Drug Discovery* **2007**, *6*, 391-403.

40. Bialy, L.; Waldmann, H. *Angew. Chem., Int. Ed.* **2005**, *44*, 3814-3839.

41. Umezawa, K.; Kawakami, M.; Watanabe, T. *Pharmacol. Ther.* **2003**, *99*, 15-24.

42. Tautz, L.; Pellecchia, M.; Mustelin, T. *Expert Opin. Ther. Targets* **2006**, *10*, 157-177.

43. Lazo, J. S.; Wipf, P. *Oncol. Res.* **2003**, *13*, 347-352.

44. Elchebly, M.; Payette, P.; Michaliszyn, E.; Cromlish, W.; Collins, S.; Loy, A. L.; Normandin, D.; Cheng, A.; Himms-Hagen, J.; Chan, C. C.; Ramachandran, C.; Gresser, M. J.; Tremblay, M. L.; Kennedy, B. P. *Science* **1999**, *283*, 1544-1548.

45. Schmidt, A.; Rutledge, S. J.; Endo, N.; Opas, E. E.; Tanaka, H.; Wesolowski, G.; Leu, C. T.; Huang, Z.; Ramachandaran, C.; Rodan, S. B.; Rodan, G. A. *Proc. Natl. Acad. Sci. U. S. A.* **1996**, *93*, 3068-3073.

46. Miski, M.; Shen, X.; Cooper, R.; Gillum, A. M.; Fisher, D. K.; Miller, R. W.; Higgins, T. J. *Bioorg. Med. Chem. Lett.* **1995**, *5*, 1519-1522.

47. Hasrat, J. A.; DeBruyne, T.; DeBacker, J. P.; Vauquelin, G.; Vlietinck, A. J. *J. Pharm. Pharmacol.* **1997**, *49*, 1145-1149.

48. Hamaguchi, T.; Sudo, T.; Osada, H. *FEBS Lett.* **1995**, *372*, 54-58.

49. Gunasekera, S. P.; McCarthy, P. J.; KellyBorges, M.; Lobkovsky, E.; Clardy, J. *J. Am. Chem. Soc.* **1996**, *118*, 8759-8760.

50. Sodeoka, M.; Sampe, R.; Kojima, S.; Baba, Y.; Usui, T.; Ueda, K.; Osada, H. *J. Med. Chem.* **2001**, *44*, 3216-3222.

51. Ye, B.; Akamatsu, M.; Shoelson, S. E.; Wolf, G.; Giorgettiperaldi, S.; Yan, X. J.; Roller, P. P.; Burke, T. R. *J. Med. Chem.* **1995**, *38*, 4270-4275.

52. Burke, T. R.; Ye, B.; Akamatsu, M.; Ford, H.; Yan, X. J.; Kole, H. K.; Wolf, G.; Shoelson, S. E.; Roller, P. P. *J. Med. Chem.* **1996**, *39*, 1021-1027.

53. Moran, E. J.; Sarshar, S.; Cargill, J. F.; Shahbaz, M. M.; Lio, A.; Mjalli, A. M. M.; Armstrong, R. W. *J. Am. Chem. Soc.* **1995**, *117*, 10787-10788.

54. Fu, H.; Park, J.; Pei, D. H. *Biochemistry (Moscow)* **2002**, *41*, 10700-10709.

55. Malamas, M. S.; Sredy, J.; Moxham, C.; Katz, A.; Xu, W. X.; McDevitt, R.; Adebayo, F. O.; Sawicki, D. R.; Seestaller, L.; Sullivan, D.; Taylor, J. R. *J. Med. Chem.* **2000**, *43*, 1293-1310.

56. Sohn, J.; Kiburz, B.; Li, Z. T.; Deng, L.; Safi, A.; Pirrung, M. C.; Rudolph, J. *J. Med. Chem.* **2003**, *46*, 2580-2588.

57. Liu, G.; Xin, Z. L.; Liang, H.; Abad-Zapatero, C.; Hajduk, P. J.; Janowick, D. A.; Szczepankiewicz, B. G.; Pei, Z. H.; Hutchins, C. W.; Ballaron, S. J.; Stashko, M. A.; Lubben, T. H.; Berg, C. E.; Rondinone, C. M.; Trevillyan, J. M.; Jirousek, M. R. *J. Med. Chem.* **2003**, *46*, 3437-3440.

58. Barr, A. J. *Future Med. Chem.* **2010**, *2*, 1563-1576.

59. Zhang, S.; Chen, L.; Kumar, S.; Wu, L.; Lawrence, D. S.; Zhang, Z. Y. *Methods* **2007**, *42*, 261-267.

60. Tautz, L.; Mustelin, T. *Methods* **2007**, *42*, 250-260.

61. McGovern, S. L.; Caselli, E.; Grigorieff, N.; Shoichet, B. K. *J. Med. Chem.* **2002**, *45*, 1712-1722.

62. Guertin, K. R.; Setti, L.; Qi, L.; Dunsdon, R. M.; Dymock, B. W.; Jones, P. S.; Overton, H.; Taylor, M.; Williams, G.; Sergi, J. A.; Wang, K.; Peng, Y.; Renzetti, M.; Boyce, R.; Falcioni, F.; Garippa, R.; Olivier, A. R. *Bioorg. Med. Chem. Lett.* **2003**, *13*, 2895-2898.

63. Montalibet, J.; Skorey, K. I.; Kennedy, B. P. *Methods* **2005**, *35*, 2-8.

64. Kenner, K. A.; Anyanwu, E.; Olefsky, J. M.; Kusari, J. *J. Biol. Chem.* **1996**, *271*, 19810-19816.

65. Vintonyak, V. V.; Antonchick, A. P.; Rauh, D.; Waldmann, H. *Curr. Opin. Chem. Biol.* **2009**, *13*, 272-283.

66. Zhang, S.; Zhang, Z.-Y. *Drug Discovery Today* **2007**, *12*, 373-381.

67. Blaskovich, M. A. T. *Curr. Med. Chem.* **2009**, *16*, 2095-2176.

68. Heneberg, P. *Curr. Med. Chem.* **2009**, *16*, 706-733.

69. Lipinski, C. A.; Lombardo, F.; Dominy, B. W.; Feeney, P. J. *Adv. Drug Delivery Rev.* **2001**, *46*, 3-26.

70. Russell, A. DPhil Thesis, University of Oxford, **2004**.

71. Aly, A. A.; Mourad, A. F. E.; Hassan, A. A.; Mohamed, N. K.; Ali, B. A.; El-Sayed, M. M. *Arch. Pharm.* **2004**, *337*, 133-139.

72. Bondock, S.; Tarhoni, A. E. G.; Fadda, A. A. *Phosphorus, Sulfur Silicon Relat. Elem.* **2007**, *182*, 1915-1936.

73. Mendgen, T.; Steuer, C.; Klein, C. D. *J. Med. Chem.* **2012**, *55*, 743-753.

74. Baell, J. B.; Holloway, G. A. *J. Med. Chem.* **2010**, *53*, 2719-2740.

75. Suzuki, K.; Hori, Y.; Kobayashi, T. *Adv. Synth. Catal.* **2008**, *350*, 652-656.

76. Watanabe, T.; Miyaura, N.; Suzuki, A. *Synlett* **1992**, 207-210.

77. Suzuki, A.; Miyaura, N. *J. Synth. Org. Chem.* **1993**, *51*, 1043-1052.

78. Parry, P. R.; Bryce, M. R.; Tarbit, B. *Org. Biomol. Chem.* **2003**, *1*, 1447-1449.

79. Dubernet, M.; Caubert, V.; Guillard, J.; Viaud-Massuard, M. C. *Tetrahedron* **2005**, *61*, 4585-4593.

80. Mavoungou-Gomes, L. *Bull. Soc. Chim. Fr.* **1967**, *5*, 1753-1758.

81. Korolev, D. N.; Bumagin, N. A. *Tetrahedron Lett.* **2006**, *47*, 4225-4229.

82. McClure, M. S.; Glover, B.; McSorley, E.; Millar, A.; Osterhout, M. H.; Roschangar, F. *Org. Lett.* **2001**, *3*, 1677-1680.

83. Castanet, A. S.; Colobert, F.; Desmurs, J. R.; Schlama, T. *J. Mol. Catal.* **2002**, *182*, 481-487.

84. Suzuki, A. J. *J. Organomet. Chem.* **1999**, *576*, 147-168.

85. Khurana, J. M.; Chauhan, S.; Bansal, G. *Monatsh. Chem.* **2004**, *135*, 83-87.

86. Deb, M. L.; Bhuyan, P. J. *Tetrahedron Lett.* **2005**, *46*, 6453-6456.

87. Hochuli, E.; Dobeli, H.; Schacher, A. *J. Chromatogr.* **1987**, *411*, 177-184.

88. Chernoff, J.; Li, H. C. *Arch. Biochem. Biophys.* **1983**, *226*, 517-530.

89. Zhao, Z.; Zander, N. F.; Malencik, D. A.; Anderson, S. R.; Fischer, E. H. *Anal. Biochem.* **1992**, *202*, 361-366.

90. Zhang, Z. Y.; Maclean, D.; Thiemesefler, A. M.; Roeske, R. W.; Dixon, J. E. *Anal. Biochem.* **1993**, *211*, 7-15.

91. Protocol kindly provided by O. King, SGC, Oxford.

92. Lorenz, U. *Current protocols in immunology*, John Wiley & Sons, **2011**, *93*, Unit 11.17.

93. Vanveldhoven, P. P.; Mannaerts, G. P. *Anal. Biochem.* **1987**, *161*, 45-48.

94. Lanzetta, P. A.; Alvarez, L. J.; Reinach, P. S.; Candia, O. A. *Anal. Biochem.* **1979**, *100*, 95-97.

95. Kuhl, P. W. *Biochem. J.* **1994**, *298*, 171-180.

96. Studies carried out by Nick Muldal, University of Oxford.

97. Karver, M. R.; Krishnamurthy, D.; Kulkarni, R. A.; Bottini, N.; Barrios, A. M. *J. Med. Chem.* **2009**, *52*, 6912-6918.

98. MacKeigan, J. P.; Murphy, L. O.; Blenis, *Nat. Cell Biol.* **2005**, *7*, 591-600.

99. Clark, O. PhD Thesis, University College London, **2011**.

CHAPTER 3

Targeting Protein Tyrosine Phosphatases with Drug-Like Small Molecule Inhibitors for Neuroblastoma Drug Discovery (II)

3.1 Hit Identification: Tetrahydroquinoline Compounds P00104 and P00341 as Potential Inhibitors of Protein Tyrosine Phosphatases

From the library of drug-like small molecules targeted to PTPs described in section 1.6, two further compounds were identified displaying moderate inhibitory potency against PTPN22 and the set of related phosphatases. These compounds belong to the tetrahydroquinoline family, named **P00104** and **P00341** (Figure 3.1). The IC_{50} values for these molecules against the five PTPs are shown in figure 3.1. It was envisaged that synthesizing a panel of analogues of these two compounds, followed by biological screening, could help to identify drug-like PTP inhibitors with increased potency, selectivity and improved physical properties.

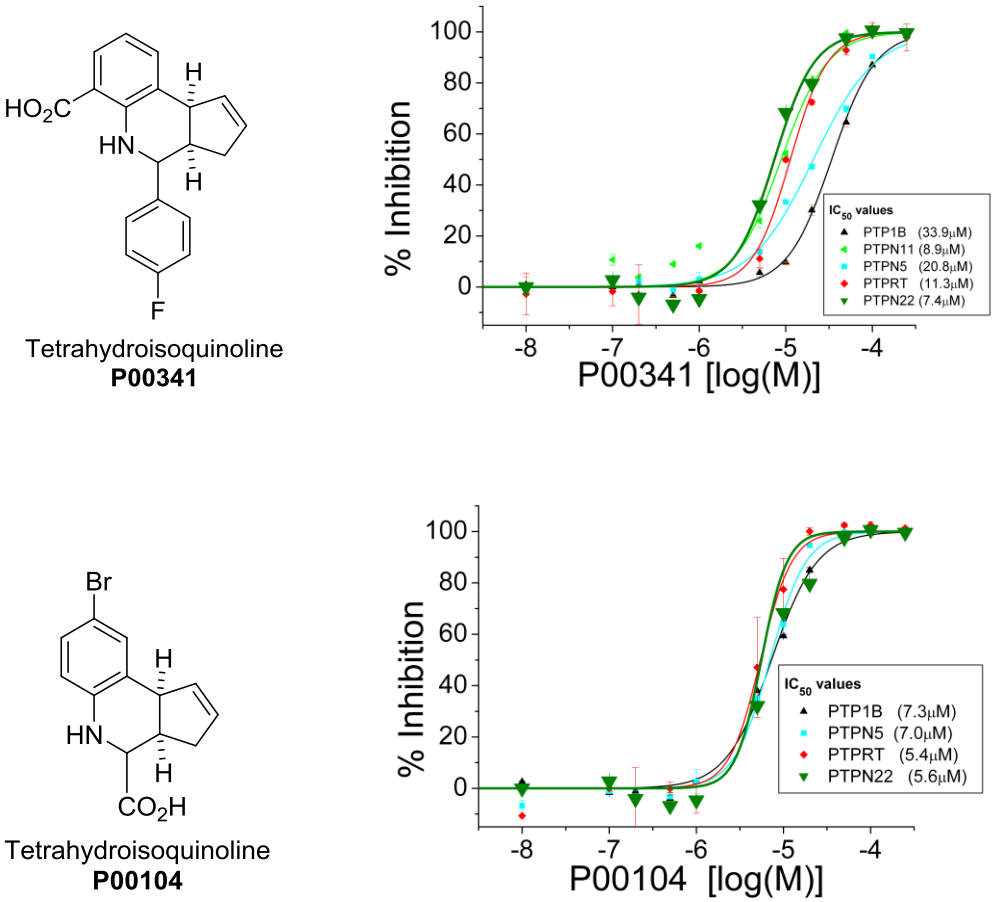


Figure 3.1: IC_{50} values (□M) for the tetrahydroquinoline inhibitors **P00104** and **P00341** against PTP1B, PTPN11, PTPN5, PTPRT and PTPN22.[1]

3.1.1 Tetrahydroquinolines

Tetrahydroquinolines (THQs) and their derivatives are important structural features of many natural products. They have attracted considerable attention due to their diverse biological and pharmaceutical activities.[2,3] Many relatively simple synthetic tetrahydroquinolines are currently being used as drugs, such as oxamniquine **72**[4] and virantmycin **73**[5] and many are being tested as potential drugs, including L-6X9.560 **74**, which is one of the most potent NMDA antagonists yet found (Figure 3.2).[6] Consequently, many research groups have focused on finding efficient methodologies for the synthesis of tetrahydroquinoline derivatives and various methods have been reported in the literature that offer good results.[2,7-9] The most common methods include the Povarov reaction[10] and various reductions of quinolines.

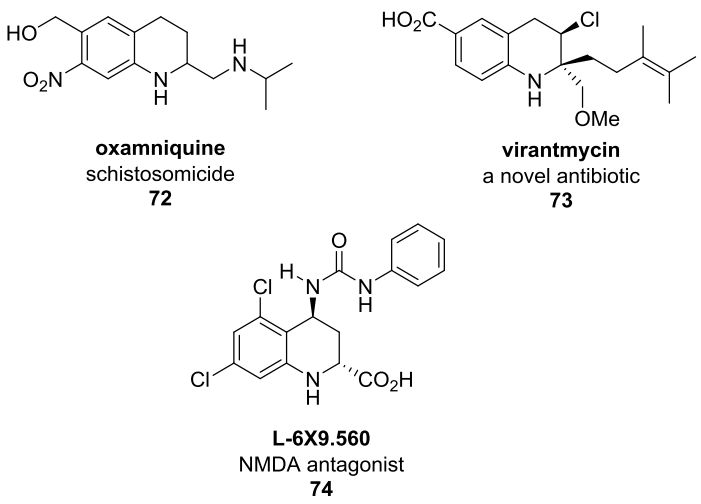
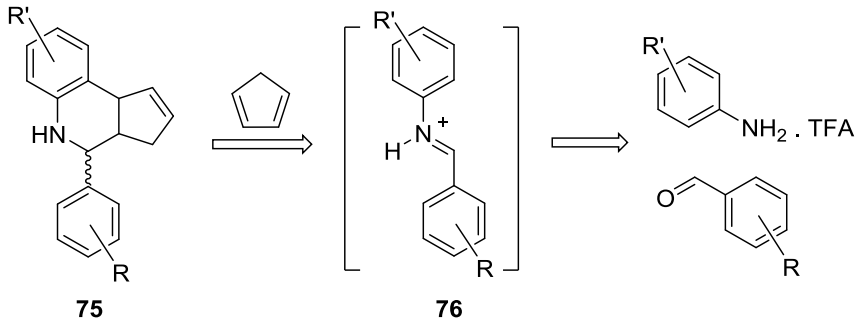


Figure 3.2: Tetrahydroquinoline derivatives used as drugs or with potential drug activity.

3.1.2 Retrosynthesis and SAR Strategies

The aza-Diels-Alder reaction is one of the most powerful synthetic routes for constructing nitrogen containing six-membered heterocycles. Imines derived from aromatic amines can act as heterodienes and undergo an amino-Diels-Alder reaction with various dienophiles,

leading to tetrahydroquinolines [Scheme 3.1]. Lewis acids and Brönsted acids such $BF_3 \cdot OEt_2$ and TFA are known to catalyse this type of condensation reaction.[11] Many imines are known to be hygroscopic, unstable at high temperature, and difficult to purify by distillation or column chromatography,[12] and therefore a one-pot three-component coupling protocol is highly convenient.



Scheme 3.1: A retrosynthetic study indicated the possibility of using three-component cycloaddition as the primary pathway to the development of the library.

For the SAR study of the two identified hits **P00104** and **P00341**, the core tetrahydroquinoline was divided into three regions in order to analyse the specific impact of each of these components on activity against PTPN22 and related PTPs (Figure 3.3).

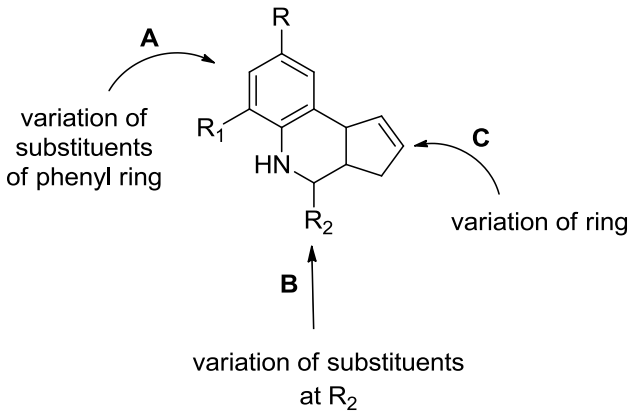
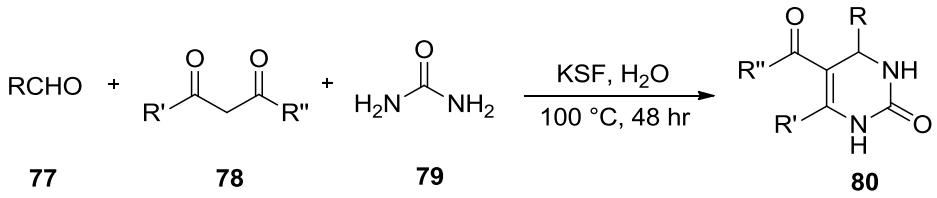


Figure 3.3: Structure-activity relationship study of compounds **P00104** and **P00341**.

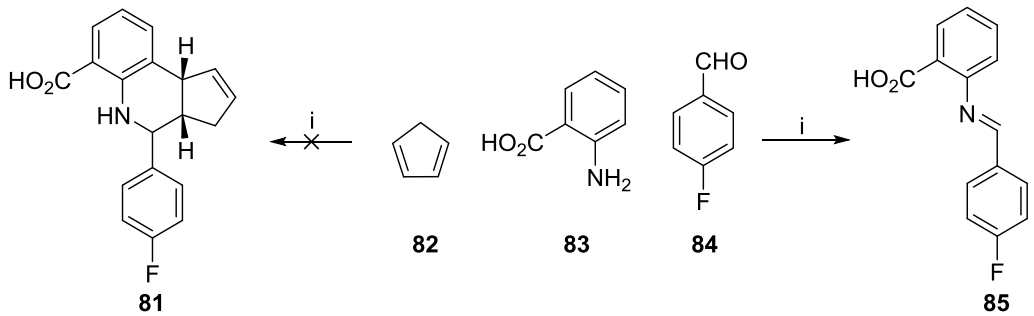
3.2 Initial Investigations and Resynthesis of Tetrahydroquinolines P00104 and P00341

For the synthesis of **P00341**, a one-pot Aza-Diels-Alder type reaction between the imine formed *in situ* from *p*-fluorobenzaldehyde **83,** and anthranilic acid **84**, and cyclopentadiene was initially investigated using TFA in acetonitrile at room temperature; unfortunately this led to degradation of the starting materials and none of the desired product could be detected. Similar multicomponent reactions for the synthesis of substituted dihydropyrimidines and chromenes have been performed in water under clay catalysis [Scheme 3.2].[13, 14]



Scheme 3.2: KSF clay-promoted three-component one-pot synthesis of dihydropyrimidines.[13]

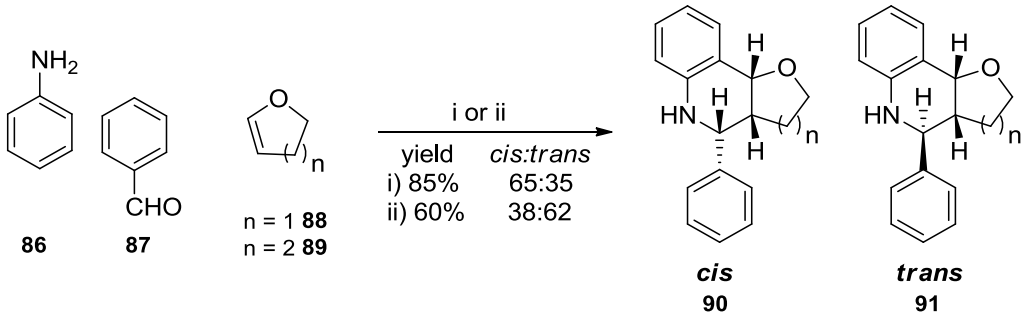
Treatment of the three reagents with montmorillonite KSF in water at 100-150 °C for 48 h in an autoclave afforded only the imine [Scheme 3.3]. The same reaction was then carried out in microwave increasing the temperature gradually; however, the same result was obtained. The purified imine was also subjected to TFA in acetonitrile and cyclopentadiene, without any success, with only imine starting material **85** being returned.



Scheme 3.3: i) Montmorillonite KSF, H_2O, 100-150 °C, 48 hr.

It was envisaged that the carboxylic acid group on the aniline moiety could be suppressing the cycloaddition reaction and therefore all of the above reactions were attempted using methyl-2-aminobenzoate; all conditions led only to imine formation. Furthermore, the effects of solvents (*e.g.* CH_2Cl_2, Et_2O, THF, MeOH), the time of reactions as well as using heat and microwave were investigated, all with no success.

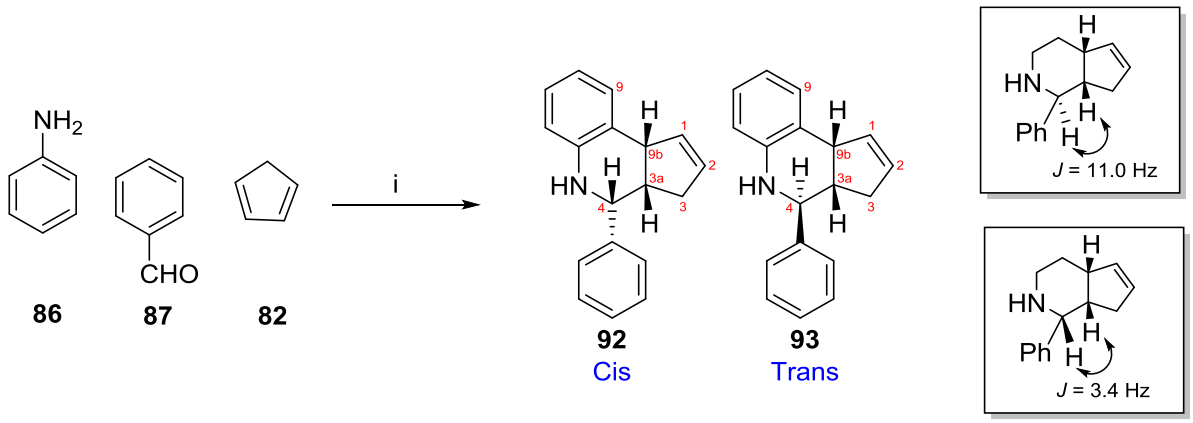
It was suspected that the lack of success of these reactions could partly be due to the reactivity of the imine or of the dienophile. The one-pot synthesis was therefore attempted using aniline **86**, benzaldehyde **87**, and electron-rich dienophiles, dihydrofuran **88** and dihydropyran **89**, using literature procedures involving sulfamic acid[15] and $KHSO_4$[16] as catalysts, respectively [Scheme 3.4]. These reactions successfully afforded the corresponding heterocycles **90** and **91**. However, when cyclopentene was used as a dienophile under the same conditions only the corresponding imine was afforded, and when cyclopentadiene was used very low yields of product were obtained, 42% and 38% respectively.



Scheme 3.4: *Reagents and conditions:* i) 50 mol% sulfamic acid, rt; ii) 40 mol% $KHSO_4$, rt.

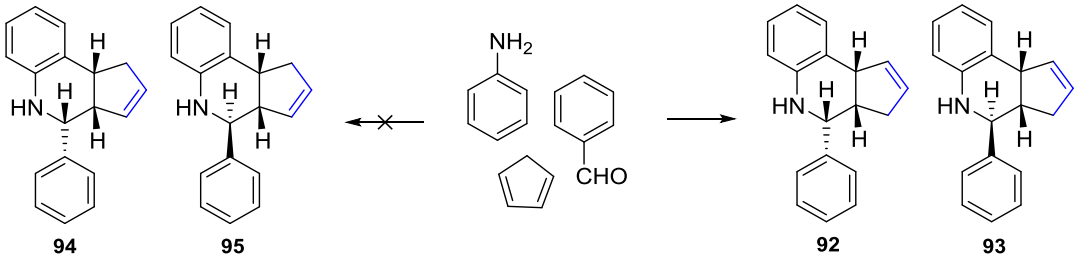
The pioneering work of Povarov is a powerful and efficient means for the construction of tetrahydroquinolines, employing Lewis acids such as $BF_3{\cdot}OEt_2$ as catalyst in a reaction where an imine/Schiff base is treated with an alkene.[17] The lack of success with the above reaction led to the application of this principle to the convergent three-component reaction of

benzaldehyde, aniline and cyclopentadiene. This reaction was catalysed by $BF_3{\cdot}OEt_2$ in the presence of $MgSO_4$, which resulted in a mixture of the desired products **92** and **93** as *cis*- and *trans*-isomers (with respect to H-3a and H-4) in a ratio of 87:13 in an overall yield of 80% [Scheme 3.5]. Acetonitrile proved to be the best solvent compared to THF, MeOH, toluene and CH_2Cl_2.



Scheme 3.6: *Reagents and conditions:* i) Povarov reaction - $BF_3{\cdot}OEt_2$ (20 mol%), MeCN, rt, $MgSO_4$.

The identity of *cis*-**92** as the major product was supported by IR, ^{1}H NMR, ^{13}C NMR and MS. There is a strong NH stretching band at 3200-3450 cm^{-1} in the IR spectra. The most diagnostic parameter for structural assignment of this diastereoisomer is the scalar coupling constant between protons H-3a and H-4 [Scheme 3.6]. In this isomer, the J(3a, 4) = 3.4 Hz is significantly small and typical for a gauche conformation.[18] As expected for this configuration, reciprocal H-H COSY interaction was observed among protons H-3a, H-4, and H-9b [Scheme 3.6]. Attempts to separate the major isomer from the minor isomeric product (using normal and reverse silica gel, neutral and basic alumina or preparative HPLC) were, unfortunately, not successful. The minor isomer was assigned as *trans*-**93**, rather than the possible regioisomeric product, on the basis of ^{1}H NMR and COSY assignments and is consistent with literature precedent [Scheme 3.7].



Scheme 3.7: The isomer mixture of **92** and **93** afforded in the Povarov reaction.

3.3 Optimisation of the General Synthetic Method and Application to the Synthesis of Analogues

Different Lewis acids were tested in order to improve the *cis/trans* isomer ratio and the yield.[17-21] Benzaldehyde and aniline were treated with cyclopentadiene in the presence of $MgSO_4$ and catalytic amount (20 mol%) of a number of Lewis acids such as ytterbium and yttrium triflate and gadolinium trichloride, in acetonitrile at rt (Table 3.1). $Sc(OTf)_3$ gave the highest yield of 90% and highest *cis:trans* isomer ratio (9:91).

Entry	Reaction condition	Crude percentage ratio isomers *trans : cis*	Isolated percentage yield of the isomeric mixture 92 and 93
1	$Yb(OTf)_3$	13 : 87	40
2	$BF_3{\cdot}OEt_2$	13 : 87	80
3	$GdCl_3$	13 :87	65
4	$Y(OTf)_3$	16 : 84	89
5	$Sc(OTf)_3$	9 : 91	90
6	$MgSO_4$	-	0

Table 3.1: Synthesis of tetrahydroisoquinolines **92** and **93** using different Lewis acids.

In these reactions, $MgSO_4$ was used as a drying agent to trap the water released during imine formation and in doing so, prevent the deactivation of the Lewis acids. Keeping the same idea

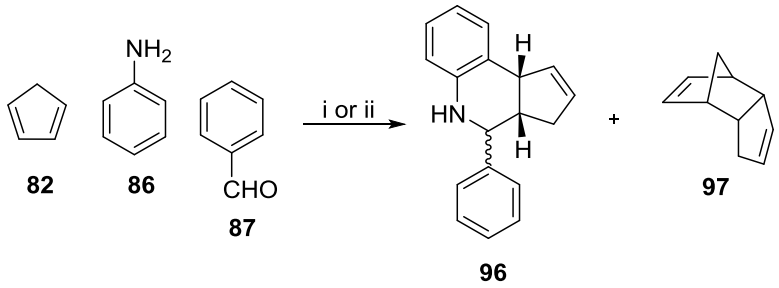
in mind, the initially investigated one-pot condensation reaction using TFA (20 mol%) was carried out under the same conditions but this time in the presence of $MgSO_4$. This time the isomeric product mixture **92** and **93** was obtained in 45:55 *cis/trans* isomer ratio in total yield of 48%.

As $MgSO_4$ is also a Lewis acid, the above reaction was carried out in the presence of catalytic and stoichiometric amounts of $MgSO_4$ alone; however, only the starting material was returned (Table 3.1).

Most Lewis acids used were triflic acid salts; consequently, it is possible that triflic acid alone could act as the catalyst in these reactions. This theory was investigated by subjecting aniline, benzaldehyde and cyclopentadiene to 10 mol% triflic acid. The desired tetrahydroquinoline **96** was isolated in 75:25 *cis/trans* isomer ratio in total yield of 29%. The ratio of product to dimerized cyclopentadiene **97** in this reaction was 47:53. It should be noted that cyclopentadiene used in each reaction was prepared freshly *via* a retro-Diels-Alder reaction of dicyclopentadiene at 150 °C. The reaction is reversible and at room temperature cyclopentadiene slowly dimerizes to reform the cyclopentadiene dimer.

The effect of different amounts of both triflic acid and TFA on the rate of the tetrahydroquinoline reaction, in relation to dimerization of cyclopentadiene, was investigated and is reported in figure 3.4. Increasing the amount of triflic acid to more than 10 mol% did not have a significant effect on the ratio of product to dicyclopentadiene, whereas using five equivalents of TFA increased the amount of product **96** by three-fold, although it was still substantially lower than the percentage of cyclopentadiene dimerization. In the one-pot reactions where a Lewis acid was used as a catalyst, no dicyclopentadiene peaks were observed in the ^{1}H-NMR spectrum. This indicates that the rate of tetrahydroquinoline formation is much higher in the presence of Lewis acids than the rate of cyclopentadiene

dimerization, and certainly using Lewis acids as a catalyst in this transformation is more effective than the use of protic acids.



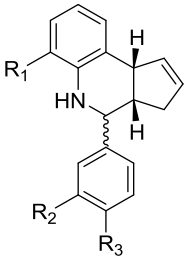
82 **86** **87** **96** **97**

	Dicyclopentadiene (97) : Product (96) Ratio	
Mole percentage	**Triflic Acid**	**TFA**
1	100:0	89:11
5	72:28	91:9
10	53:47	91:9
50	45:55	91:9
100	43:57	79:21
500	no product	60:40

Figure 3.4: *Reagents and conditions:* i) triflic acid, CH_3CN, $MgSO_4$, rt; ii) TFA, CH_3CN, $MgSO_4$, rt.

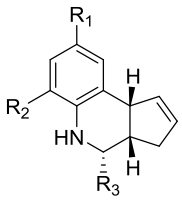
As $BF_3 \cdot OEt_2$ produced excellent yield and was the cheapest amongst the investigated Lewis acids, it was used for the synthesis of **P00341, P00104** and a library of their analogues for SAR analysis (Figure 3.5).

Carboxylic acid derivatives of aniline and benzaldehyde (**86** and **87**), afforded low yields due to production of many side products. Using ester derivatives increased the yield and simple hydrolysis with lithium hydroxide afforded the desired compound **111** in higher overall yields of over 75%.



Compound P00341 and Structural Analogues

Compound	R_1	R_2	R_3	Yield (%)
P00341	CO_2H	F	H	12
98	H	F	H	65
99	CO_2Me	F	H	82
100	Br	F	H	85
101	NO_2	F	H	69
102	OMe	F	H	82
103	OH	F	H	79
104	CN	F	H	72
105	Me	F	H	86
106	*t*-Butyl	F	H	69
107	CF_3	F	H	65
108	CO_2Me	NO_2	H	75
109	H	Cl	H	87
110	CO_2H	F	F	32
111	CO_2H	H	F	28



Compound P00104 and Structural Analogues

Compound	R_1	R_2	R_3	Yield (%)
P00104	Br	H	CO_2H	45
112	Br	H	CO_2Me	64
113	H	H	CO_2H	52
114	CO_2H	H	CO_2H	37
115	H	OH	CO_2H	48

Figure 3.5: P00341, P00104 and analogues *via* Povarov one-pot reaction catalysed by $BF_3{\cdot}OEt_2$.

3.4 Triflic Acid as Catalyst in the Synthesis of Furanoquinolines

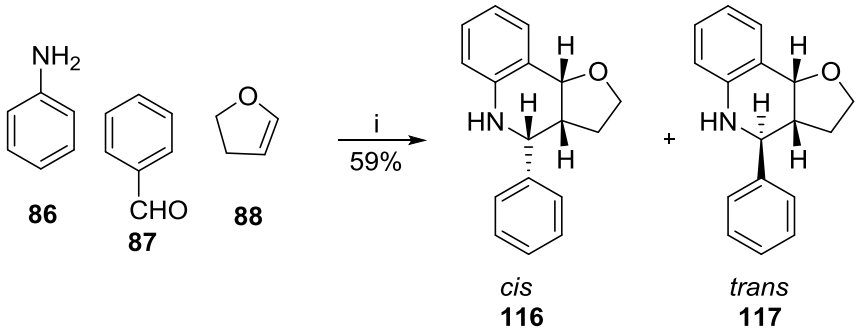
In a preliminary attempt at using triflic acid as the catalyst for the convergent three-component synthesis of cyclopentaquinoline, it was observed that cyclopentadiene dimerized at a fast rate whilst the reaction proceeded. This resulted in a low yield of product and consequently it was decided to use different commercially available alkenes to test the catalytic activity of triflic acid in the cyclization reactions. In addition, use of different dienophiles in the synthesis of tetrahydroquinoline analogues will aid future SAR studies on these compounds, as it will be possible to elucidate if the cyclopentene moiety in part C of the structure (Figure 3.3) is required for the biological activity of this chemotype.

1,3-Cyclohexadiene was selected and its reactivity was tested using one of the prior successful reactions conditions (*i.e.* using $Y(OTf)_3$ as catalyst); unfortunately only starting material was retrieved. Using a more reactive amine (2-aminopyridine), preformed imine and heating *via* microwave also did not push this reaction forward. It was concluded that this dienophile is not reactive enough for [4+2] cycloaddition reactions.

The lack of success with this approach prompted the use of an alternate dienophile, *i.e.* dihydrofuran. A series of Lewis acids such as $Ln(OTf)_3$,[22] $GdCl_3$,[18] and Selectfluor™ [23] have been reported to be effective catalysts for the three-component synthesis of furanoquinolines. These compounds have many attractive and useful biological activities such as having the ability to act as broad-spectrum anti-tumour agents by inhibiting cRAF1 kinases.[24] Consequently, a mild, economical and more efficient one-pot protocol for the synthesis of these compounds is still in great demand. Herein protic acids are explored as novel catalysts for the synthesis of these compounds.

Initially, benzaldehyde, aniline and dihydrofuran were subjected to 10 mol%, 50 mol%, 1 and 5 equivalents of TFA in the presence of $MgSO_4$ in parallel reactions, none of which afforded

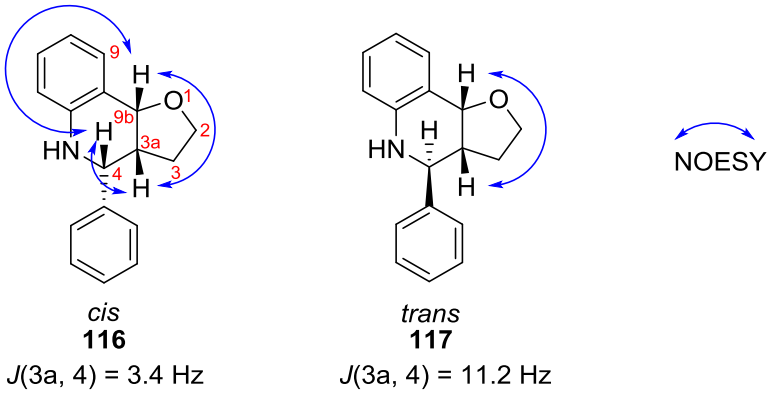
the desired product. Baudelle *et al.* have reported a successful synthesis of a series of 45:55 *cis/trans* stereoisomer ratio pyranoquinolines using one equivalent of TFA in the absence of $MgSO_4$.[25] Applying these conditions to the above reaction yielded the furanoquinolines **116** and **117** in an overall yield of 59%. The two isomers have the same polarity and could not be separated by chromatographic purification. The same reaction under catalytic amounts of TFA (10 mol%) afforded the products **116** and **117** in a similar isomeric ratio of 48:52 with a reduced yield of 28%.



Scheme 3.8: *Reagents and conditions:* i) 1 equiv. TFA, CH_3CN, rt.

Next, the more reactive 4-nitrobenzaldehyde, dihydrofuran and aniline were subjected to 10 mol% triflic acid in the absence of $MgSO_4$. The corresponding tetrahydroquinoline **119** was produced in 99% yield in a *cis/trans* isomer ratio of 46:54. This result is very exciting, as it potentially provides a novel, high yielding, cheap and efficient route towards these useful compounds. The effect of increasing the concentration of triflic acid was also tested. Using one equivalent of triflic acid returned the starting material but five equivalents produced a black tar. The results shown in Figure 3.6 clearly indicate the scope and generality of this [4+2] cycloaddition reaction with respect to various aryl and alkyl aldehydes and anilines in the presence of 10 mol% triflic acid. In all cases, the reactions proceeded smoothly to furnish

the desired tetrahydroquinoline derivatives in 46-94% yield as a mixture of *cis*- and *trans*-isomers, which were easily separated by column chromatography.



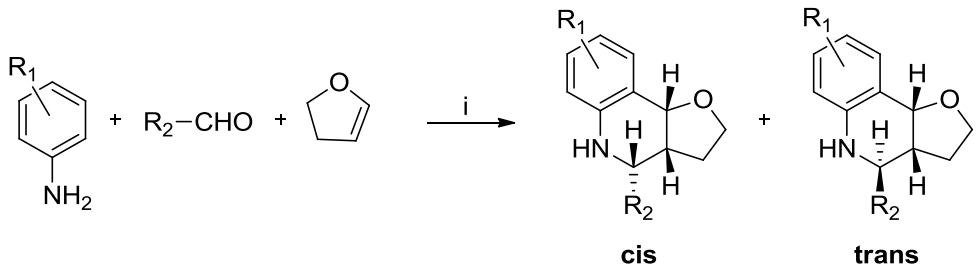
cis
116
J(3a, 4) = 3.4 Hz

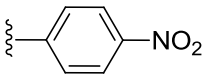
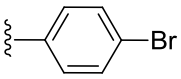
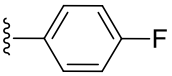
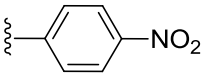
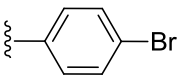
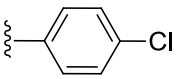
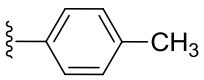
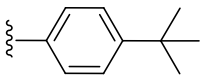
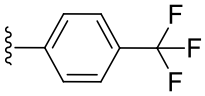
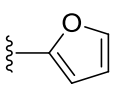
trans
117
J(3a, 4) = 11.2 Hz

Scheme 3.9: Chemical shift values and H-H cross-peaks observed in NOE spectra for compound **116** and **117**.

The stereochemistry of the *cis*- and *trans*-isomers was assigned based on the coupling constant values between proton H_{3a} and H_4 and NOE studies [Scheme 3.9]. For example, in the *cis*-isomer of structure **116** the coupling constant *J*(3a, 4) = 3.4 Hz, which is small and indicative of a gauche conformation. As expected for this configuration, NOE cross peaks were observed among protons H_{3a}, H_4 and H_{9b}. The *J*(3a, 4) value of 11.2 Hz in the *trans*-isomer **117** is appropriate and indicative of antiperiplanar orientation of protons H_{3a} and H_4. This configuration is also confirmed by the presence of NOE cross peaks between H_{3a} and H_{9b} and its absence between H_{3a} and H_4 and its. In all cases, *J*(3a, 9b) was found to be 2.6-2.9 Hz indicating a *cis* ring junction between the quinoline and furan rings which is in accord with literature values.[26]

In summary, it can be concluded that catalytic amounts of triflic acid can act as an efficient catalyst in the one-pot coupling reactions of various aryl and alkyl aldehydes, aryl amines and dihydrofuran, to afford furanoquinolines in high yields under mild conditions.



Product	R_1-NH_2	R_2-CHO	Yield (%)	Stereoisomer (*cis : trans*)
118	H	C_6H_5	90	48:52
119	H		99	46:54
120	H		82	100:0
121	H		79	52:48
122		C_6H_5	61	78:22
123		C_6H_5	82	45:55
124		C_6H_5	84	45:55
125		C_6H_5	85	48:52
126		C_6H_5	81	45:55
127	H		76	44:56
128	H		88	98:2
129	H		75	100:0

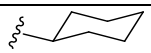
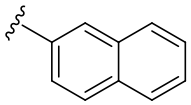
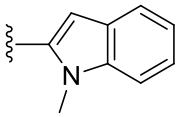
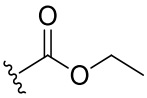
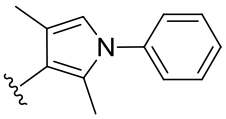
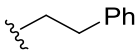
130	H		46	93:7
131	H		75	87:13
132	H		59	87:13
133	H		69	100:0
134	H		66	18:82
135	H		0	0
136	H		0	0

Figure 3.6: *Reagents and conditions:* i) 10 mol% triflic acid, CH_3CN, rt.

3.5 Synthesis of Carboxylic Acid Bioisosteres of Tetrohydroquinoline P00341

The concept of bioisosterism was first introduced by Friedman[27] in 1951 and was defined as molecules or functional groups which have chemical and physical similarities and produce broadly similar biological properties.[28] The structural knowledge gained from protein crystallography since then has led to an improved understanding of intermolecular interactions between molecules such as proteins and their ligands. Consequently, the bioisostere definition has been refined to include molecules or functional groups that are structurally different but retain biological activity by forming similar intermolecular interactions.[28]

Bioisosteres have been classified as either classical or nonclassical.[29] Classical bioisosteres are molecules that have similar steric and electronic features and the same number of atoms as the substituent moiety they are replacing. In contrast, nonclassical bioisosteres do not have the same number of atoms but are capable of maintaining similar biological activity by mimicking the spatial arrangement, electronic properties, or some other physicochemical property of the molecule or functional group that is critical for the retention of biological activity.

In the contemporary practice of medicinal chemistry and drug design, the rationale for the development and application of bioisosteres during lead optimisation stage is to enhance the desired properties of a biologically active compound or minimise its adverse effects. The utility of bioisosteres is broad in nature and includes improving pharmacokinetic properties, enhancing potency, improving selectivity, reducing or redirecting metabolism and eliminating or modifying toxicophores.[30]

The tetrahydroquinoline compounds **P00104** and **P00341,** and the thiobarbituric acid **P00337** that showed activity against PTPN22 and related phosphatases in the initial high-throughput screening, all contain a carboxylic acid moiety and showed low solubility in aqueous buffers. Within the last century drugs containing a carboxylate functionality, such as non-steroidal anti-inflammatory drugs, β-lactam antibiotics, and statins have resulted in important advancements in the field of medicine. However, a significant number of these carboxylic acid-containing drugs have been withdrawn from clinical use due to recurrent occurrence of idiosyncratic adverse drug reactions (such as hepatotoxicity).[31, 32] There are a number of factors that are associated with the side effects caused by such compounds. Firstly, compounds with a carboxylate functionality are known to be susceptible to Phase II metabolism *in vivo* (Figure 3.7). They go through conjugation reactions to form electrophilic ester metabolites of the carboxylic acid group. Such metabolites can react with critical proteins disturbing cellular functionality or induce an immune response eliciting adverse effects that in serious cases can be fatal.[33] In addition, carboxylic acid containing compounds tend to be neutral in the acidic environment of the stomach but are negatively charged in the higher pH of the small intestine, where drugs have a longer time to be absorbed. As only neutral species readily cross biological membranes, carboxylic acid containing drugs tend to be absorbed from the stomach and, consequently have a relatively short amount of time to reach the maximum plasma concentration of the drug (T_{max}). As a result they have poor oral absorption due to their low permeability.[34] Furthermore, carboxylic acid containing drugs bind extensively (> 98%) to plasma proteins, such as albumin, and consequently tend to have a small volume of distribution (Vd).

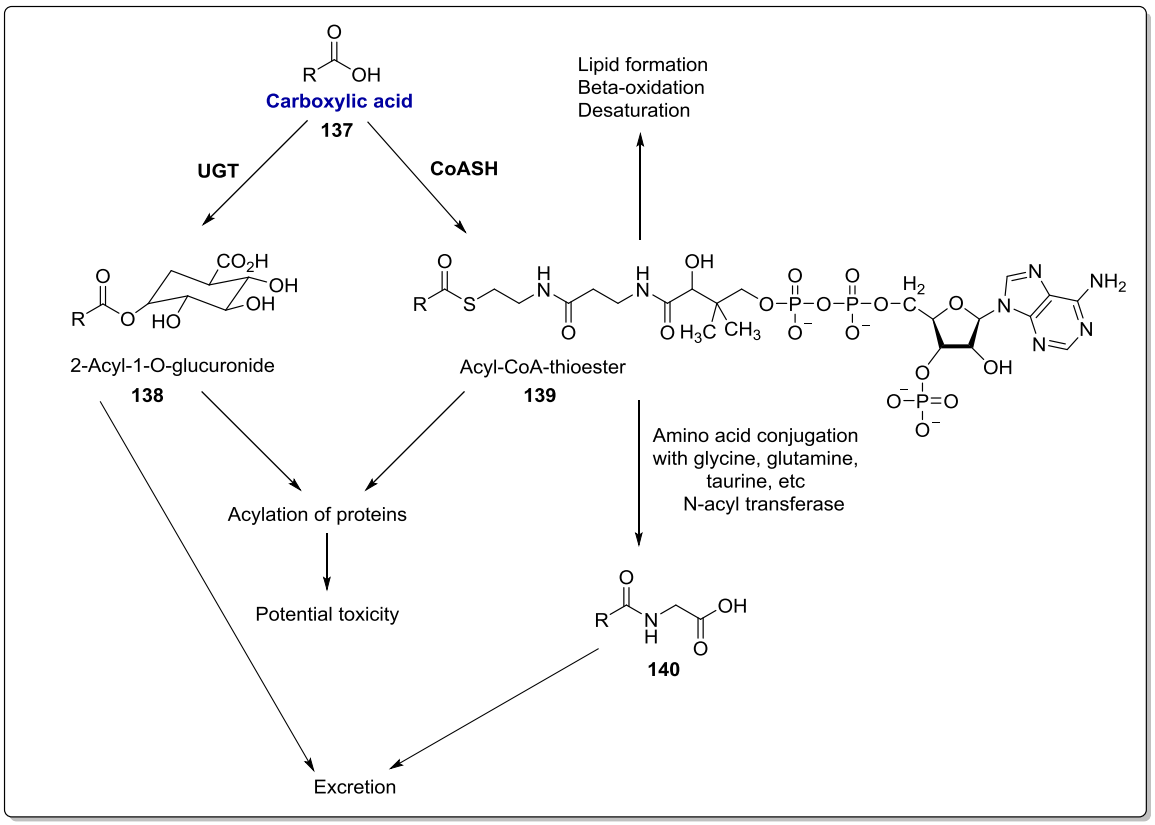


Figure 3.7: Overview of carboxylic acid metabolism and some processes in which the metabolites may be involved. Metabolism of carboxylic acid occurs via two major pathways – UDP-Glucuronosyl-tranferase (UGT) catalysed in conjugation with glucuronic acid and acyl coenzyme A synthetase (CoASH) catalysed formation of acyl CoA thioester.[33]

Studies on bioisoteric replacement of the carboxylic acid functionality of many drugs have typically focused on enhancing potency, reducing polarity, and increasing lipophilicity in order to improve membrane permeability, enhancing pharmacokinetic properties *in vivo* and reducing the potential for toxicity.

The presence of the carboxylate functionality, or an isosteric replacement was envisaged to be critical for the PTP activity of compounds **P00104**, **P00341** and **P00337**. A variety of inhibitors for PTPs has been reported in the literature that incorporate this functionality such as such as cinnamic acids[35] and 2-(oxalylamino)-benzoic acids,[36] and structural modelling studies have revealed it to function as a phosphate mimics.[37-39]

In order to bypass the problems associated with the carboxylate functionality and to examine the pharmacological consequences of replacing such groups, initially a series of carboxylic acid bioisosteres of compound **P00341** was synthesised for SAR analysis along with its other structural analogues. The bioisosteres synthesized included heterocyclic non-classical isosteres, phosphonic acid and sulphonic esters.

3.5.1 Planar Acidic Heterocycle-Based Isosteres

Approximately 70% of all pharmaceuticals and agrochemicals contain at least one heterocyclic ring.[40] The major reason for the tremendous value of heterocycles in the lead optimization stage is the positive impact they have on the synthetic accessibility and physicochemical properties of a drug, driving values of lipophilicity and solubility toward the optimal balanced range regarding uptake and bioavailability.[30]

Several different heterocyclic rings such as tetrazoles, triazoles,[41] oxadiazolones,[42] and hydroxythiadiazoles,[30] have proven track records of being good isosteric replacements for the carboxylic acid moiety in many drugs.

3.5.1.1 Synthesis of Tetrazole Bioisostere

The most prominent example of a carboxylic acid bioisosteric replacement involves the 5-substituted 1*H*-tetrazole.[43,44] Tetrazole **141** exists as a nearly 1:1 ratio of 1H- and 2H-tautomeric forms, and due to being able to stabilise negative charge *via* electron delocalization, the free N-H bond imparts acidity (Figure 3.5). This planar heterocycle displays a pKa similar to the corresponding carboxylic acids (~4.5-4.9)[45] and like its carboxylate counterpart ionizes at physiological pH 7.4. It is, however, almost 10 times more

lipophilic and therefore has much better absorption properties. In addition, tetrazole metabolizes as a non-electrophilic glucuronide and hence can avoid toxicity.

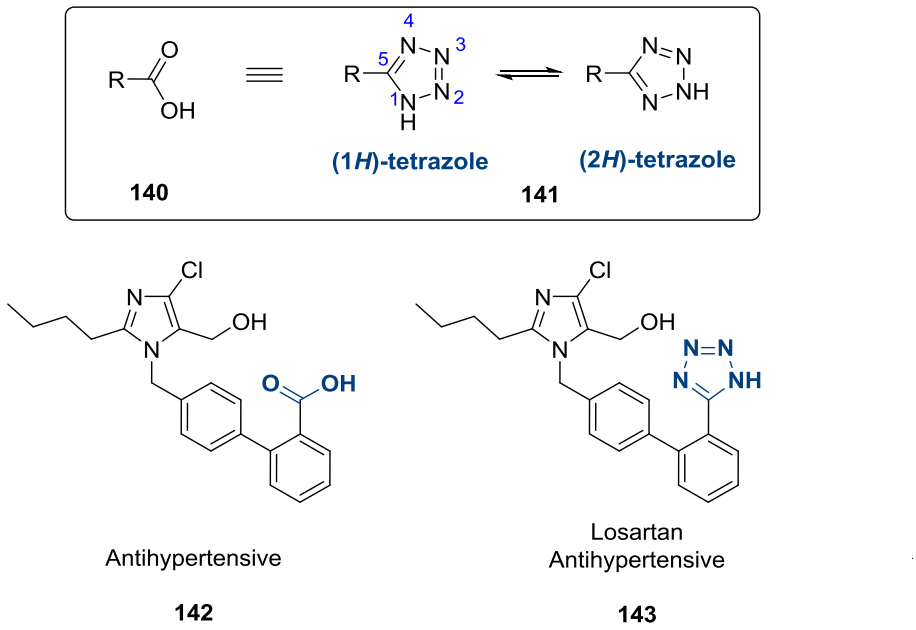


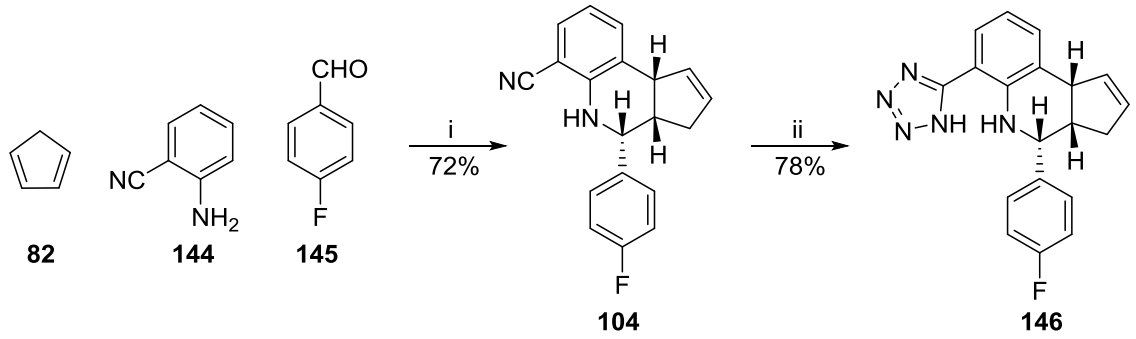
Figure 3.8: The tetrazole derivative losartan **143** as carboxylic acid bioisosteres.

One of the successful examples of the tetrazole-carboxylate isosterism involves the angiotensin II receptor antagonist losartan **143** (Figure 3.8). This antihypertensive drug **143** and its carboxylic acid lead structure **142** possess similar acidity (pKa of 5.0 and 4.5, respectively) but differ significantly in lipophilicity (log *P* of 4.5 and 1.2, respectively). The higher lipophilicity of losartan results in considerably improved oral bioavailability.[46,47]

There are many literature precedents for the synthesis of 5-substituted tetrazoles, the majority involving the reactions of nitriles with azides under different conditions.[43] This process is generally thought to occur by a concerted 1,3-dipolar cycloaddition mechanism, in which the nitrile acts as the dipolarophile toward the azide that serves as the 1,3-dipolar species.[48]

In order to prepare the nitrile analogue of tetrahydroquinoline **P00341**, *p*-fluorobenzaldehyde and 2-aminobenzonitrile were reacted with cyclopentadiene in the presence of a catalytic amount of $BF_3 \cdot OEt_2$ (20 mol %) in acetonitrile at room temperature. The reaction proceeded

smoothly to afford the corresponding tetrahydroquinoline **104** in 72% yield [Scheme 3.10]. Nitrile **104** was successfully converted to tetrazole derivative **146** in 78% yield by treatment with sodium azide and ammonium chloride in DMF at 80 ºC.



Scheme 3.10: *Reagents and conditions:* i) $BF_3{\cdot}OEt_2$ (20 mol %), CH_3CN, $MgSO_4$, rt; ii) NH_4Cl, NaN_3, DMF, 80 ºC, 24 h.[49]

3.5.1.2 Synthesis of 1,2,4-Oxadiazole and Oxo-Oxadiazole Bioisosteres

Oxadiazoles are a heterocyclic compound containing an oxygen atom and two nitrogen atoms in a five-membered ring.[50] There are four known isomers: 1,2,4-oxadiazole **148**, 1,3,4-oxadiazole **149**, 1,2,3-oxadiazole **150** and 1,2,5-oxadiazole **151** (Figure 3.9).[51] The first two have attracted interest in medicinal chemistry as surrogates for carboxylic acids, esters and carboxamides and have been more widely studied by researchers due to their many important chemical and biological properties.[52] Due to the increased hydrolytic and metabolic stabilities of the oxadiazole ring, improved pharmacokinetic and *in vivo* performance is often observed. In addition, 1,2,4-oxadiazoles have been reported to exhibit a range of biological activities such as being analgesic and having antitumour, anti-inflammatory and antimicrobial properties.[53,54]

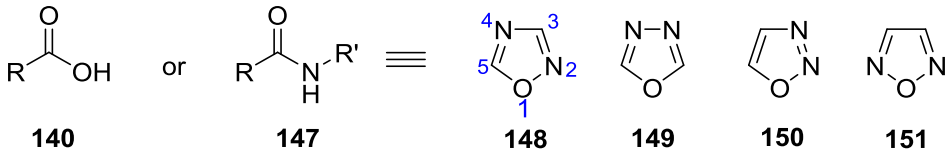
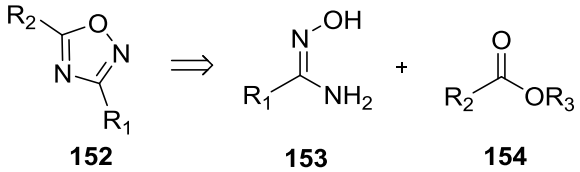


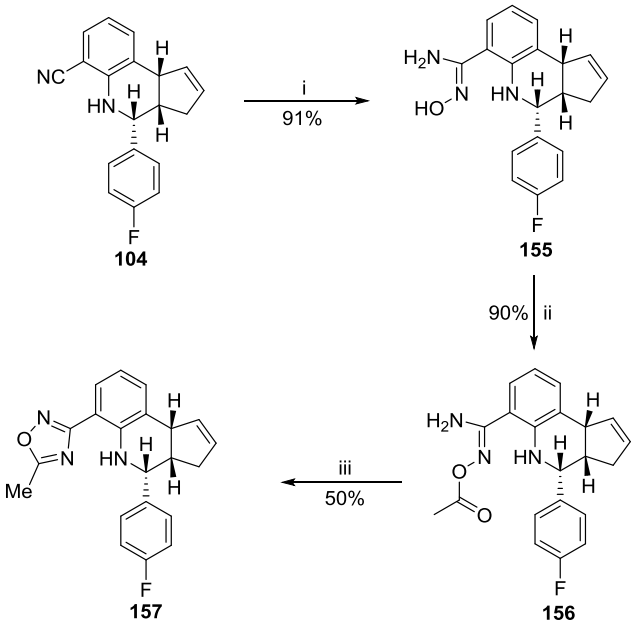
Figure 3.9: Isomers of oxadiazole as surrogates for $–CO_2H$ or $–CO_2R$.

Therefore, attention was turned to the synthesis of the 1,2,4-oxadiazole derivative of compound **P00341**. A wide range of reaction conditions have been published for the synthesis of 1,2,4-oxadiazoles in solution and on solid phase.[55] The syntheses are based mostly on the use of primary amidoximes and acylating agents as the initial reactants [Scheme 3.11].



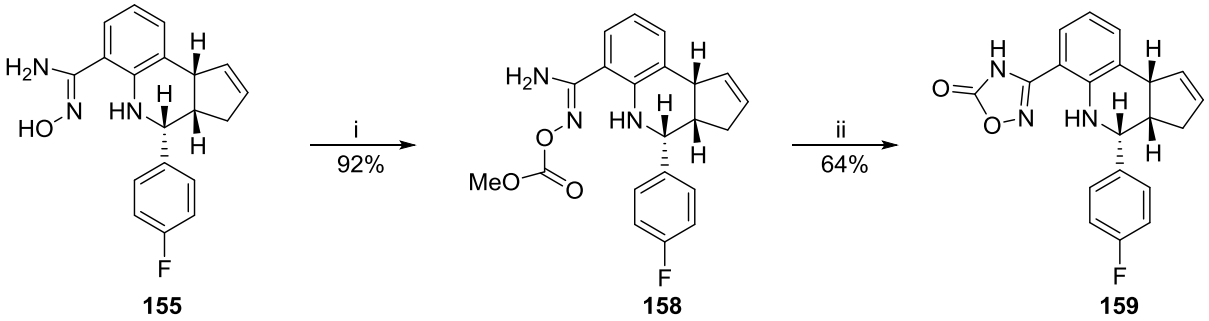
Scheme 3.11: Retrosynthesis of 1,2,4-oxadiazole.

The amidoxime precursor **155** was prepared in 91% yield by treating nitrile **104** with hydroxylamine hydrochloride and sodium carbonate in DMF at 70 °C. Acylation of amidoxime **155** with acetic anhydride in DMSO, in the presence of triethylamine afforded the corresponding carboximidamide **156** in 90% yield. Cyclization was then achieved by heating **156** in DMSO at 90 °C in the presence of acetic anhydride, to afford the 1,2,4-oxadiazole derivative **157** in 50% yield after 24 hours [Scheme 3.12].



Scheme 3.12: *Reagents and conditions:* i) $NH_2OH{\cdot}HCl$, DMF, 70 ºC, 24 h;[56] ii) $(CH_3CO)_2O$, Et_3N, DMSO, rt, 12 h;[57] iii) Ac_2O, DMSO, 90 ºC, 24 h.[57]

Another class of acidic bioisotere that can be synthesized through a similar route from amidoxime is the 5-oxo-1,2,4-oxadiazole ring.[56] The amidoxime **155**, which was prepared from nitrile **104** with hydroxylamine, was treated with methyl chloroformate in the presence of triethylamine in DMF to afford acylamidoxime **158** in 92% yield. Cyclization of **158** by refluxing in xylene provided the 5-oxo-1,2,4-oxadiazole derivative **159** in 64% yield [Scheme 3.13].



155 **158** **159**

Scheme 3.13: *Reagents and conditions:* i) $ClCO_2Me$, Et_3N, DMF, rt, 18 h; ii) xylene, 145 °C, 24 h.[2,57]

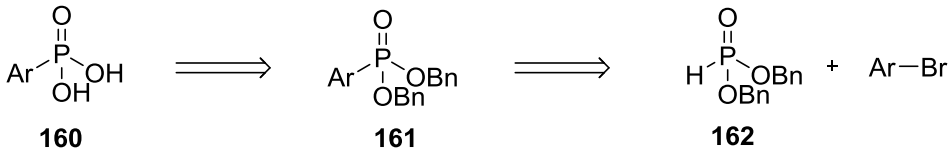
3.5.2 Synthesis of Phosphonic acid Bioisosteres

In recent years phosphonic acids have also attracted considerable attention in medicinal chemistry due to their ability to function as effective bioisosteres for the carboxylic acid group.[58] A study of a range of carboxylic and phosphonic acids analogues indicated that substitution of a phosphonic acid for a carboxylic acid group lowers the value of log P by about 1 log unit.[59] However, there is an increase in acidity in the range of 1.0 to 1.5 pH units, which may be a limiting factor in the absence of active transport.[59] In addition, while carboxylic groups are monoprotic acids (pKa of CH_3COOH = 4.76), phosphonic groups are diprotic (for $CH_3PO_3H_2$: pKa_1 = 3.4; pKa_2 = 7.8).[44,60]

During the lead optimisation stage, if it is desired to lower the log P of the active compound, and increased acidity is not a limiting factor, substitution of a carboxylic acid group by a phosphonic acid would be a viable approach.[59] The presence of marketed drugs containing a

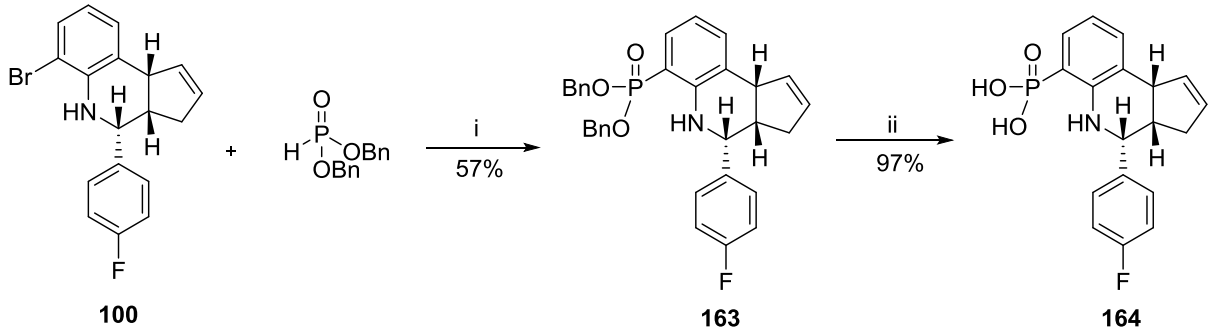
phosphonic acid group indicates that this bioisosteric group has an important role in drug design.

A number of methods have been described in the literature for the synthesis of aryl phosphonates, including the esterification of arylphosphonic dichlorides with alcohols[61] and the decarbonylation of arylketophosphonates.[62] However, the current state of the art method for the direct formation of *sp2* hybridized carbon-phosphorous bonds (first introduced by Hirao *et al.*)[63] involves Pd-catalyzed cross-coupling reaction of H-phosphonates with aryl and vinyl halides [Scheme 3.14]. It was envisaged that a benzyl protected phosphonate **161** could be introduced *via* this route to the bromo-tetrahydroquinoline **100**, followed by catalytic hydrogenation or hydrolysis to yield the desired phosphonic acid derivative **160**.



Scheme 3.14: Retrosynthesis of an aryl-phosphonate derivative **160**.

Stawinski *et al.* introduced an efficient and fast microwave-assisted Pd-catalysed cross-coupling of aryl halides with H-phosphonate diesters.[64] This procedure was employed for the synthesis of a phosphonic acid bioisostere derivative of compound **P00341**. First, the bromo-tetrahydroquinoline **100** was subjected to dibenzyl phosphite in THF in the presence of 5 mol% $Pd(PPh_3)_4$ and caesium carbonate. The mixture was heated to 120 ºC in a microwave for 30 minutes to afford the corresponding dibenzyl phosphonate **163** in 57% yield. This was followed by hydrolysis of the diester with bromotrimethylsilane in CH_2Cl_2 to afford the desired phosphonic acid derivative **164** in 97% yield [Scheme 3.15].

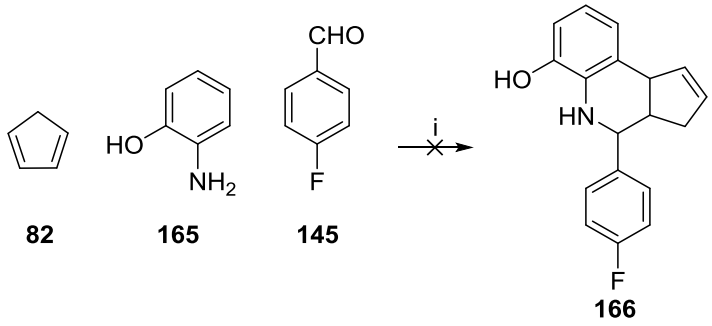


Scheme 3.15: *Reagents and conditions:* i) $Pd(PPh_3)_4$ (5 mol%), Cs_2CO_3, CH_2Cl_2, 120 ºC, 30 min; ii) TMSBr, CH_2Cl_2, 18 h, MeOH, 12 h.

3.5.3 Synthesis of Sulfonate Bioisostere

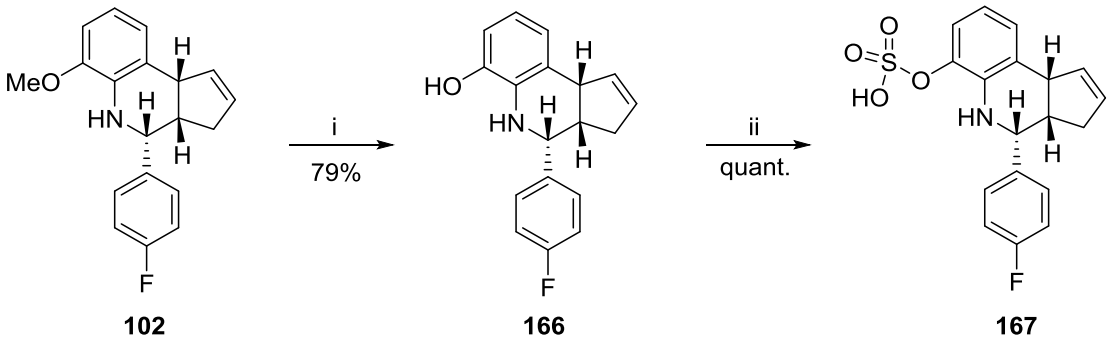
Sulfonic acidic groups, like phosphonates have been classified as non-planar bioisosteric surrogates of the carboxylic acid function and have been extensively used in drug development.[44] Like carboxylic acids, they are ionized at physiological pH but have a considerably better pharmacokinetic profile. Compounds with a sulfonic acid groups are much more acidic with the pKa of CH_3SO_3H being -2.6 relative to 4.76 for CH_3COOH and tend to form longer hydrogen bonding interactions than carboxylic and phosphonic groups.[59] Synthesis of these bioisosteres typically involves sulfation of alcohols using chlorosulfonic acid or sulfur trioxide reagents to produce the characteristic C-SO_3 configuration.

In order to prepare the phenolic analogue **166** of tetrahydroquinoline **P00341** which could then be converted into the sulfonic acid bioisostere, *p*-fluorobenzaldehyde and 2-aminophenol were reacted with cyclopentadiene in the presence of a catalytic amount of $BF_3{\cdot}OEt_2$. However, this attempted one-pot synthesis afforded a complex mixture of products from which the product **166** could not be isolated [Scheme 3.16].



Scheme 3.16: i) $BF_3 \cdot OEt_2$ (20 mol %), CH_3CN, $MgSO_4$, rt.

It was envisaged that the methoxy-tetrahydroquinoline **102** previously synthesised could be demethylated to release the desired phenolic analogue. Such a reaction was reported by Konieczny *et al.* where they described the use of boron trifloride-methyl sulfide complex for the selective cleavage of a range of allyl- and phenyl ethers.[65] Methyl ether **102** was deprotected using six equivalents of this reagent in CH_2Cl_2 at room temperature and after six hours **166** was afforded in 79% pure yield. Subsequent reaction of this compound with ten equivalents of pyridine-sulfur trioxide complex in DMF/Pyridine (1:1) afforded the sulfonic acid derivative **167** in quantitative yield [Scheme 3.17]. This sulphonate ester was found to be relatively stable with a shelf-life of several months, as judged by ^{1}H NMR analysis.



Scheme 3.17: i) $BF_3 \cdot SMe_2$, CH_2Cl_2, rt, 6 h; ii) pyridine-sulfur trioxide complex, DMF/Pyridine (1:1), rt, 20 h.[66]

3.6 Biological Testing

The synthesised compounds **P00104** and **P00341** and their analogues were tested for inhibitory activity against tyrosine phosphatase PTPN22, using both optimised malachite green and *p*-NPP assays (as described in chapter 2). The cytotoxicity of these compounds was also tested against two neuroblastoma cell lines SH-N-SY and LAN5. Compounds displaying significant neuroblastoma cell death were further subjected to selectivity tests using the control cell line 293T (as described in chapter 2).

3.6.1 Malachite Green and *p*-NPP Assay Results

From all of the analogues tested, including the bioisosteres of compound **P00341**, none showed any inhibitory activity against PTPN22 in either assay (Figure 3.10 and 3.11). On average, all compounds tested seemed to have enhanced the enzymatic activity by about 30% (Figure 3.10 and 3.11).

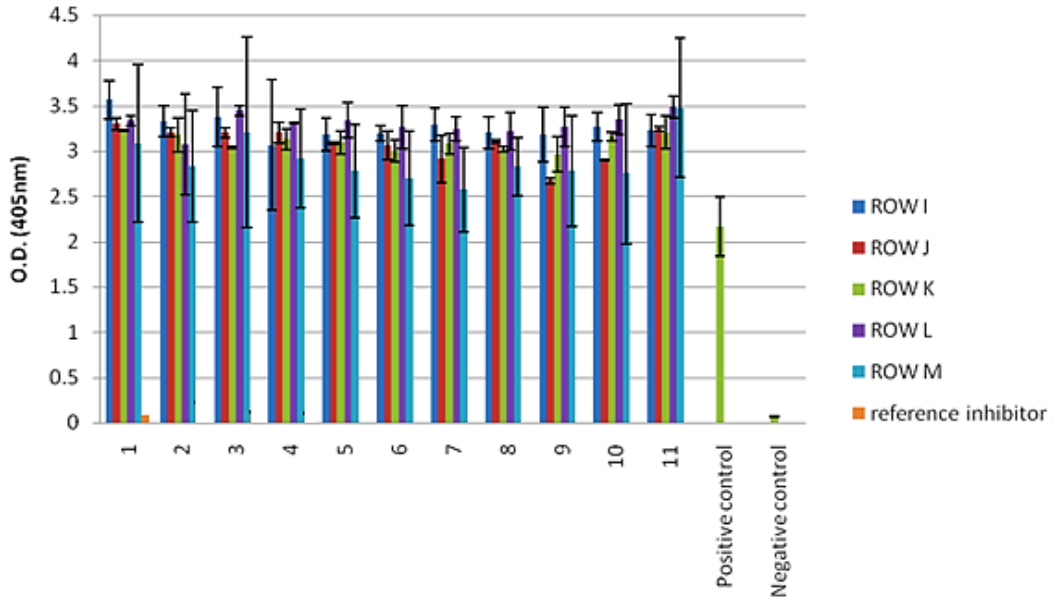


Figure 3.10: Determination of the level of inhibition exhibited by compounds P00104 and P00341 and analogues using the malachite green assay, at an enzyme concentration of 0.13 µM and a substrate concentration of 20 µM (buffer pH 7.2). The reaction was quenched after 30 min incubation with malachite green ammonium molybdate dye solution (50 µl). The assay was performed in duplicates. Reference inhibitor = vanadate.

The observed overactivity can be due to many number of factors, as discussed in detail in chapter two, including inhibition of enzyme aggregation or possible non-specific activation of the enzyme. In summary, the tetrahydroquinoline compounds **P00104** and **P00341** and their derivatives display no inhibitory activity against phosphatase PTPN22.

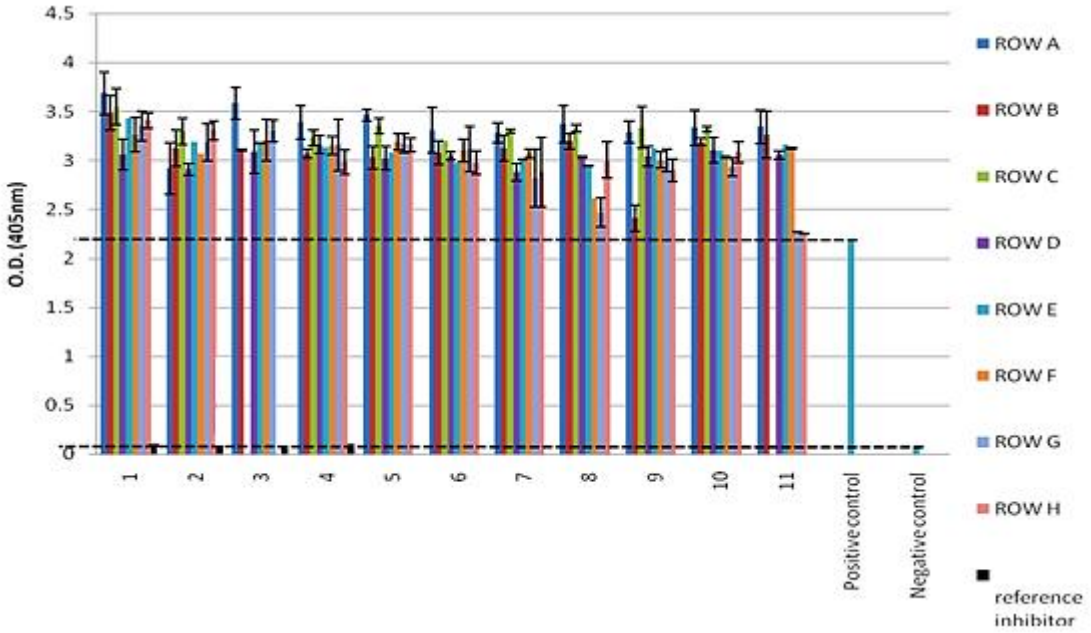


Figure 3.11: Determination of the inhibitory activity of compound P00337 analogues using the *p*-NPP assay, at an enzyme concentration of 500 nM and a substrate concentration of 2 mM (buffer pH 7.5). The reaction was quenched after 60 min incubation with 0.5 M NaOH. The assay was performed in duplicate. The data are presented as mean value ± SD, N=1. Reference inhibitor = vanadate.

3.6.2 Neuroblastoma cell line assays

The effect of each **P00104** and **P00341** analogue was tested against the neuroblastoma cell line SH-N-SY at concentrations ranging from 5 μM to 200 μM, under standard culture conditions (see appendix for protocol). After the treatment period of 6 days, only compounds **101**, **104** and **122** caused considerable cell death of more than 90% at 50 μM (Figure 3.12).

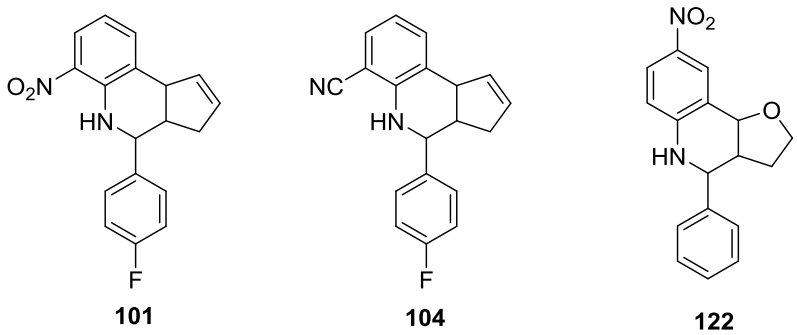


Figure 3.12: The structure of **P00341** analogues that were cytotoxic towards the neuroblastoma cell line SH-N-SY at 50 μM.

The specificity of the cytotoxic compounds **101**, **104**, and **122** was further investigated using the neuroblastoma cell line, LAN5 and the control cell line, 293T. All three compounds exhibited no selectivity towards neuroblastoma cells as they displayed high cytotoxicity towards the control cell line 293T as well (Figure 3.13).

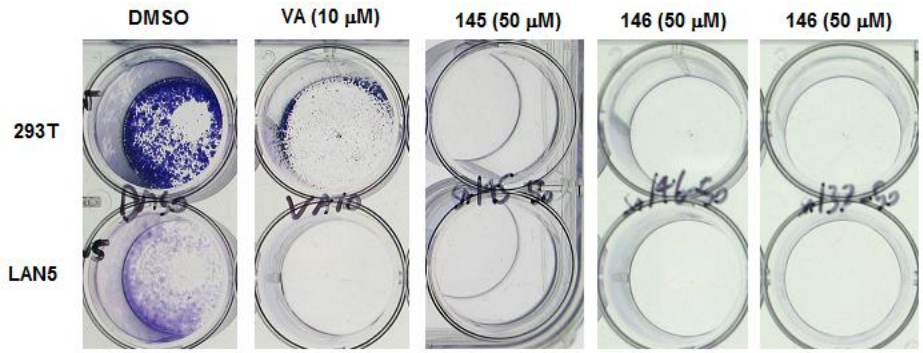


Figure 3.13: Compounds **101**, **104** and **122** induce cytotoxicity in an unselective manner against neuroblastoma cell LAN5 and the normal cell representative 293T. After the 6 days treatment period, all neuroblastoma and 293T cells were killed at 50 µM concentration of each compound. VA = vanadate (a general non-specific PTP inhibitor).

3.7 Conclusion and Future Work

A stereoselective route to tetrahydroquinolines **P00104** and **P00341** and their analogues was identified and optimised. A range of analogues of both compounds was prepared, including a series of bioisosteric replacements of the carboxylate functionality for **P00341**. Unfortunately, none of the compounds, including the authentic samples of the hits were confirmed as PTP inhibitors, and whilst some analogues induced cell death in neuroblastoma cell lines, no selective cytotoxicity was observed when compared to non-transformed cells.

As the hits obtained from the high-throughput screening proved ineffective, attention was turned towards another synthetic strategy for the development of a neuroblastoma inhibitor. This route involved investigations into finding a versatile synthetic route to the recently discovered natural product lead with promising anti-tumour activity, *i.e.* the synthesis of methyl jasmonate and its analogues.

3.8 References

1. Russell, A. DPhil Thesis, University of Oxford, **2004**.
2. Katritzky, A. R.; Rachwal, S.; Rachwal, B. *Tetrahedron* **1996**, *52*, 15031-15070.
3. Murarka, S.; Zhang, C.; Konieczynska, M. D.; Seidel, D. *Org. Lett.* **2009**, *11*, 129-132.
4. Kokwaro, G. O.; Taylor, G. *Drug Chem. Toxicol.* **1990**, *13*, 347-354.
5. Williamson, N. M.; March, D. R.; Ward, A. D. *Tetrahedron Lett.* **1995**, *36*, 7721-7724.
6. Reynolds, G. P.; Pearson, S. J.; Hutson, P. H. *J. Neurol. Sci.* **1994**, *125*, 46-49.
7. Ryabukhin, S. V.; Plaskon, A. S.; Volochnyuk, D. M.; Pipko, S. E.; Tolmachev, A. A. *Synth. Commun.* **2008**, *38*, 3032-3043.
8. Patti, A.; Pedotti, S. *Tetrahedron* **2010**, *66*, 5607-5611.
9. Sridharan, V.; Avendano, C.; Menendez, J. C. *Synthesis* **2008**, 1039-1044.
10. Kouznetsov, V. V. *Tetrahedron* **2009**, *65*, 2721-2750.
11. Kruszynski, R.; Wieczorek, W. *Heteroat. Chem.* **2005**, *16*, 613-620.
12. Sabitha, G.; Reddy, M. S. K.; Arundhathi, K.; Yadav, J. S. *ARKIVOC* **2006**, 153-160.
13. Bigi, F.; Carloni, S.; Frullanti, B.; Maggi, R.; Sartori, G. *Tetrahedron Lett.* **1999**, *40*, 3465-3468.
14. Ballini, R.; Bigi, F.; Conforti, M. L.; De Santis, D.; Maggi, R.; Oppici, G.; Sartori, G. *Catal. Today* **2000**, *60*, 305-309.
15. Nagarajan, R.; Magesh, C. J.; Perumal, P. T. *Synthesis* **2004**, 69-74.
16. Kumar, R. S.; Nagarajan, R.; Perumal, P. T. *Synthesis* **2004**, 949-959.
17. Povarov, L. S. *Russ. Chem. Rev.* **1967**, *36*, 656-660.
18. Ma, Y.; Qian, C. T.; Xie, M. H.; Sun, J. *J. Org. Chem.* **1999**, *64*, 6462-6467.
19. Crousse, B.; Begue, J. P.; Bonnet-Delpon, D. *J. Org. Chem.* **2000**, *65*, 5009-5013.
20. Kobayashi, S.; Ishitani, H.; Nagayama, S. *Chem. Lett.* **1995**, 423-424.
21. Mellor, J. M.; Merriman, G. D. *Tetrahedron* **1995**, *51*, 6115-6132.
22. Kobayashi, S.; Nagayama, S. *J. Am. Chem. Soc.* **1996**, *118*.
23. Yadav, J. S.; Reddy, B. V. S.; Sunitha, V.; Reddy, K. S. *Adv. Synth. Catal.* **2003**, *345*, 1203-1206.
24. Wood, E.; Crosby, R. M.; Dickerson, S.; Frye, S. V.; Griffin, R.; Hunter, R.; Jung, D. K.; McDonald, O. B.; McNutt, R.; Mahony, W. B.; Peel, M. R.; Ray, J.; Lackey, K. *Anti-Cancer Drug Des.* **2001**, *16*.
25. Baudelle, R.; Melnyk, P.; Deprez, B.; Tartar, A. *Tetrahedron* **1998**, *54*.
26. Mahesh, M.; Reddy, C. V.; Reddy, K. S.; Raju, P. V. K.; Reddy, V. V. N. *Synth. Commun.* **2004**, *34*.

27. Friedman, H. L. *Influence of isosteric replacements upon biological activity, Symposium on Chemical-Biological Correlation,* National Research Council Publication, Washington, DC, **1951**.

28. Watson, P.; Willett, P.; Gillet, V. J.; Verdonk, M. L. *J. Comput. Aided Mol. Des.* **2001**, *15*.

29. Burger, A. *Prog. Rech. Pharm.* **1991**, *37*, 287-371.

30. Meanwell, N. A. *J. Med. Chem.* **2011**, *54*, 2529-2591.

31. Kalgutkar, A. S.; Daniels, J. S. *Metabolism, Pharmacokinetics and Toxicity of Functional Groups: Impact of Chemical Building Blocks on ADMET*, **2010**, *0*, 99-167

32. Skonberg, C.; Olsen, J.; Madsen, K. G.; Hansen, S. H.; Grillo, M. P. *Expert Opin. Drug Metab. Toxicol.* **2008**, *4*, 425-438.

33. Olsen, J.; Bjornsdottir, I.; Tjornelund, J.; Hansen, S. H. *J. Pharm. Biomed. Anal.* **2002**, *29*, 7-15.

34. Parkinson, A.; Ogilvie, B. W.; Paris, B. L.; Hensley, T. N.; Loewen, G. J. In *Biotransformation and Metabolite Elucidation of Xenobiotics*; John Wiley & Sons, Inc., **2010**, 1-77.

35. Moran, E. J.; Sarshar, S.; Cargill, J. F.; Shahbaz, M. M.; Lio, A.; Mjalli, A. M. M.; Armstrong, R. W. *J. Am. Chem. Soc.* **1995**, *117*, 10787-10788.

36. Andersen, H. S.; Iversen, L. F.; Jeppesen, C. B.; Branner, S.; Norris, K.; Rasmussen, H. B.; Moller, K. B.; Moller, N. P. H. *J. Biol. Chem.* **2000**, *275*, 7101-7108.

37. Huang, P.; Wei, C. C.; Tang, P. C.; Liang, C.; Ramphal, J.; Jallal, B.; Biltz, J.; Li, S.; Mattson, M.; McMahon, G.; Koenig, M. U.S. Patent 6596772, March 24, **2003**.

38. Ibrahimi, O. A.; Wu, L.; Zhao, K.; Zhang, Z. Y. *Bioorg. Med. Chem. Lett.* **2000**, *10*, 457-460.

39. Sodeoka, M.; Baba, Y. *J. Synth. Org. Chem. Japan* **2001**, *59*, 1095-1102.

40. Bartlett, D. W.; Clough, J. M.; Godwin, J. R.; Hall, A. A.; Hamer, M.; Parr-Dobrzanski, B. *Pest Manag. Sci.* **2002**, *58*, 649-662.

41. Eden, J. M.; Higginbottom, M.; Hill, D. R.; Horwell, D. C.; Hunter, J. C.; Martin, K.; Pritchard, M. C.; Rahman, S. S.; Richardson, R. S.; Roberts, E. *Eur. J. Med. Chem.* **1993**, *28*, 37-45.

42. Gezginci, M. H.; Martin, A. R.; Franzblau, S. G. *J. Med. Chem.* **2001**, *44*, 1560-1563.

43. Herr, R. J. *Biorg. Med. Chem.* **2002**, *10*, 3379-3393.

44. King, F. D. *Medicinal chemistry: Principles and practice*; 2nd edition; Royal Society of Chemistry, **2003**.

45. Hansch, C.; Leo, A.; Hoekman, D. *Exploring QSAR: Hydrophobic, electronic, and steric constants*; American Chemical Society **1995**; Vol. 2.

46. Nie, Y.-y.; Da, Y.-j.; Zheng, H.; Yang, X.-x.; Jia, L.; Wen, C.-h.; Liang, L.-s.; Tian, J.; Chen, Z.-l. *Biorg. Med. Chem.* **2012**, *20*, 2747-2761.

47. Lamberth, C.; Dinges, J. u. *Bioactive Heterocyclic Compound Classes: Agrochemicals*, Wiley VCH, First edition, **2012**.

48. Dinadayalane, T. C.; Punnagai, M.; Sastry, G. N. *J. Mol. Struct.* **2003**, *626*, 247-262.

49. Hasegawa, M.; Takenouchi, K.; Takahashi, K.; Takeuchi, T.; Komoriya, K.; Uejima, Y.; Kamimura, T. *J. Med. Chem.* **1997**, *40*, 395-407.

50. Goldberg, K.; Groombridge, S.; Hudson, J.; Leach, A. G.; MacFaul, P. A.; Pickup, A.; Poultney, R.; Scott, J. S.; Svensson, P. H.; Sweeney, J. *Med. chem. comm.* **2012**, *3*, 600-604.

51. de Oliveira, C. S.; Lira, B. F.; Barbosa-Filho, J. M.; Lorenzo, J. G. F.; de Athayde-Filho, P. F. *Molecules* **2012**, *17*, 10192-10231.

52. Bostrom, J.; Hogner, A.; Llinas, A.; Wellner, E.; Plowright, A. T. *J. Med. Chem.* **2012**, *55*, 1817-1830.

53. Kumar, D.; Narayanam, M. K.; Chang, K.-H.; Shah, K. *Chem. Biol. Drug Des.* **2011**, *77*, 182-188.

54. de Melo, S. J.; Sobral, A. D.; Lopes, H. D.; Srivastava, R. M. *J. Braz. Chem. Soc.* **1998**, *9*, 465-468.

55. Kayukova, L. A.; Gapparova, G. I. *Khim.-Farm. Zh.* **2005**, *39*, 32-40.

56. Kohara, Y.; Imamiya, E.; Kubo, K.; Wada, T.; Inada, Y.; Naka, T. *Bioorg. Med. Chem. Lett.* **1995**, *5*, 1903-1908.

57. Jakopin, Z.; Dolenc, M. S. *Curr. Org. Chem.* **2008**, *12*, 850-898.

58. Kehler, J.; Hansen, H. I.; Sanchez, C. *Bioorg. Med. Chem. Lett.* **2000**, *10*, 2547-2548.

59. Franz, R. D. *AAPS Pharmsci* **2001**, *3*, E10.

60. March, J. *Advanced Organic Chemistry*; Third edition, Wiley, **1985**.

61. Siddall, T. H.; Prohaska, C. A. *J. Am. Chem. Soc.* **1962**, *84*, 2502-&.

62. Nakazawa, H.; Matsuoka, Y.; Yamaguchi, H.; Kuroiwa, T.; Miyoshi, K.; Yoneda, H. *Organometallics* **1989**, *8*, 2272-2274.

63. Hirao, T.; Masunaga, T.; Yamada, N.; Ohshiro, Y.; Agawa, T. *Bull. Chem. Soc. Jpn.* **1982**, *55*, 909-913.

64. Kalek, M.; Ziadi, A.; Stawinski, J. *Org. Lett.* **2008**, *10*, 4637-4640.

65. Konieczny, M. T.; Maciejewski, G.; Konieczny, W. *Chem. Inform.* **2005**, *36*, 1575-1577

66. Larsen, S. D.; Barf, T.; Liljebris, C.; May, P. D.; Ogg, D.; O'Sullivan, T. J.; Palazuk, B. J.; Schostarez, H. J.; Stevens, F. C.; Bleasdale, J. E. *J. Med. Chem.* **2002**, *45*, 598-622.

CHAPTER 4

Synthesis of Methyl Jasmonate

4.1 Introduction

The stress hormone methyl jasmonate and its derivatives occur widely in the plant kingdom (Figure 4.1). Methyl jasmonate is a fragrant volatile compound that was first isolated and characterized in 1962 by Demole and coworkers from the oil derived from *Jasminum grandiflorum*.[1] Jasmonates are fatty acid derived cyclopentanones and share structural and biofunctional similarities to the prostaglandin hormone in mammals. These plant hormones help regulate plant growth and development, are signal transmitters in interplant communication and play a major role in mediating responses against biotic and abiotic stresses.[2-5]

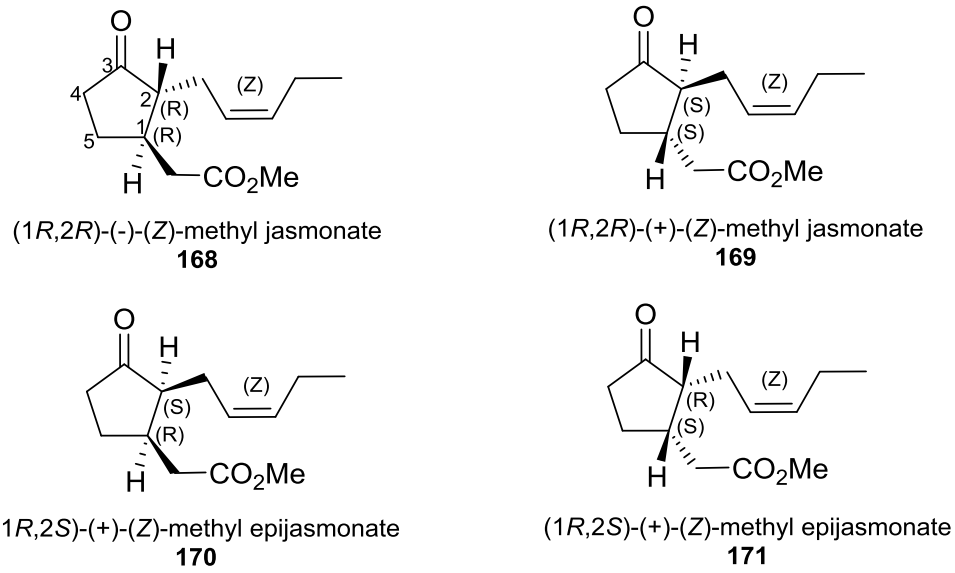


Figure 4.1: Structures of the four stereoisomers of jasmonate.

The elegant, radiant and rich floral jasmine scent is associated with methyl jasmonate and few of its analogues and have made this highly expensive molecule central to the perfume industry for centuries.[6] Four stereoisomers of methyl jasmonate have been observed in nature: (1*R*,2*S*)-(+)-(*Z*)-methyl epijasmonate **171** has the strongest odour whereas (1*R*,2*R*)-(-)-(*Z*)-methyl jasmonate **168** has a weak odour and the remaining two isomers **169** and **170** are odourless.[7]

Although it has been a synthetic target for many years due to its significance in perfumery industries, in recent years several groups have reported a novel property of this compound. Methyl jasmonate and some of its synthetic derivatives have been shown to exhibit anticancer activity *in vitro* and *in vivo* against a number of neoplasms.[8-10] In addition, methyl jasmonate increased the life span of EL-4 lymphoma-bearing mice and is capable of inducing cancer cell death *via* a mechanism independent of protein translation, p53 expression and cellular mRNA transcription, which means it may act directly on mitochondria.[11,12]

4.1.1 Biosynthesis

Methyl jasmonate and jasmonic acid, collectively known as jasmonates, are synthesized in plants *via* an octadecanoid pathway (Figure 4.2). α-Linolenic acid is released from the membrane lipid by phospholipases in response to a certain stimuli: lipoxygenase (LOX) then oxygenates the linolenic acid to form 13-(*S*)-hydroxy linolenic acid (13-HPOT), which is then converted into an unstable allene oxide by allene oxide synthase (AOS). Allene oxide cyclase (AOC) converts the allene oxide into 12-oxo-phytodienoic acid (OPDA) and the jasmonic acid is then afforded after a further reduction and three β-oxidation steps. Catabolization of jasmonic acid by a carboxyl methyltransferase (JMT) and epimerization yields the volatile methyl jasmonate.[3,5]

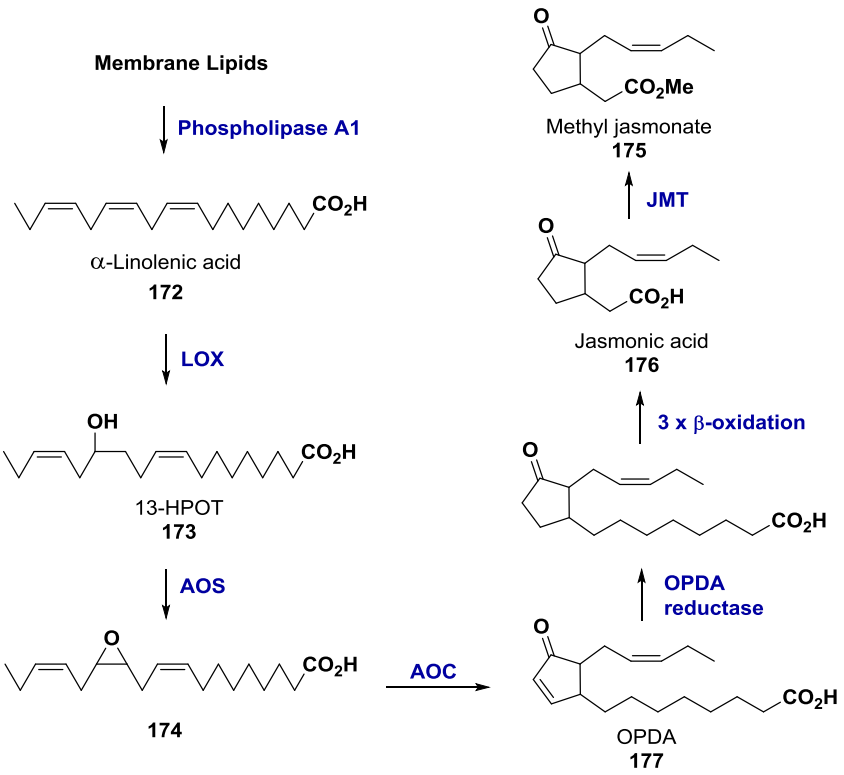


Figure 4.2: The main pathway of methyl jasmonate biosynthesis.

4.1.2 Methyl Jasmonate in Cancer

Cancer, medically known as malignant neoplasm, is a group of more than two hundred different and distinctive diseases, characterized by an abnormal growth of cells which tend to proliferate in an uncontrolled manner. It is the leading cause of death worldwide, accounting for around 13% of all deaths in 2008.[13] Consequently, there has been an extensive search of various natural products, especially plant-derived natural products, as a source of potential anticancer drugs. This research can be dated back as early as the Ebers Papyrus in 1550 BC but a more systematic investigation began with Hartwell's group in 1960s.[14,15] Thus far, over 60% of currently used anticancer agents are derived from natural sources including the well-known paclitaxel, camptothecin, vinblastine and vincristine.[16-18]

Salicylic acid, a plant stress hormone, suppresses the growth of various types of cancer cells. Based on this knowledge, in 2002 Flescher *et al.* began their investigation of the potential anticancer properties of the major plant stress hormone family called the jasmonates.[11] This group, along with a number of others have since reported that jasmonates and some of their natural derivatives, exhibit anti-cancer activity *in vitro* and *in vivo* (Figure 4.3). Flescher *et al.* have reported that jasmonates inhibited cellular proliferation and induced cell death in several human and murine cancer cell lines including prostate, breast, melanoma, lymphoblastic leukaemia and lymphoma carcinoma cells, as well as lung and myeloid leukaemia cells.[11] Jasmonates were also shown to induce suppression of cellular proliferation and death in lung and myeloid leukaemia cells.[8-10]

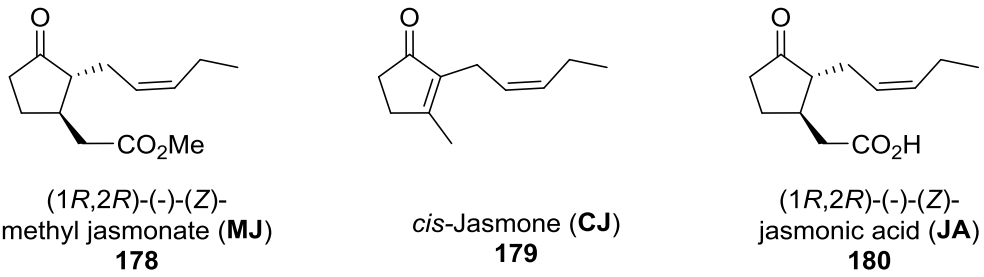


Figure 4.3: Structures of naturally occurring jasmonates.

Furthermore, these molecules were observed to have selective cytotoxicity towards cancer cells in a mixed population of leukaemic and normal cells drawn from the blood of chronic lymphocytic leukaemia (CLL) patients, as well as increasing the life span of T-cell lymphoma-bearing mice.[11,19] The most important properties of jasmonates are certainly their high selective cytotoxicity towards cancer cells whilst being inactive towards normal healthy cells, and having the ability to act on drug resistant cells.[20] The evidence for the first characteristic was confirmed by the study of Fingrut and Flescher on the leukaemic MOLT-4 cell line, where methyl jasmonate (MJ) was proven to be considerably more cytotoxic towards

this malignant cell line than towards normal lymphocytes.[11] Jasmonate anticancer activity against drug resistant cells was validated using two clones of B-lymphoma cells of the same line differing in their p53 expression; wild type p53 *versus* mutant p53. The response of these two clones to the cytotoxic drug bleomycin and the radiomimetic neocarzinostatin (NCS) weas drastically different, *i.e.* the p53 mutant clone was considerably less susceptible to these drugs.[20] In contrast, both clones were equally sensitive towards the jasmonate-induced cytotoxic effects. MJ mostly caused apoptotic death in the wild type cells and necrotic death in the mutant cells, which indicates that jasmonates can circumvent drug resistance in mutant p53-expressing cells by inducing a non-apoptotic mode of cell death.[19]

The three naturally occurring jasmonates that have been studied as anti-cancer agents are methyl jasmonate, jasmonic acid (JA) and *cis*-jasmone (CJ) (Figure 4.3). While molecular target(s) have yet to be elucidated, several studies have revealed that MJ exhibits the most activity and accordingly have been further studied in various cellular systems. Whilst comparing the effects of naturally occurring MJ and JA *in vitro* using leukaemia, lymphoma, breast, prostate and melanoma cancer cells as targets, Flescher observed that MJ showed greater cytotoxicity and activation of caspase-3 which is a marker of apoptosis.[20] Studies conducted by Samaila *et al*. concluded that the order of sensitivity of two prostate cancer cell lines was found to be MJ > CJ > JA.[10] The same order of sensitivity was also observed by Fingrut *et al* on the leukemic cells of CLL patients.[12] The methyl ester group seems to be strongly associated with the cytotoxic effect of MJ which could be the result of higher affinity for the supposed target or improved permeation of cells, although a definitive conclusion has yet to be established.[19]

The ability of MJ to inhibit the metastatic process was also investigated by Reischer *et al.* in the model of metastatic melanoma.[21] Metastatic cancer cells are able to move within tissues by their own motility mechanism and can invade and localize distant tissues and organs. Once

metastasis begins, local therapy alone is not sufficient to cure the patients and alternative treatment is necessary to control the migration of malignant cells. MJ at a concentration that neither reduces cell number nor affects cellular ATP stores has been shown to interfere with the melanoma cell motility *in vitro*. Exposure of murine lung melanoma to 75 mg/kg of MJ *in vivo* (the highest non-toxic dose), has also revealed a significant reduction in growth. These findings show that MJ as well as inducing cell death and suppressing proliferation can also affect other functions of cancer cells, in this case, cellular motility.[21]

Ezekwudo *et al*. studied the combined effect of MJ and γ-radiation on the human prostate cell line PC-3.[22] When hormone refractory human prostate cancer cell lines are exposed to radiation, they activate anti-apoptotic proteins of the Bcl-2 family and hence are resistant to radiotherapy. The combination of MJ and γ-radiation therapy proved to be much more effective than the single treatments. As predicted, radiation alone caused little or no caspase-3 activity, therefore having minimal cytotoxic effect on these cells. However, a five-fold increase in caspase-3 activity was observed when cells were treated with MJ following irradiation, and the data showed a 1.5-fold increase in caspase-3 activity in comparison with the cells receiving the MJ therapy alone.[23]

Flescher *et al.*also investigated the combined effects of MJ with four anticancer drugs, all with different modes of action, namely carmustine, cisplatin, taxol and doxorubicin. Carmustine functions as an alkylating agent by forming covalent bonds with different functional groups of biologically important molecules. Taxol blocks the cell cycle in mitosis by promoting microtubular assembly and stability. Doxorubicin, an antimalignant antibiotic, interacts with DNA by intercalation and inhibits macromolecular biosynthesis. Although the mechanisms of action of these drugs are different to MJ, they all mediate cytotoxic effects *via* indirect mitochondrial perturbation. A cooperative effect of these combined treatments was observed in six cancer cell lines *in vitro* as well as an *in vivo* synergistic effect between MJ

and doxorubicin on murine BCL1 leukaemia. The IC_{50} values of the anticancer drugs were drastically reduced when combined with MJ, therefore revealing a great potential in reduction of unwanted side-effects.[24]

In order to find a novel way of controlling acute myelogenous leukaemia, Ishii *et al* tested the ability of MJ and a series of its derivatives in inducing differentiation of several human myeloid leukaemia cells (Figure 4.4).[8] The results showed that prolonged exposure to relatively low concentrations of MJ (0.2 – 0.4 mM) inhibited growth and induced re-differentiation of acute myelogenous leukaemia cells in a mitogen-activated protein kinase (MAPK)-dependent manner. All the MJ derivatives tested were relatively more potent than MJ itself; in particular, methyl 4,5-didehydrojasmonate was approximately 30 times more potent. It can therefore be concluded that introducing a double bond at the 4,5-position of the cyclopentanone ring, greatly enhances the anticancer activity of MJ and proves that systematic and detailed investigations of SARs may afford an even more effective jasmonate. Studies on a number of cyclopentenone-bearing compounds such as prostaglandins, clavulones and falconensones, have revealed their anticancer properties induced *via* different mechanisms on a wide spectrum of intracellular targets, ranging from nuclear factors to mitochondria.[25]

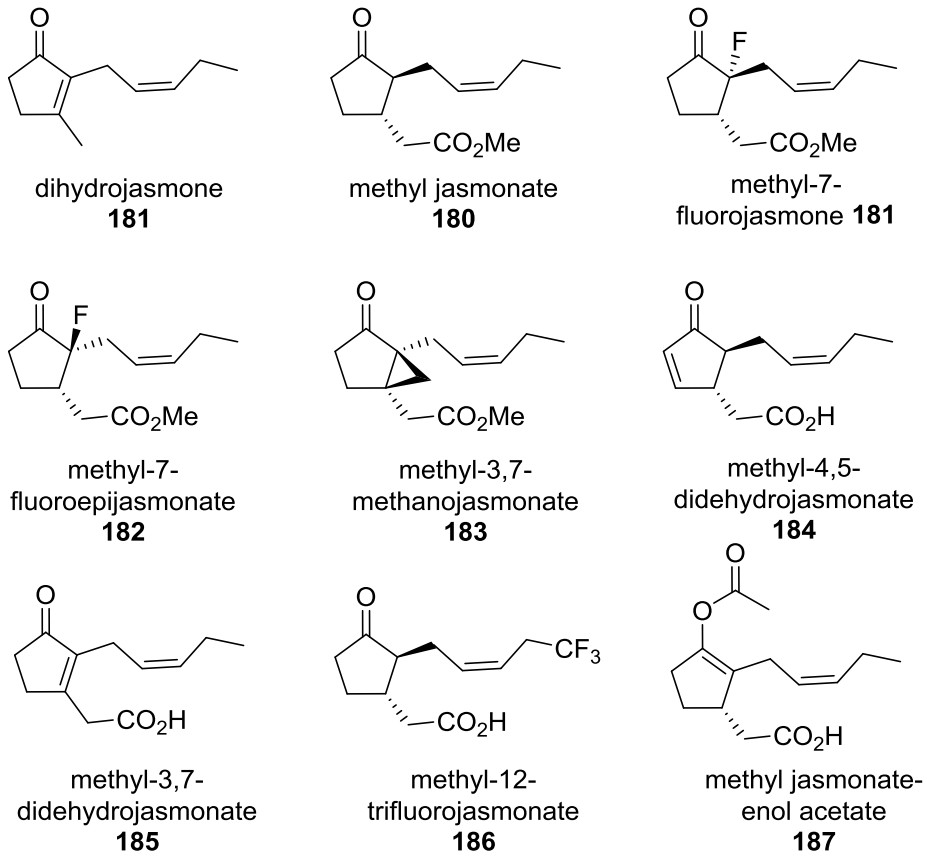


Figure 4.4: Structures of jasmonate derivatives.

In conclusion, jasmonates have proven efficacy against various neoplastic growths and exhibit selective cytotoxicity towards transformed cells. These novel anticancer agents provide hope for the development of new cancer therapeutics and will attract further scientific and pharmaceutical interest.

4.1.3 Mechanism of Action of Jasmonates

Cell death occurs *via* two major mechanisms: necrosis and apoptosis (Figure 4.5). Necrosis, also known as "cell murder", is mediated through external damage *via* destruction of the plasma membrane or the biochemical integrity of the cell's intracellular organelles and

molecules. Necrotic cells appear swollen under the microscope, and the plasma membrane lyses to release cytoplasmic components to the neighbouring tissue. The released necrotic contents attract inflammatory cells causing tissue destruction; this occurs in a matter of few seconds. Some tissues can resolve necrotic death of single cells; however large numbers of cells dying by necrosis leads to permanent modification of tissue architecture as the result of inflammation and subsequent repair and scarring.[26]

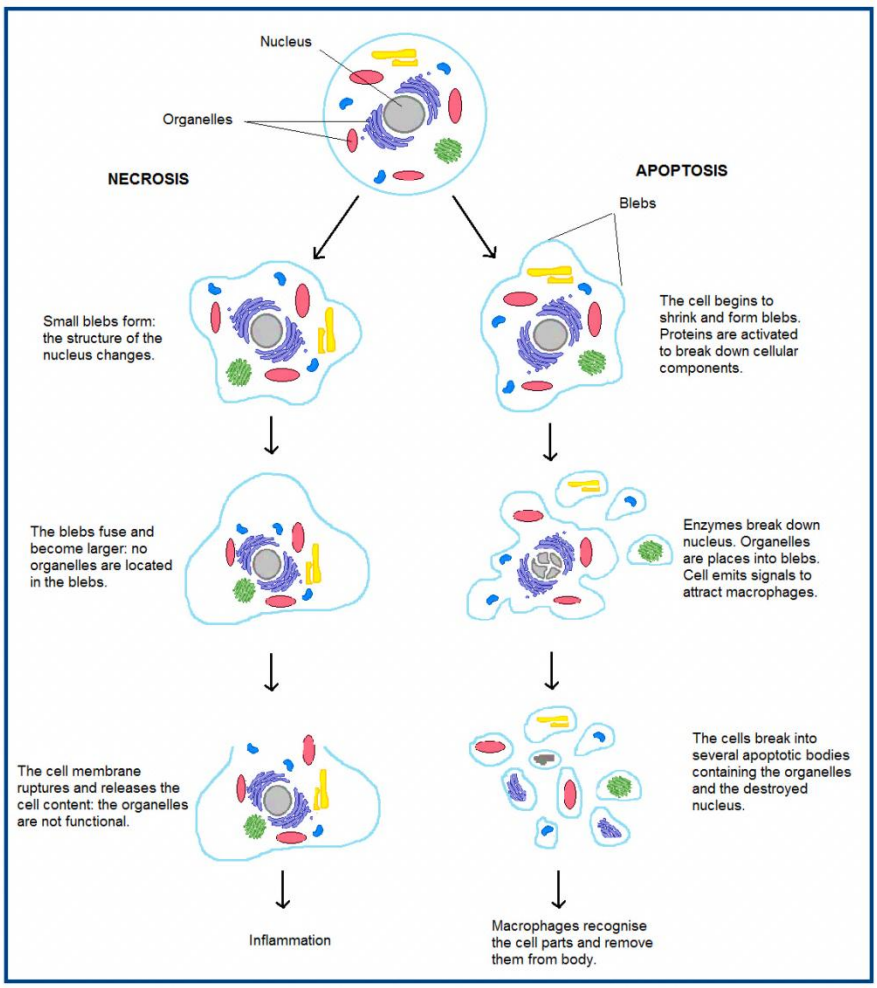


Figure 4.5: Apoptotic verses necrotic morphology.

The second type of cell death is based on the concept of programmed cell death, which entails a genetically coded program of highly controlled biochemical and morphological set of

events which terminates in apoptosis. This type of cell death plays a major role in numerous physiological processes during foetal development and in adult tissue. Defects in apoptotic cell death regulation leads to several diseases, including conditions which result in cell proliferation (cancer, restenosis) or disorders causing cell loss (stroke, heart failure, neurodegeneration, AIDS). This death is similar to "cell suicide" as it is the consequence of intracellular molecular signals and, unlike necrosis, is a much slower process, taking a few hours to several days depending on the initiating signal.[27] Apoptosis begins with acinus, which is accompanied by shrinking of the cell and is followed by nucleus fragmentation, cell surface transformation and splitting of the entire cell content into apoptotic bodies attached to the membrane. The final stage of apoptosis involves activation of caspases, a series of specific cytoplasmic proteases (Figure 4.6). There are multiple initiators of various tightly regulated cascades of events leading to activation of these self-catalytic caspases, two of which have been identified: the extrinsic and intrinsic pathways. The extrinsic pathway is initiated through the stimulation of the transmembrane death receptors, such as the Fas receptors, located on the cell membrane. In contrast, the intrinsic pathway is initiated through the release of signal factors (cytochrome c) by mitochondria within the cell.[26,27]

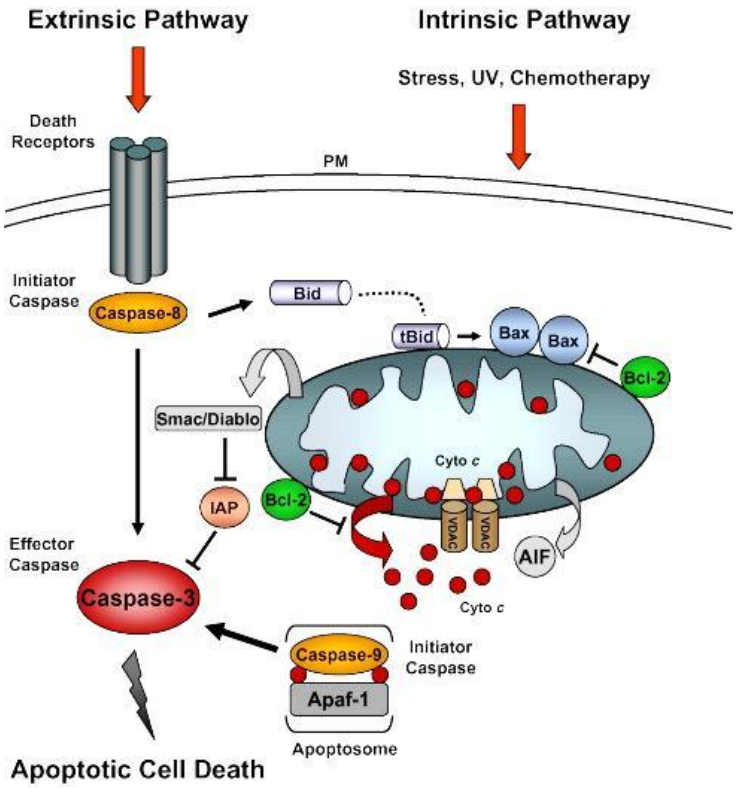


Figure 4.6: A simplified model of the two apoptosis signalling pathways converging to a common execution phase. In the extrinsic, the death receptor at the plasma membrane (PM) is activated, leading to activation of initiator caspase-8 that activates the executioner caspase-3, which in turn, cleaves cellular substrates and brings about formation of apoptotic bodies. In the intrinsic, mitochondria-mediated pathway, multiple stimuli such as Bax can trigger mitochondrial membrane permeabilization, leading to the release of mitochondrial apoptogenic factors (Cyto *c*, AIF) triggering caspase-9 activation which cleaves effector caspases, such as caspase-3.[28]

Chemotherapeutic drugs generally work by inducing apoptosis in cancer cells.[29] The mechanism by which jasmonates suppress cancer cell growth is not fully defined nor are the molecular target(s) with which they interact; however, so far three mechanisms have been proposed to explain their anticancer properties. These include mitochondrial perturbation causing severe ATP depletion in cancer cells, manipulation of mitogen-activated kinase activity to induce re-differentiation of human myeloid leukaemia cells, and generation of hydrogen peroxide and pro-apoptotic proteins of the Bcl-2 family in lung carcinoma cells which induces oxygen species-mediated apoptosis.[24]

4.1.3.1 The Bio-energetic mechanism

Apart from their central bioenergetic role of supplying ATP, mitochondria are commonly known to be pivotal to life and death decisions in cells. Indeed, mitochondrial perturbation may result in both apoptotic and necrotic death.[30] Upon introduction of adverse conditions, permeability transition of mitochondria is initiated *via* the permeability transition pore complex (PTPC). Adenine nucleotide translocator, cyclophilin D, and the voltage-dependent anion channel (VDAC) are central constituents of PTPC. Dissipation of the inner membrane mitochondrial potential occurs as a result of prolonged opening of the PTPC, leading to osmotic swelling of the mitochondrial matrix and release of cytochrome c, and finally cell death by necrosis or apoptosis.[31]

During the last few years, Flescher *et al.* have demonstrated the cytotoxic effects of MJ on mitochondria isolated from cancer cells as well as on the mitochondria of intact, normal and cancer cells.[19] MJ induced perturbation of mitochondria, caused swelling and cytochrome c release in isolated as well as several intact cancer cell lines including lymphocytes drawn from chronic lymphocytic leukaemia patients, whilst having no effect on normal human lymphocytes or non-transformed 3T3 cells.[24,30] Cancer and normal mitochondria differ in several aspects: cancer cell mitochondria have a higher membrane potential, possible modulation of the expression of PTPC constituents, and enhanced rates of ATP generation through glycolysis rather than through oxidative phosphorylation (the latter phenomenon commonly known as the Warburg effect) in cancer cells, perhaps explaining the selective action of jasmonates on these cells. It has been shown that MJ reduces the ATP cellular levels in various cancer cells long before exerting its cytotoxic effect. A positive correlation between susceptibility of cancer cells towards the cytotoxic effect of MJ and the amount of ATP depletion was also observed.[19] As mitochondria have been shown to be the target organelles of MJ, decreases in ATP levels were found to be independent of pyruvate and oligomycin, a

substrate and inhibitor of oxidative phosphorylation, respectively, suggesting the effect of MJ on mitochondrial ATP generation to be substantial and irreversible.[19] In contrast, high glucose levels protected cancer cells from MJ-induced ATP depletion, whilst synergistic effects of the glycolysis inhibitor 2-deoxyglucose (2DG) were observed when administered in combination with MJ.[30]

Furthermore, as jasmonates act directly on the mitochondria of cancer cells in a PTPC-mediated manner, this should grant them with the ability to bypass pre-mitochondrial anti-apoptotic mutations, thus making this compound potentially active against diverse drug-resistant tumours.[19]

A target enzyme of MJ associated with cancer cell mitochondria was discovered to be hexokinase, the initial enzyme in the glycolytic pathway.[30] Its isozymes, hexokinase type I and hexokinase type II associate with mitochondrial VDAC *via* hydrophobic interactions.[32] Mitochondrial perturbation and consequent cell death is linked with dissociation of hexokinase from VDAC. In cancer cells, there is an overexpression of mitochondria-bound hexokinase and VDAC. This factor along with its glucose phosphorylation activity, plays a major role in cancer cell growth rate and survival.[33] Flescher *et al.* have shown that MJ binds specifically to mammalian hexokinase and interferes with its interaction with VDAC, dissociating hexokinase from mitochondria followed by release of cytochrome c. In addition, MJ only disturbs hexokinase-bound mitochondria and overexpression of hexokinase decreases the cytotoxicity of MJ. All these events result in perturbation of mitochondrial permeability and therefore overall cellular bio-energetics.[24,30]

4.1.3.2 The Re-Differentiation Mechanism

Re-differentiation is a procedure *via* which the genetic program of cancer cells is modified to generate a more differentiated genotype and phenotype, thereby "normalizing" an undifferentiated cancer cell by losing its earlier neoplastic characteristics. This modified state proliferates at a slower rate. It was suggested that retinoids, a family of natural and synthetic nuclear receptor ligands, act *via* this mechanism. Re-differentiation of acute promyelocytic leukaemia cells is induced by the FDA-approved All-Trans Retinoic Acid (ATRA); however, it is not very effective as a single treatment agent for other haematopoietic malignancies.[34] Likewise, the family of cytokinin plant hormones also induce re-differentiation in leukemic cells. Hence the cancer cell re-differentiation capability of jasmonates was subjected to study. Suppression of proliferation was observed when MJ was exposed to a number of human malignant cells.[8]

Additionally, Ishii *et al.* investigated the role of several signalling pathways in the MJ-induced re-differentiation of HL-60 cells and concluded that MJ induced the activity of mitogen activated protein kinase (MAPK) in HL-60 cells, and a MAPK inhibitor suppressed re-differentiation induced by MJ as seen by NBT reduction. Therefore, MAPK signalling is probably essential in the re-differentiation induced by MJ.[8]

4.1.3.3 Reactive Oxygen Species (ROS) Mediated Apoptosis

The potential cytotoxic involvement of ROS such as superoxide ion, hydrogen peroxide hydroxyl radical and singlet oxygen in MJ-induced apoptosis was evaluated. Studies by Kim *et al.* showed that apoptosis in human lung carcinoma cells induced by MJ seems to be facilitated by a cascade involving the generation of hydrogen peroxide, and an increased expression of pro-apoptotic members of the Bcl-2 family.[9]

Oh *et al*. observed that MJ stimulates heat shock protein 72 (HSP72) in C6 glioma cells along with increasing levels of cellular hydrogen peroxide, superoxide ions and mitochondrial ROS. Inhibition of hydrogen peroxide and hydroxyl radicals prevented this observed activity. It therefore appears that depending on the type of cancer cell being studied, distinct ROS may mediate the different activities of MJ.[9,20,24]

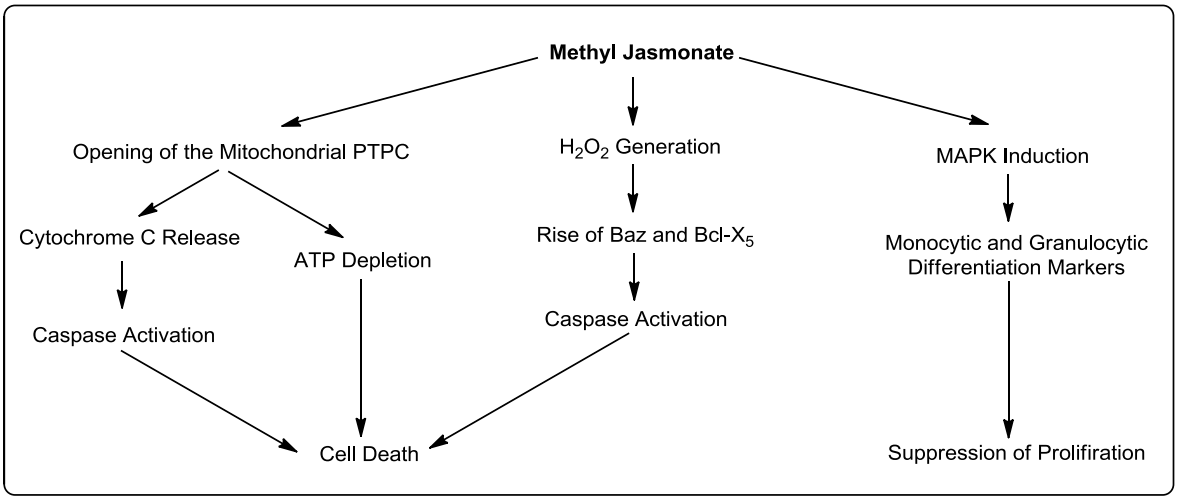


Figure 4.7: Possible pathways of jasmonate action against cancer cells.

In conclusion, the above proposed mechanisms of action suggest that interaction of MJ with cancer cells will either result in re-differentiation or induction of apoptosis (Figure 4.7). The fact that re-differentiation is associated with suppression of proliferation, as well as the abolition of the activity of MJ when inhibitors of the bio-energetic mediators and ROS are used, points towards these three mechanisms being instrumental for the anti-cancer effects of methyl jasmonate.[9,12,20,35]

4.2 Cytotoxic Effect of Methyl Jasmonate on Human Neuroblastoma Cell Lines

Neuroblastoma derived from the neural crest element of the sympathetic nervous system is a highly malignant solid tumour, which accounts for around 10% of all childhood malignancies and 50% of cancer deaths in children.[36] Neuroblastoma patients show heterogeneous clinical courses ranging from life-threatening progression to spontaneous regression and are classified into low-risk, intermediate-risk, and high-risk groups.[37] The molecular mechanisms involved in neuroblastoma development and progression are well understood, which stems from amplification of the N-myc proto-oncogene, deletion of chromosome 1p, and complete or partial gain of the long arm of chromosome 17.[12] Despite the treatment procedures available, including radiation therapy, and high-dose chemotherapy with stem cell rescue, there is still no effective treatment/therapy and poor prognosis for patients with late-stage neuroblastoma as resistance to chemotherapy is common. There is therefore a great need for novel treatments.

Tong *et al.* are the first and only scientists to date who have investigated the effects of MJ on human neuroblastoma cells.[38] Their first study demonstrated that MJ suppressed the growth of human SK-N-SH and BE(2)-C neuroblastoma cell lines in a dose-dependent and time-dependent manner. The mechanism by which MJ exerts its effect was found to be by downregulating proliferating cell nuclear antigen (PCNA) expression in the neuroblastoma cell lines, thereby facilitating cell cycle arrest at G0/G1 phase.[38]

Survivin and X-linked inhibitor of apoptosis protein (XIAP) are the most important members of the inhibitor of apoptosis protein (IAP) family. In neuroblastoma cell lines, expression of survivin is associated with enhanced proliferation rates and more resistance towards drug-mediated or immune-mediated cell death, whereas XIAP expression suppresses apoptosis *via* inhibition of caspase-3 and caspase-7.[39] Inhibitors of IAPs play an essential role in the

regulation of apoptosis of tumour cells.[39] Tong *et al.* demonstrated that MJ induced apoptosis in the SK-N-SH and BE(2)-C cell lines by reducing the expression levels of both XIAP and survivin.[38]

In their second study, Tong *et al* demonstrated that natural jasmonates, *i.e.* methyl jasmonate, jasmonic acid and *cis*-jasmone (Figure 4.3), all suppressed cell proliferation and induced apoptosis in human neuroblastoma SH-SY5Y cells *in vitro* in a dose- and time-dependent manner, but had no effect on a cultured human embryonic kidney (HEK) cell line HEK 293, which is consistent with the previous finding that normal cells are resistant to the cytotoxicity induced by jasmonates.[40]

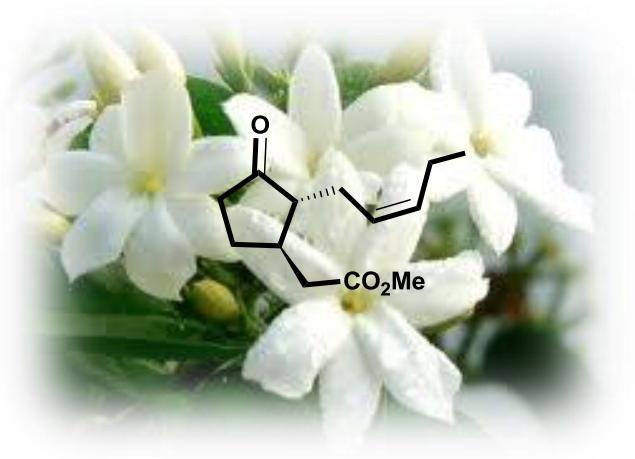
Proliferating cell nuclear antigen (PCNA) and N-myc, are both critical proteins involved in neuroblastoma development and progression. Levels of PCNA directly correlate with the rate of cellular proliferation, and high levels of PCNA expression are associated with poor survival rates. N-myc is a member of proto-oncogene myc family, which has strong oncogenic potential.[41] Overexpression and amplification of the N-myc proto-oncogene are seen in approximately 30% of primary untreated neuroblastomas, which represent an advanced stage of disease, rapid progression and poor prognosis.[42] The downregulation of N-myc expression has been shown to reduce proliferation and/or prompt neuronal differentiation of neuroblastoma cells. It was observed that MJ downregulated PCNA and N-myc in SH-SY5Y cells, which might correlate with the jasmonate-mediated anticancer activity against these neuroblastoma cells.[40]

MJ and CJ were shown to induce apoptosis by triggering G_2/M phase arrest in cultured SH-SY5Y cells. The downregulation of XIAP and survivin by MJ in this cell line was also confirmed. The anticancer activities of the natural jasmonates on SH-SY5Y cells were as follow: methyl jasmonate > *cis*-jasmone > jasmonic acid, confirming that the methyl ester functionality appears to contribute significantly to the cytotoxic effects of MJ.[40]

These findings by Tong *et al.* warrant further investigation into the mechanism of MJ-mediated anticancer activity in neuroblastoma cells. As the structure of jasmonates are different to the current available anticancer drugs, and as they represent new hope for development of cancer therapeutics with less toxicity to healthy cells, potential future research should be directed at the identification of the actual jasmonate target molecule(s), and thus a full SAR analysis to discover new derivatives with superior therapeutic index should be carried out.

4.3 Previous Synthesis of Methyl Jasmonate

Methyl jasmonate (MJ) has great commercial value in the perfumery industry and has been a synthetic target since the early 1960s, as procedures for its extraction have proven laborious and low yielding. MJ represents up to 2-3% of jasmine oil and around 15,000 jasmine blossoms are needed to produce 1.5 g of jasmine oil.



Methyl jasmonate

Due to the high commercial value as well as structural and biological interest in MJ, investigations for the efficient racemic, enantio- and diastereo-selective synthesis of this compound and some of its natural derivatives has received a considerable amount of attention in the past five decades. The synthesis of cyclopentane ring-bearing compounds such as cyclopentanoid natural products and some pharmaceutically important agents remains a challenging task, due to the lack of a general method for construction of appropriately substituted cyclopentane rings in a stereodefined and regiodefined manner.

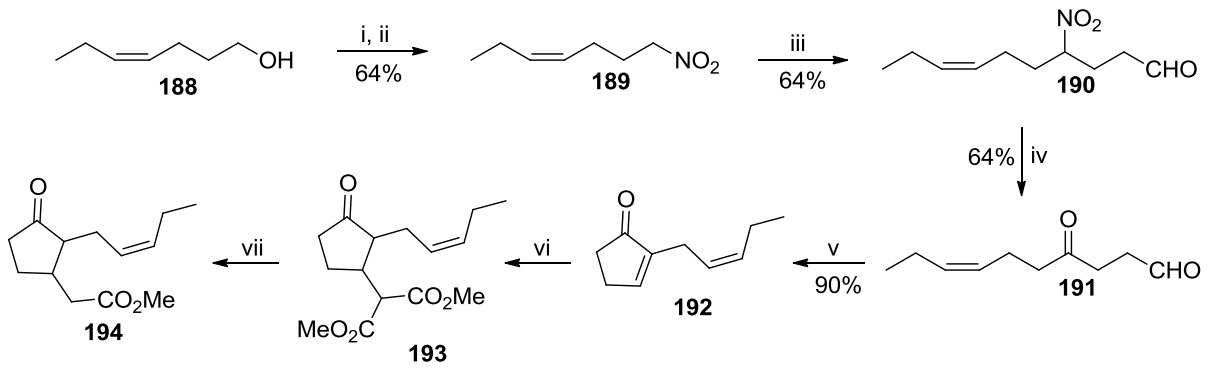
The synthesis of the racemic form of MJ has been achieved via diverse routes from many different precursors. These include addition of substituents to α- and β- position of 2-cyclopentenone and its derivatives *via* different mechanisms; or by starting from acyclic open chain precursors and utilizing different cyclization techniques to construct the disubstituted

cyclopentanone. A handful of asymmetric syntheses have been reported by the use of chiral auxiliaries, asymmetric catalysis or stereocontrolled cyclization using asymmetric induction. A few examples to illustrate the range of reported methods are described below.

4.3.1 Use of Acyclic Compounds as Precursors of MJ

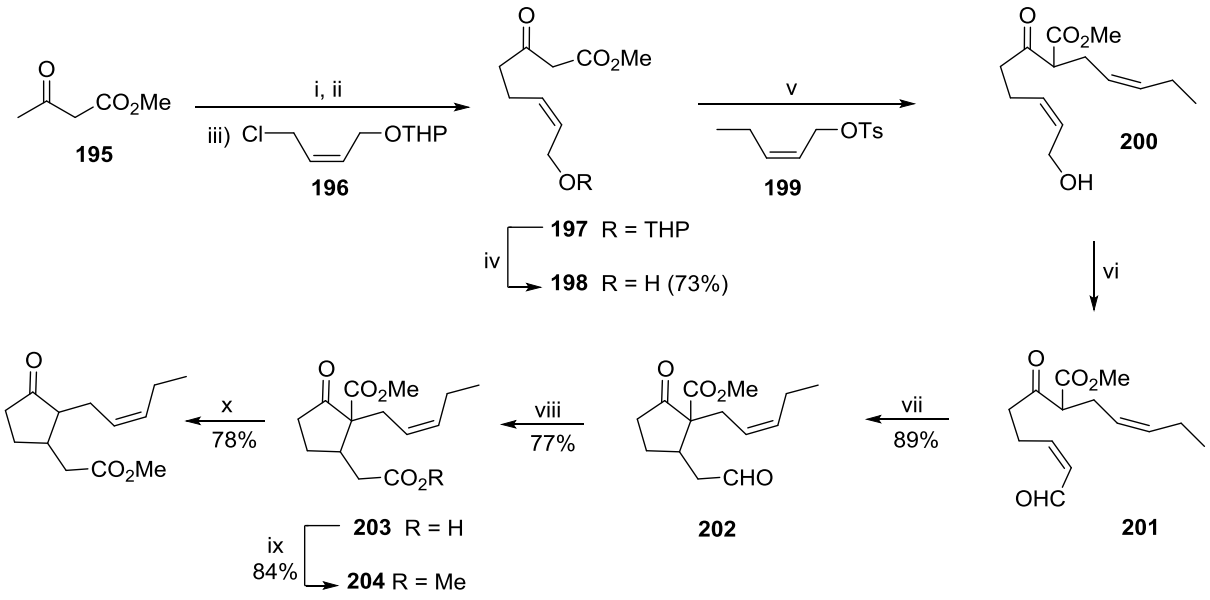
Many groups have reported syntheses of MJ from readily available acyclic precursors, and different cyclization techniques were employed for the preparation of the desired 2,3-disubsituted cyclopentanone.[43-45]

Recognizing that nitro moieties have been used extensively as activating groups for the formation of C-C bonds, Ballini *et al.* have reported an elegant synthesis of methyl jasmonate from the precursor (*Z*)-7-nitro-3-heptene **190** [Scheme 4.1].[46] Conjugate addition of the anion derived from α-deprotonation of the nitro compound to acrolein (by heterogeneous catalysis), followed by a Nef reaction afforded (*Z*)-1,4-dioxodec-7-ene **191**, which is then easily converted into (*Z*)-2-(2-pentenyl)-2-cyclopenten-1-one **193** by cyclodehydration in an aldol-elimination step. Following the Buchi and Egger method,[47] the latter compound was converted into methyl jasmonate.[45,48]



Scheme 4.1: *Reagents and conditions:* i) PBr_3; ii) $NaNO_2$, DMF; iii) acrolein, Al_2O_3 (cat); iv) MeONa, MeOH, H_2SO_4, -25 ºC; v) NaOH, Et_2O; vi) Michael addition of methyl malonate, decarboxylative hydrolysis and esterification.

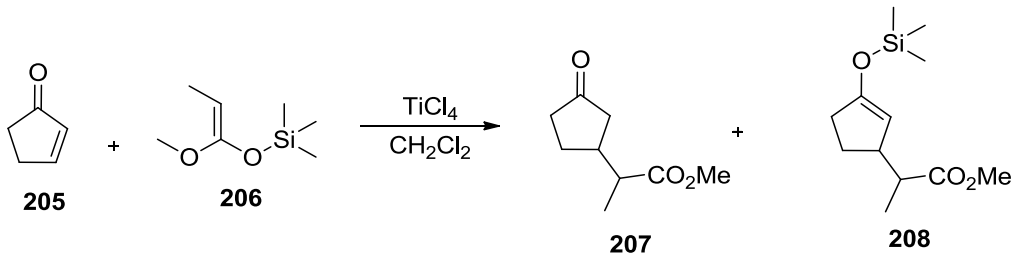
Intramolecular Michael addition has found widespread use in cyclopentane annulation. Lee *et al*. reported a synthetic route towards racemic MJ in which the key intermediate unsaturated aldehyde **201** was prepared from sequential alkylation of methyl acetoacetate **195** with the allylic functionalities 4-chloro-*cis*-2-butenyl THP ether **196** and *cis*-2-penten-1-yl tosylate **199**, followed by an oxidation step [Scheme 4.2]. Cyclization *via* intramolecular Michael addition was achieved by treatment of **201** with caesium fluoride to afford the cyclopentanone **202**. Subsequent oxidation, esterification and Krapcho decarbomethoxylation afforded methyl *dl*-jasmonate.[49] The authors did not comment on the selectivity of the decarbomethoxylation step, but reported the major product as having spectroscopic data consistent with the *trans*-diastereomer.



Scheme 4.2: *Reagents and conditions:* i) NaH, THF, 0 ºC; ii) *n*-BuLi; iii) 4-chloro-*cis*-2-butenyl THP ether **196**; iv) *p*-TsOH, MeOH; v) K_2CO_3, acetone, *cis*-2-penten-1-yl tosylate **199**, reflux; vi) PCC, CH_2Cl_2, 3 h; vii) CsF, THF, 2h; viii) PDC, DMF; ix) MeI, DBU; x) NaCl, wet DMSO, 180 ºC.

4.3.2 Conjugate Addition to Cyclopentenone

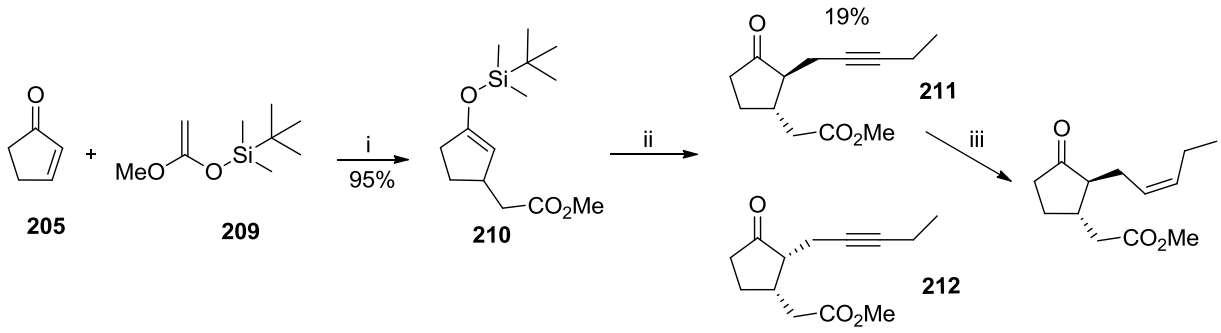
The versatility of cyclopentenone functionalities makes them particularly useful precursors for the synthesis of various cyclopentyl compounds. Cyclopentenone undergoes the classic enone reactions of α,β-unsaturated ketones, including nucleophilic conjugate addition, Baylis–Hillman reaction, and Michael addition. A few groups have synthesized MJ by conjugate addition of various functionalized carbanions to the β-position of cyclopentenone, followed by allylation of the resulting enolate. The Michael donors employed included carboxymethyl anion equivalents such as silylketene and oxazoline cyanocuprate[50] or the use of lithium diallylcuprate moieties as acetic acid synthons.[51,52] The subsequent allylation of the resulting enolates was generally achieved by the use of allylic halides. Many studies have described the general difficulties associated with attaining allylation of regio-defined cyclopentenolates with stereo- and regiodefined allylic electrophiles, especially those with (*Z*)-isomer stereochemistry. These difficulties include loss of stereochemical integrity within the allyl group and low regioselectivity with respect to the ring, mediocre product yields of less than 50% and the need for a large excess of allylic halides.[52]



Scheme 4.3: An example of Michael addition of acetals to enones by the Mukaiyama reaction.

Tamura *et al.* have reported conjugate addition of silylketene acetals to a series of α,β-unsaturated carbonyl compounds.[53] This type of Michael addition was reported as unsuccessful until Mukaiyama *et al.* managed to react acetals with enones *via* an activating

method using titanium tetrachloride [scheme 4.3]. Tamura *et al.* carried out the same type of reaction by enhancing the reactivity of the silylketene acetals with acetonitrile solvent, without the need for an activating catalyst. Their reactions led to the corresponding O-silylated Michael adduct rather than the ketone hydrolysis product, which was predicted to readily allow the introduction of an α-substituent thereafter. This theory was applied to the synthesis of MJ. Even though ketene methyl trimethylsilyl acetal **206** is the ideal synthon, its synthesis and purification was found to be quite labour intensive, thus, methyl dimethyl-*t*-butylsilylketene acetal **209** was used instead. Alkylation of the resulting *O*-silylated Michael adduct **210** with 1-bromopent-2-yne in presence of caesium fluoride gave a mixture of **211** and **212**. Epimerization of **212** to **211** using triethylamine, followed by hydrogenation using Lindlar's catalyst generated (±)-methyl jasmonate [Scheme 4.4].

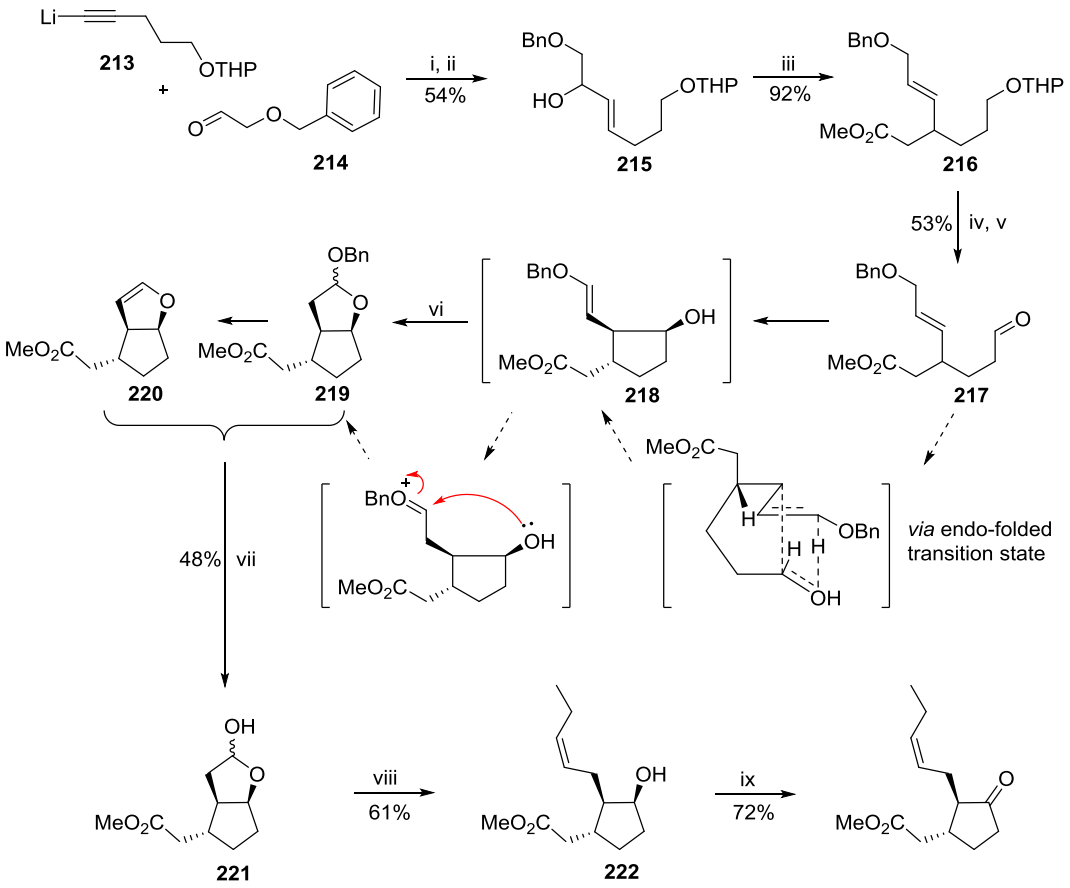


Scheme 4.4: *Reagents and conditions:* i) CH_3CN; ii) 1-bromo-pent-2-yne, CsF, CH_3CN; iii) H_2, Lindlar's catalyst.

4.3.3 Ene-Based Methodology

A few groups have synthesized methyl jasmonate in a stereocontrolled manner using intramolecular ene-cyclization as the key step.[54,55] An example reported by Nakai *et al.* described a sequential Claisen-ene approach for the stereocontrolled synthesis of cyclopentanoids, where the aldehyde functionality was used as the internal enophile [Scheme

4.5].[56] Addition of lithium acetylide **213** to benzyloxyacetaldehyde, **214** followed by trans-selective reduction of the alkyne moiety, yielded the precursor allylic alcohol (±)-**215**. The requisite ene substrate **217** was derived by Johnson-Claisen rearrangement of **215** to the unsaturated ester **216**, and subsequent deprotection and oxidation step by pyridinium chlorochromate. The ene reaction of **217** proceeded at 220 ºC, although it did not reach completion even after three days. A mixture of bicyclic compounds **219** and **220** were afforded along with benzyl alcohol and the recovery of **217**. The Nakai group suggested that once the ene product **218** was formed it underwent intramolecular addition of the hydroxyl group to the enol ether moiety spontaneously to afford the bicyclic acetal **219**, from which the bicyclic enol ether **220** was afforded by elimination of benzyl alcohol. The resulting mixture was hydrolysed to give cyclopentanolactol **221** as a single product with an exceptionally high diastereo (1,2-*cis*) and diastereofacial (2,3-*trans*) selectivity. Subjecting **221** to Wittig olefination furnished cyclopentanol **222** which went through Jones oxidation to afford (±)-methyl jasmonate.[56]



Scheme 4.5: *Reagents and conditions:* i) -78 ºC, Et_2O; ii) $LiAlH_4$, THF; iii) $CH_3C(OCH_3)_3$, 2,6-xylenol, 220 ºC, 18 h; iv) *p*-TsOH; v) PCC, CH_2Cl_2; vi) 220 ºC, 3 days; vii) 1 M HCl, 25 ºC; viii) *n*-$PrPPh_3^+$ Br^-, *n*-BuLi, THF; ix) CrO_3, aq. H_2SO_4, acetone.

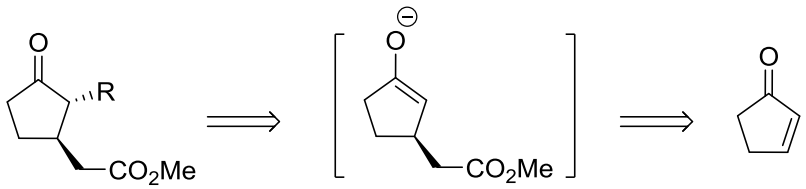
In conclusion, the synthesis of racemic MJ has been achieved *via* many diverse routes starting with various precursors, but the majority involve lengthy synthetic routes of over ten steps, are low yielding and/or most of the starting materials or synthetic intermediates were too expensive or not readily available. In addition, none provide a facile versatile route for methyl jasmonate analogue synthesis. Therefore, there is still a need for an efficient and rapid route for the synthesis of this biologically important compound and its analogues.

4.4 Results and Discussion

In this chapter, all attempted and successful synthetic routes towards methyl jasmonate and analogues are discussed. The aim was to find a general synthetic procedure whereby substituents could be introduced at the α- and β-positions of cyclopentenone and systematic variation of these substituents, and their corresponding ring-expanded homologues, would provide easy access to methyl jasmonate and its analogues, ready for a more detailed SAR study of these compounds against different cancer cell lines and molecular targets.

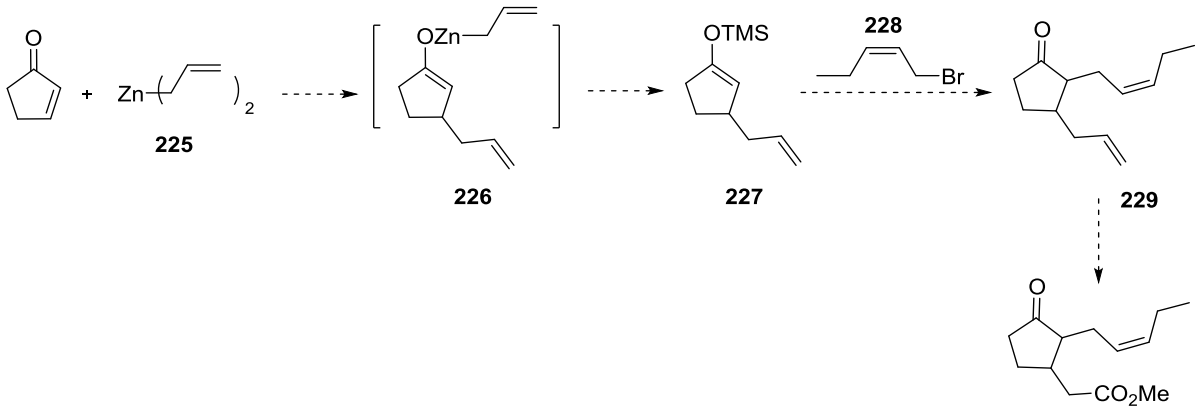
4.4.1 *Via* a Tandem Conjugate Addition and Enolate Trapping

It was envisaged that methyl jasmonate could be synthesized *via* a cascade of conjugate addition of a carboxymethyl anion equivalent to cyclopentenone, trapping the enolate that is formed, followed by an electrophilic addition of an alkynyl or allylic halide [Scheme 4.6].



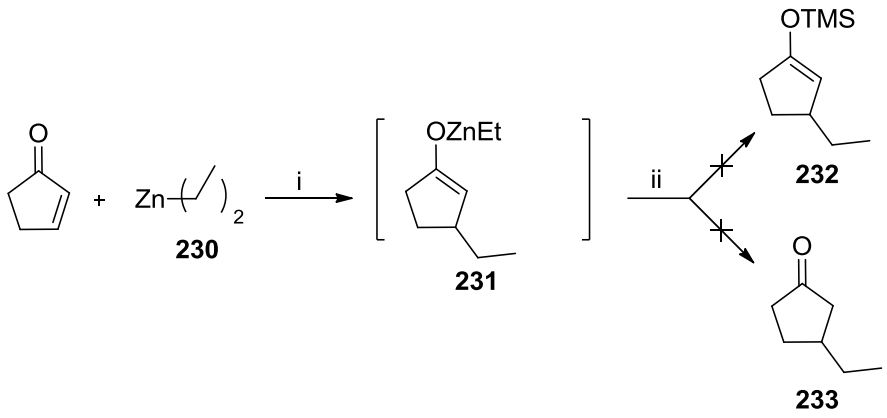
Scheme 4.6: Retrosynthesis of envisaged tandem conjugate addition and enolate trapping.

Alexakis *et al.* reported a tandem conjugate addition of dialkyl zinc reagents to cyclohexenone, and trapping of the zinc enolate formed as the corresponding silyl enol ethers.[57] In addition, Noyori *et al.* have shown that a variety of enol silyl ethers can be alkylated selectively with active alkylating agents with the aid of a fluoride ion source such as tris(dialkylamino)sulfonium difluorotrimethylsiliconate.[58]



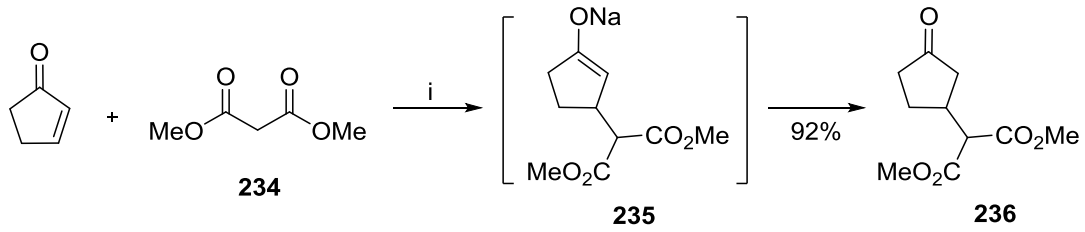
Scheme 4.7: Proposed route to methyl jasmonate.

To test this proposed route, the literature procedure of tandem conjugate addition and trapping of zinc enolate **225** by Alexakis *et al.*[57] was applied to cyclopentenone. Addition of commercially available diethyl zinc to a mixture of cyclopentenone, copper (II) triflate and the ligand PPh_3 in CH_2Cl_2 at -30 ºC to form the zinc enolate intermediate *in situ*, followed by addition of TMSOTf, or TMSCl and NEt_3 at -20 ºC to trap the enolate as stated in the literature, only afforded the starting material **205** [Scheme 4.8].



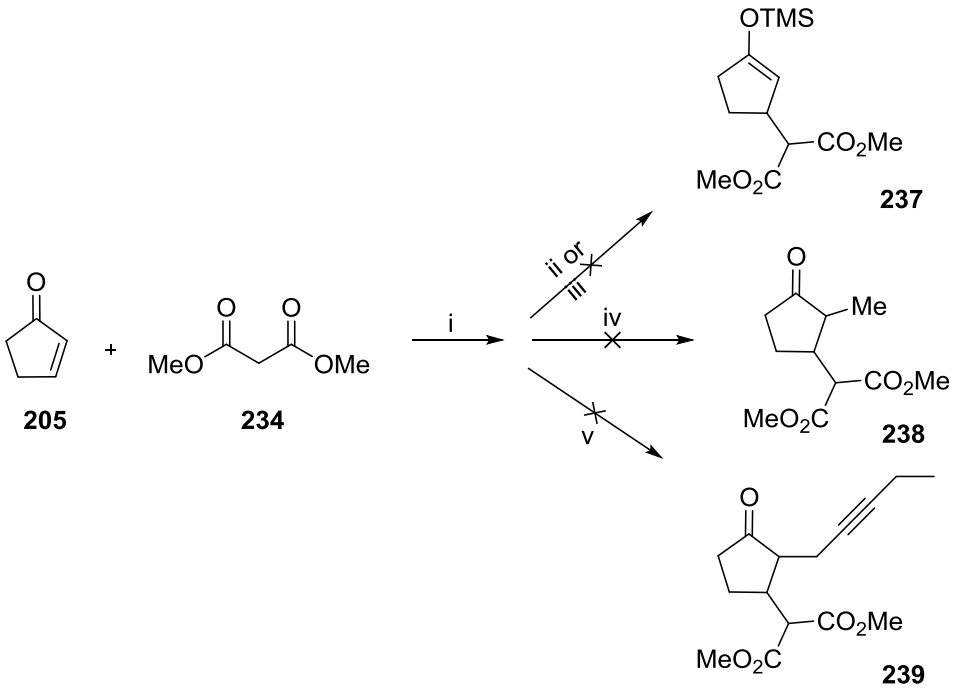
Scheme 4.8: *Reagents and conditions:* i) 20 mol% $Cu(OTf)_2$, 40 mol% PPh_3, Et_2O, -30 ºC, 3 h; ii) TMSCl, NEt_3, $ZnEt_2$, -20 ºC → rt, 2 h.

As trapping of the zinc enolate did not take place, it was thought that it may be possible to trap other enolate salts with a silyl group. To test this theory, another conjugate addition reaction was tested. Following a literature procedure,[59] dimethyl malonate in the presence of sodium methoxide was slowly added to cyclopentenone to give the Michael addition product **236** in 92% yield [Scheme 4.9]. It was envisaged that the sodium enolate **235** that is formed in the above reaction could be trapped at a low temperature using TMSCl. Thus, the reaction was performed at -30 ºC and after completion of the conjugate addition as judged by the disappearance of starting material TLC (20 h), TMSCl was added to the reaction mixture at -20 ºC. No sign of enolate trapping was observed after 24 hours at -30 ºC. Increasing the temperature to 25 ºC or the use of TMSOTf did not lead to enolate trapping and only afforded the Michael adduct **236** [Scheme 4.9].



Scheme 4.9: *Reagents and conditions:* i) NaOMe, MeOH, rt, 18 h.

Since enolate trapping was unsuccessful, at this point a one-pot synthesis of methyl jasmonate via a tandem Michael addition-enolate alkylation was also investigated. Addition of methyl iodide, a highly reactive electrophile, and bromopentyne in parallel reactions to the presumed sodium enolate compound formed was also not successful and yielded only the Michael addition product [Scheme 4.10]. It was postulated that the proton from the protic solvent methanol or possibly proton transfer from the more acidic dimethyl malonate may be responsible for quenching of the enolate as formed.

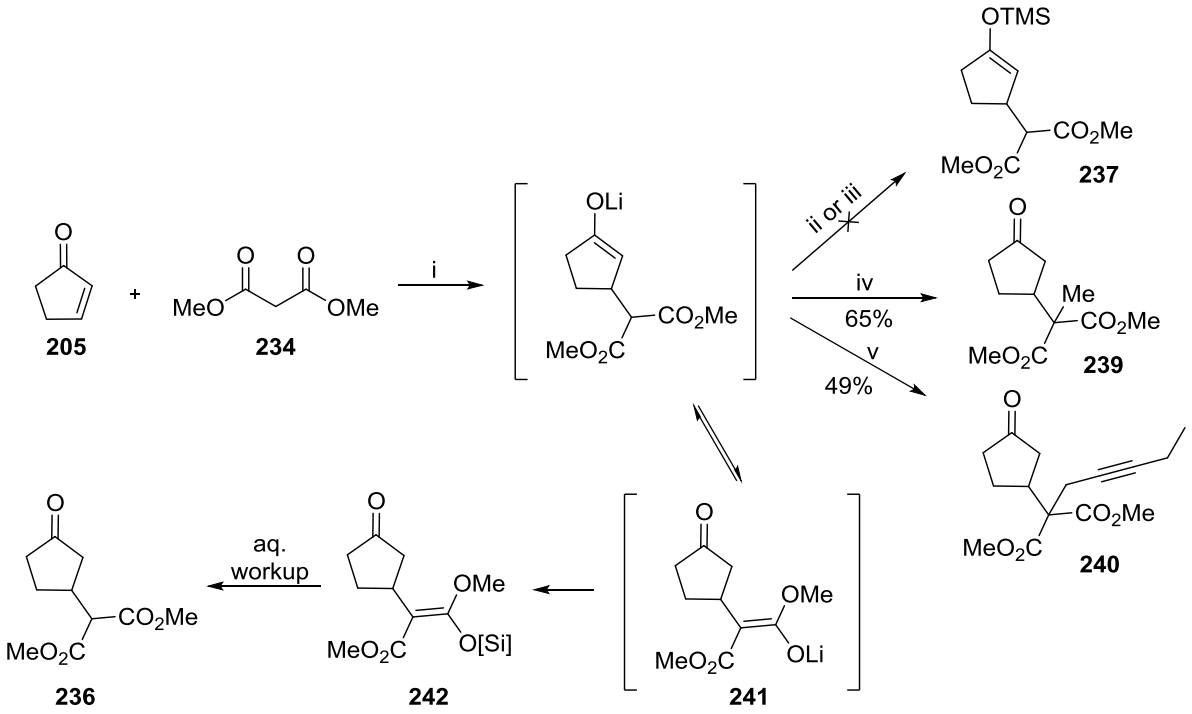


Scheme 4.10: *Reagents and conditions:* i) NaOMe, MeOH, rt, 12 h; ii) TMSCl, THF, -30 ºC; iii) TMSOTf, THF, -30 ºC; iv) MeI, THF, -30 ºC; v) 1-bromo-2-pentyne, THF, -30 ºC.

Subsequently, to prevent the problem of premature quenching of the intermediate enolate **235**, use of an alternative base in an aprotic solvent for the Michael conjugation addition was investigated. To a mixture of methyl malonate and *n*-BuLi in THF was slowly added cyclopentenone at -78 ºC in the presence of 4Å molecular sieves, providing the desired Michael product **236** in 20% yield after 12 hours [Scheme 4.11]. Increasing the temperature to -40 ºC, however, afforded **236** in quantitative yield in the same time period. Nevertheless, the lithium enolate intermediate also could not be trapped using TMSCl or TMSOTf even with the variation of reaction time and temperature ranging between -20 ºC to room temperature [Scheme 4.11].

Tandem Michael addition and enolate alkylation using methyl iodide and bromopentyne in parallel reactions, however, afforded **239** and **240** in 65% and 49% yields, respectively

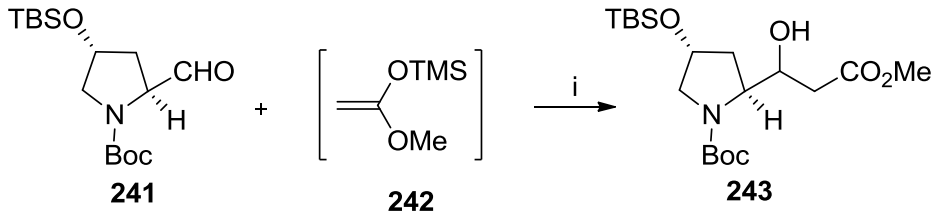
[Scheme 4.11]. This result is entirely consistent with the highly acidic proton between the methyl esters quenching the lithium enolate as soon as it is formed by a proton transfer, and the ester enolate that is subsequently formed attacks the alkyl halide to give the observed products.



Scheme 4.11: *Reagents and conditions:* i) *n*-BuLi, THF, -78 ºC → -40 ºC, 12 h; ii) TMSCl, THF, -78 ºC → -40 ºC; iii) TMSOTf, -78 ºC → -40 ºC; iv) MeI, THF-78 ºC → -40 ºC; v) 1-bromo-2-pentyne, THF, -78 ºC → -40ºC.

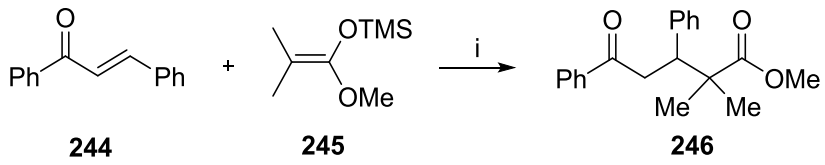
To eliminate the problem of proton transfer, the reactions above were attempted in parallel using methyl acetate instead of dimethyl malonate. Many different reaction conditions were tested, none of which resulted in the generation of the desired products **239** and **240** and all conditions returned only starting material. It can therefore be concluded that under basic conditions the equilibrium lies highly towards methyl acetate rather than its corresponding enolate lithium salt, as the methyl group has a pKa of ~25 relative to dimethyl malonate which has a pKa of 13, hence making methyl acetate a poor Michael donor.[60]

It was postulated that this problem could be resolved if the lithium enolate salt of methyl acetate could be trapped *in situ* and used as the Michael donor. Ohtake *et al.* have described an aldol reaction of the aldehyde group of a carbapenem with *in situ* generated ketene acetal in the presence of Lewis acids such as $TiCl_4$ [Scheme 4.12].[61]



Scheme 4.12: *Reagents and conditions:* i) Lewis acid, THF.

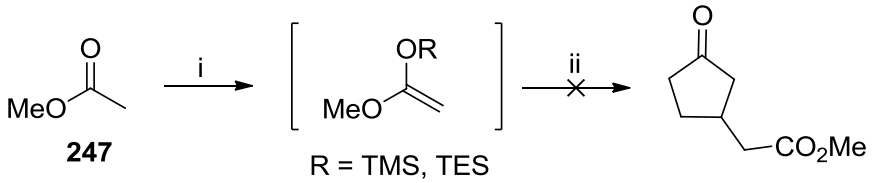
Mukaiyama and co-workers have also successfully reacted ketene acetals with several acyclic enones and cyclohexenone in the presence of $TiCl_4$ [Scheme 4.13].[62]



Scheme 4.13: *Reagents and conditions:* i) $TiCl_4$, CH_2Cl_2, -78 ºC.

To apply the combination of both procedures described above to the synthesis of methyl jasmonate, the generation of ketene methyl trimethylsilyl acetal *in situ* was attempted by treating methyl acetate with LiHMDS and TMSCl successively at -78 ºC for three hours. Addition of cyclopentenone and $TiCl_4$, however, did not yield the desired compound [Scheme 4.14]. The reactions were also attempted using TESCl, which is known to be more stable than

TMSCl, and also using LDA as the base for the *in situ* generation of the ketene acetal, none of which resulted in yielding the desired product.



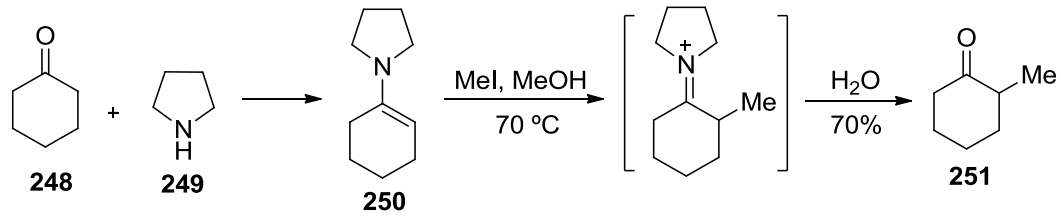
Scheme 4.14: *Reagents and conditions:* i) LiHMDS or LDA, THF, TMSCl or TESCl, -78 ºC; ii) Cyclopentenone, $SnCl_4$, THF, -78 ºC → 0 ºC.

Although ketene methyl trimethylsilyl acetal would be an ideal synthon for methyl jasmonate synthesis, its synthesis has been reported to be problematic compared to methyl- or dimethylketene methyl trimethylsilyl acetals. Tamura *et al.* did use another more readily available methyl acetate equivalent, ketene methyl dimethyl-*t*-butylsilyl acetal, in their very low yielding synthetic route towards methyl jasmonates.[53] However, the latter route using methyl dimethyl-*t*-butylsilyl ketene acetal was not pursued, as subsequent steps would have been required to remove the *gem*-dimethyl substituent and we were seeking a novel and high yielding route towards methyl jasmonate.

4.4.2 *Via* a Cascade Organocatalysis Strategy

The next synthetic strategy towards methyl jasmonate was inspired by the work of Gilbert Stork.[63,64] Since the publication of his historic paper on enamine alkylation and acylation of aldehydes and ketones, a vast array of transformations has been achieved *via* preformed enamine chemistry.[65] In such reactions an enamine is generated by treating a carbonyl compound with an amine under dehydration conditions. Reaction of the enamine can proceed *via* an addition or substitution route depending on the nature of the electrophile. In either case,

iminium ions are usually formed, which are then hydrolyzed to afford the products [Scheme 4.15]. Enamines currently play a major role in organocatalysis.



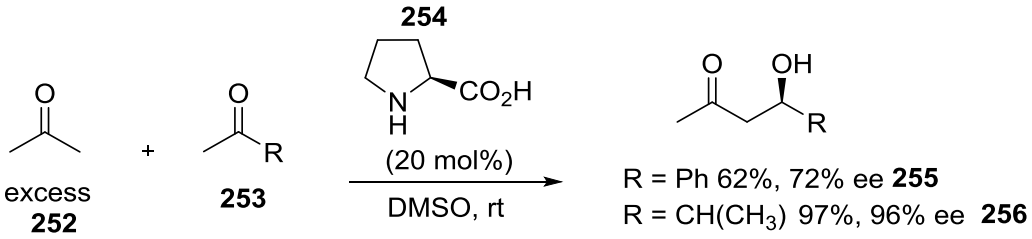
Scheme 4.15: An example of enamine alkylation of a carbonyl compounds by Gilbert Stork.[63]

Organocatalysis is the acceleration of a chemical reactions with a sub-stoichiometric amount of an organic compound which does not contain a metal atom.[66] Enantioselective organocatalysis has emerged as a powerful synthetic paradigm and has had a significant impact in chemical synthesis over the past decade.[66-70] Of particular relevance is the emergence of drug candidates with one or more non-racemic, asymmetric centres. Ideally, for catalysis to be used widely in pharmaceutical synthesis, it needs to be efficient, facile, reliable and economic and organocatalysis has provided such a platform.[71] Although many of these reactions have complementary approaches in the well-studied fields of organometallic catalysis, asymmetric organocatalysis offers several significant advantages. For example, they have a much lower toxicity profile relative to conventional metal catalysis, can tolerate water and air, and are often easy to perform.[70]

The basis of enamine catalysis is the reversible generation of an enamines from a catalytic amount of an amine and a carbonyl compound, and key to this enamine formation is the LUMO lowering effect and the substantial increase in C-H acidity upon initial conversion of the carbonyl compound into an iminium ion.[65] Enamine-based organocatalysis has been shown to be efficient in many direct catalytic asymmetric reactions such as α-

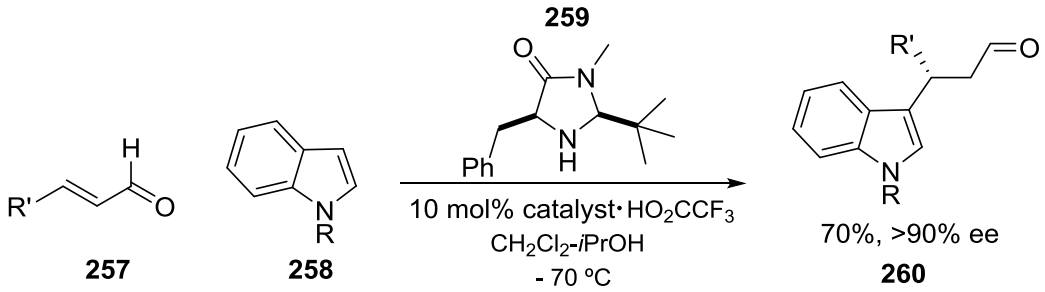
functionalization of carbonyl compounds, intramolecular α-alkylation of aldehydes, and aldol and Mannich reactions.

List *et al.* developed the first amine-catalysed, asymmetric direct intermolecular aldol reaction in 2000.[72] This involved the reaction of excess acetone with aromatic and alkyl-branched aldehydes in the presence of a catalytic amount of (*S*)-proline (20-30 mol%) in DMSO to provide the corresponding acetone aldols **255** and **256** with good yields and enantioselectivities [Scheme 4.16].



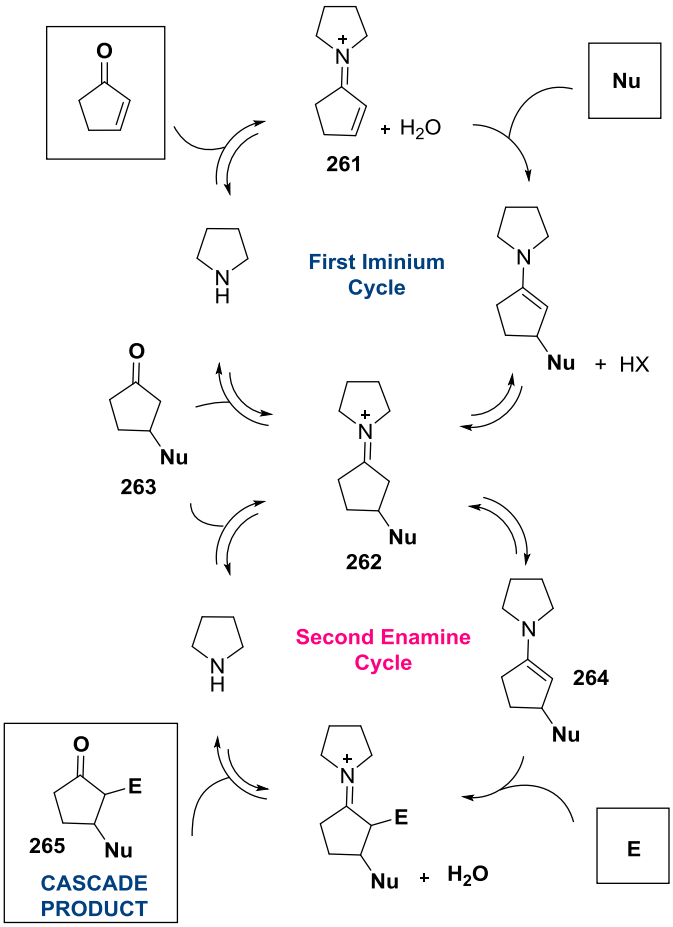
Scheme 4.16: Proline-catalyzed direct asymmetric intermolecular aldol reactions.[72]

Moreover, during the same period another useful secondary amine catalysis was introduced by Macmillan *et al.* which involved the use of chiral amines as catalysts to activate enals *via* the corresponding iminium ion [Scheme 4.17]. This catalysis provided an alternative to conventional Lewis acid catalysis of α,β-unsaturated compounds. In this iminium species, the LUMO orbital is lowered in energy such that it can more readily interact with suitable coupling reagents through either conjugate addition or pericyclic reactions.[71]



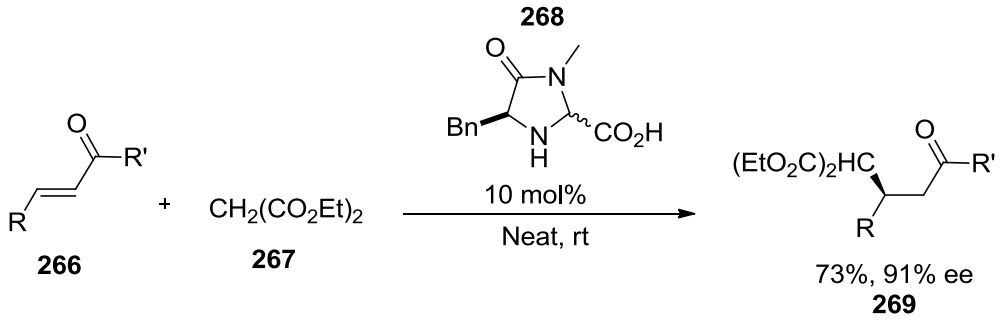
Scheme 4.17: An example of secondary amine-catalysed conjugate addition of indole to enals.[67]

A closer inspection of the mechanism of the latter reaction reveals that the conjugate addition of a nucleophile to iminium-activated forms an enamine. For the synthesis of racemic methyl jasmonate, it was envisaged that exposure of cyclopentenone to pyrrolidine would generate activated iminium species **261**, which could undergo a nucleophilic conjugate addition by dimethyl malonate [Scheme 4.18]. It was assumed that, upon rapid hydrolysis of the resulting iminium species **262**, the conjugate addition adduct **263** would then enter a second cycle wherein enamine activation **264** would enable α-addition of an alkyl group. This synthetic procedure, if proved successful, would then provide the opportunity for asymmetric synthesis of methyl jasmonate using appropriately designed chiral secondary amines [scheme 4.18].



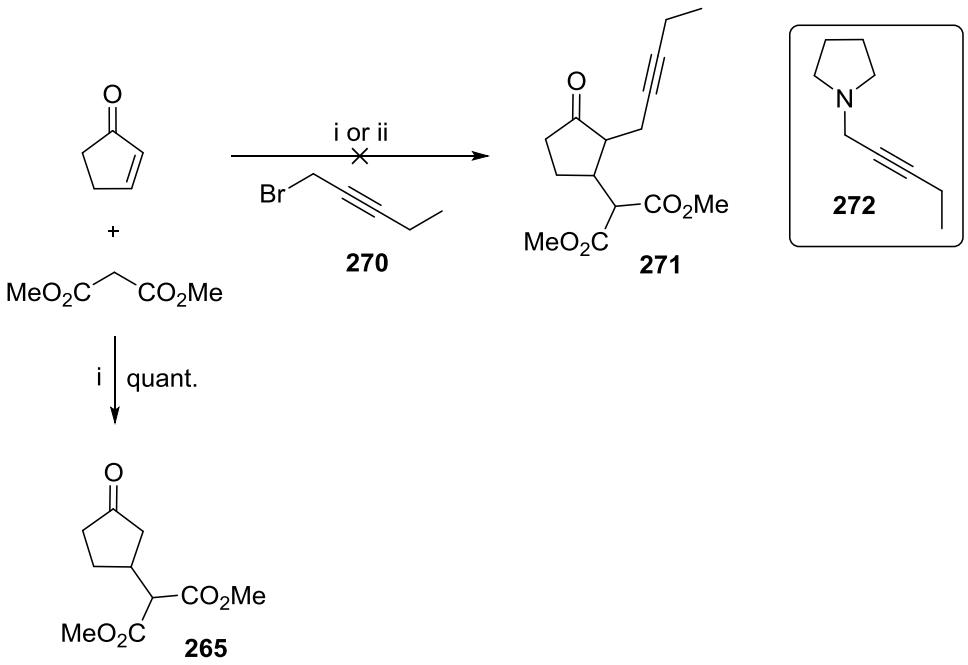
Scheme 4.18: Proposed one-pot synthesis of methyl jasmonate: merged iminium-enamine activation. E = alkyl halide, Nu = dimethyl malonate.

The first example of highly enantioselective organocatalytic conjugative addition of malonates to acyclic α,β-unsaturated acyclic enones (*vs.* enals) has been reported by Jørgensen *et al.* [Scheme 4.19].[73] This solvent-free reaction proceeds in 48 hours *via* the addition of seven equivalents of malonate **266** to an acyclic enone **267** in the presence of 10 mol% of an imidazolidine catalyst **268**. Adopting this procedure, reaction of dimethyl malonate with cyclopentenone in the presence of 10 mol% of pyrrolidine at room temperature, afforded the racemic conjugate product **265** in quantitative yield after 48 hours [Scheme 4.20]. Reducing the malonate to three equivalents reduced the yield drastically to 27%.



Scheme 4.19: Enantioselective Michael addition of malonate to acyclic enones.[73]

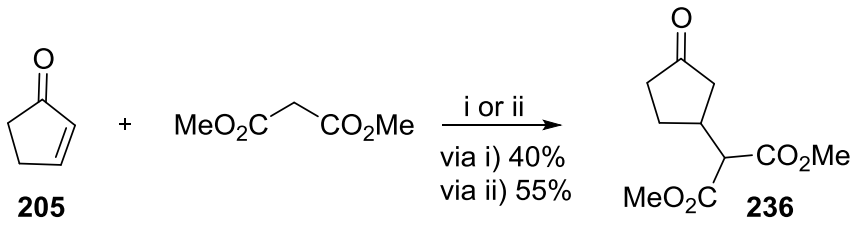
A rapid fluorescence assay was used by Tanaka *et al.* to find ways of optimising the use of enamine based catalysts. They concluded that most of the pyrrolidine-derived catalyst analysed for reactions such as the Michael addition demonstrated a higher reactivity and enantioselectivity when used in combination with a lewis acid, especially triflic acid. The lewis acid is thought to accelerate the formation of the enamine intermediate. Both of the above reactions were repeated in the presence of the pyrrolidine/TFA bifunctional catalyst, but only starting material was obtained even after 72 hours [Scheme 4.20].[74]



Scheme 4.20: *Reagents and conditions:* i) 10 mol% pyrrolidine, rt; ii) 10 mol% pyrrolidine, 10 mol% TFA, rt.

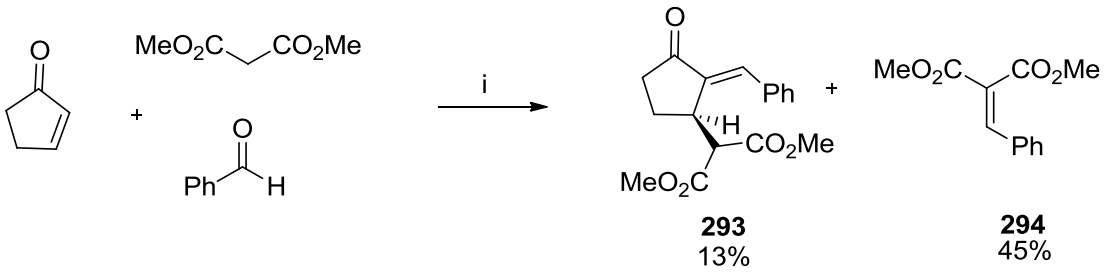
Next, the proposed one-pot cascade synthesis of methyl jasmonate was attempted. Addition of dimethyl malonate and one equivalent of 1-bromo-2-pentyne **270** to cyclopentenone in the presence of 10 mol% pyrrolidine after 48 hours returned starting material contaminated with 1-(pent-2-yn-1-yl)pyrrolidine **272** [Scheme 4.20]. All of the pyrrolidine catalyst seems to have reacted with the bromopentyne before the conjugate addition could take place.

It was hypothesized that dilution of the reaction using a co-solvent would slow down the competing nucleophilic addition of 1-bromo-2-pentyne to pyrrolidine, and therefore allow the reaction to proceed. The conjugation addition under the reported conditions in THF gave **265** in 40% yield. The same reaction in the presence of a pyrrolidine/TFA bifunctional catalyst instead, increased the yield to 55% [Scheme 4.21].



Scheme 4.21: *Reagents and conditions:* i) 10 mol% pyrrolidine, THF, rt; ii) 10 mol% pyrrolidine, 10 mol% TFA, THF, rt.

The one-pot synthesis using the latter conditions returned only the conjugated adduct **236**. Increasing the number of equivalents of 1-bromo-2-pentyne and use of iodopentyne and allylic iodide as superior electrophiles, in all cases did not allow the alkylation step to proceed. Given the unsuccessful nature of α-alkylation of the *in situ* enamine intermediate using alkyl halides, an aldol reaction was attempted instead by using one equivalent of benzaldehyde. In this instance, the cascade product **293** was obtained in 13% yield, along with the side product **294** arising from the direct Knoevenagel-type condensation of malonate and aldehyde [Scheme 4.22]. This reaction was not optimised but it did help in drawing the conclusion that the allylic and propargylic halides are not reactive enough for α-alkylation of the enamine intermediate in the proposed cascade synthesis.



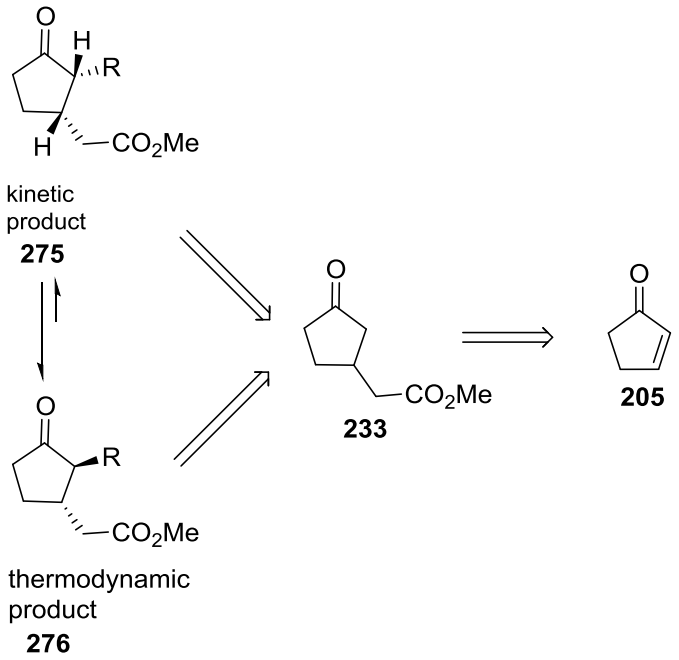
4.22: *Reagents and conditions:* i) 10 mol% pyrrolidine-TFA, THF, rt.

It should be noted that although a range of catalytic iminium-enamine tandem reactions has been reported that give rise to densely functionalised non-racemic compounds, to date no research group have reported such tandem reactions that has been successful in forming C-C bonds in both steps. Therefore, the latter reaction [Scheme 4.22] is worth perusing and optimising in future. A process that involves C-C bond formation in both steps of iminium and enamine mediated tandem reaction, especially in an enantioselective manner upon using an appropriate secondary amine catalyst, would be a powerful method in synthesis.

In addition, despite the superficial similarities between aldehydes and ketones, the steric and electronic properties they exhibit with respect to catalytic interactions are very different and most secondary amine catalysts such as proline, which are efficient in enantio-enriching aldehyde synthons, are not successful in activating ketonic motifs. In 2010, Macmillan *et al.* reported the synthesis of a set of secondary amine catalysts that worked well as catalysts in enantioselective α-allylation of a range of cyclic ketones accomplished *via* singly occupied molecular orbital (SOMO) catalysis (although not successful in mono α-allylation of cyclopentenone).[75] The Jørgensen catalyst [Scheme 4.19] is also another recently reported catalyst that is successful in acting as a highly enantioselective catalyst in conjugate addition of malonates to acyclic α,β-unsaturated enones. In a preliminary study, it was shown that Jørgensen's catalyst could be used in in conjugate addition of dimethyl malonate to cyclopentenone, producing the conjugate product in quantitative yield. However, as the main object of the project was initial racemic synthesis of methyl jasmonate, the e.e. of this reaction was not determined. Nonetheless, this sets the ground for future work in optimising the novel reaction displayed in scheme 4.22 and designing a second generation catalyst based on Macmillan's and Jørgensen's catalysts that is optimal in both tandem iminium-catalysed conjugation addition step and the enamine-catalysed α-alkylation step (although in this

reaction post aldol step, the compound undergoes a spontaneous E1cB elimination to form a double bond).

The lack of success *via* the organocatalysis cascade route for the synthesis of racemic methyl jasmonate prompted the abandoning of the one-pot synthesis strategy, and attention was turned instead towards finding an optimized route to α-alkylation of cyclopentanone that could be applied to **233** *via* the next proposed synthetic route depicted in scheme 4.23.

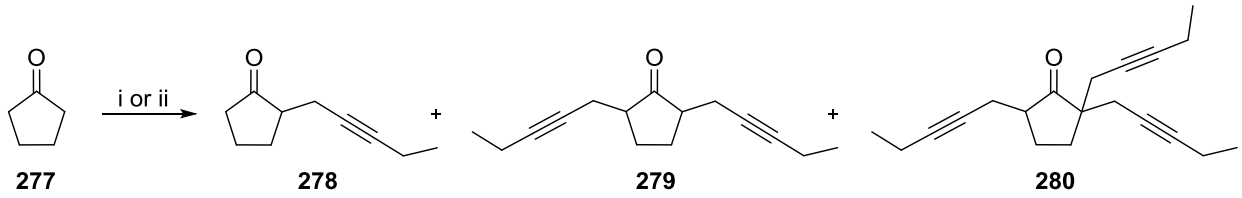


Scheme 4.23: Retrosynthetic route towards methyl jasmonate from cyclopentenone.

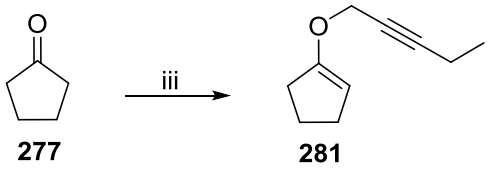
4.4.3 α-Alkylation of Cyclopentanone

One of the most fundamental and widely used methods for carbon-carbon bond formation is the alkylation of ketone enolates. Unfortunately, due to the symmetric nature of the enolate π-system, apart from few exceptions, this process does not lend itself to enantioselective or regioselective control, and therefore, in simple, flexible structures, asymmetric and regioselective C-C bond-forming reactions are not feasible.

The attempted α-alkylation of cyclopentanone using bases such as LDA and LiHMDS, as presumed, led to a mixture of mono-, di-, and tri-alkylated (**278**, **279**, and **280**) cyclopentanone [Scheme 4.24]. The yields of monoalkylated cyclopentanone were 35 and 36%, respectively. These results suggest that the rate of cyclopentanone enolate equilibration is relatively higher than enolate alkylation. Use of potassium *tert*-butoxide as base, however, led to *O*-alkylation product **281** rather than *C*-alkylation [Scheme 4.24].



	Percentage Yield		
	Monoalkylation	Dialkylation	Trialkylation
i) LDA	35	41	0.7
ii) LiHMDS	36	50	0.3



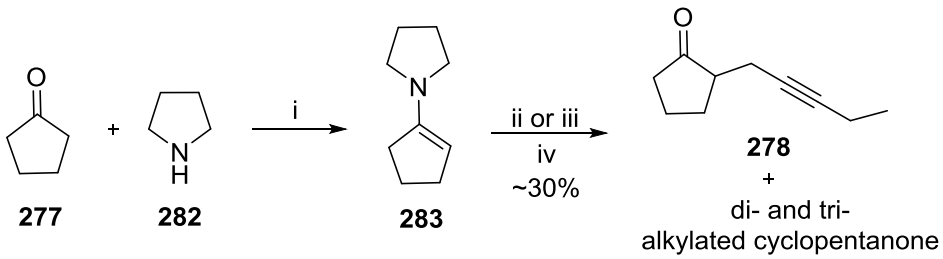
Scheme 4.24: *Reagents and conditions:* i) LDA, THF, -78 ºC, 1-bromo-2-pentyne, -78 ºC → rt, 18 h; i) LiHMDS, THF, -78 ºC, 1-bromo-2-pentyne, -78 ºC → rt, 18 h; iii) KO^{t}Bu, THF, -78 ºC, 1-bromo-2-pentyne, -78 ºC → rt.

It was suspected that this overalkylation problem can be solved by Stork enamine formation. Stork *et al.* showed that alkylation of enamines derived from carbonyl compounds such as cyclohexanone and its derivatives with simple primary alkyl bromides or iodides only gives a modest yield of 2-alkyl ketones. However, very high monoalkylated yields were obtained with strongly electrophilic halides, including allylic, benzylic, and propargylic halides.[64] This monoalkylation obtained is said to be the result of the much lower reactivity of the alkylated

enamine relative to its corresponding monoalkylated carbonyl and thus a lower rate of enamine equilibration suppressing over-alkylation.[63]

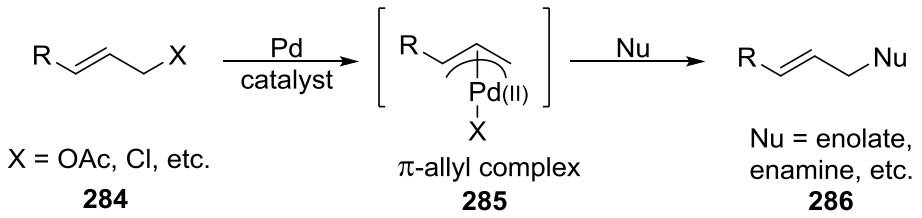
Villemin *et al.* described a two-step Stork procedure for alkylation and acylation of cyclohexanone. In the first step, the enamine was prepared *in situ* by reaction of cyclohexanone and morpholine in the presence of a catalyst, KSF clay, under azeotropic distillation. In the second step, the enamine was monoalkylated or acylated using a range of alkyl halides and olefin electrophiles.[76] Application of the same procedure to cyclopentanone returned only the starting material. It was suspected that morpholine is not reactive enough and that forming a pyrrolidine enamine instead might be more favourable. It can be presumed that the rate of enamine formation would be higher with pyrrolidine than with morpholine on the basis of the difference in the strength of the parent base. The strength of the base would also be important in the transition state of the alkylation step, where electron removal from nitrogen takes place.

The pyrrolidine enamine of cyclopentanone **283** was synthesized using a literature procedure [Scheme 4.25].[77] A general Stork procedure was followed for alkylation of **283**, which involved refluxing a mixture of the enamine and an equimolar quantity of 1-bromo-2-pentyne in acetonitrile for 18 hours, followed by its decomposition to the ketone by heating the reaction with water for an extra hour [Scheme 4.25].[78] The reaction yielded 33% of the monoalkylated product **278** and surprisingly, a mixture of di- and trialkylated side products. Thus, it can be concluded that in contrast to the alkylated enamine of cyclohexanone, the monoalkylated enamine of cyclopentanone is as reactive as its corresponding ketone, and can therefore go through further alkylation steps. Furthermore, use of a catalytic amount of sodium iodide reduced the reaction time of the above reaction to four hours but did not have a significant effect on the yield of monoalkylated product.



Scheme 4.25: *Reagents and conditions:* i) $MgSO_4$, cyclohexane; ii) $BrCH_2C{\equiv}CCH_2CH_3$, CH_3CN, reflux, 18 h, 33%; iii) $BrCH_2C{\equiv}CCH_2CH_3$, NaI, EtOH, reflux, 4 h, 31%; iv) H_2O, reflux, 1 h.

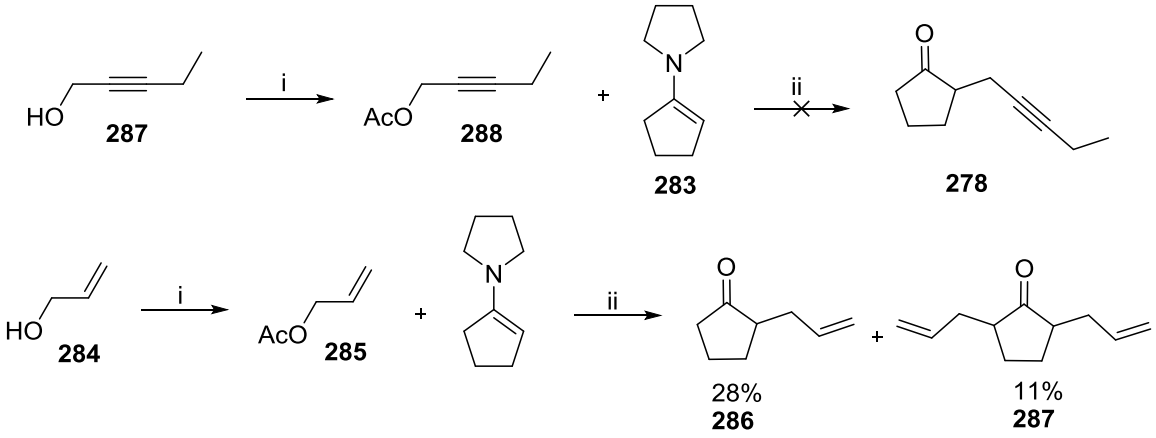
Transition metal-catalyzed carbon-carbon bond-forming reactions have emerged as powerful tools in alkylation of nucleophiles, and amongst these new methods the Tsuji-Trost reaction has attracted much attention over the last decades [Scheme 4.26].[44] The Tsuji-Trost reaction is a palladium-catalysed substitution reaction of a nucleophile with a substrate containing a leaving group, such as halide or acetate, in an allylic position.[44]



Scheme 4.26: Tsuji-Trost Pd-catalyzed allylation of nucleophiles.

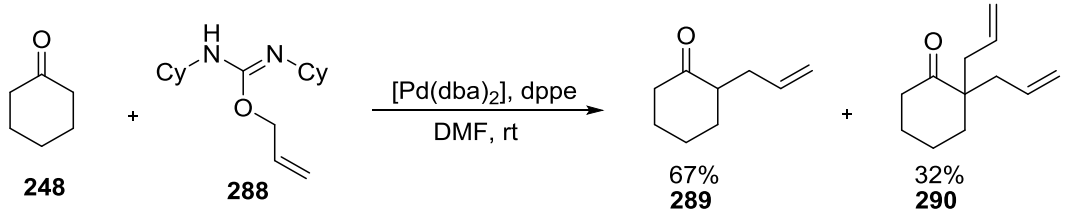
Enamines are considered to be strong nucleophiles. Tsuji reported a Pd-catalyzed reaction procedure for allylation of cyclohexanone enamines with butadiene and allyl acetate. The reaction is thought to proceed through nucleophilic attack of the enamine on an intermediate π-allylic palladium complex of allyl acetate or butadiene with the palladium compound. Reaction of cyclopentanone enamine with pentynyl acetate under similar conditions returned only the starting material, whereas use of allyl acetate afforded 28% monoalkylated **286** and

11% dialkylated product **287** [Scheme 4.27]. The yield obtained from this procedure was felt to be too low to be applied to the total synthesis of methyl jasmonate and alternative leaving groups to acetate were investigated.



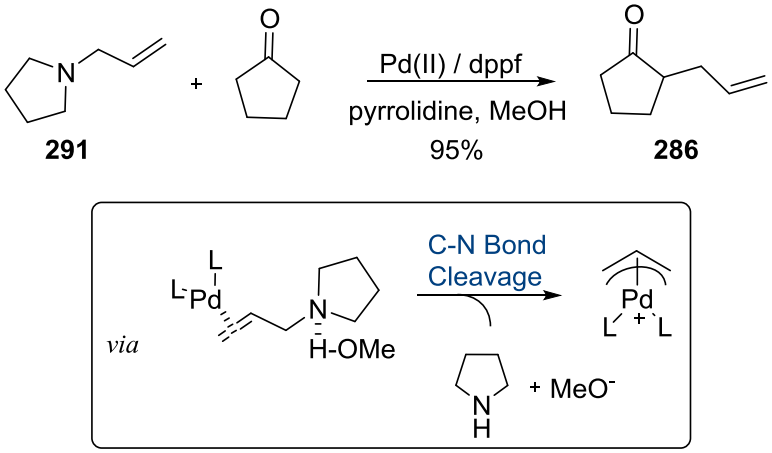
Scheme 4.27: *Reagents and conditions:* i) acetic anhydride, NEt_3, CH_2Cl_2; ii) $Pd(OAc)_2$, PPh_3, CH_3CN, 80 ºC, 5 h, aq. HCl, 50 ºC, 30 min.

Inoue *et al*. described the use of 2-allylisourea as an effective agent for direct α-allylation of a range of ketones and aldehydes assisted by palladium [Scheme 4.28]. Using the same principle, cyclopentanone was treated with 2-pentylisourea. The isourea derivative was prepared by heating pent-2-ynol with DCC at 70 ºC in the presence of catalytic amount of copper (I) chloride. Treatment of cyclopentanone and cyclohexanone with 2-pentylisourea, under the Pd-catalyzed condition only returned the starting material. This reaction was also ineffective for the addition of 2-allylisourea to cyclopentanone.



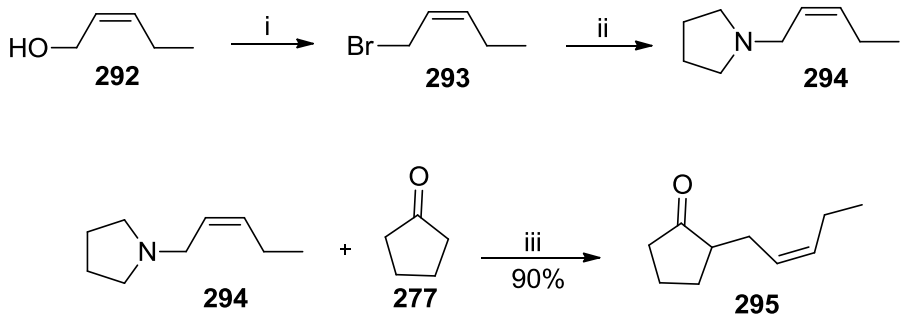
Scheme 4.28: Inoue's procedure for direct α-allylation of ketones and aldehydes with 2-allylisourea.

As described previously, the Pd-catalyzed allylic alkylation reaction of Tsuji and Trost involves formation of a C-C bond *via* cleavage of a carbon-oxygen bond of a leaving group. It is known that allylic compounds with a good leaving group are indispensable for this type of Pd-catalyzed reaction. Carbon-nitrogen bonds are common in many structures including in allylic compounds. Consequently, it was thought that utilizing an amino moiety as a leaving group in this type of allylic alkylation would be useful. However, the cleavage of the C-N bond of allylic amines has proven to be difficult due to their high stability. Since the 1980s, many groups have devoted their efforts to resolving this challenge and have come up with different routes to overcome this matter. One such example is a new method developed by Zhang *et al.* for Pd-catalyzed allylic alkylation of carbonyl compounds using allylic amines. They reported that the C-N bond cleavage of allylic amines is thought to take place *via* hydrogen bond activation using alcohol solvents such as methanol [Scheme 4.29]. The reaction of 1-allylpyrrolidine with cyclopentanone were performed in the presence of pyrrolidine using 2.5 mol% $[Pd(\eta^3\text{-}C_3H_5)Cl]_2$ and 6 mol% dppe in MeOH. The reaction after 3 hours at room temperature was described to give 2-allylcyclopentanone in 95% yield. The results obtained by this group suggest that the protic solvent is responsible for the cleavage of the C-N bond, releasing a Pd-olefin complex which is then attacked by the *in situ* generated enamine [Scheme 4.29].



Scheme 4.29: Zhang Pd-catalyzed allylic alkylation of cyclopentanone *via* the proposed reaction mechanism.

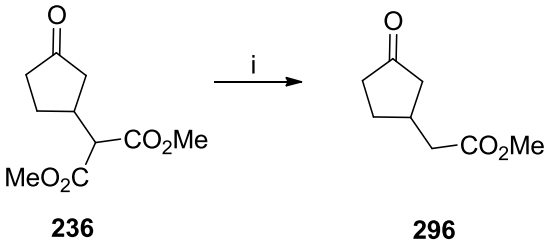
To apply this methodology to the total synthesis of methyl jasmonate, (*Z*)-1-(pent-2-enyl)pyrrolidine **294** was first prepared *via* a two-step procedure from (*Z*)-pent-2-enol [Scheme 4.30]. The addition of this allylic amine to cyclopentanone under the Pd-catalyzed conditions afforded the desired (*Z*)-2-(pent-2-en-1-yl)cyclopentanone **295** in over 90% yield with no di/tri alkylated species observed.



Scheme 4.30: *Reagents and conditions:* i) PBr_3, Et_2O, rt, 4 h; ii) 0 °C → rt, 12 h; iii) 2.5 mol% $[Pd(\eta^3\text{-}C_3H_5)Cl]_2$, 6 mol% dppe, pyrrolidine, MeOH, 3 h.

With a synthetic route for α-alkylation of cyclopentanone in good yield at hand, attention was turned to the proposed synthetic route towards methyl jasmonate [Scheme 4.23]. For this synthetic route to be successful, the α-alkylation of **296** using the latter procedure had to be investigated.

The decarboxylation of the Michael product **236** was achieved following a literature procedure.[79] Starting material **236** in aqueous *N*-Methylpyrrolidine was heated at 220 °C in a microwave reactor to afford **296** in quantitative yield [Scheme 4.31].

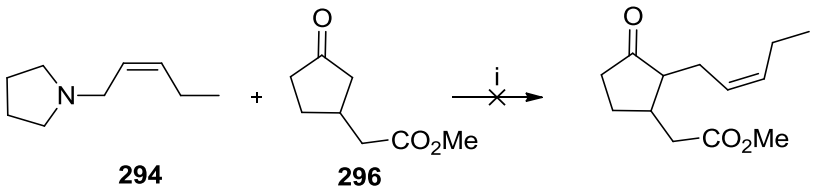


236 **296**

Scheme 4.31: *Reagents and conditions:* i) NMP, H_2O (1 equiv.), microwave, 220 ºC, 90 min.

Regiospecific generation and alkylation of one enolate structural isomer of unsymmetrical enones has proven to be difficult. The Michael addition and decarboxylation steps gave an overall yield of 96% and the α-alkylation of cyclopentanone afforded the product in 91% yield. Considering this, it was assumed that combining both steps should provide a reasonable yield of methyl jasmonate despite the characteristic lack of regiospecificity of α-alkylation of unsymmetrical cyclic ketones.

Attempted α-alkylation of **296** with (*Z*)-1-(pent-2-enyl)pyrrolidine **294** under Zhang's Pd-catalyzed conditions, however, only returned the starting material [Scheme 4.32]. Increasing the reaction time, heating the reaction for 72 hours, increasing the molar percentage of the Pd catalyst, as well as using the next recommended protic solvent, ethanol, all had no positive effect on the reaction and only returned starting material.



294 **296**

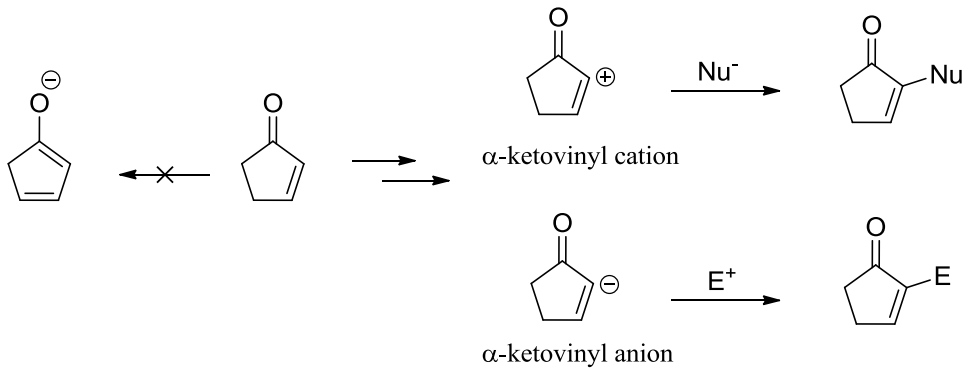
Scheme 4.32: *Reagents and conditions:* i) 2.5 - 10 mol% $[Pd(\eta^3\text{-}C_3H_5)Cl]_2$, dppe, pyrrolidine, MeOH or EtOH.

Subjecting **233** to LiHMDS followed by alkylation with bromopentyne (as in scheme 4.24), as expected resulted in a complex mixture from which the product could not be isolated.

The lack of success of the approaches *via* direct α-substitution of the Michael adduct **296** prompted investigations into an alternative synthetic route, *i.e. via* direct α-alkylation of cyclopentenone, followed by a conjugate addition reaction using a carboxymethyl anion equivalent.

4.4.4 *Via* α-Substituted Cyclopentenone

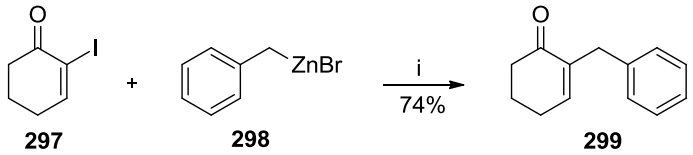
This synthetic approach was centred on a two-step regiospecific protocol involving an initial α-substitution of cyclopentenone with an allylic moiety followed by conjugate addition of a carboxymethyl anion equivalent to the resulting α-substituted cyclopentenone. An ideal route to α-substituted cyclic α,β-enones would involve the direct substitution of the corresponding parent enone devoid of the intervening thermodynamic dienolates. This protocol would entail the generation of the corresponding α-ketovinyl anion or the cation, proceeding by its capture by an appropriate electrophile or nucleophile, respectively [Scheme 4.33].



Scheme 4.33: Proposed theory for α-substitution of cyclic α,β-enones.

Negishi *et al.* introduced a method for regiocontrolled α-monosubstitution of cyclic carbonyl compounds with alkynyl and alkyl groups [Scheme 4.34]. These reactions took place *via* Pd-

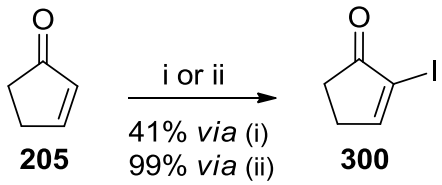
catalyzed coupling of cyclic α-iodoenones with organozinc substrates, which was envisioned to be an ideal route for the initial step of the proposed methyl jasmonate synthesis.[80]



Scheme 4.34: Pd-catalyzed coupling of cyclic α-iodoenones with organozincs. i) 5 mol% $Pd(PPh_3)_2$, THF/DMF.

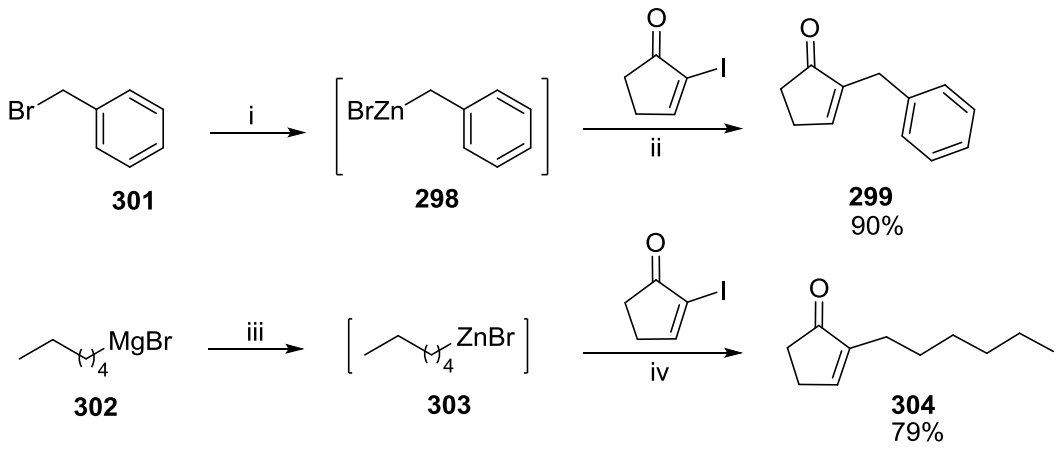
The precursor α-iodocyclopentenone **300** was first synthesized according to a procedure reported by Johnson *et al.* which involved the addition of iodine to cyclopentenone in a 1:1 solution of pyridine and tetrachloromethane.[81] The pyridine acts as a nucleophilic catalyst and co-solvent, and the reaction is thought to proceed *via* a Baylis-Hillman type pathway. Using this procedure only 41% of the desired product **300** was obtained after 24 hours [Scheme 4.35].

In order to improve the yield another route by Krafft *et al*. was used, in which cyclopentenone was exposed to iodine in the presence of a catalytic amount of DMAP and K_2CO_3 in a 1:1 solution of water and THF.[82] DMAP is more nucleophilic than pyridine and thus may be acting as a superior catalyst. With the addition of K_2CO_3 to remove the *in situ* generated HI, full conversion to **300** was observed after one hour [Scheme 4.35].



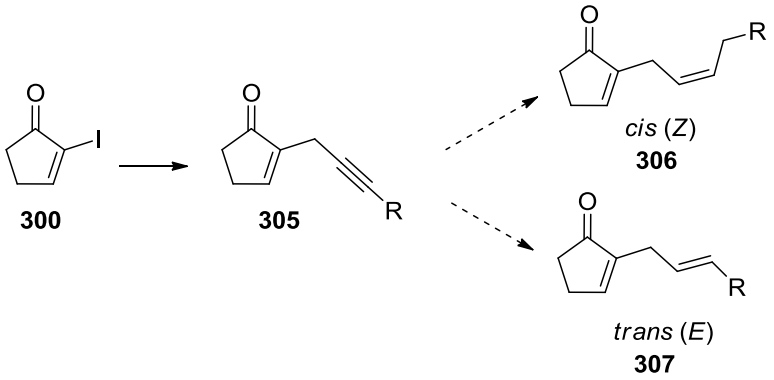
Scheme 4.35: Reagents and conditions: i) I_2, CCl_4/pyridine, rt, 24h; ii) I_2, DMAP (20 mol%), K_2CO_3, H_2O/THF, rt, 1h.

In order to assess the applicability of Negishi's methodology of α-alkylation of α-iodoenones to the preparation of the key intermediates, two representative literature procedures were carried out.[80] The requisite alkylzinc moieties were generated *in situ* via different methods by insertion into aryl halide or transmetallation from the corresponding Grignard reagent. Firstly, benzyl bromide was treated with zinc dust in the presence of 1,2-bromoethane in refluxing THF, and subsequently subjected to α-iodocyclopentenone **299** in the presence of 5 mol% of $Pd(PPh_3)_2Cl_2$ at 0 ºC to afford α-benzylcyclopentenone in 90% yield. Secondly, zinc bromide was treated with *n*-hexylmagnesium bromide at -78 ºC and was transferred *via* cannula into a solution of α-iodocyclopentenone in THF in the presence of 5 mol% of $Pd(PPh_3)_2Cl_2$ at 0 ºC, to also afford α-*n*-hexylcyclopentenone **304** in 79% yield [Scheme 4.36].



Scheme 4.36: *Reagents and conditions:* i) Zn dust, 1,2-dibromoethane, THF, reflux, 10 min; ii) 5 mol% $Pd(PPh_3)_2$, DMF, 0 ºC → rt, 2h; iii) $ZnBr_2$, THF, -78 ºC → 0 ºC; iv) 5 mol% $Pd(PPh_3)_2$, DMF, 0 ºC → rt, 2h.

In order to apply this procedure to the synthesis of methyl jasmonate, the commercially available 1-bromo-2-pentyne was employed as reaction partner. This moiety would also allow further diversity of the synthetic route towards methyl jasmonate analogues as both *cis* and *trans* isomers of methyl jasmonate can be prepared from the pentyne derivative *via* different hydrogenation steps [Scheme 4.37].

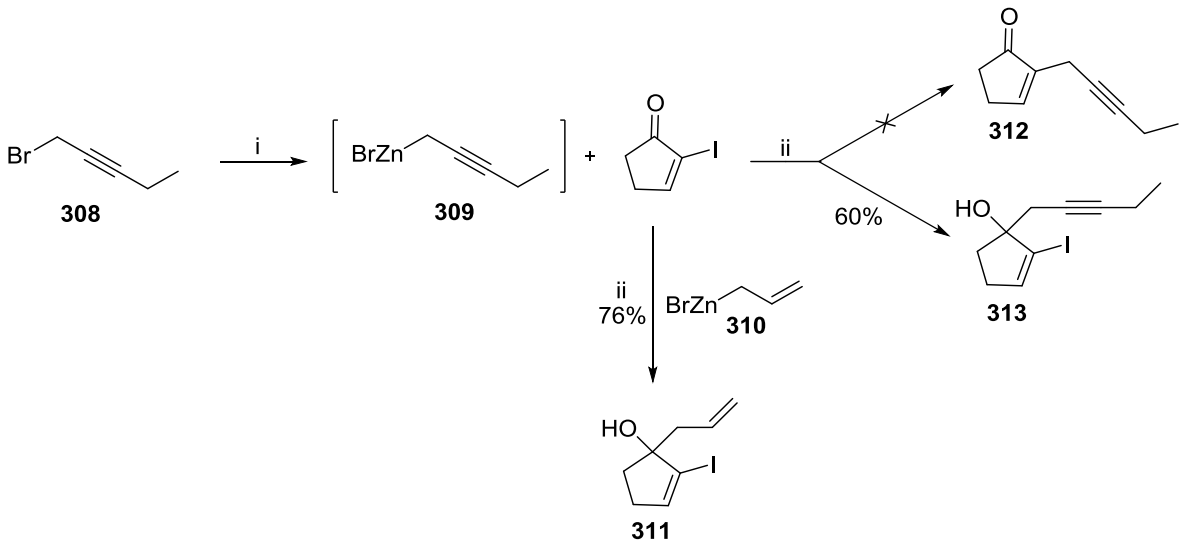


Scheme 4.37: Use of alkyne halide to allow further diversity to the synthetic route towards methyl jasmonate.

Addition of the reagents generated either directly *via* reduction with zinc, or *via* formation of Grignard reagents described above, to 1-bromo-2-pentyne and α-iodocyclopentenone returned only starting material even after 24 hours [Scheme 4.38]. It was suspected that the oxidative zincation of bromopentyne was not taking place and therefore different routes of activating the zinc metal were applied. No reaction was observed by following another procedure by Negishi *et al.* in which catalytic amount of iodine and magnesium were added to $ZnBr_2$ followed by the addition of bromopentyne at 0 ºC.[80] Increasing the temperature to 25 ºC and heating the reaction at reflux also had no effect [Scheme 4.38].

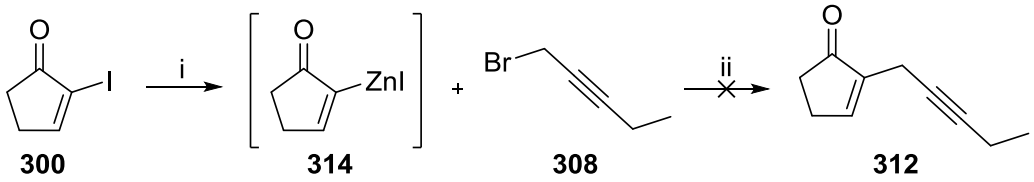
Knowing that zinc powder will become more activated if exposed to a combination of activating agents such as Me_3SiCl/1,2-dibromoethane rather than 1,2-dibromoethane alone, the procedure for allylzinc bromide preparation by Yamamoto *et al.* was applied to the generation of alkynylzinc bromide.[83] Zinc powder and 1,2-dibromoethane in THF was refluxed for few minutes and the mixture was cooled to rt, after which TMSCl was added and stirred for a further 20 minutes. Slow addition of pentynyl bromide **308** at 0 ºC over one hour did provide the pentynylzinc bromide **309**; however, under the Pd-catalyzed conditions the reaction underwent an exclusive 1,2-addition to the carbonyl group and no α-allylation was observed [Scheme 4.38].

To confirm that the alkyne functionality did not prevent α-alkylation, under the same conditions, allylzinc bromide **310** generated *in situ* was reacted with 2-iodocyclopentenone **300**, which also afforded the 1,2-addition product **311** in 76% yield [Scheme 4.38].



Scheme 4.38: *Reagents and conditions:* i) Zn dust, 1,2-dibromoethane, TMSCl, THF, 1h; ii) 5 mol% $Pd(PPh_3)_2$, DMF, 0 ºC → rt, 2h.

Knochel *et al.* reported a procedure *via* which they prepared highly functionalized aromatic, heteroaromatic, and alkenyl zinc reagents, which involved exposure of zinc dust to 1,2-dibromoethane in THF under reflux, followed by addition of trimethylsilyl chloride and the iodo- moieties successively at rt and stirring for one hour.[84] It was assumed that the Pd-catalyzed reaction may proceed between α-iodozinc-cyclopentenone and bromopentyne, thus Knochel's procedure was applied to α-iodocyclopentenone and proceeded by addition of bromopentyne under Pd-catalyzed conditions, but again starting materials were retrieved [Scheme 4.39].

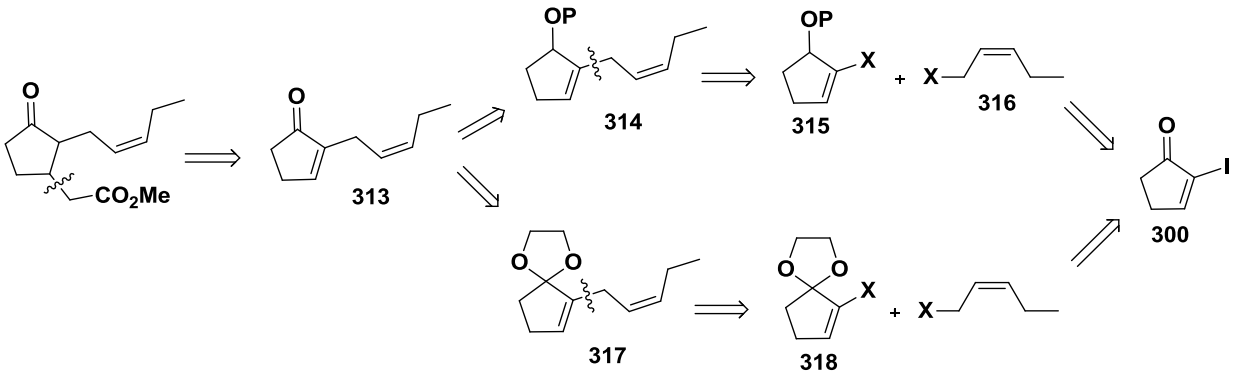


Scheme 4.39: *Reagents and conditions:* i) Zn dust, 1,2-dibromoethane, TMSCl, THF, 70 ºC, 1h; 5 mol% $Pd(PPh_3)_2$, THF/DMF.

The lack of success *via* this route prompted the abandoning of this type of strategy in favour of direct α-allylation of the parent cyclopentenone.

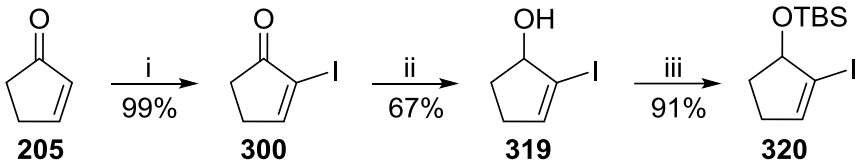
4.4.5 *Via* a Protected α-Halocyclopentenol

It was envisaged that α-alkylation of cyclopentenone could be accomplished through a regioselective halo-lithium permutation of a protected 2-halocyclopentenol **315** and its subsequent reaction with an electrophile. Methyl jasmonate could then be synthesized by conjugate addition of a carboxymethyl anion equivalent to the deprotected and oxidized resulting compound **314** [Scheme 4.40].



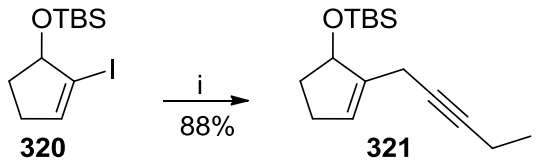
Scheme 4.40: Proposed retrosynthetic analysis of methyl jasmonate from **300**. X = I, Br; P = protecting group.

The synthesis was initiated by Luche reduction of α-iodocyclopentenone **300** using cerium (III) chloride and sodium borohydride to give **319** in 67% yield [Scheme 4.41]. Treatment of this compound with *tert*-butylchlorodimethylsilane in presence of imidazole and DMAP afforded the desired *O*-TBS protected 2-iodocyclopentenol **320** in 91% isolated yield [Scheme 4.41].



Scheme 4.41: *Reagents and conditions:* i) I_2, DMAP, K_2CO_3, H_2O/THF, rt, 1 h; ii) $NaBH_4$ (0.8 equiv), $CeCl_3 \cdot 7H_2O$, MeOH, 0 ºC → rt, 3 h; iii) TBSCl, imidazole, DMAP, CH_2Cl_2, 12 h.

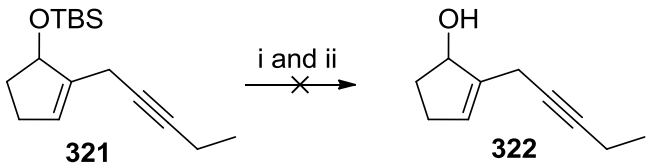
The proposed α-alkylation of this compound was investigated by its exposure to *n*-BuLi (1.1 equiv.) at -78 ºC in THF for 10 minutes, followed by quenching the resulting pale yellow vinyl anion formed by the addition of 1-bromo-2-pentyne. This successfully led to the alkylated product **321** in 88% yield [Scheme 4.42].



Scheme 4.42: *Reagents and conditions:* i) 1.6 M *n*-BuLi (1.1 equiv.), THF, -78 ºC, 10 min, 1-bromo-2-pentyne (1.2 equiv.), -78 ºC → -30 ºC over 4 h.

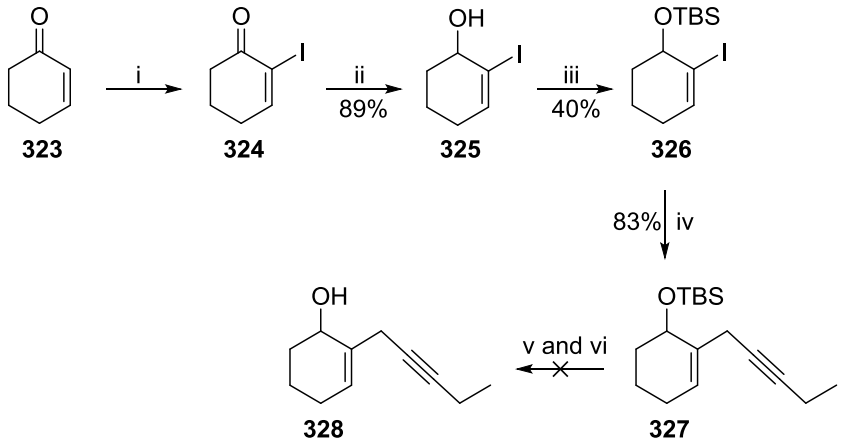
Two procedures were attempted to mediate TBS-deprotection of compound **321**. Following a literature procedure for desilylation of silyl ethers under acidic conditions (3:1 AcOH/H_2O at

50 ºC), only returned the starting materials [Scheme 4.43].[85] Using an alternative literature procedure, treatment of **321** with TBAF in THF at both 0 ºC and room temperature resulted in a complex mixture of products.[86] It was suspected that the decomposition may be occurring due to the highly basic nature of the fluoride ion, which may be forming corrosive hydrofluoric acid in the presence of residual water.[87] However, the use of flame-dried powdered molecular sieves in an attempt to eliminate this assumed problem also proved unsuccessful.



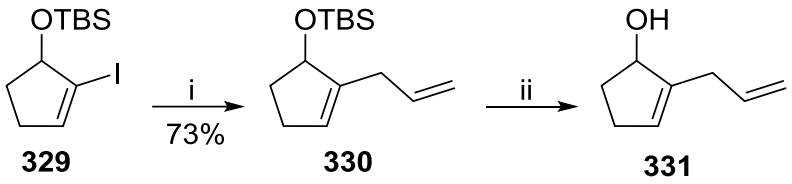
Scheme 4.43: Reagents and conditions: i) TBAF, THF, 0 ºC → rt; ii) THF/AcOH/H_2O 3:1:1, 50 ºC.

It was assumed that the lack of success in the deprotection of the silyl group of **321** may be related to the common difficulty that has been encountered thus far by working with 5-membered ring systems. The viability of this approach was therefore tested *via* the synthesis of of cyclohexenone derivative of **324** from α-iodocyclohexenone **323**, and its subsequent exposure to both of the deprotection procedures. Similar to **321**, return of starting material under acidic conditions and decomposition of compound **327** using the TBAF conditions were observed [Scheme 4.44].



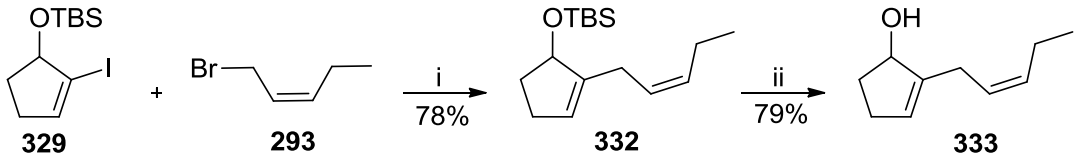
Scheme 4.44: *Reagents and conditions:* i) I_2, DMAP, K_2CO_3, H_2O/THF, rt, 1 h; ii) $NaBH_4$ (0.8 equiv), $CeCl_3 \cdot 7H_2O$, MeOH, 0 ºC → rt, 3 h; iii) TBSCl, imidazole, DMAP, CH_2Cl_2, 12 h; iv) 1.6 M *n*-BuLi (1.1 equiv), THF, -78 ºC, 10 min, 1-bromo-2-pentyne (1.2 equiv), -78 ºC → -30 ºC over 4 h; v) TBAF, THF, 0 ºC → rt; vi) THF/AcOH/H_2O 3:1:1, 50 ºC.

The successful deprotection of silyl ethers of many cyclopentenone and cyclohexenone derivatives under both conditions has been reported in the literature. Consequently, it was suspected that the pentyne side chain may be interfering with the deprotection step. To test this theory, the silyl ether deprotection was tested on 2-allyl *O*-TBS protected cyclopentenone **330** [Scheme 4.45]. This compound was prepared in 73% yield by treatment of **329** with allyl bromide. Silyl ether deprotection of **330** took place successfully using TBAF in presence of flame dried powdered 4Å molecular sieves, furnishing the deprotected alcohol **331** in 83% yield. Lack of molecular sieves prevented the reaction from proceeding and gave starting material only.



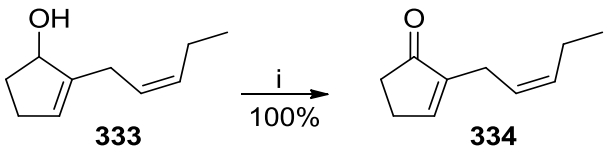
Scheme 4.45: *Reagents and conditions:* i) 1.6 M *n*-BuLi (1.1 equiv), THF, -78 ºC, 10 min, allyl bromide (1.2 equiv), -78 ºC → -30 ºC over 4 h; ii) TBAF, THF, 4Å molecular sieves, 0 ºC → rt.

With an effective step-wise protocol for the α-alkylation of cyclopentenone in hand, attention was again turned to the total synthesis of methyl jasmonate. Applying the alkylation procedure described above to **329** and the previously prepared (*Z*)-pent-2-enol **293**, followed by O-TBS deprotection produced (*Z*)-2-(pent-2-en-1-yl)cyclopent-2-enol **333** in 79% yield over two steps [scheme 32].



Scheme 4.46: *Reagents and conditions:* i) 1.6 M *n*-BuLi (1.1 equiv), THF, -78 ºC, 10 min, -78 ºC → -30 ºC over 4 h; ii) TBAF, THF, 4Å molecular sieves, 0 ºC → rt.

Finally, Dess-Martin periodinate oxidation of **381** successfully provided the desired α-allylated cyclopentenone **383**, in quantitative yield [Scheme 4.47].[88]

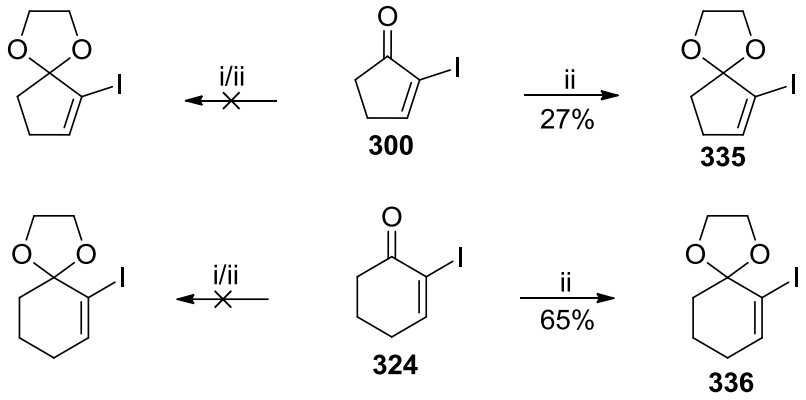


Scheme 4.47: *Reagents and conditions:* i) Dess-Martin periodinate (1.1 equiv), CH_2Cl_2, rt, 30 min.

Furthermore, in order to enable a more direct access to ketone **334**, the methodology was extended to acetal protection of ketone **300**. Attempted acetalization of **300** *via* the classic method of refluxing the ketone in toluene in the presence of ethylene glycol and pyridinium *p*-toluenesulfonate (PPTS) catalyst, under azeotropic distillation was not successful, possibly as ketone **300** did not fully dissolve in toluene.[89] The same reaction was therefore repeated with benzene at 85 ºC overnight, which mostly led to substrate decomposition to an undefinable mixture of products.[90]

In the search for another route at a milder temperature, the procedure by Chan *et al*. was investigated[91] and **300** was treated with ethylene glycol and TMSCl at room temperature. However, even after 72 hours only the starting material was retrieved. This procedure was also ineffective for the iodocyclohexenone **324**.

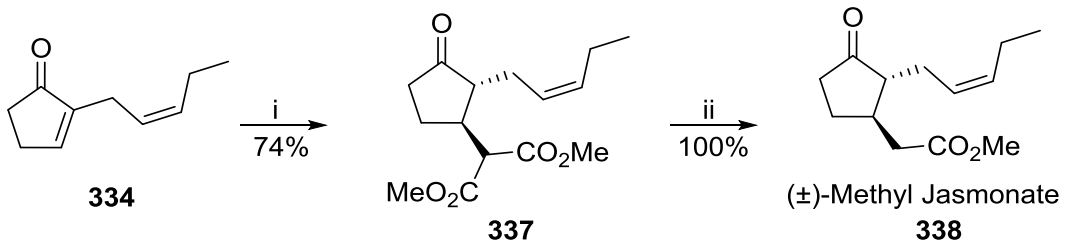
In accord with literature precedent, ethylene glycol in the presence of 1,2-bis(trimethylsilyloxy)ethane (BTSE) and TMS triflate can acetalize α-iodocyclohexenone at -20 ºC in 72 hours. In order to demonstrate this methodology the literature representative procedure was carried out using α-iodocyclohexenone **324**. The acetal protected ketone **336** was furnished in 65% yield after purification [Scheme 4.48]. However, applying the same reaction conditions to α-iodocyclopentenone **300**, afforded the desired acetal protected product **335** in only 27% yield after 120 hours.



Scheme 4.48: *Reagents and conditions:* i) ethylene glycol, PPTS, toluene or benzene, reflux, 18 h; ii) ethylene glycol, TMSCl, rt, 72 h; iii) BTSE, TMSOTf, CH_2Cl_2, -20 ºC.

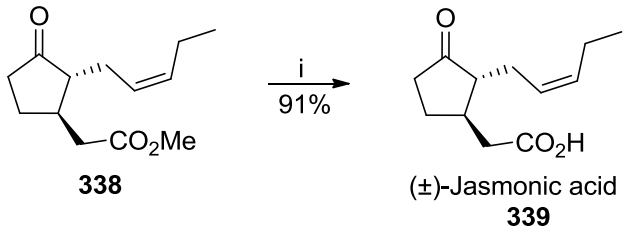
In an attempt to increase the yield of **335**, as well as to reduce the reaction time, the procedure was repeated at 0 ºC. However, analysis of the crude NMR spectrum revealed only a 19% conversion to product even after 120 hours. Due to the long reaction time and the poor yields obtained, the use of this direct protection route for the total synthesis of methyl jasmonate was abandoned.

Following on with the total synthesis of methyl jasmonate, Michael addition of dimethyl malonate to **334** and microwave mediated decarboxylation of **337**, finally afforded (±)-methyl jasmonate in excellent yield [Scheme 4.49]. The NMR spectral data for compound **388** were consistent with those reported in the literature.[92]



Scheme 4.49 *Reagents and conditions:* i) NaOMe, MeOH, rt, 18 h; ii) NMP, H_2O (1 equiv.), microwave, 220 ºC, 90 min.

Under hydrolysis conditions, the corresponding jasmonic acid was also prepared in 91% yield.



338 (±)-Jasmonic acid **339**

Scheme 4.50: *Reagents and conditions:* i) KOH, MeOH, H_2O, 45 ºC, 3h.

In conclusion, a novel versatile synthetic route to methyl jasmonate was developed, with the key steps in this total synthesis comprising of a step-wise α-alkylation of cyclopentenone, followed by a conjugation addition reaction. Methyl jasmonate was synthesized in eight steps from the cyclopentenone precursor in an overall yield of 89%.

4.5 Biological Testing

The first preliminary tests on investigating the cytotoxicity of methyl jasmonate and jasmonic acid against a range of neuroblastoma cell lines have been conducted by Andrew Stoker at the Institute of Child Health, UCL.

Methyl jasmonate has been reported to have selective cytotoxic activity against a series of tumour cells at concentrations ranging from 1-3 mM. Consequently, 0.5 mM, 1.5 mM, and 3 mM of each compound in absolute ethanol was initially tested against two neuroblastoma cell lines (Kelly cells and SK-N-SH cells) for 24 hours, in duplicate, under standard culture conditions. The jasmonic acid was reported to exhibit very little to no cytotoxicity even at the highest concentration tested, whereas 3mM of methyl jasmonate efficiently killed about 50% of the SK-N-SH cells and all the Kelly cells after 24 hours. The lower doses of 0.5 and 1 mM showed very low cytotoxicity. These results agree with that reported by Tong *et al.*, in that methyl jasmonate was found to be much more cytotoxic than jasmonic acid.[40]

Both compounds were then further tested against another two neuroblastoma cell lines, LAN5 and SHSY5Y and were repeated on Kelly and SK-N-SH cells. In general, the results were similar to the initial tests. Jasmonic acid had little or no effect on any cells, whereas methyl jasmonate killed all neuroblastoma cells at 3 mM and induced around 50% cell death at 1 mM in some of the cells. There is therefore a clear pattern with methyl jasmonate being most effective at cytotoxic dose range between 1 mM and 3 mM.

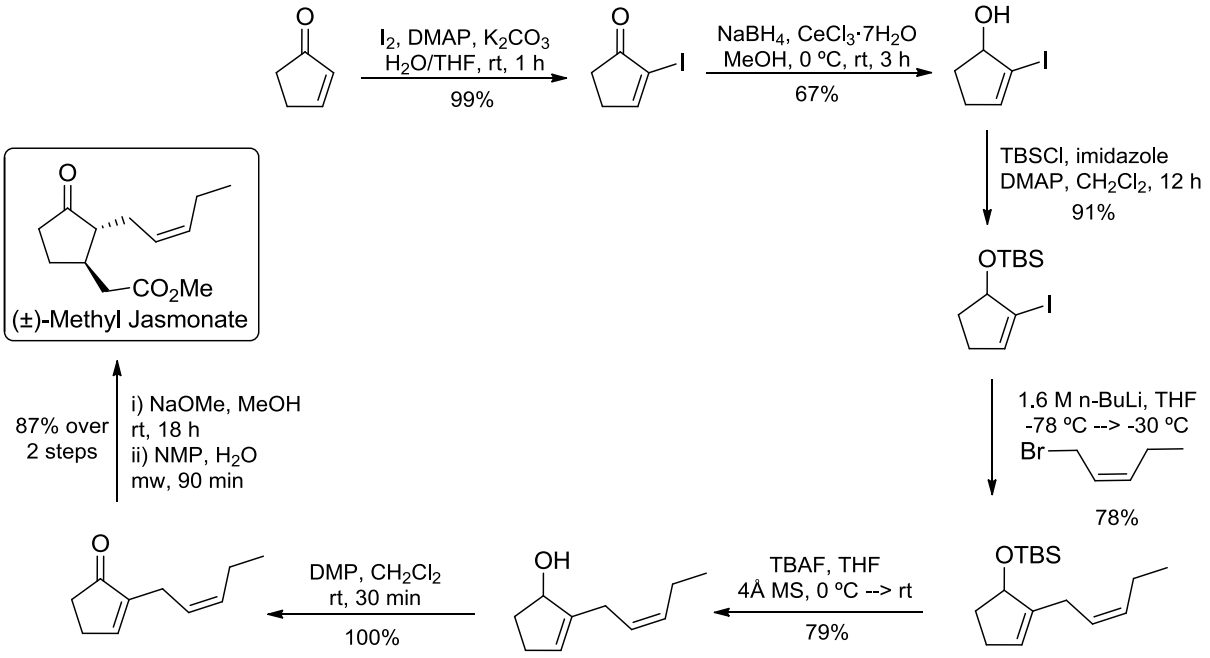
In past studies, methyl Jasmonate has been reported to significantly increase the survival of lymphoma-bearing mice and induced death in human neuroblastoma, leukaemia, prostate, breast and melanoma cell lines, as well as in leukemic cells from chronic lymphocytic leukaemia patients.[11,19,35] Conversely, normal lymphocytes, peripheral blood erythrocytes and human sperm cells were found to be resistant to jasmonate cytotoxicity.[11,20] These results strongly support the conclusion that jasmonates specifically target transformed cells.[20]

As the significant cytotoxicity of methyl jasmonate on neuroblastoma cells has now been confirmed in our studies, the next step would be to confirm the resistance of normal cells to the cytotoxicity of methyl jasmonate. Subsequently, the mechanism by which this compound causes neuroblastoma cell death will be investigated. In particular, attention will be focused on the effects of methyl jasmonate on the classical pathways regulated by PTPs (Erk, AKT, FAK, *etc.*) to see if PTP inhibition is the likely mechanism of action.

4.6 Conclusion and Future Work

Over the past decade, methyl jasmonate has been proven to have cytotoxic effects against various tumours both *in vitro* and *in vivo*. Studies have revealed that the cytotoxicity of this molecule against transformed cells is highly selective, thus suggesting that low levels of side-effects would be encountered in comparison with existing cytotoxic drugs. As the research on the anti-cancer properties of methyl jasmonate is still at early stages, and also due to the lack of a versatile synthetic procedure for the preparation of its structural derivatives, detailed SAR studies of this compound have not yet been conducted.

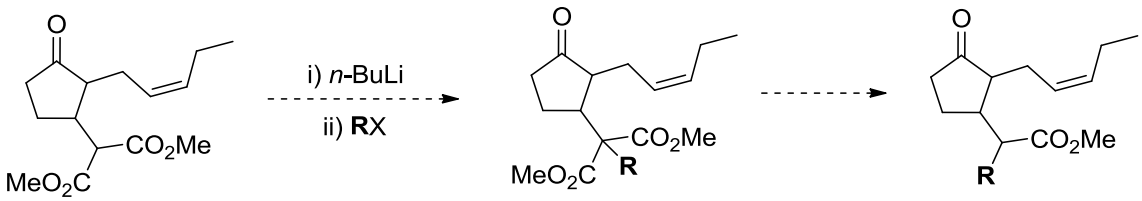
In the course of this project, a novel versatile synthetic route to methyl jasmonate was developed [Scheme 4.51]. The key steps in this total synthesis include step-wise α-alkylation of cyclopentenone, followed by a conjugation addition reaction. Methyl jasmonate was synthesized in eight steps from the cyclopentenone precursor in an overall yield of 89%.



Scheme 4.51: Total synthesis of methyl jasmonate.

The cytotoxic activity of methyl jasmonate was confirmed against a range of neuroblastoma cell lines including SK-N-SH, SHSY5Y, LAN5 and the Kelly cells. A further study on the mechanism by which methyl jasmonate induces neuroblastoma cell death is currently underway. Particular attention is being focused on the effect of this compound on the classical pathways regulated by protein tyrosine phosphatases, to clarify if PTP inhibition is the likely mechanism of action.

In conclusion, with this novel synthetic procedure, substituents can be readily introduced at the α- and β-position of cyclopentenone. In addition, further diversity could be introduced at C2 of methyl jasmonate core structure *via* utilising one of the failed routes towards the one-pot synthesis of this compound [Scheme 4.52]. Systematic variation of these substituents, and their corresponding ring-expanded homologues, will allow for future extensive SAR studies of methyl jasmonate in tumour cells, in particular in neuroblastoma.



Scheme 4.52: Proposed route for addition of substituents at C2 with alkyl halides.

Furthermore, there are many high yielding synthetic routes in the literature for the acetal protection of α-bromocyclopentenone. Future studies will include synthesis of methyl jasmonate from an α-bromocyclopentenone precursor. If successful, the total synthesis of methyl jasmonates using the above principles may be achieved in fewer numbers of steps.

4.7 References

1. Demole, E.; Lederer, E.; Mercier, D. *Helv. Chim. Acta* **1962**, *45*, 675-685.

2. Wasternack, C. *Ann. Bot. (Oxford, U. K.)* **2007**, *100*, 681-697.

3. Cheong, J. J.; Choi, Y. D. *Trends Genet.* **2003**, *19*.

4. Farmer, E. E.; Ryan, C. A. *Proc. Natl. Acad. Sci. U. S. A.* **1990**, *87*.

5. Creelman, R. A.; Mullet, J. E. *Annu. Rev. Plant Physiol. Plant Mol. Biol.* **1997**, *48*, 355-381

6. Frater, G.; Bajgrowicz, J. A.; Kraft, P. *Tetrahedron* **1998**, *54*, 7633-7703.

7. Acree, T. E.; Nishida, R.; Fukami, H. *J. Agric. Food Chem.* **1985**, *33*, 425-427.

8. Ishii, Y.; Kiyota, H.; Sakai, S.; Honma, Y. *Leukemia* **2004**, *18*, 1413-1419.

9. Kim, J. H.; Lee, S. Y.; Oh, S. Y.; Han, S. I.; Park, H. G.; Yoo, M. A.; Kang, H. S. *Oncol. Rep.* **2004**, *12*, 1233-1238.

10. Samaila, D.; Toy, B. J.; Wang, R. C.; Elegbede, J. A. *Anticancer Res.* **2004**, *24*, 3089-3095.

11. Fingrut, O.; Flescher, E. *Leukemia* **2002**, *16*, 608-616.

12. Fingrut, O.; Reischer, D.; Rotem, R.; Goldin, N.; Altboum, I.; Zan-Bar, I.; Flescher, E. *Br. J. Pharmacol.* **2005**, *146*, 800-808.

13. World Health Organization, cancer. http://www.who.int/mediacentre/factsheets/fs297/en/.

14. Hartwell, J. L. *Lloydia* **1971**, *34*, 386-425.

15. Srivastava, V.; Negi, A. S.; Kumar, J. K.; Gupta, M. M.; Khanuja, S. P. S. *Biorg. Med. Chem.* **2005**, *13*, 5892-5908.

16. Zhang, L.; Demain, A. L. *Natural Products: Drug Discovery and Therapeutic Medicine*; Humana Press, **2005**.

17. Balunas, M. J.; Kinghorn, A. D. *Life Sci.* **2005**, *78*, 431-441.

18. Gragg, G. M.; Newman, D. J. *J. Ethnopharmacol.* **2005**, *100*, 72–79.

19. Flescher, E. *Anticancer Drugs* **2005**, *16*, 911-916.

20. Heyfets, A.; Flescher, E. *Cancer Lett.* **2007**, *250*, 300-310.

21. Reischer, D.; Heyfets, A.; Shimony, S.; Nordenberg, J.; Kashman, Y.; Flescher, E. *Br. J. Pharmacol.* **2007**, *150*, 738-749.

22. Ezekwudo, D.; Shashidharamurthy, R.; Devineni, D.; Bozeman, E.; Palaniappan, R.; Selvaraj, P. *Cancer Lett.* **2008**, *270*, 277-285.

23. Schimmer, A. D.; Welsh, K.; Pinilla, C.; Wang, Z. L.; Krajewska, M.; Bonneau, M. J.; Pedersen, I. M.; Kitada, S.; Scott, F. L.; Bailly-Maitre, B.; Glinsky, G.; Scudiero, D.; Sausville, E.; Salvesen, G.; Nefzi, A.; Ostresh, J. M.; Houghten, R. A.; Reed, J. C. *Cancer Cell* **2004**, *5*, 25-35.

24. Cohen, S.; Flescher, E. *Phytochemistry* **2009**, *70*, 1600-1609.

25. Conti, M. *Anticancer Drugs* **2006**, *17*, 1017-1022.

26. Willingham, M. C. *J. Histochem. Cytochem.* **1999**, *47*, 1101-1109.

27. Kaufmann, S. H.; Earnshaw, W. C. *Exp. Cell Res.* **2000**, *256*, 42-49.

28. Shoshan-Barmatz, V.; De Pinto, V.; Zweckstetter, M.; Raviv, Z.; Keinan, N.; Arbel, N. *Mol. Aspects Med.* **2010**, *31*, 227-285.

29. Bailly, J. D.; Skladanowski, A.; Bettaieb, A.; Mansat, V.; Larsen, A. K.; Laurent, G. *Leukemia* **1997**, *11*, 1523-1532.

30. Goldin, N.; Arzoine, L.; Heyfets, A.; Israelson, A.; Zaslavsky, Z.; Bravman, T.; Bronner, V.; Notcovich, A.; Shoshan-Barmatz, V.; Flescher, E. *Oncogene* **2008**, *27*, 4636-4643.

31. Cai, J. Y.; Yang, J.; Jones, D. P. *Biochim. Biophys. Acta* **1998**, *1366*, 139-149.

32. Nakashima, R. A.; Mangan, P. S.; Colombini, M.; Pedersen, P. L. *Biochemistry (Moscow)* **1986**, *25*, 1015-1021.

33. Hammerman, P. S.; Fox, C. J.; Thompson, C. B. *Trends Biochem. Sci.* **2004**, *29*, 586-592.

34. Zhang, J. W.; Gu, J.; Wang, Z. Y.; Chen, S. J.; Chen, Z. *J. Biosci.* **2000**, *25*, 275-284.

35. Rotem, R.; Heyfets, A.; Fingrut, O.; Blickstein, D.; Shaklai, M.; Flescher, E. *Cancer Res.* **2005**, *65*, 1984-1993.

36. Schor, N. F. *J. Neurooncol.* **1999**, *41*, 159-166.

37. Oberthuer, A.; Berthold, F.; Warnat, P.; Hero, B.; Kahlert, Y.; Spitz, R.; Ernestus, K.; Konig, R.; Haas, S.; Eils, R.; Schwab, M.; Brors, B.; Westermann, F.; Fischer, M. *J. Clin. Oncol.* **2006**, *24*, 5070-5078.

38. Tong, Q.; Jiang, G.; Zheng, L.; Tang, S.; Cai, J.; Liu, Y.; Zeng, F.; Dong, J. *Anticancer Drugs* **2008**, *19*, 573-581.

39. Fuldo, S. *Expert Rev. Anticancer Ther.* **2007**, *7*, 1255-1264.

40. Tong, Q.; Jiang, G.; Zheng, L.; Tang, S.; Cai, J.; Liu, Y.; Zeng, F.; Dong, J. *Acta Pharmacol. Sin.* **2008**, *29*, 861-869.

41. Kusafuka, T.; Fukuzawa, M.; Oue, T.; Yoneda, A.; Okada, A.; Satani, M. *J. Pediatr. Surg.* **1994**, *29*, 543-547.

42. Brodeur, G. M. *Nat. Rev. Cancer* **2003**, *3*, 203-216.

43. Naoshima, Y.; Nishimoto, K.; Wakabayashi, S.; Hayashi, S. *Agric. Biol. Chem.* **1980**, *44*, 687-688.

44. Kataoka, H.; Yamada, T.; Goto, K.; Tsuji, J. *Tetrahedron* **1987**, *43*, 4107-4112.

45. Ballini, R.; Petrini, M.; Marotta, M. *Synthetic comm.* **1989**, *19*, 573-583.

46. Ballini, R.; Bigi, F.; Conforti, M. L.; De Santis, D.; Maggi, R.; Oppici, G.; Sartori, G. *Catal. Today* **2000**, *60*, 305-309.

47. Buchi, J.; Egger, B. *J. Org. Chem.* **1971**, *36*, 2021-2023.

48. Amaratunga, M.; Fluhr, K.; Jarrett, J. T.; Drennan, C. L.; Ludwig, M. L.; Matthews, R. G.; Scholten, J. D. *Biochemistry (Moscow)* **1996**, *35*, 2453-2463.

49. Lee, W. Y.; Jang, S. Y.; Kim, M.; Park, O. S. *Synth. comm.* **1992**, *22*, 1283-1291.

50. Santos, A. A. d.; Clososki, G. C.; Simonelli, F.; Oliveira, A. R. M. d.; Marques, F. d. A.; Zarbin, P. H. G. *J. Braz. Chem. Soc.* **2001**, *12*, 673-679.

51. Greene, A. E.; Crabbe, P. *Tetrahedron Lett.* **1976**, *52*, 4867-4870.

52. Luo, F.-T.; Negishi, E.-i. *Tetrahedron Lett.* **1985**, *26*, 2177-2180.

53. Tamura, M.; Gu, J. G.; Danen, E. H. J.; Takino, T.; Miyamoto, S.; Yamada, K. M. *J. Biol. Chem.* **1999**, *274*, 20693-20703.

54. Sarkar, T. K.; Ghorai, B. K.; Nandy, S. K.; Mukherjee, B.; Banerji, A. *J. Org. Chem.* **1997**, *62*, 6006-6011.

55. Sarkar, T. K.; Mukherjee, B.; Ghosh, S. K. *J. ChemInf.* **1998**, *29*, no-no.

56. Takahashi, K.; Sato, H.; Mikami, K.; Nakai, T. *Chem. Lett.* **1989**, 247-250.

57. Knopff, O.; Alexakis, A. *Org. Lett.* **2002**, *4*, 3835-3837.

58. Noyori, R.; Nishida, I.; Sakata, J. *J. Am. Chem. Soc.* **1983**, *105*, 1598-1608.

59. Reddy, S. H. K.; Chiba, K.; Sun, Y.; Moeller, K. D. *J. ChemInf.* **2001**, *32*, no-no.

60. Bernasconi, C. F.; Leyes, A. E.; Ragains, M. L.; Shi, Y.; Wang, H.; Wulff, W. D. *J. Am. Chem. Soc.* **1998**, *120*, 8632-8639.

61. Ohtake, N.; Jona, H.; Okada, S.; Okamoto, O.; Imai, Y.; Ushijima, R.; Nakagawa, S. *Tetrahedron: Asymmetry* **1997**, *8*, 2939-2947.

62. Saigo, K.; Osaki, M.; Mukaiyama, T. *Chem. Lett.* **1976**, *5*, 163-164.

63. Stork, G.; Terrell, R.; Szmuszkovicz, J. *J. Am. Chem. Soc.* **1954**, *76*, 2029-2030.

64. Stork, G.; Brizzolara, A.; Landesman, H.; Szmuszkovicz, J.; Terrell, R. *J. Am. Chem. Soc.* **1963**, *85*, 207-222.

65. Rappoport, Z. *The Chemistry of Enamines*, Wiley, **1994**.

66. Dalko, P. I.; Moisan, L. *Angew. Chem., Int. Ed.* **2004**, *43*, 5138-5175.

67. Dalko, P. I.; Moisan, L. *Angew. Chem., Int. Ed.* **2001**, *40*, 3726-3748.

68. Seayad, J.; List, B. *Org. Biomol. Chem.* **2005**, *3*, 719-724.

69. Houk, K. N.; List, B. *Acc. Chem. Res.* **2004**, *37*, 487-487.

70. List, B. *Adv. Synth. Catal.* **2004**, *346*, 1021-1021.

71. Gaunt, M. J.; Johansson, C. C. C.; McNally, A.; Vo, N. T. *Drug Discovery Today* **2007**, *12*, 8-27.

72. List, B. *Tetrahedron* **2002**, *58*, 5573-5590.

73. Halland, N.; Aburel, P. S.; Jørgensen, K. A. *Angew. Chem. Int. Ed.* **2003**, *42*, 661-665.

74. Mase, N.; Tanaka, F.; Barbas, C. F. *Angew. Chem. Int. Ed.* **2004**, *43*, 2420-2423.

75. Mastracchio, A.; Warkentin, A. A.; Walji, A. M.; MacMillan, D. W. *Proc. Natl. Acad. Sci. U. S. A.* **2010**, *107*, 20648-20651.

76. Hammadi, M.; Villemin, D. *Synth. Commun.* **1996**, *26*, 2901-2904.

77. Zhao, X.; Liu, D.; Xie, F.; Zhang, W. *Tetrahedron* **2009**, *65*, 512-517.

78. Varga, T. R.; Nemes, P.; Mucsi, Z.; Scheiber, P. *Tetrahedron Lett.* **2007**, *48*, 1159-1161.

79. Curran, D. P.; Zhang, Q. *Adv. Synth. Catal.* **2003**, *345*, 329-332.

80. Negishi, E.; Tan, Z.; Liou, S. Y.; Liao, B. Q. *Tetrahedron* **2000**, *56*, 10197-10207.

81. Johnson, C. R.; Adams, J. P.; Braun, M. P.; Senanayake, C. B. W.; Wovkulich, P. M.; Uskokovic, M. R. *Tetrahedron Lett.* **1992**, *23*, 917–918.

82. Krafft, M. E.; Cran, J. W. *Synlett* **2005**, 1263-1266.

83. Ashcroft, J.; LaPlante, S. R.; Borer, P. N.; Cowburn, D. *J. Am. Chem. Soc.* **1989**, *111*, 363-365.

84. Majid, T. N.; Knochel, P. *Tetrahedron Lett.* **1990**, *31*, 4413-4416.

85. Gurjar, M. K.; Wakharkar, R. D.; Singh, A. T.; Jaggi, M.; Borate, H. B.; Shinde, P. D.; Verma, R.; Rajendran, P.; Dutt, S.; Singh, G.; Sanna, V. K.; Singh, M. K.; Srivastava, S. K.; Mahajan, V. A.; Jadhav, V. H.; Dutta, K.; Krishnan, K.; Chaudhary, A.; Agarwal, S. K.; Mukherjee, R.; Burman, A. C. *J. Med. Chem.* **2007**, *50*, 1744-1753.

86. Gonçalves-Martin, M. G.; Saxer, A.; Renaud, P. *Synlett* **2009**, *2009*, 2801-2802.

87. Davies, S. G.; Nicholson, R. L.; Smith, A. D. *Org. Biomol. Chem.* **2004**, *2*, 3385-3400.

88. Suzuki, K.; Inomata, K.; Endo, Y. *Org. Lett.* **2004**, *6*, 409-411.

89. Babler, J. H.; Malek, N. C.; Coghlan, M. J. *J. Org. Chem.* **1978**, *43*, 1821-1823.

90. Crimmins, M. T.; Deloach, J. A. *J. Am. Chem. Soc.* **1986**, *108*, 800-806.

91. Chan, T. H.; Brook, M. A.; Chaly, T. *Synthesis* **1983**, *1983*, 203-205.

92. Seto, H.; Nomura, E.; Fujioka, S.; Koshino, H.; Suenaga, T.; Yoshida, S. *Biosci., Biotechnol., Biochem.* **1999**, *63*, 361-367.

CHAPTER 5

Experimental

5.1 General Procedures

5.1.1 Reagents

All reactions involving organometallic or other moisture-sensitive reagents were carried out under a nitrogen or argon atmosphere using standard vacuum line techniques and glassware that was flame dried and cooled under nitrogen before use. Solvents were dried according to the procedure outlined by Grubbs and co-workers. All reagents were used as supplied (analytical or HPLC grade) without prior purification. Reactions performed below room temperature were cooled by means of an acetone/dry ice bath, with the exception of reactions at 0 °C which were cooled by means of an ice bath. Organic layers were dried over Na_2SO_4.

5.1.2 Chromatography

TLC was performed on aluminium plates coated with 60 F_{254} silica. Plates were visualised using UV light (254 nm), iodine, 1% aq $KMnO_4$, or 10% ethanolic phosphomolybdic acid. Flash column chromatography was performed on Kieselgel 60 silica on a glass column, or on a Biotage SP4 automated flash column chromatography platform.

5.1.3 Spectroscopy

NMR spectra were recorded on Bruker Avance spectrometers in the deuterated solvent stated. Chemical shifts (δ) are reported in ppm and coupling constants (J) in Hz and are uncorrected. Residual signals from the solvents were used as an internal reference. Spectral peaks were assigned using DEPT-135, HMQC and HMBC where appropriate.

IR spectra were recorded on a Bruker Tensor 27 FT-IR spectrometer as either a thin film on NaCl plates (film), a KBr disc (KBr) or using an ATR module (ATR), as stated. Selected

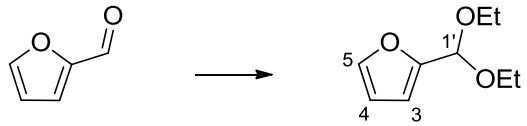
characteristic peaks are reported in cm^{-1}. Melting points were recorded on a Gallenkamp Hot Stage apparatus and are uncorrected.

Low-resolution mass spectra were recorded on either a VG MassLab 20-250 or a Micromass Platform–1 spectrometer. Accurate mass measurements were run on either a Bruker MicroTOF internally calibrated with polyalanine, or a Micromass GCT instrument fitted with a Scientific Glass Instruments BPX5 column (15 m × 0.25 mm) using amyl acetate as a lock mass, by the mass spectrometry department of the Chemistry Research Laboratory, University of Oxford, UK.

5.2 Experimental for Chapter 2

5.2.1 Synthesis of Thiobarbituric Acid Analogues

2-(Diethoxymethyl)furan 17



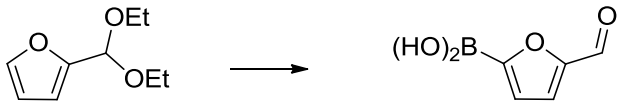
Method A

Triethyl orthoformate (3.41 g, 23.0 mmol) was added to a solution of furan-2-carbaldehyde **15** (2.0 g, 20.82 mmol) and ammonium chloride (0.58 g, 19.7 mmol) in EtOH (3.6 mL). The reaction was heated at reflux for 18 h. Upon cooling, solvent was removed *in vacuo*. The residue was dissolved in EtOAc (50 mL), washed with saturated aqueous $NaHCO_3$ (30 mL), dried ($MgSO_4$), and concentrated *in vacuo*. Purification *via* flash column chromatography (silica, petroleum ether/EtOAc 85:15) afforded the pure product **16** (1.59 g, 45%) as a colourless oil.

Method B

To a solution of furan-2-carbaldehyde **15** (9.60 g, 99.96 mmol) in EtOH (200 mL) was added triethyl *ortho*formate (14.81 g, 99.96 mmol) and pyridinium *p*-toluenesulfonate (2.51 g, 9.99 mmol). The reaction was stirred at room temperature overnight. The solvent was removed *in vacuo* and the resulting residue was dissolved in EtOAc (100 mL). This solution was washed with saturated aqueous $NaHCO_3$ (50 mL), dried ($MgSO_4$) and concentrated *in vacuo*. Purification *via* flash column chromatography (silica, petroleum ether/EtOAc 95:5) furnished the pure product **16** (17.0 g, 74%) as a colourless oil. Data were consistent with those in the literature.[1] **^{1}H NMR** (400 MHz, $CDCl_3$) 7.43-7.21 (1H, m, C(5)*H*), 6.43-6.41 (1H, m, C(3)*H*), 6.37-6.35 (1H, m, C(4)*H*), 5.55 (1H, s, C(1')*H*), 3.67-3.56 (4H, m, CH_2CH$_3$), 1.24 (6H, t, *J* = 7.1 Hz, CH_3); **LRMS** (ESI$^+$) 171 ([M+H]$^+$, 100%).

5-Formyl-2-furylboronic acid 17



To a stirred solution of 2-(diethoxymethyl)furan **16** (6.13 g, 35.80 mmol) in THF (51 mL) at -78 °C was added *n*-BuLi (19.6 mL, 1.6 M in hexane) dropwise and the reaction was stirred for 2 h at -78 °C. Triisopropyl borate (5.61 g, 29.83 mmol) was then added and the resulting solution was allowed to warm to room temperature. The reaction mixture was stirred for 18 h before solvent was removed *in vacuo*. The resulting residue was taken up in water (40 mL) and the pH was adjusted to 10 by the addition of 1M NaOH solution. The aqueous solution was washed with Et_2O (3 x 40 mL) and was acidified to pH 4 with aqueous HBr solution (48%). The precipitated product was filtered and triturated with cold Et_2O (3 x 10 mL) to afford the pure product **17** (2.31 g, 55%) as a light brown powder. Data were consistent with those in the literature.[2] **Mp** 151-152 °C (lit[2] 150-151 °C); **^{1}H NMR** (400 MHz, DMSO-d_6) 9.67 (1H, s, C*H*O), 8.69 (2H, s, B(O*H*)$_2$), 7.48 (1 H, d, *J* = 3.5 Hz, C(3)*H*), 7.22 (1 H, d, *J* = 3.5 Hz, C(4)*H*); **LRMS** (ESI$^+$) 138 ([M+H]$^+$, 100%).

5.2.1.1 Palladium-Catalysed Cross-Coupling Reactions

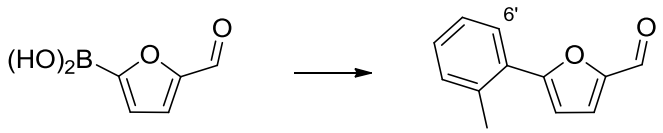
GENERAL PROCEDURE 5.1: Ligandless Suzuki-Miyaura coupling under phase-transfer conditions

To a suspension of boronic acid **17** (1.0 eq) and aryl iodide (1.2 eq) in EtOH/H_2O (6 mL/mmol boronic acid, 1:1) was added $Pd(OAc)_2$ (0.3 mol%), TBAl (1.0 eq) and Na_2CO_3 (2.5 eq). The resulting suspension was stirred at room temperature until completion of the reaction (determined by TLC). The solvent was removed *in vacuo* and the residue was taken up in water (10 mL/mmol boronic acid). The aqueous phase was extracted with EtOAc and the combined organic layers were stirred over charcoal for 30 min. The mixture was filtered and the filtrate was dried ($MgSO_4$) and concentrated *in vacuo*. The crude product was purified by flash column chromatography (silica, petroleum ether/EtOAc).

GENERAL PROCEDURE 5.2: Ligandless Suzuki-Miyaura coupling under homogeneous conditions for polar compounds

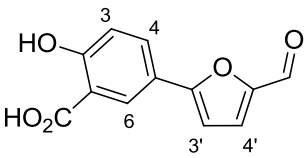
Palladium acetate (0.1 mol%) was added to a stirred suspension of boronic acid **17** (1.05 eq) and aryl iodide (1.0 eq) in water (5 mL/mmol). The mixture was degassed (nitrogen was bubbled through the solution for 5 min) and NaOH (3.0 eq) was added. The temperature of reaction was gradually increased to 75 ºC and the resultant mixture was stirred until completion of the reaction (determined by TLC). The solution was acidified to pH 2 by addition of 1M HCl solution. The aqueous phase was extracted with EtOAc and the combined organic layers was dried ($MgSO_4$) and concentrated *in vacuo*. The crude product was purified by flash column chromatography (silica, petroleum ether/EtOAc).

5-(2-Methylphenyl)-2-furaldehyde 28



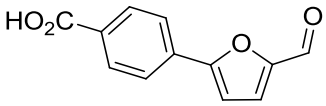
5-Formylfuran-2-boronic acid **17** (500 mg, 3.53 mmol) and 2-iodotoluene **20** (860 mg, 4.23 mmol) were subjected to general procedure 5.1. The crude product was purified *via* flash column chromatography (silica, 9:1 petroleum ether/EtOAc) to furnish the pure compound **28** (280 mg, 86%) as an orange oil. Data were consistent with those in the literature.[3] **^{1}H NMR** (400 MHz, $CDCl_3$) 9.73 (1H, s, C*H*O), 7.85 (1H, d, *J* = 7.0 Hz, C(6')*H*), 7.40 (1H, *J* = 3.8 Hz, C(3)*H*), 7.37-7.29 (3H, m), 6.80 (1H, d, *J* = 3.8 Hz, C(4)*H*), 2.61 (3H, s, CH_3); **LRMS** (ESI^+) 187 ($[M+H]^+$, 100%).

5-(5-formylfuran-2-yl)-2-hydroxybenzoic acid 19



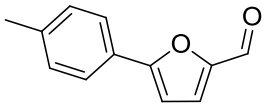
5-Formylfuran-2-boronic acid **17** (250 mg, 1.76 mmol) and 5-iodosalicylic acid **18** (440 mg, 1.67 mmol) were subjected to the general procedure 5.2. The crude product was purified *via* flash column chromatography (silica, 9:1 petroleum ether/EtOAc) to afford the pure compound **19** (180 mg, 45%) as beige powder. Data were consistent with those in the literature.[4] **Mp** 247 °C (lit [4] 245-247 °C); **^{1}H NMR** (400 MHz, $CDCl_3$) 9.68 (1H, s, OH), 9.58 (1H, s, C*H*O), 8.25 (1H, d, *J* = 2.3 Hz, C(6)*H*), 8.05 (1H, d, *J* = 8.7, 2.3 Hz, C(4)*H*), 7.65 (1H, d, *J* = 3.8 Hz, C(4')*H*), 7.24 (1H, *J* = 3.7 Hz, C(3')*H*), 7.12 (1H, *J* = 8.7 Hz, C(3)*H*); **LRMS** (ESI^+) 231 ($[M+H]^+$, 100%).

4-(5-Formylfuran-2-yl) benzoic acid 30



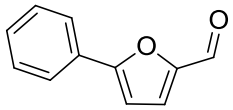
4-Iodobenzoic acid **22** (500 mg, 2.01 mmol) and 5-formylfuran-2-boronic acid **17** (300 mg, 2.12 mmol) were subjected to the general procedure 5.2. The crude product was purified *via* flash column chromatography (silica, 9:1 petroleum ether/EtOAc) to afford the pure compound **30** (226 mg, 52%) a white solid. Data were consistent with those in the literature.[5] **Mp** 310 °C (lit[5] 306-310 °C; **^{1}H NMR** (400 MHz, $CDCl_3$) 9.67 (1H, s, C*H*O), 8.06 (2H, d, *J* = 8.3 Hz, C(2)*H*, C(6)*H*), 8.0 (2H, d, *J* = 8.3 Hz, C(3)*H*, C(5)*H*), 7.71 (1H, d, *J* = 3.8 Hz, C(3')*H*), 7.47 (1H, *J* = 3.8 Hz, C(4')*H*); **LRMS** (ESI^+) 215 ($[M+H]^+$, 100%).

5-*p*-Tolylfuran-2-carbaldehyde 29



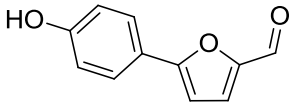
5-Formylfuran-2-boronic acid **17** (500 mg, 3.53 mmol) and 4-iodotoluene **21** (920 mg, 4.23 mmol) were subjected to general procedure 5.1. The crude product was purified *via* flash column chromatography (silica, 9:1 petroleum ether/EtOAc) to afford the pure compound **29** (487 mg, 74%) as a orange oil. Data were consistent with those in the literature.[6] **^{1}H NMR** (400 MHz, $CDCl_3$) 9.59 (1H, s, C*H*O), 7.78 (2H, d, *J* = 8.2, 2.0 Hz, C(2')*H*, C(6')*H*), 7.65 (1H, d, *J* = 3.8 Hz, C(3)*H*), 7.33 (2H, d, *J* = 8.2 Hz, C(3')*H*, C(5')*H*), 7.47 (1H, *J* = 3.8 Hz, C(4)*H*), 2.36 (3H, s, CH_3); **LRMS** (ESI^+) 187 ($[M+H]^+$, 100%).

5-Phenylfuran-2-carbaldehyde 32



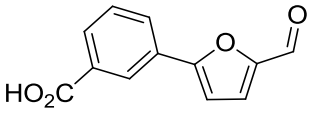
5-Formylfuran-2-boronic acid **17** (500 mg, 3.53 mmol) and phenyl iodide **24** (860 mg, 4.23 mmol) were subjected to general procedure 5.1. The crude product was purified *via* flash column chromatography (silica, 9:1 petroleum ether/EtOAc) to afford the pure compound **32** (150 mg, 84%) as a orange oil. Data were consistent with those in the literature.[6] **^{1}H NMR** (400 MHz, $CDCl_3$) 9.67 (1H, s, C*H*O), 7.86-7.83 (2H, m), 7.49-7.39 (3H, m), 7.34 (1H, *J* = 3.7 Hz, C(3)*H*), 6.86 (1H, *J* = 3.7 Hz, C(4)*H*); **LRMS** (ESI^+) 173 ($[M+H]^+$, 100%).

5-(4-Hydroxyphenyl)furan-2-carbaldehyde 33



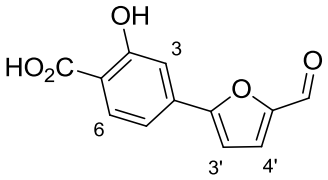
5-Formylfuran-2-boronic acid **17** (420 mg, 2.96 mmol) and *p*-iodophenol **25** (780 mg, 3.55 mmol) were subjected to general procedure 5.1. The crude product was purified *via* flash column chromatography (silica, 9:1 petroleum ether/EtOAc) to afford the pure compound **33** (557 mg, 88%) as brown solid. Data were consistent with those in the literature.[6] **Mp** 177 °C (lit[6] 178-180 °C); **^{1}H NMR** (400 MHz, $CDCl_3$) 10.05 (1H, s, O*H*), 9.53 (1H, s, C*H*O), 7.71 (1H, d, *J* = 8.7 Hz, C(3')*H*, C(5')*H*), 7.61 (1H, d, *J* = 3.8 Hz, C(3)*H*), 7.07 (1H, *J* = 3.7 Hz, C(4)*H*), 6.89 (2H, d, *J* = 8.7 Hz, C(2')*H*, C(6')*H*); **LRMS** (ESI^+) 188 ($[M+H]^+$, 100%).

3-(5-Formylfuran-2-yl) benzoic acid 34



2-Iodobenzoic acid **26** (900 mg, 3.42 mmol) and 5-formylfuran-2-boronic acid **17** (510 mg, 3.60 mmol) were subjected to the general procedure 5.2. The crude product was purified *via* flash column chromatography (silica, 9:1 petroleum ether/EtOAc) to afford the pure compound **38** (226 mg, 52%) as a white solid. Data were consistent with those in the literature.[7] **Mp** 267-268°C (lit[7] 266-267 °C); **^{1}H NMR** (400 MHz, $CDCl_3$) 9.65 (1H, s, C*H*O), 8.38 (1H, s, C(2)*H*, C(5')*H*), 8.12 (1H, d, *J* = 7.8 Hz, C(6)*H*), 7.99 (1H, d, *J* = 7.7 Hz, C(4)*H*), 7.67 (1H, d, *J* = 2.9 Hz, C(4')*H*), 7.65 (1H, t, *J* = 7.7 Hz, C(5)*H*), 7.40 (1H, d, *J* = 3.0 Hz, C(3')*H*); **LRMS** (ES^-) 215 ($[M-H]^-$).

4-(5-formylfuran-2-yl)-2-hydroxybenzoic acid 31



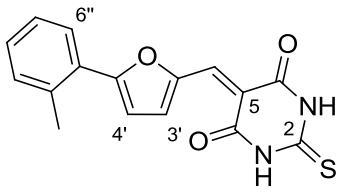
4-Iodosalicylic acid **23** (180 mg, 0.62 mmol) and 5-formylfuran-2-boronic acid (100 mg, 0.72 mmol) were subjected to the general procedure 5.2. The crude product was purified *via* flash column chromatography (silica, 9:1 petroleum ether/EtOAc) to afford the pure compound **31** (124 mg, 75%) as light brown solid. **Mp** 242-244 °C; **^{1}H NMR** (400 MHz, $CDCl_3$) 9.68 (CO_2H), 9.57 (1H, s, C*H*O), 8.23 (1H, s, C(3)*H*), 7.98 (1H, dd, *J* = 8.4, 2.2 Hz, C(5)*H*), 7.65 (1H, d, *J* = 3.8 Hz, C(4')*H*), 7.21 (1H, d, *J* = 3.8 Hz, C(3')*H*), 7.05 (1H, d, *J* = 8.8 Hz, C(6)*H*); **^{13}C NMR** (DMSO-d_6) 178.2 (*C*HO), 171.8 (CO_2H), 161.7 (*C*-OH), 156.9 (furan *C*-O), 151.3 (furan *C*-O), 128.8, 127.3, 123.2 (*C*(4')), 118.4, 115.6, 114.5, 109.2 (*C*(3')); $\boldsymbol{\nu_{max}}$

(disk)/cm^{-1} 3419, 3106, 2960, 2539, 1679, 1648, 1616, 1536, 1200; **HRMS** (ES$^-$): calcd. for $C_{12}H_7O_5$, 231.0299; found, 231.0293.

GENERAL PROCEDURE 5.3: Base and Solvent-Free Knoevenagel condensation

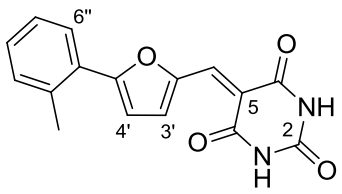
A suspension of corresponding aldehyde (1.0 eq) in water (10m mL/mmol) was added in one portion to a stirred suspension of barbituric acid derivative (1.0 eq) in water (10 mL/mmol). The reaction mixture was sonicated for 5 min and heated to 80 °C for 30 minutes. Upon cooling, the precipitate was filtered, triturated with cold diethyl ether and dried *in vacuo* to give the desired compound in high purity (> 95%).

2-Thioxo-5-((5-*o*-tolylfuran-2-yl)methylene)dihydropyrimidine-4,6(1*H*,5*H*)-dione 40



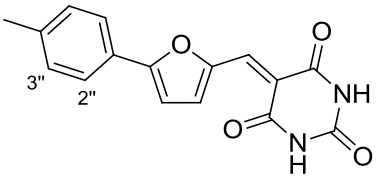
Aldehyde **28** (66 mg, 0.36 mmol) and thiobarbituric acid (51 mg, 0.36 mmol) were subjected to general procedure 5.3 to afford the title compound **40** (69 mg, 96%) as a orange solid. **^{1}H NMR** (400 MHz, DMSO-d_6) 8.65 (1H, *J* = 3.9 Hz, C(3')*H*), 8.12 (1H, s, C=C*H*), 7.93 (1H, d, *J* = 6.5 Hz, Ar(6'')*H*), 7.41-7.37 (3H, m), 7.33 (1H, d, 4.0 Hz, C(4')*H*), 2.59 (3H, s, CH_3); **^{13}C NMR** (DMSO-d_6) 178.5 (*C*=S), 159.9 (*C*=O), 159.2 (*C*=O), 156.8 (furan *C*-O), 145.0 (furan *C*-O), 138.6, 136.0 (H*C*=C), 131.3, 129.8, 128.6, 126.2, 125.8, 122.4, 112.6 (*C*(3')), 112.4 (*C*(4')), 21.9 (*C*H$_3$); $\boldsymbol{\nu}_{\mathbf{max}}$ (disk)/cm^{-1} 3142, 2910, 1703, 1647, 1581, 1566, 1551, 1527, 1506, 1469, 1299, 1038; **HRMS** (ESI$^-$): calcd. for $C_{16}H_{11}N_2O_3S$, 311.0496; found, 311.0491)

5-((5-*o*-Tolylfuran-2-yl)methylene)pyrimidine-2,4,6(1*H*,3*H*,5*H*)-trione 41



Aldehyde **28** (66 mg, 0.36 mmol) and barbituric acid (43 mg, 0.36 mmol) were subjected to general procedure 5.3 to afford the title compound **41** (88 mg, 100%) as a orange solid. **^{1}H NMR** (400 MHz, DMSO-d_6) 11.36 (1H, s, NH), 11.27 (1H, s, NH), 8.59 (1H, *J* = 3.7 Hz, C(3')*H*), 8.12 (1H, s, C=C*H*), 7.91 (1H, d, *J* = 6.5 Hz, Ar(6'')*H*), 7.40-7.36 (3H, m), 7.28 (1H, d, 3.9 Hz, C(4')*H*), 2.58 (3H, s, CH_3); **^{13}C NMR** (DMSO-d_6) 162.5 (*C*=O), 160.7 (*C*=O), 155.8 (furan *C*-O), 152.4 (furan *C*-O), 150.4 (O=*C*(2)), 137.9, 136.2 (H*C*=C), 131.0, 129.8, 128.6, 126.7, 122.9, 120.5, 112.2 (*C*(3')), 112.1 (*C*(4')), 21.9 (*C*H$_3$); $\boldsymbol{\nu_{max}}$ (disk)/cm^{-1} 3540, 3471, 3172, 3056, 2835, 1731, 1694, 1664, 1561, 1497, 1445, 1425, 1214, 1091; **LRMS** (ES$^-$) 295 ([M-H]$^-$); **HRMS** (ESI$^-$): calcd. for $C_{16}H_{11}N_2O_4$, 295.0724; found, 295.0718

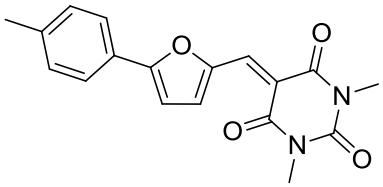
5-((5-*p*-Tolylfuran-2-yl)methylene)pyrimidine-2,4,6(1*H*,3*H*,5*H*)-trione 44



Aldehyde **29** (120 mg, 0.64 mmol) and barbituric acid (83 mg, 0.64 mmol) were subjected to general procedure 5.3 to afford the title compound **44** (175 mg, 96%) as a bright yellow solid. **^{1}H NMR** (400 MHz, DMSO-d_6) 11.32 (1H, s, NH), 11.23 (1H, s, NH), 8.56 (1H, d, *J* = 3.7 Hz, C(3')*H*), 8.10 (1H, s, C=C*H*), 7.86 (2H, dd, *J* = 8.1, 2.0 Hz, C(2'')*H*, C(6'')*H*), 7.41 (1H, d, 3.9 Hz, C(4')*H*), 7.35 (2H, dd, *J* = 8.3, 2.0 Hz, C(3'')*H*, C(5'')*H*), 2.37 (3H, s, CH_3); **^{13}C NMR** (DMSO-d_6) 164.3 (*C*=O), 161.5 (*C*=O), 155.0 (furan *C*-O), 153.3 (furan *C*-O), 150.8 (O=*C*(2)), 136.8 (H*C*=C), 130.7, 126.6, 126.2, 124.8, 120.1, 112.6 (*C*(3')), 112.3 (*C*(4')), 21.9

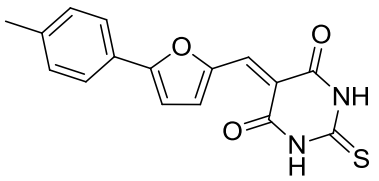
(CH_3); ν_{max} (disk)/cm^{-1} 3189, 3057, 2839, 1809, 1607, 1290, 1221, 1070, 955; **LRMS** (ES^-) 295 ($[M-H]^-$); **HRMS** (ESI^-): calcd. for $C_{16}H_{11}N_2O_4$, 295.0724; found, 295.0718.

1,3-Dimethyl-5-((5-*p*-tolylfuran-2-yl)methylene)pyridine-2,4,6(1*H*,3*H*,5*H*)-trione 45



Aldehyde **29** (120 mg, 0.64 mmol) and 1,3-dimethylbarbituric acid (100 mg, 0.64 mmol) were subjected to general procedure 5.3 to afford the title compound **45** (130 mg, 65%) as a orange solid. **^{1}H NMR** (400 MHz, DMSO-d_6) 8.63 (1H, *J* = 3.9 Hz, C(3')*H*), 8.19 (1H, s, C=C*H*), 7.87 (2H, dd, *J* = 8.1, 2.0 Hz, C(2'')*H*, C(6'')*H*), 7.43 (1H, d, 3.9 Hz, C(4')*H*), 7.35 (2H, dd, *J* = 8.3, 2.0 Hz, C(3'')*H*, C(5'')*H*), 3.24 (6H, s, N-CH_3), 2.37 (3H, s, CH_3); **^{13}C NMR** (DMSO-d_6) 162.5 (*C*=O), 162.4 (*C*=O), 155.9 (furan *C*-O), 153.8 (furan *C*-O), 151.4 (O=*C*(2)), 136.8 (H*C*=C), 130.1, 127.8, 126.0, 124.4, 121.0, 111.8 (*C*(3')), 111.2 (*C*(4')), 30.0 (N-*C*H_3), 21.8 (*C*H_3); ν_{max} (disk)/cm^{-1} 1726, 1655, 1586, 1569, 1476, 1411, 1370, 1389, 1031, 956, 809; **LRMS** (ESI^+) 325 ($[M+H]^+$); **HRMS** (ESI^+): calcd. for $C_{18}H_{17}N_2O_4$, 325.1144; found, 325.1132.

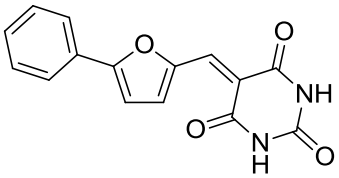
2-Thioxo-5-((5-*p*-tolylfuran-2-yl)methylene)dihydropyrimidine-4,6(1*H*,5*H*)-dione 46



Aldehyde **29** (120 mg, 0.64 mmol) and thiobarbituric acid (92 mg, 0.64 mmol) were subjected to general procedure 5.3 to afford the title compound **46** (130 mg, 65%) as a red solid. **^{1}H NMR** (400 MHz, DMSO-d_6) 12.41 (1H, s, NH), 12.35 (1H, s, NH), 8.63 (1H, d, *J* = 4.0 Hz,

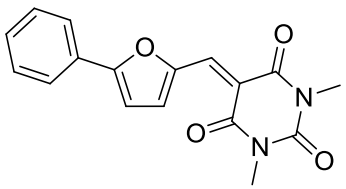
C(3')*H*), 8.11 (1H, s, C=C*H*), 7.89 (2H, dd, *J* = 8.1, 2.0 Hz, C(2'')*H*, C(6'')*H*), 7.45 (1H, d, 4.0 Hz, C(4')*H*), 7.36 (2H, dd, *J* = 8.2, 2.0 Hz, C(3'')*H*, C(5'')*H*), 2.37 (3H, s, CH_3); **^{13}C NMR** (DMSO-d_6) 178.8 (*C*=S), 162.6 (*C*=O), 160.9 (*C*=O), 155.2 (furan *C*-O), 153.8 (furan *C*-O), 141.6, 137.8 (H*C*=C), 130.0, 126.8, 124.8, 120.1, 112.6 (*C*(3')), 112.3 (*C*(4')), 22.0 (*C*H_3); $\boldsymbol{\nu_{max}}$ (disk)/cm^{-1} 3151, 2903, 1700, 1646, 1541, 1516, 1474, 1442, 1376, 1072; **LRMS** (ES$^-$) 311 ([M-H]$^-$); **HRMS** (ESI$^-$): calcd. for $C_{16}H_{11}N_2O_3S$, 311.0569; found, 311.0566.

5-((5-Phenylfuran-2-yl)methylene)pyrimidine-2,4,6(1*H*,3*H*,5*H*)-trione 47



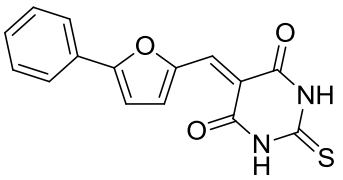
Aldehyde **32** (100 mg, 0.58 mmol) and barbituric acid (74 mg, 0.58 mmol) were subjected to general procedure 5.3 to afford the title compound **47** (94 mg, 60%) as a dark yellow solid. **^{1}H NMR** (400 MHz, DMSO-d_6) 11.34 (1H, s, NH), 11.25 (1H, s, NH), 8.56 (1H, d, *J* = 4.0 Hz, C(3')*H*), 8.10 (1H, s, C=C*H*), 7.96 (2H, d, *J* = 8.6), 7.55-7.44 (4H, m); **^{13}C NMR** (DMSO-d_6) 162.2 (*C*=O), 161.8 (*C*=O), 153.4 (furan *C*-O), 151.2 (furan *C*-O), 150.8 (O=*C*(2)), 136.6 (H*C*=C), 129.8, 128.7, 128.2, 121.8, 120.4, 110.7 (*C*(3')), 110.5 (*C*(4')); $\boldsymbol{\nu_{max}}$ (disk)/cm^{-1} 3145, 3048, 2848, 1743, 1703, 1651, 1562, 1545, 1511, 1472, 1377, 1093, 1041, 962; **LRMS** (ES$^-$) 281 ([M-H]$^-$); **HRMS** (ESI$^-$): calcd. for $C_{15}H_9N_2O_4$, 281.0568; found, 281.0568.

1,3-Dimethyl-5-((5-phenylfuran-2-yl)methylene)pyrimidine-2,4,6(1*H*,3*H*,5*H*)-trione 48



Aldehyde **32** (100 mg, 0.58 mmol) and 1,3-dimethylbarbituric acid (91 mg, 0.58 mmol) were subjected to general procedure 5.3 to afford the title compound **48** (135 mg, 78%) as a light orange solid. **^{1}H NMR** (400 MHz, DMSO-d_6) 8.63 (1H, *J* = 4.0 Hz, C(3')*H*), 8.17 (1H, s, C=C*H*), 7.84 (2H, dd, *J* = 8.6, 2.0 Hz, C(2'')*H*, C(6'')*H*), 7.56-7.49 (3H, m), 7.30 (1H, d, 3.9 Hz, C(4')*H*), 3.24 (6H, s, N-CH_3); **^{13}C NMR** (DMSO-d_6) 161.8 (*C*=O), 161.7 (*C*=O), 152.8 (furan *C*-O), 152.5 (furan *C*-O), 150.4 (O=*C*(2)), 130.3, 128.0, 127.7, 125.4, 124.6, 120.5, 110.4 (*C*(3')), 111.0 (*C*(4')), 29.2 (N-*C*H_3); $\boldsymbol{\nu}_{\mathbf{max}}$ (disk)/cm^{-1} 1724, 1656, 1566, 1549, 1513, 1455, 1407, 1370, 1129, 1099, 980; **LRMS** (ES$^-$) 310 ([M-H]$^-$); **HRMS** (ESI$^-$): calcd. for $C_{17}H_{14}N_2O_4$, 310.0954; found, 310.0964.

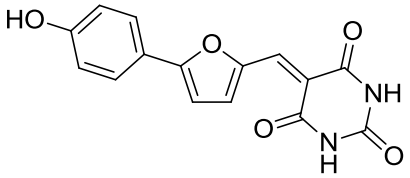
5-((5-Phenylfuran-2-yl)methylene)-2-thioxodihydropyrimidine-4,6(1*H*,5*H*)-dione 49



Aldehyde **32** (100 mg, 0.58 mmol) and 1,3-dimethylbarbituric acid (84 mg, 0.58 mmol) were subjected to general procedure 5.3 to afford the title compound **52** (147 mg, 88%) as a orange solid. **^{1}H NMR** (400 MHz, DMSO-d_6) 12.43 (1H, s, NH), 12.37 (1H, s, NH), 8.63 (1H, d, *J* = 4.0 Hz, C(3')*H*), 8.11 (1H, s, C=C*H*), 7.99-7.96 (2H, m), 7.46-7.49 (4H, m); **^{13}C NMR** (DMSO-d_6) 178.9 (*C*=S), 160.5 (*C*=O), 160.3 (*C*=O), 153.5 (furan *C*-O), 145.8 (furan *C*-O), 136.2 (H*C*=C), 129.7, 128.6, 128.0, 122.9, 120.5, 110.5 (*C*(3')), 110.3 (*C*(4')); $\boldsymbol{\nu}_{\mathbf{max}}$

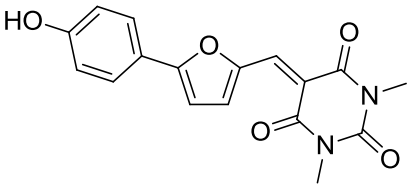
(disk)/cm^{-1} 3148, 3066, 2923, 2902, 1700, 1644, 1540, 1506, 1376, 1238, 1171, 955; **LRMS** (ES$^-$) 297 ([M-H]$^-$); **HRMS** (ESI$^-$): calcd. for $C_{15}H_{10}N_2O_3S$, 297.0446; found, 297.0443.

5-((5-(4-Hydroxyphenyl)furan-2-yl)methylene)pyrimidine-2,4,6(1*H*,3*H*,5*H*)-trione 50



Aldehyde **33** (120 mg, 0.64 mmol) and barbituric acid (82 mg, 0.64 mmol) were subjected to general procedure 5.3 to afford the title compound **50** (94 mg, 96%) as a dark yellow solid. **^{1}H NMR** (400 MHz, DMSO-d_6) 11.26 (1H, s, NH), 11.17 (1H, s, NH), 10.20 (1H, s, OH), 8.59 (1H, d, *J* = 3.9 Hz, C(3')*H*), 8.08 (1H, s, C=C*H*), 7.82 (2H, dd, *J* = 8.8, 2.0 Hz, C(2'')*H*, C(6'')*H*), 7.27 (1H, d, 3.9 Hz, C(4')*H*), 6.90 (2H, dd, *J* = 8.8, 2.0 Hz, C(3'')*H*, C(5'')*H*); **^{13}C NMR** (DMSO-d_6) 161.6 (*C*=O), 161.3 (*C*=O), 156.5 (*C*-OH), 152.7 (furan *C*-O), 152.6 (furan *C*-O), 150.0 (O=*C*(2)), 136.6 (H*C*=C), 128.3, 122.6, 120.4, 117.9, 110.9 (*C*(3')), 110.8 (*C*(4')); $\boldsymbol{\nu_{max}}$ (disk)/cm^{-1} 3027, 2839, 1719, 1693, 1609, 1534, 1174, 955, 519; **LRMS** (ESI$^-$) 297 ([M-H]$^-$); **HRMS** (ESI$^-$): calcd. for $C_{15}H_9N_2O_5$, 297.0623; found, 297.0613.

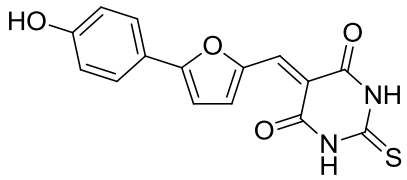
5-((5-(4-hydroxyphenyl)furan-2-yl)methylene)-1,3-dimethylpyrimidine-2,4,6-(1*H*,3*H*,5*H*)-trione 51



Aldehyde **33** (120 mg, 0.64 mmol) and 1,3-dimethylbarbituric acid (100 mg, 0.64 mmol) were subjected to general procedure 5.3 to afford the title compound **51** (178 mg, 89%) as a orange solid. **^{1}H NMR** (400 MHz, DMSO-d_6) 10.25 (1H, br. s), 8.61 (1H, *J* = 4.0 Hz, C(3')*H*), 8.10

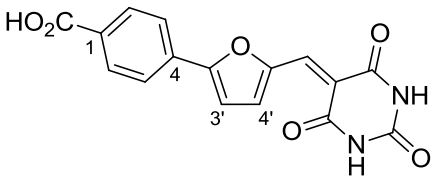
(1H, s, C=C*H*), 7.79 (2H, dd, *J* = 7.7, 2.0 Hz, C(2'')*H*, C(6'')*H*), 7.25 (1H, d, 4.0 Hz, C(4')*H*), 6.89 (2H, dd, *J* = 7.7, 2.0 Hz, C(3'')*H*, C(5'')*H*), 3.20 (6H, s, N-CH_3); **^{13}C NMR** (DMSO-d_6) 160.7 (*C*=O), 160.6 (*C*=O), 156.6 (*C*-OH), 152.5 (furan *C*-O), 151.4 (furan *C*-O), 148.2 (O=*C*(2)), 127.8, 124.4, 123.7, 120.6, 117.4, 109.5 (*C*(3')), 109.2 (*C*(4')), 29.2 (N-*C*H_3); $\boldsymbol{\nu_{max}}$ (disk)/cm^{-1} 3293, 3174, 3119, 3024, 2959, 1723, 1608, 1591, 1480, 1336, 1172, 1076, 936; **LRMS** (ES$^-$) 325 ([M-H]$^-$); **HRMS** (ESI$^-$): calcd. for $C_{17}H_{13}N_2O_5$, 325.0830; found, 325.0832.

5-((5-(4-hydroxyphenyl)furan-2-yl)methylene)-2-thioxodihydropyrimidine-4,6(1*H*,5*H*)-dione 52



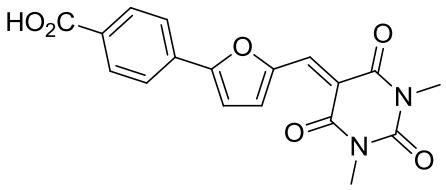
Aldehyde **33** (120 mg, 0.64 mmol) and thiobarbituric acid (92 mg, 0.64 mmol) were subjected to general procedure 5.3 to afford the title compound **52** (159 mg, 83%) as a orange solid. **^{1}H NMR** (400 MHz, DMSO-d_6) 12.36 (1H, s, NH), 12.30 (1H, s, NH), 8.63 (1H, d, *J* = 4.0 Hz, C(3')*H*), 8.08 (1H, s, C=C*H*), 7.85 (2H, dd, *J* = 7.9, 2.0 Hz, C(2'')*H*, C(6'')*H*), 7.34 (1H, d, 4.0 Hz, C(4')*H*), 6.93-6.87 (2H, m); **^{13}C NMR** (DMSO-d_6) 178.4 (*C*=S), 159.6 (*C*=O), 159.2 (*C*=O), 156.7 (furan *C*-O), 154.8 (furan *C*-O), 146.1, 137.4 (H*C*=C), 128.6, 122.5, 120.5, 117.9, 110.1 (*C*(3')), 109.6 (*C*(4')); $\boldsymbol{\nu_{max}}$ (disk)/cm^{-1} 1906, 1643, 1611, 1529, 1473, 1369, 1268, 948, 838, 526; **LRMS** (ES$^-$) 313 ([M-H]$^-$); **HRMS** (ESI$^-$): calcd. for $C_{15}H_9N_2O_4S$, 313.0289; found, 313.0282.

4-(5-((2,4,6-Trioxotetrahydropyrimidine-5(6*H*)-ylidene)furan-2-yl)benzoic acid 53



Aldehyde **30** (50 mg, 0.23 mmol) and barbituric acid (30 mg, 0.64 mmol) were subjected to general procedure 5.3 to afford the title compound **53** (72 mg, 97%) as a dark yellow solid. **^{1}H NMR** (400 MHz, DMSO-d_6) 12.36 (1H, s, NH), 12.30 (1H, s, NH), 8.68 (1H, d, J = 3.8 Hz, C(4')*H*), 8.08 (1H, s, C=C*H*), 7.85 (2H, dd, J = 8.7, 2.0 Hz, C(2'')*H*, C(6'')*H*), 7.34 (1H, d, 4.0 Hz, C(3')*H*), 6.87 (2H, dd, J = 8.7, 2.0 Hz, C(3'')*H*, C(5'')*H*); **^{13}C NMR** (DMSO-d_6) 179.2 (CO_2H), 163.9 (*C*=O), 162.5 (*C*=O), 153.9 (furan *C*-O), 153.1 (furan *C*-O), 150.2 (O=*C*(2)), 136.6 (H*C*=C), 135.5, 130.2, 127.9, 124.4, 123.3, 109.9 (*C*(4')), 109.4 (*C*(3')); $\boldsymbol{\nu_{max}}$ (disk)/cm^{-1} 3456, 3066, 2923, 2902, 1700, 1644, 1540, 1506, 1376, 1238, 1171, 955; **LRMS** (ES$^-$) 325 ([M-H]$^-$); **HRMS** (ESI$^-$): calcd. for $C_{16}H_9N_2O_6$, 325.0343; found, 325.0345.

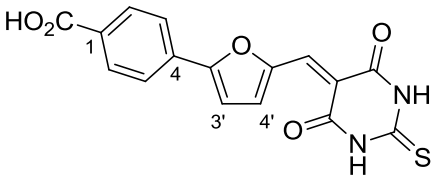
4-(5-((1,3-Dimethyl-2,4,6-trioxotetrahydropyrimidine-5(6*H*)-ylidene)furan-2-yl)benzoic acid 54



Aldehyde **30** (50 mg, 0.23 mmol) and 1,3-dimethylbarbituric acid (30 mg, 0.64 mmol) were subjected to general procedure 5.3 to afford the title compound **54** (66 mg, 82%) as a dark yellow solid. **^{1}H NMR** (400 MHz, DMSO-d_6) 12.34 (1H, s, NH), 12.31 (1H, s, NH), 8.63 (1H, J = 3.9 Hz, C(4')*H*), 8.21 (1H, s, C=C*H*), 8.06-8.00 (4H, m), 7.56 (1H, d, 3.9 Hz, C(3')*H*), 3.25 (6H, s, N-CH_3); **^{13}C NMR** (DMSO-d_6) 179.8 (CO_2H), 164.9 (*C*=O), 164.3 (*C*=O), 159.7 (furan *C*-O), 156.8 (furan *C*-O), 151.0 (O=*C*(2)), 135.4, 129.9, 128.1, 124.4,

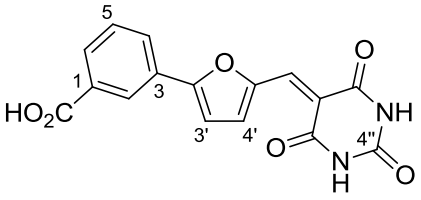
123.7, 120.6, 109.6 (*C*(4')), 109.2 (*C*(3')), 28.4 (N-*C*H_3); ν_{max} (disk)/cm^{-1} 3427, 2959,1728, 1663, 1697, 1569, 1469, 1236, 1127, 940; **LRMS** (ES^-) 353 ([M-H]$^-$); **HRMS** (ESI^-): calcd. for $C_{18}H_{13}N_2O_6$, 353.0779; found, 353.0773.

4-(5-((4,6-Dioxo-2-thioxotetrahydropyrimidine-5(6*H*)-ylidene)furan-2-yl)benzoic acid 55



Aldehyde **30** (50 mg, 0.23 mmol) and thiobarbituric acid (30 mg, 0.64 mmol) were subjected to general procedure 5.3 to afford the title compound **55** (63 mg, 76%) as a orange solid. **^{1}H NMR** (400 MHz, DMSO-d_6) 8.62 (1H, d, *J* = 3.9 Hz, C(4')*H*), 8.13-8.06 (5H, m), 7.64 (1H, d, 4.0 Hz, C(3')*H*), 6.93-6.87 (2H, m); **^{13}C NMR** (DMSO-d_6) 179.5 (CO2H), 178.7 (*C*=S), 164.2 (*C*=O), 163.3 (*C*=O), 162.8 (furan *C*-O), 158.1 (furan *C*-O), 146.8, 136.9 (H*C*=C), 131.1, 129.7, 128.3, 120.3, 110.5, (*C*(4')), 109.4 (*C*(3')); ν_{max} (disk)/cm^{-1} 3050, 2899, 1690, 1644, 1608, 1578, 1512, 1426, 1315, 1270, 1038, 958; **LRMS** (ES^-) 341 ([M-H]$^-$); **HRMS** (ESI^-): calcd. for $C_{16}H_9N_2O_5S$, 341.0238; found, 341.0240.

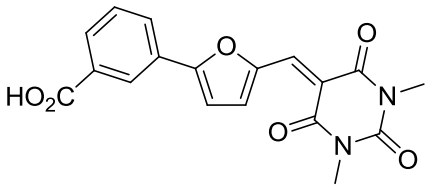
3-(5-((2,4,6-Trioxotetrahydropyrimidine-5(6*H*)-ylidene)methyl)furan-2-yl) benzoic acid 56



Aldehyde **34** (200 mg, 0.93 mmol) and barbituric acid (120 mg, 0.93 mmol) were subjected to general procedure 5.3 to afford the title compound **56** (260 mg, 86%) as a orange solid. **^{1}H NMR** (400 MHz, DMSO-d_6) 13.31 (1H, br. s, CO_2H), 11.36 (1H, s, NH), 11.28 (1H, s, NH),

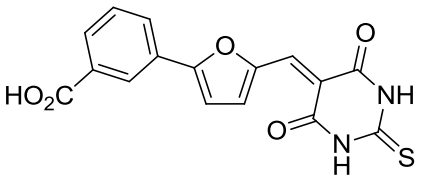
8.55 (1H, *J* = 4.0 Hz, C(4')*H*), 8.44 (1H, m, C(2)*H*), 8.20 (1H, dt, *J* = 7.8, 2.0 Hz, C(6)*H*), 8.12 (1H, s, C=C*H*), 8.01 (1H, dt, *J* = 7.8, 2.0 Hz, C(4)*H*), 7.66 (1H, t, *J* = 7.8 Hz, C(5)*H*), 7.57 (1H, d, 3.9 Hz, C(3')*H*); **^{13}C NMR** (DMSO-d_6) 167.5 (CO_2H), 164.2 (*C*=O), 163.0 (*C*=O), 159.7 (furan *C*-O), 153.0 (furan *C*-O), 151.1 (O=*C*(4")), 136.9 (H*C*=C), 132.7, 131.4, 130.6, 130.2, 130.0, 129.7, 126.5, 113.5 (*C*(4')), 113.0 (*C*(3')); $\boldsymbol{\nu}_{\mathbf{max}}$ (disk)/cm^{-1} 3481, 3203, 3072, 2819, 2637, 1743, 1678, 1568, 1447, 1422, 1223, 1130, 960; **LRMS** (ES$^-$) 325 ([M-H]$^-$); **HRMS** (ESI$^-$): calcd. for $C_{16}H_9N_2O_6$, 325.0466; found, 325.0468.

3-(5-((1,3-Dimethyl-2,4,6-trioxotetrahydropyrimidine-5(6*H*)-ylidene)methyl)-furan-2-yl) benzoic acid 57



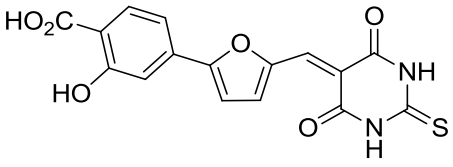
Aldehyde **34** (200 mg, 0.93 mmol) and 1,3-dimethylbarbituric acid (140 mg, 0.93 mmol) were subjected to general procedure 5.3 to afford the title compound **57** (285 mg, 95%) as a orange solid. **^{1}H NMR** (400 MHz, DMSO-d_6) 13.30 (1H, br. s, CO_2H), 8.60 (1H, *J* = 3.9 Hz, C(4')*H*), 8.43 (1H, s, C(2)*H*), 8.21 (1H, m, C(6)*H*), 8.19 (1H, s, C=C*H*), 8.00 (1H, m, C(4)*H*), 7.66 (1H, t, *J* = 7.8 Hz, C(5)*H*), 7.58 (1H, d, 3.9 Hz, C(3')*H*), 3.23 (6H, s, N-CH_3); **^{13}C NMR** (DMSO-d_6) 167.9 (CO_2H), 163.0 (*C*=O), 162.6 (*C*=O), 158.4 (furan *C*-O), 156.6 (furan *C*-O), 151.7 (O=*C*(4")), 144.2, 135.6, 129.0, 127.5, 125.7, 120.9, 116.7, 110.7 (*C*(4')), 109.7 (*C*(3')), 29.5 (N-*C*H_3), 28.8 (N-*C*H_3); $\boldsymbol{\nu}_{\mathbf{max}}$ (disk)/cm^{-1} 3165, 1723, 1592, 1576, 1552, 1507, 1475, 1416, 1275, 1416, 1275, 1113, 1037, 987; **LRMS** (ES$^-$) 323 ([M-H]$^-$); **HRMS** (ESI$^-$): calcd. for $C_{18}H_{13}N_2O_6$, 353.0779; found, 353.0774.

3-(5-((4,6-Dioxo-2-thioxotetrahydropyrimidine-5(6*H*)-ylidene)methyl)furan-2-yl) benzoic acid 58



Aldehyde **34** (200 mg, 0.93 mmol) and 1,3-dimethylbarbituric acid (130 mg, 0.93 mmol) were subjected to general procedure 5.3 to afford the title compound **58** (276 mg, 92%) as an orange solid. **^{1}H NMR** (400 MHz, DMSO-d_6) 13.29 (1H, br. s, CO_2H), 12.46 (1H, s, NH), 12.40 (1H, s, NH), 8.62 (1H, *J* = 4.0 Hz, C(4')*H*), 8.47 (1H, m, C(2)*H*), 8.24 (1H, dt, *J* = 7.8, 2.7 Hz, C(6)*H*), 8.14 (1H, s, C=C*H*), 8.03 (1H, dt, *J* = 7.8, 2.5 Hz, C(4)*H*), 7.80 (1H, t, *J* = 7.8 Hz, C(5)*H*), 7.63 (1H, d, 4.0 Hz, C(3')*H*); **^{13}C NMR** (DMSO-d_6) 177.5 (*C*=S), 167.6 (CO_2H), 159.5 (*C*=O), 156.0 (*C*=O), 152.4 (furan *C*-O), 146.8 (furan *C*-O), 136.6 (H*C*=C), 133.4, 132.8, 131.7, 129.6, 122.5, 120.8, 117.0, 110.8 (*C*(4')), 109.4 (*C*(3')); $\boldsymbol{\nu_{max}}$ (disk)/cm^{-1} 3441, 3066, 2900, 1699, 1646, 1544, 1503, 1445, 1374, 1275, 1170, 1131, 997; **LRMS** (ES$^-$) 341 ([M-H]$^-$)**; HRMS** (ESI$^-$): calcd. for $C_{16}H_9N_2O_5S$, 341.0238; found, 341.0250.

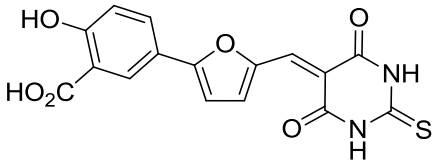
4-(5-((4,6-Dioxo-2-thioxotetrahydropyrimidin-5(2H)-ylidene)methyl)furan-2-yl)-2-hydroxybenzoic acid 42



Aldehyde **31** (50 mg, 0.22 mmol) and thiobarbituric acid (31 mg, 0.22 mmol) were subjected to general procedure 5.3 to afford the title compound **42** (68 mg, 88%) as a dark red solid. Data were consistent with those in the literature.[8] **^{1}H NMR** (400 MHz, DMSO-d_6) 11.40 (1H, s, NH), 11.32 (1H, s, NH), 8.53 (1H, d, *J* = 4.0 Hz, C(3')*H*), 8.12 (1H, s, *H*C=C), 7.92 (1H, d,

J = 8.0 Hz, C(5)*H*), 7.43-7.71 (3H, m); **HRMS** (ES^-): calcd. for $C_{16}H_9N_2O_6S$, 357.0181; found, 357.0187.

5-(5-((4,6-Dioxo-2-thioxotetrahydropyrimidin-5(2H)-ylidene)methyl)furan-2-yl)-2-hydroxybenzoic acid P00337

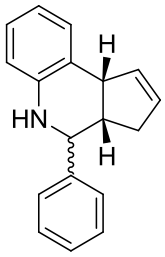


Aldehyde **19** (80 mg, 0.35 mmol) and thiobarbituric acid (50 mg, 0.35 mmol) were subjected to general procedure 5.3 to afford the title compound **P00337** (109 mg, 88%) as a purple solid. Data were consistent with those in the literature.[8] **^{1}H NMR** (400 MHz, DMSO-d_6) 12.39 (1H, s, NH), 12.33 (1H, s, NH), 8.63 (1H, *J* = 4.0 Hz, C(4')*H*), 8.32 (1H, m, C(6)*H*), 8.12 (1H, s, C=C*H*), 8.05-8.03 (1H, m, C(4)*H*), 7.43 (1H, d, 4.0 Hz, C(3')*H*), 7.09 (1H, d, *J* = 8.0 Hz, C(3)*H*); **HRMS** (ES^-): calcd. for $C_{16}H_9N_2O_6S$, 357.0181; found, 357.0187.

5.3 Experimental for chapter 3

5.3.1 Synthesis of Tetrahydroquinolines

4-Phenyl-3a,4,5,9b-tetrahydro-3*H*-cyclopenta[*c*]quinolone 92



Method A: Lewis acid-catalysed one-pot Diels-Alder reaction - $Yb(OTf)_3$, $Y(OTf)_3$ or $Sc(OTf)_3$ used as the catalyst.

Benzaldehyde (5.37 mmol) and aniline (5.37 mmol) were added to a suspension of Lewis acid (20 mol%) and $MgSO_4$ (500 mg) in MeCN (15 mL) at room temperature. The reaction mixture was stirred for 5 min before the addition of cyclopentadiene (16.11 mmol) in MeCN (5 mL). The reaction was stirred at room temperature overnight. After the completion of reaction, solvent was removed *in situ* and the residue was taken up in saturated aqueous $NaHCO_3$. The product was extracted with CH_2Cl_2 (3 x 30 mL) and the combined organic layers were washed with brine, dried ($MgSO_4$) and concentrated *in vacuo*. The crude product was purified *via* flash column chromatography (silica, petroleum ether/EtOAc) to afford the pure product **92** as a colourless oil.

Method 2: $GdCl_3$-catalysed one-pot Diels-Alder reaction.

A solution of benzaldehyde (5.37 mmol) and aniline (5.91 mmol) in MeCN (8 mL) was added to a suspension of $GdCl_3$ (20 mol%) and $MgSO_4$ (500 mg) in MeCN (4 mL) was added at room temperature. The mixture was stirred for 5 min before the addition of cyclopentadiene (7.52 mmol) in MeCN (4 mL). The reaction mixture was stirred at room temperature

overnight. The resulting suspension was then filtered through a short plug of silica gel and concentrated *in vacuo*. The crude product was purified *via* flash column chromatography (silica, petroleum ether/EtOAc) to afford the pure product **92** (865 mg, 65%) as a colourless oil.

Method 3: TFA-catalysed one-pot Diels-Alder reaction.

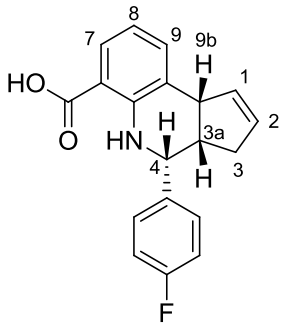
To a suspension of TFA (20 mol%) and $MgSO_4$ (500 mg) in MeCN (15 mL) was added benzaldehyde (5.37 mmol) and aniline (5.37 mmol). The mixture was stirred for 5 before the addition of a solution of cyclopentadiene (16.11 mmol) in MeCN (5 mL) was added and the mixture was stirred at room temperature overnight. The solvent was co-evaporated with toluene and the crude product was purified *via* flash column chromatography (silica, petroleum ether/EtOAc) to afford the pure product **92** (580 mg, 46%) as a white solid.

Data were consistent with those in the literature.[9] *cis* isomer: **Mp** 116–117 °C (lit[9] 117-118 °C).[1]**H NMR** (400 MHz, $CDCl_3$) 7.27 – 7.47 (5H, m), 7.07 (1H, d, *J* = 8.0 Hz), 6.99 (1H, m), 6.76 (1H, m), 6.64 (1H, d, *J* = 8.0 Hz), 5.67 (1H, m), 4.66 (1H, d, *J* = 2.9 Hz), 4.13 (1H, d, *J* = 8.6 Hz), 3.73 (1H, br. s), 3.00 (1H, m), 2.63 (1H, m), 1.80 (1H, m); **^{13}C NMR** ($CDCl_3$) 145.6, 142.8, 134.0, 130.3, 129.0, 128.4, 127.2, 126.4, 126.3, 126.0, 119.1, 115.9, 58.0, 46.4, 46.0, 31.5; **LRMS** (ES^+) 248 ($[M+H]^+$).

GENERAL PROCEDURE 5.4: Synthesis of tetrahydroquinolines P00104 and P00341 and their structural analogues using $BF_3.OEt_2$ as the catalyst in one-pot Diels-Alder reaction

The requisite substituted benzaldehyde (5.37 mmol) and aniline (5.37 mmol) were added to a suspension of $BF_3.OEt_2$ (20 mol%) and $MgSO_4$ (500 mg) in MeCN (15 mL) at room temperature. The reaction mixture was stirred for 5 min before the addition of cyclopentadiene (16.11 mmol) in MeCN (5 mL). The reaction was stirred at room temperature overnight. After the completion of reaction, solvent was removed *in situ* and the residue was taken up in saturated aqueous $NaHCO_3$. The product was extracted with CH_2Cl_2 (3 x 30 mL) and the combined organic layers were washed with brine, dried ($MgSO_4$) and concentrated *in vacuo*. The crude product was purified *via* flash column chromatography (silica, petroleum ether/EtOAc) to afford the pure product**.**

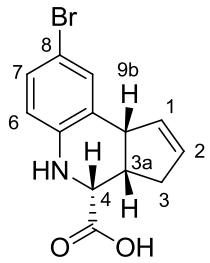
4-(4-Fluorophenyl)-3a,4,5,9b-tetrahydro-3H-cyclopenta[c]quinoline-6-carboxylic acid P00341



Anthranilic acid (0.74 g, 5.37 mmol), *p*-fluorobenzaldehyde (0.67 g, 5.37 mmol) and cyclopentadiene (1.06 g, 16.11 mmol) were subjected to general procedure 5.4. Purification *via* flash column chromatography (silica, 7:3 petroleum ether/EtOAc) afforded the pure product *cis*-**P00341** (158 mg, 12%) as a light brown solid. **Mp** 213-215 ºC; **^{1}H NMR** (400 MHz, $CDCl_3$) 7.82-7.78 (1H, m, C(7)*H*), 7.64 (1H, d, *J* = 8.0 Hz, C(9)*H*), 7.48 (2H, dd, *J* = 8.1, 5.7 Hz), 7.27-7.25 (2H, m), 6.64 (1H, t, *J* = 7.3 Hz, C(8)*H*), 5.86-5.84 (1H, m,

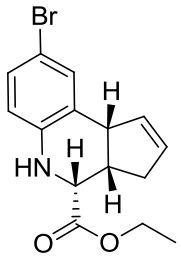
C(1)*H*), 5.59 (1H, d, *J* = 5.3 Hz, C(2)*H*), 4.70 (1H, d, *J* = 3.0 Hz, C(4)*H*), 4.44 (1H, br. s, N*H*), 4.12 (1H, d, *J* = 8.8 Hz, C(9b)*H*), 3.02-2.96 (1H, m, C(3a)*H*), 2.38 (1H, dd, *J* = 14.8, 9.6 Hz, C(3)*H*), 1.69 (1H, dd, *J* = 14.8, 9.6 Hz, C(3)*H*); **^{13}C NMR** ($CDCl_3$) 170.7 (*C*O_2H), 150.1 (*C*-F), 135.7 (*C*-NH), 134.8, 130.5, 129.8, 128.9, 128.8, 127.4, 117.1, 116.3, 116.1, 112.5, 55.9 (*C*(4)), 46.3 (*C*(9b)), 45.2 (*C*(3a)), 32.3 (*C*(3)), $\boldsymbol{\nu}_{\mathbf{max}}$ (thin film)/cm^{-1} 3353, 1608, 1478; **LRMS** (ES^-) 308 ($[M-H]^-$, 100%); **HRMS** (ESI): calcd. for $C_{19}H_{15}FNO$, 308.1199; found, 308.1202.

8-Bromo-3a,4,5,9b-tetrahydro-3*H*-cyclopenta[*c*]quinoline-4-carboxylic acid P00104



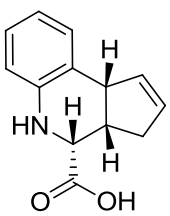
Glyoxilic acid (0.40 g, 5.37 mmol), *p*-bromoaniline (0.92 g, 5.37 mmol) and cyclopentadiene (1.06 g, 16.11 mmol) were subjected to general procedure 5.4. Purification *via* flash column chromatography (silica, 8:2 petroleum ether/EtOAc) afforded the pure product *cis*-**P00104** (0.47 g, 45%) as a green solid. **Mp** 108-110 ºC; **^{1}H NMR** (400 MHz, DMSO-d_6) 7.09 (1H, d, *J* = 2.0 Hz, C(9)*H*), 6.96 (1H, dd, *J* = 8.5, 2.2 Hz, C(7)*H*), 6.71 (1H, d, *J* = 8.5 Hz, C(6)*H*), 5.76 (1H, dd, *J* = 5.4, 2.3 Hz, C(1)*H*), 5.61 (1H, d, *J* = 5.4 Hz, C(2)*H*), 3.94 (1H, d, *J* = 8.9 Hz, C(9b)*H*), 3.79 (1H, d, *J* = 3.2 Hz, C(4)*H*), 3.15 (1H, m, C(3a)*H*), 2.32-2.14 (2H, m, C(3)*H*); **^{13}C NMR** (DMSO-d_6) 173.2 (*C*O_2H), 144.6, 134.5 (*C*(1)), 130.5, 129.8 (*C*(2)), 128.3, 127.6, 117.2, 107.6, 55.9 (*C*(4)), 45.6 (*C*(9b)), 40.5 (*C*(3a)), 32.2 (*C*(3)); $\boldsymbol{\nu}_{\mathbf{max}}$ (thin film)/cm^{-1} 3381, 1704, 1488, 1123, 875, 808, 715, 614; **LRMS** (ESI^-) 293 ($[M-H]^-$, 100%); **HRMS** (ESI): calcd. for $C_{13}H_{11}BrNO_2$, 293.0051; found, 293.0048.

8-Bromo-3a,4,5,9b-tetrahydro-3*H*-cyclopenta-[*c*]quinoline-4-carboxylic acid ethyl ester 112



Glyoxilic acid (0.40 g, 5.37 mmol), aniline (0.92 g, 5.37 mmol) and cyclopentadiene (1.06 g, 16.11 mmol) were subjected to general procedure 5.4. Purification *via* flash column chromatography (silica, 8:2 petroleum ether/EtOAc) afforded the pure product *cis*-**112** (2.22 g, 64%) as a green solid. **Mp** 100-102 ºC; **^{1}H NMR** (400 MHz, DMSO-d_6) 7.14 (1H, d, J = 2.2 Hz, C(9)*H*), 7.01 (1H, dd, J = 8.6, 2.2 Hz, C(7)*H*), 6.74 (1H, d, J = 8.6 Hz, C(6)*H*), 5.80 (1H, dd, J = 5.2, 2.5 Hz, C(1)*H*), 5.65 (1H, s, N*H*), 5.62 (1H, d, J = 5.2 Hz, C(2)*H*), 4.30-4.08 (2H, m, OCH_2), 4.05-3.97 (2H, m, C(4)*H*, C(9b)*H*), 3.10 (1H, m, C(3a)*H*), 2.35-2.13 (2H, m, C(3)*H*), 1.23 (3H, t, J = 7.3 Hz, CH_3); **^{13}C NMR** (DMSO-d_6) 171.3 (CO_2H), 144.0, 134.5 (*C*(1)), 130.5, 129.8 (*C*(2)), 128.4, 127.3, 117.1, 108.4, 60.0 (O*C*H), 55.1 (*C*(4)), 45.5 (*C*(9b)), 40.2 (*C*(3a)), 32.2 (*C*(3)), 14.0 (CH_3); $\boldsymbol{\nu_{max}}$ (thin film)/cm^{-1} 3349, 1715, 1491, 1170, 885, 860, 645; **LRMS** (ESI$^+$) 323 ([M+H]$^+$, 100%); **HRMS** (ESI$^+$): calcd. for $C_{15}H_{17}BrNO_2$, 323.0344; found, 323.0347.

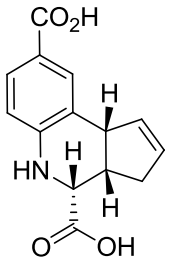
3a,4,5,9b-Tetrahydro-3*H*-cyclopenty[*c*]quinoline-4-carboxylic acid 113



Ethyl glycolate (1.10 g, 5.37 mmol), aniline (0.50 g, 5.37 mmol) and cyclopentadiene (1.06 g, 16.11 mmol) were subjected to general procedure 5.4. Purification *via* flash column

chromatography (silica, 8:2 petroleum ether/EtOAc) afforded the pure product *cis*-**113** (0.52 g, 52%) as a light green solid. **Mp** 98 ºC; **^{1}H NMR** (400 MHz, DMSO-d_6) 6.91 (1H, d, *J* = 7.4 Hz, C(9)*H*), 6.82 (1H, dd, *J* = 7.8, 7.3 Hz, C(7)*H*), 6.68 (1H, d, *J* = 7.7 Hz, C(6)*H*), 6.51 (1H, dd, *J* = 7.4 Hz, C(8)*H*), 5.71 (1H, dd, *J* = 5.6, 2.5 Hz, C(1)*H*), 5.69 (1H, d, *J* = 5.6 Hz, C(2)*H*), 3.93 (1H, d, *J*=8.8 Hz, C(9)*H*), 4.01 (1H, d, *J* = 3.4 Hz, C(4)*H*), 3.14 (1H, m, C(3a)*H*), 2.24 (2H, m, C(3)*H*); **^{13}C NMR** (DMSO-d_6) 173.5 (*C*O_2H), 145.6, 134.8 (*C*(1)), 130.0, 129.5 (*C*(2)), 128.4, 125.6, 125.1, 117.0, 114.9, 56.3 (*C*(4)), 46.2 (*C*(9b)), 40.9 (*C*(3a)), 32.3 (*C*(3)); $\boldsymbol{\nu}_{\mathbf{max}}$ (thin film)/cm^{-1} 3365, 1586, 1231, 751, 710, 682; **LRMS** (ESI^{-}) 214 ([M−H]$^{-}$, 100%); **HRMS** (ESI^{+}): calcd. for $C_{13}H_{14}NO_2$, 216.1019; found, 216.1022.

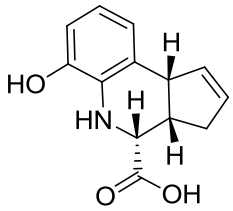
3a,4,5,9b-Tetrahydro-3H-cyclopenta[c]quinoline-4,8-dicarboxylic acid 114



4-Aminobenzoic acid (0.74 g, 5.37 mmol), glyoxilic acid (0.40 g, 5.37 mmol), and cyclopentadiene (1.06 g, 16.11 mmol) were subjected to general procedure 5.4. Purification *via* flash column chromatography (silica, 8:2 petroleum ether/EtOAc) afforded the pure product *cis*-**114** (0.51 g, 37%) as a solid. **Mp** 247-248 ºC; **^{1}H NMR** (400 MHz, DMSO-d_6) 7.51 (1H, s, C(9)*H*), 7.43 (1H, d, *J* = 8.2 Hz, C(7)*H*), 6.68 (1H, d, *J* = 8.5 Hz, C(6)*H*), 5.77 (1H, dd, *J* = 5.8, 2.4 Hz, C(1)*H*), 5.60 (1H, d, *J* = 5.9 Hz, C(2)*H*), 3.93 (1H, d, *J* = 8.8 Hz, C(9)*H*), 3.62 (1H, d, *J* = 3.5 Hz, C(4)*H*), 3.19 (1H, m, C(3a)*H*), 2.21 (2H, m, C(3)*H*); **^{13}C NMR** (DMSO-d_6) 173.5 (*C*O_2H), 168.2 (Ar-*C*O_2H), 149.3, 135.2 (*C*(1)), 130.0, 129.8 (*C*(2)), 127.7, 123.8, 119.4, 114.0, 56.3 (*C*(4)), 45.8 (*C*(9b)), 41.0 (*C*(3a)), 32.2 (*C*(3)); $\boldsymbol{\nu}_{\mathbf{max}}$ (thin

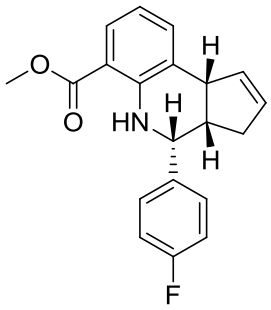
film)/cm^{-1} 3408, 1561, 1270, 1221, 1130, 1108; **LRMS** (ESI$^-$) 258 ([M−H]$^-$, 100%); **HRMS** (ESI$^-$): calcd. for $C_{14}H_{14}NO_4$, 258.045; found, 258.0848.

6-Hydroxy-3a,4,5,9b-tetrahydro-3*H*-cyclopenta[*c*]quinoline-4-carboxylic acid 115



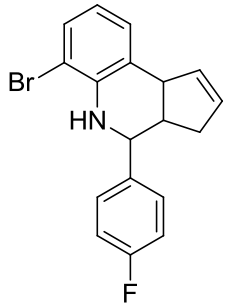
Glyoxilic acid (0.40 g, 5.37 mmol), *o*-aminophenol (0.59 g, 5.37 mmol), and cyclopentadiene (1.06 g, 16.11 mmol) were subjected to general procedure 5.4. Purification *via* flash column chromatography (silica, 8:2 petroleum ether/EtOAc) afforded the pure product *cis*-**115** (0.60 g, 48%) as a white solid. **Mp** 116 ºC; 6.52-6.35 (3H, m), 5.72 (1H, dd, *J* = 5.4, 2.9 Hz, C(1)*H*), 5.58 (1H, d, *J* = 5.4 Hz, C(2)*H*), 3.93 (1H, d, *J* = 8.8 Hz, C(9b)*H*), 3.76 (1H, d, *J* = 3.0 Hz, C(4)*H*), 3.21 (m, C(3a)*H*), 2.37-2.14 (2H, m, C(3)*H*); **^{13}C NMR** (DMSO-d_6) 173.2 (*C*O_2H), 144.4, 135.0 (*C*(1)), 133.5, 129.6 (*C*(2)), 125.6, 118.7, 117.0, 111.1, 56.3 (*C*(4)), 45.9 (*C*(9b)), 40.8 (*C*(3a)), 32.2 (*C*(3)); $\boldsymbol{\nu_{max}}$ (thin film)/cm^{-1} 3385, 1592, 1360, 1284, 1247, 750; **LRMS** (ESI$^+$) 232 ([M+H]$^+$, 100%); **HRMS** (ESI$^+$): calcd. for $C_{13}H_{14}NO_3$, 232.0968; found, 232.0962.

Methyl 4-(4-fluorophenyl)3a,4,5,9b-tetrahydro-3*H*-cyclopenta[*c*]quinoline-6 carboxylate 99



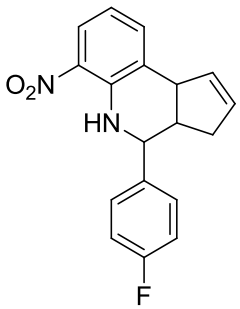
Methyl anthranilate (0.66 g, 5.37 mmol), *p*-fluorobenzaldehyde (0.67 g, 5.37 mmol) and cyclopentadiene (1.07 g, 16.11 mmol) were subjected to general general procedure 5.4. The crude product was purified *via* flash column chromatography (silica, 96:4 petroleum ether/EtOAc) to furnish the pure compound **99** (1.42 g, 82%) as a light brown oil, in a diastereomeric *cis/trans* ratio of 97:3. *cis* isomer: **^{1}H NMR** (400 MHz, $CDCl_3$) 7.76-7.79 (2H, m), 7.44 (2H, dd, *J* = 8.2, 5.6 Hz), 7.19 (1H, d, *J* = 7.3 Hz, $CH_3CO_2ArH_{para}$), 7.08 (2H, m), 6.66 (1H, m), 5.83-5.81 (1H, m, C(1)*H*), 5.65 (1H, m, C(2)*H*),), 4.71 (1H, d, *J* = 3.1 Hz, C(4)*H*), 4.15 (1H, d, *J* = 8.7 Hz, C(9b)*H*), 3.84 (3H, s, CO_2CH_3), 3.02 (1H, qd, *J*= 9.0, 3.3 Hz, C(3a)*H*), 2.57-2.51 (1H, m, C(3)*H*), 1.85-1.79 (1H, m, C(3)*H*); **^{13}C NMR** ($CDCl_3$) 168.9 (CO_2Me), 149.5 (*C*-F), 142.4 (*C*-NH), 134.2, 134.0, 130.6, 129.0, 127.8, 127.7, 126.8, 116.4, 115.6, 115.3, 56.1 (OCH_3), 51.6 (*C*(4)), 46.0 (*C*(9b)), 45.4 (*C*(3a)), 31.7 (*C*(3)); $\boldsymbol{\nu_{max}}$ (thin film)/cm^{-1} 3321, 1710, 1486, 1244, 752; **LRMS** (ESI$^+$) 324 ([M+H]$^+$, 100%); **HRMS** (ESI$^+$): calcd. for $C_{20}H_{19}FNO_2$, 324.1355; found, 324.1357.

6-Bromo-4-(4-fluorophenyl)-3a,4,5,9b-tetrahydro-3*H*-cyclopenta[*c*]quinoline 100



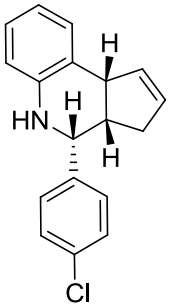
p-Fluorobenzaldehyde (1.13 g, 10.74 mmol), *o*-bromoaniline (1.85 g, 10.74 mmol) and cyclopentadiene (2.63 mL, 32.22 mmol) were subjected to general procedure 5.4. The crude product was purified *via* flash column chromatography (silica, 96:4 petroleum ether/EtOAc) to furnish the pure compound **100** (3.04 g, 85%) as an orange oil. **^{1}H NMR** (400 MHz, $CDCl_3$) 7.48-7.44 (2H, m), 7.28 (1H, d, *J* = 6.7 Hz, C(9)*H*), 7.13-7.09 (2H, m), 7.03-7.01 (1H, m), 6.65 (1H, t, *J* = 7.5 Hz, C(8)*H*), 5.86-5.83 (1H, m, C(1)*H*), 5.68 (1H, d, *J* = 5.1 Hz, C(2)*H*), 4.66 (1H, d, *J* = 3.0 Hz, C(4)*H*), 4.40 (1H, s, N*H*), 4.15 (1H, d, *J* = 8.9 Hz, C(9b)*H*), 3.01 (1H, dq, *J* = 8.9, 3.2 Hz, C(3a)*H*), 2.65-2.57 (1H, m, C(3)*H*), 1.86-1.79 (1H, m, C(3)*H*); **^{13}C NMR** ($CDCl_3$) 142.7 (*C*-F), 142.4 (*C*-NH), 138.0 (*C*-Br), 133.7, 130.7, 129.1, 128.1, 128.0, 127.6, 119.6, 115.6, 115.4, 110.5, 57.2, 50.4 (*C*(4)), 46.2 (*C*(9b)), 45.2 (*C*(3a)), 31.5 (*C*(3)); $\boldsymbol{\nu_{max}}$ (thin film)/cm^{-1} 3345, 1484; **LRMS** (ESI^+) 345 ($[M+H]^+$, 100%); **HRMS** (ESI^+): calcd. for $C_{18}H_{16}BrFN$, 325.0351; found, 325.0357.

4-(4-Fluorophenyl)-6-nitro-3a,4,5,9b-tetrahydro-3*H*-cyclopenta[*c*]quinolone 101



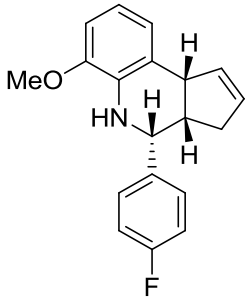
p-Fluorobenzaldehyde (1.13 g, 10.74 mmol), *o*-nitroaniline (1.48 g, 10.74 mmol) and cyclopentadiene (2.63 mL, 32.22 mmol) were subjected to general procedure 5.4. The crude product was purified *via* flash column chromatography (silica, 96:4 petroleum ether/EtOAc) to furnish the pure compound **101** (2.30 g, 69%) as a light brown oil, in a diastereomeric *cis/trans* ratio of 98:2. Data were consistent with those in the literature.[10] *cis* isomer: **^{1}H NMR** (400 MHz, $CDCl_3$) 8.02-7.99 (1H, m, C(7)*H*), 7.70 (1H, d, *J* = 8.0 Hz, C(9)*H*), 7.39-7.34 (2H, m), 7.12-7.06 (2H, m), 6.74 (1H, t, *J* = 7.5 Hz, C(8)*H*), 5.75-5.70 (1H, m, C(1)*H*), 5.45 (1H, d, *J* = 5.6 Hz, C(2)*H*), 4.84 (1H, d, *J* = 3.1 Hz, C(4)*H*), 4.14 (1H, qd, *J* = 7.1, 3.1 Hz, C(9b)*H*), 3.14-3.11 (1H, m, C(3a)*H*), 2.80-2.73 (1H, m, C(3)*H*), 1.91-1.79 (1H, m, C(3)*H*); **LRMS** (ESI^-) 309 ($[M-H]^-$, 100%).

(3a*S*,4*R*,9b*R*)-4-(4-chlorophenyl)-3a,4,5,9b-tetrahydro-3H-cyclopenta[c]quinolone 109



p-Chlorobenzaldehyde (0.75 g, 5.37 mmol), aniline (0.92 g, 5.37 mmol) and cyclopentadiene (1.06 g, 16.11 mmol) were subjected to general procedure 5.4. The crude product was purified *via* flash column chromatography (silica, 96:4 petroleum ether/EtOAc) to furnish the pure compound **109** (1.40 g, 87%). **Mp** 139 °C (lit 141–142 °C), **^{1}H NMR** (400 MHz, $CDCl_3$) 7.57-7.35 (4H, m), 7.13–6.71 (2H, m), 6.79–6.73 (1H, m), 6.64 (1H, d, *J* = 7.7 Hz), 5.86–5.84 (1H, m, C(1)*H*), 5.66 (1H, m, C(2)*H*), 4.62 (1 H, d, *J* = 3.0 Hz, C(4)*H*), 4.13 (1 H, d, *J* = 8.5 Hz, C(9b)*H*), 3.70 (1H, br. s, N*H*), 3.03–2.92 (1H, m, C(3a)*H*), 2.67–2.55 (1 H, m, C(3)*H*), 1.85–1.74 (1 H, m, C(3)*H*); **LRMS** (ESI^+) 282 ($[M+H]^+$, 100%).

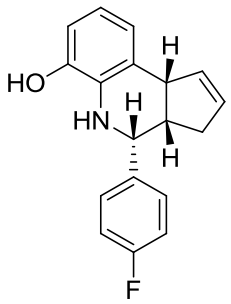
4-(4-Fluorophenyl)-6-methoxy-3a,4,5,9b-tetrahydro-3H-cyclopenta[c]quinolone 102



p-Fluorobenzaldehyde (1.33 mg, 10.74 mmol), 2-methoxyaniline (1.32 g, 10.74 mmol) and cyclopentadiene (2.13 g, 32.22 mmol) were subjected to general procedure 5.4. Purification *via* flash column chromatography (silica, 8:2 petroleum ether/EtOAc) afforded the pure product *cis*-**102** (2.84 g, 82%) as a light orange oil. **^{1}H NMR** (400 MHz, $CDCl_3$) 7.47 (2H,

dd, *J* = 8.6, 5.4 Hz), 7.10-7.05 (2H, m), 6.74-6.72 (2H, m), 6.66-6.63 (1H, m), 5.88-5.85 (1H, m, C(1)*H*), 5.67-5.65 (1H, m, C(2)*H*), 4.58 (1H, d, *J* = 3.2 Hz, C(4)*H*), 4.16-4.11 (1H, d, *J* = 8.7 Hz, C(9b)*H*), 3.83 (3H, s, OCH_3), 3.02 (1H, m, C(3a)*H*), 2.98 (1H, dd, *J* = 8.8, 3.4 Hz, C(3)*H*), 2.69-2.61 (1H, m, C(3)*H*); **^{13}C NMR** ($CDCl_3$) 147.1 (*C*-F), 138.8 (*C*-NH), 135.1, 133.9, 130.6, 128.1, 128.0, 126.2, 120.8, 118.2, 115.3, 107.0, 57.1 (*C*(4)), 55.4 (OCH_3), 46.2 (*C*(9b)), 46.0 (*C*(3a)), 31.3 (*C*(3)); $\boldsymbol{\nu_{max}}$ (thin film)/cm^{-1} 3457, 3381, 2944, 2907, 1739, 1360, 1215, 720; **HRMS** (FI^+): calcd. for $C_{19}H_{18}FNO$, 295.1372; found, 295.1383.

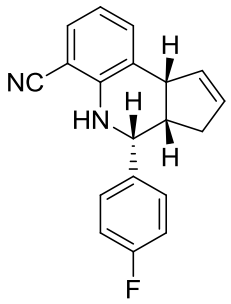
4-(4-Fluorophenyl)-3a,4,5,9b-tetrahydro-3H-cyclopenta[c]quinolin-6-ol 103



Boron trifluoride-methyl sulphide complex (2.64 g, 20.34 mmol) was added to a solution of **186** in CH_2Cl_2 (5 mL) and the reaction mixture was stirred at rt for 12 h. The reaction was quenched with MeOH, filtered through celite plug and the solvent was removed *in vacuo*. Purification *via* flash column chromatography (silica, 8:2 petroleum ether/EtOAc) afforded the pure product *cis*-**103** (0.75 g, 79%) as a orange oil. **^{1}H NMR** (400 MHz, $CDCl_3$) 7.47 (2H, dd, *J* = 8.5, 5.6 Hz, 7.10-7.05 (2H, m), 6.72 (1H, d, *J* = 7.7 Hz), 6.64 (1H, t, *J* = 7.7 Hz), 6.56 (1H, d, *J* = 7.7 Hz), 5.86 (1H, m, C(1)*H*), 5.67 (1H, m, C(2)*H*), 4.60 (1H, d, *J* = 3.0 Hz, C(4)*H*), 4.12 (1H, d, *J* = 8.8 Hz, C(9b)*H*), 2.99 (1H, dq, *J* = 9.0, 3.3 Hz, C(3a)*H*), 2.67-2.60 (1H, m, C(3)*H*), 1.83 (1H, dd, *J* = 16.3, 8.7 Hz, C(3)*H*); **^{13}C NMR** ($CDCl_3$) 142.9, 138.6, 137.5, 133.9, 130.3, 128.1, 127.9, 121.3, 118.4, 115.3, 115.1, 111.8, 57.0, 46.2, 45.9, 31.3;

ν_{max} (thin film)/cm^{-1} 3342, 3052, 2970, 2922, 1739, 1591, 1220, 749; **HRMS** (FI$^+$): calcd. for $C_{18}H_{16}FNO$, 281.1216; found, 281.1214.

4-(4-Fluorophenyl)-3a,4,5,9b-tetrahydro-3H-cyclopenta[c]quinoline-6-carbonitrile 104



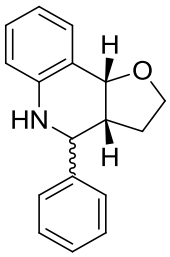
2-Aminobenzonitrile (0.63 g, 5.37 mmol), *p*-fluorobenzaldehyde (0.58 g, 5.37 mmol) and cyclopentadiene (1.31 mL, 16.11 mmol) were subjected to general procedure 5.4. The crude product was purified by flash chromatography (silica gel, pet. ether/EtOAc 8:2) to afford title compound **104** (1.12 g, 72%) as beige powder. **Mp** 197-199 °C; **^{1}H NMR** (400 MHz, $CDCl_3$) 7.42 (2H, dd, *J* = 8.5, 5.4 Hz), 7.29-7.27 (2H, m), 7.23 (1H, d, *J* = 7.6 Hz), 7.11 (1H, t, *J* = 8.6 Hz), 6.76 (1H, t, *J* = 7.6 Hz), 5.85 (1H, m, C(1)*H*), 5.71 (1H, m, C(2)*H*), 4.72 (1H, d, *J* = 2.9 Hz, C(4)*H*), 4.57 (1H, br. s, N*H*), 4.11 (1H, d, *J* = 8.5 Hz, C(9b)*H*), 3.04-2.98 (1H, m, C(3a)*H*), 2.60-2.53 (1H, m, C(3)*H*), 1.85 (1H, dd, *J* = 16.1, 8.5 Hz, C(3)*H*); **^{13}C NMR** ($CDCl_3$) 31.4 (*C*H_2), 45.5 (CH_2*C*H), 45.7 (*C*C=C), 56.7 (*C*NH), 97.2 (C≡N), 115.5, 117.6, 126.6, 127.9, 128.0, 130.0, 131.1, 133.2, 133.7, 140.0, 148.1, 163.5; ν_{max} (film) 3334, 3052, 2923, 2890, 2217, 1592, 1216, 719; **HRMS** (FI$^+$): calcd. for $C_{19}H_{15}FN_2$, 290.1219; found, 290.1224

5.3.2 Synthesis of Furanoquinolines

GENERAL PROCEDURE 5.5: One-Pot Synthesis of Furanoquinolines Catalyzed by Triflic Acid

Triflic acid (0.6 mmol) was added to a solution of aniline (6.0 mmol) and aldehyde (6.0 mmol) in acetonitrile (12 mL) at room temperature. The mixture was stirred for 5 min before 2,3-dihydrofuran (6.0 mmol) was added. The resulting solution was stirred overnight and the solvent was removed *in vacuo*. The residue was taken up in saturated aqueous $NaHCO_3$ (40 mL) and the product was extracted with CH_2Cl_2 (3 x 40 mL). The combined organic layers were washed with brine, dried ($MgSO_4$) and concentrated *in vacuo*. The crude product was purified *via* flash column chromatography to afford the pure product.

(3a*R*,4*R*,9b*R*)-4-Phenyl-2,3,3a,4,5,9b-hexahydrofuro[3,2-c]quinoline 118



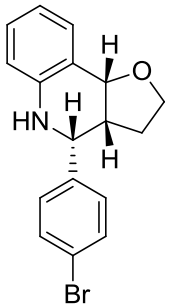
Benzaldehyde (0.63 g, 6.0 mmol) and aniline (0.58 g, 6.0 mmol) were subjected to general general procedure 5.5. The product was obtained as a mixture of *cis* and *trans* isomers (48:52, 0.97 g, 64%), which were separated by column chromatography (silica, 95:5 petroleum ether/EtOAc). Data were consistent with those in the literature.[11]

a) *trans* isomer – colourless oil. **^{1}H NMR** (400 MHz, $CDCl_3$) 7.40-7.31 (6H, m), 7.16 (1H, td, *J* = 8.3, 1.5 Hz), 6.84 (1H, td, *J* = 7.5, 1.1 Hz), 6.64 (1H, d, *J* = 8.0 Hz), 4.63 (1H, d, *J* = 5.1 Hz, OC*H*), 4.06 (1H, td, *J* = 8.4, 6.3 Hz, OCH_2), 3.87 (1H, m, OCH_2), 3.82 (1H, d, *J* = 11.2

Hz, NC*H*), 2.49 (1H, m, NCC*H*), 2.05-1.99 (1H, m, CH_2), 1.79-1.73 (1H, m, CH_2); **^{13}C NMR** ($CDCl_3$) 145.5, 141.8, 131.3, 128.9, 128.8, 128.7, 128.2, 120.1, 118.4, 114.76, 76.2, 65.2, 57.8, 43.4, 28.9; **LRMS** (ESI^-) 250 ($[M-H]^-$, 100%).

a) *cis* isomer - white solid; **Mp** 120-121 ºC, (lit[11] 117-118 ºC); **^{1}H NMR** (400 MHz, $CDCl_3$) 7.47 (2H, d, *J* = 7.3 Hz), 7.42-7.31 (4H, m), 7.10 (1H, td, *J* = 7.8, 1.5 Hz), 6.81 (1H, td, *J* = 7.7, 1.0 Hz), 6.62 (1H, dd, *J* = 7.8, 1.1 Hz), 5.26 (1H, d, *J* = 8.0 Hz, OC*H*), 4.70 (1H, d, *J* = 3.4 Hz, NC*H*), 3.84 (1H, td, *J* = 8.5, 3.4 Hz, OCH_2), 3.74-3.70 (1H, m, OCH_2), 2.81 (1H, qd, *J* = 8.8, 3.4 Hz, NCC*H*), 2.28-2.20 (1H, m), 1.58-1.51 (1H, m); **LRMS** (ESI^-) 250 ($[M-H]^-$, 100%).

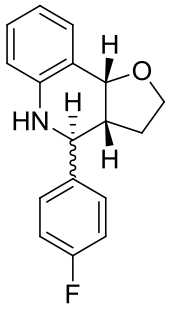
4-(4-Bromophenyl)-2,3,3a,4,5,9b-hexahydrofuro[3,2-c]quinoline 120



p-Bromobenzaldehyde (1.11 g, 6.0 mmol) and aniline (0.58 g, 6.0 mmol) were subjected to general general procedure 5.5. Purification of the crude *via* flash column chromatography (silica, 8:2 petroleum ether/EtOAc) afforded the pure product *cis*-**120** (1.62 g, 82%) as a white solid. Data were consistent with those in the literature.[12] **Mp** 146-149 ºC, (lit[12] 142-147 ºC); **^{1}H NMR** (400 MHz, $CDCl_3$) 7.58 (2H, d, *J* = 8.2 Hz, BrCC*H*), 7.39-7.42 (3H, m), 7.17-7.13 (1H, t, *J* = 8.1 Hz), 6.90-6.87 (1H, t, *J* = 7.2 Hz), 6.65 (1H, d, *J* = 8.2 Hz), 5.31 (1H, d, *J* = 8.2 Hz, OC*H*), 4.72 (1H, d, *J* = 3.2 Hz, NC*H*), 3.89-3.84 (2H, m, OCH_2), 2.83-2.77 (1H, m,

NCC*H*), 2.26-2.16 (1H, m, CH_2), 1.60-1.53 (1H, m, CH_2); $\boldsymbol{\nu_{max}}$ (disk)/cm^{-1} 3417, 1617, 1484, 1351; **LRMS** (ESI$^-$) 329 ([M−H]$^-$, 100%).

4-(4-Fluorophenyl)-2,3,3a,4,5,9b-hexahydrofuro[3,2-c]quinolone 121

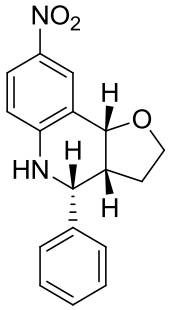


p-Fluorobenzaldehyde (0.74 g, 6.0 mmol) and aniline (0.58 g, 6.0 mmol) were subjected to general general procedure 5.5. The product was obtained as a mixture of *cis* and *trans* isomers (52:48, 1.28 g, 79%), which were separated by column chromatography (silica, 95:5 petroleum ether/EtOAc). Data were consistent with those in the literature.[13]

a) *cis* isomer – white solid. **Mp** 173 ºC, (lit[13] 173-175 ºC); **^{1}H NMR** (400 MHz, $CDCl_3$) 7.47-7.40 (2H, m, F-ArH_{ortho}), 7.36 (1H, d, *J* = 7.6 Hz), 7.16-7.06 (3H, m, F-ArH_{meta}, Ar*H*), 6.83 (1H, m), 6.64 (1H, m), 5.28 (1H, d, *J* = 4.7 Hz, OC*H*), 4.70 (1H, d, *J* = 3.1 Hz, NC*H*), 4.11 (1H, s. br, N*H*), 3.88-3.70 (2H, m, OCH_2), 2.76 (1H, qd, *J* = 8.1, 3.2 Hz, NCC*H*), 2.24-2.16 (1H, m, CH_2), 1.54 (1H, ddd, *J* = 11.5, 7.7, 3.6 Hz, CH_2); **LRMS** (ESI$^-$) 268 ([M−H]$^-$, 100%).

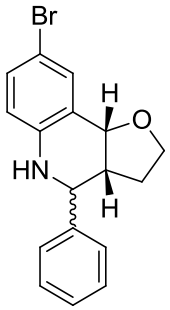
b) *trans* isomer – colourless oil. **^{1}H NMR** (400 MHz, $CDCl_3$) 7.47-7.40 (3H, m), 7.16-7.06 (3H, m, F-ArH_{meta}, Ar*H*), 6.83 (1H, m), 6.64 (1H, m), 4.61 (1H, d, *J* = 5.1 Hz, NC*H*), 4.06-4.01 (1H, m, OC*H*), 3.88-3.84 (1H, m, OC*H*), 3.76-3.70 (1H, m, NCC*H*), 2.44-2.40 (1H, m), 2.03 (1H, dd, *J* = 14.3, 5.9 Hz, CH_2), 1.71-1.66 (1H, m, CH_2); **LRMS** (ESI$^-$) 268 ([M−H]$^-$, 100%).

4-(4-Nitrophenyl)-2,3,3a,4,5,9b-hexahydrofuro[3,2-c]quinolone 122



Benzaldehyde (0.63 g, 6.0 mmol) and 4-nitroaniline (0.83 g, 6.0 mmol) were subjected to general general procedure 5.5. The product was obtained as a mixture of *cis* and *trans* isomers (78:22, 1.09 g, 61%). Purification *via* flash column chromatography (silica, 95:5 petroleum ether/EtOAc) afforded the pure product *cis*-**122** as a yellow solid. Data were consistent with those in the literature.[14] **Mp** 149-150 ºC, (lit[14] 153-155 ºC); **^{1}H NMR** (400 MHz, $CDCl_3$) 8.35 (1H, s, O_2N-ArH_{ortho}), 8.07-8.04 (1H, d, J = 8.8 Hz, O_2N-ArH_{ortho}), 7.44-7.38 (5H, m, Ar*H*), 6.60 (1H, d, J = 8.8 Hz, O_2N-ArH_{meta}), 4.90 (1H, m, OC*H*), 4.61 (1H, d, J = 3.5 Hz, NC*H*), 4.16-4.05 (1H, m, OCH_2), 3.95-3.89 (1H, m, OCH_2), 2.49-2.43 (1H, m, NCC*H*), 2.15-2.08 (1H, m, CH_2), 1.82-1.75 (1H, m, CH_2); **LRMS** (ESI$^-$) 296 ([M−H]$^-$, 100%).

8-Bromo-4-phenyl-2,3,3a,4,5,9b-hexahydrofuro[3,2-c]quinolone 123



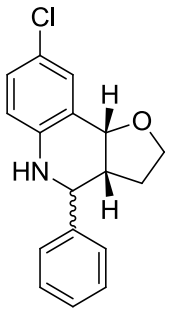
Benzaldehyde (0.63 g, 6.0 mmol) and *p*-bromoaniline (1.03 g, 6.0 mmol) were subjected to general general procedure 5.5. The product was obtained as diastereomeric mixture **3e** (52:48,

1.62 g, 82%), which was separated by flash column chromatography (silica, 95:5 petroleum ether/EtOAc). Data were consistent with those in the literature.[15]

a) *cis* isomer – white powder. **Mp** 153-155 ºC, (lit[15] 152 ºC); **^{1}H NMR** (400 MHz, $CDCl_3$) 7.53 (1H, s, Br-ArH_{ortho}), 7.48-7.31 (5H, Ar*H*), 7.16 (1H, d, *J* = 8.7 Hz, Br-ArH_{ortho}), 6.48 (1H, d, *J* = 8.6 Hz, Br-ArH_{meta}), 5.22 (1H, d, *J* = 7.8 Hz, NC*H*), 4.69 (1H, d, *J* = 3.4 Hz, OC*H*), 4.17 (1H, br. s, N*H*), 3.88-3.71 (2H, m, OCH_2), 2.76 (1H, qd, *J* = 8.0, 3.5 Hz, NCC*H*), 2.20-2.14 (1H, m, CH_2), 1.55-1.52 (1H, m, CH_2); **LRMS** (ESI^-) 328 ($[M-H]^-$, 100%).

b) *trans* isomer – white solid. **Mp** 98-99 ºC, (lit[15] 104 ºC); **^{1}H NMR** (400 MHz, $CDCl_3$) 7.44-7.31 (7H, m), 6.50 (1H, d, *J* = 8.6 Hz), 4.56 (1H, d, *J* = 5.2 Hz, OC*H*), 3.85-3.71 (3H, m, OCH_2, NC*H*), 2.47-2.42 (1H, m, NCC*H*), 2.06-2.01 (1H, m, CH_2), 1.76-1.71 (1H, m, CH_2); **LRMS** (ESI^-) 328 ($[M-H]^-$, 100%).

8-Chloro-4-phenyl-2,3,3a,4,5,9b-hexahydrofuro[3,2-c]quinoline 124

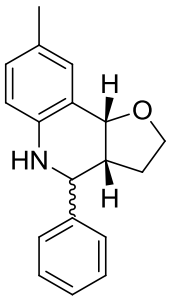


Benzaldehyde (0.63 g, 6.0 mmol) and *p*-chloroaniline (0.58 g, 6.0 mmol) were subjected to general general procedure 5.5. The product was obtained as a mixture of *cis* and *trans* isomers (45:55, 1.44 g, 84%), which were separated by column chromatography (silica, 95:5 petroleum ether/EtOAc). Data were consistent with those in the literature.[11]

a) *cis* isomer – white solid. **Mp** 157 ºC, (lit[14] 153-155 ºC); NMR [400 MHz, δ (ppm),$CDCl_3$]: 7.47-7.37 (6H, m, Ar*H*, Cl-ArH_{ortho}), 7.03 (1H, d, *J* = 8.6 Hz, Cl-ArH_{ortho}), 6.56 (1H, d, *J* = 8.6 Hz, Cl-ArH_{meta}), 5.21 (1H, d, *J* = 7.8 Hz, OC*H*), 4.69 (1H, d, *J* = 2.9 Hz, NC*H*), 4.16 (1H, s, N*H*), 3.87-3.71 (2H, m, OCH_2), 2.76 (1H, m, NCC*H*), 2.20-2.15 (1H, m, CH_2), 1.55-1.50 (1H, m, CH_2); **LRMS** (ESI^-) 284 ($[M-H]^-$, 100%).

b) *trans* isomer – white powder. **Mp** 98-99 ºC, (lit[14] 99-101°C); **^{1}H NMR** (400 MHz, $CDCl_3$) 7.47-7.38 (6H, m, Ar*H*, Cl-ArH_{ortho}), 7.05 (1H, dd, *J* = 8.6, 2.4 Hz, Cl-ArH_{ortho}), 6.55 (1H, d, *J* = 8.6 Hz, Cl-ArH_{meta}), 4.56 (1H, d, *J* = 5.2 Hz, OC*H*), 4.06-4.01 (1H, m, OCH_2), 3.87-3.71 (2H, m, OCH_2, NC*H*), 2.49-2.43 (1H, m, NCC*H*), 2.03 (1H, dt, *J* = 8.7, 5.5 Hz, CH_2), 1.77-1.71 (1H, m, CH_2); **^{13}C NMR** ($CDCl_3$) 143.7, 141.8, 130.7, 129.7, 128.8, 128.3, 128.2, 122.9, 121.6, 115.9, 75.5, 65.3, 57.8, 45.4, 28.7.

(3a*R*,9b*R*)-8-Methyl-4-phenyl-2,3,3a,4,5,9b-hexahydrofuro[3,2-c]quinoline 125



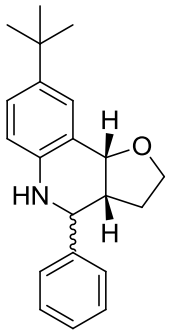
Benzaldehyde (0.63 g, 6.0 mmol) and *p*-toluidine (0.64 g, 6.0 mmol) were subjected to general general procedure 5.5. The product was obtained as a mixture of *cis* and *trans* isomers (48:52, 1.35 g, 85%), which were separated by column chromatography (silica, 95:5 petroleum ether/EtOAc). Data were consistent with those in the literature.[16]

a) *cis* isomer – colourless oil. **^{1}H NMR** (400 MHz, $CDCl_3$) 7.49-7.24 (6H, H_3C-ArH_{ortho}, Ar*H*), 6.96-6.91 (1H, m, H_3C-ArH_{ortho}), 6.50 (1H, m, H_3C-ArH_{meta}), 5.26 (1H, d, *J* = 8.0 Hz,

OC*H*), 4.66 (1H, d, *J* = 3.2 Hz, NC*H*), 3.87-3.71 (2H, m, OCH_2), 2.75 (1H, m, NCC*H*), 2.28 (3H, s, CH_3), 2.26-2.20 (1H, m, CH_2), 1.53 (1H, ddd, *J* = 11.4, 7.5, 3.6 Hz, CH_2); **LRMS** (ESI$^-$) 264 ([M−H]$^-$, 100%).

b) *trans* isomer – colourless oil. **^{1}H NMR** (400 MHz, $CDCl_3$) 7.49-7.24 (6H, H_3C-ArH_{ortho}, Ar*H*), 6.96-6.91 (1H, m, H_3C-ArH_{ortho}), 6.50 (1H, m, H_3C-ArH_{meta}), 4.60 (1H, d, *J* = 5.2 Hz, OC*H*), 4.04 (1H, td, *J* = 8.3, 6.3 Hz, OCH_2), 3.87-3.81 (1H, d, *J* = 11.3 Hz, NC*H*), 2.49 (1H, m, NCC*H*), 2.06-1.99 (1H, m, CH_2), 1.76-1.70 (1H, m, CH_2); **LRMS** (ESI$^-$) 264 ([M−H]$^-$, 100%).

(3a*R*,9b*R*)-8-(Tert-butyl)-4-phenyl-2,3,3a,4,5,9b-hexahydrofuro[3,2-c]quinoline 126



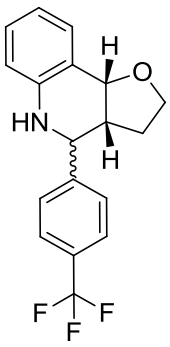
Benzaldehyde (0.63 g, 6.0 mmol) and 4-*t*-butylaniline (0.90 g, 6.0 mmol) were subjected to general general procedure 5.5. The product was obtained as a mixture of *cis* and *trans* isomers (45:55, 1.45 g, 81%), which were separated by column chromatography (silica, 95:5 petroleum ether/EtOAc).

a) *cis* isomer – colourless oil. **^{1}H NMR** (400 MHz, $CDCl_3$) 7.49-7.33 (6H, m, Ar*H*), 7.19 (1H, m, C-ArH_{ortho}), 6.61 (1H, d, *J* = 8.1 Hz, C-ArH_{meta}), 5.29 (1H, d, *J* = 8.1 Hz, OC*H*), 4.69 (1H, d, *J* = 2.9 Hz, NC*H*), 3.90-3.70 (2H, m, OCH_2), 2.82-2.78 (1H, m, NCC*H*), 2.27-2.22 (1H, m, CH_2), 1.56-1.49 (1H, m, CH_2), 1.33 (9H, s, CH_3); **^{13}C NMR** ($CDCl_3$) 143.4, 142.0,

142.1, 128.4, 127.9, 127.3, 126.9, 126.1, 121.3, 119.4, 115.2, 76.5, 65.1, 57.8, 34.2, 31.5, 28.6; **LRMS** (ESI^-) 306 ($[M-H]^-$, 100%).

b) *trans* isomer – colourless oil. **^{1}H NMR** (400 MHz, $CDCl_3$) 7.49-7.33 (6H, m, Ar*H*), 7.19 (1H, m, C-ArH_{ortho}), 6.61 (1H, d, *J* = 8.1 Hz, C-ArH_{meta}), 4.63 (1H, d, *J* = 5.1 Hz, OC*H*), 3.16-4.04 (1H, m, OCH_2), 3.90-3.84 (1H, m, OCH_2), 3.82 (1H, d, *J* = 11.4 Hz, NC*H*), 2.51-2.45 (1H, m, NCC*H*), 2.04-2.01 (1H, m, CH_2), 1.74-1.70 (1H, m, CH_2), 1.33 (9H, s, CH_3); **^{13}C NMR** ($CDCl_3$) 143.1, 142.4, 141.8, 128.6, 128.3, 127.6, 126.7, 126.3, 122.2, 119.3, 114.5, 76.2, 65.3, 57.9, 34.1, 31.5, 28.8; $\boldsymbol{\nu_{max}}$ (thin film)/cm^{-1} 3350, 2964, 2850, 1619, 1515, 1085; **LRMS** (ESI^-) 306 ($[M-H]^-$, 100%); **HRMS** (ES^+): calcd. for $C_{21}H_{26}NO$, 308.1936; found, 308.2003.

(3a*R*,9b*R*)-4-(4-(Trifluoromethyl)phenyl)-2,3,3a,4,5,9b-hexahydrofuro[3,2-c]quinoline 127

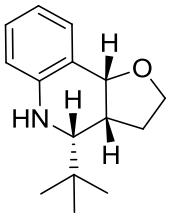


Aniline (0.58 g, 6.0 mmol) and *p*-(trifluoromethyl)benzaldehyde (1.05 g, 6.0 mmol) were subjected to general general procedure 5.5. The product was obtained as a mixture of *cis* and *trans* isomers (44:56, 1.44 g, 76%), which were separated by column chromatography (silica, 9:1 petroleum ether/EtOAc).

a) *cis* isomer – white solid. **Mp** 100-102 ºC; **^{1}H NMR** (400 MHz, $CDCl_3$) 7.68 (2H, m, F_3C-ArH_{ortho}), 7.60 (2H, m, F_3C-ArH_{meta}), 7.42 (1H, d, *J* = 7.6 Hz), 7.16 (1H, m), 6.85 (1H, m), 6.65 (1H, m), 5.30 (1H, d, *J* = 7.8 Hz, OC*H*), 4.78 (1H, d, *J* = 2.9 Hz, NC*H*), 3.90-3.80 (2H, m, OCH_2), 2.80 (1H, dtd, *J* = 10.6, 7.9, 3.1 Hz, NCC*H*), 2.24-2.14 (1H, m, CH_2), 1.54-1.46 (1H, m, CH_2); **^{13}C NMR** ($CDCl_3$) 144.9, 142.2, 131.2, 129.4, 128.6, 127.6, 126.8, 125.6, 122.5, 119.5, 115.0, 75.9, 66.7, 57.5, 45.4, 28.6; $\boldsymbol{\nu_{max}}$ (thin film)/cm^{-1} 3318, 2975, 2850, 1480, 1070; **LRMS** (ESI$^-$) 318 ([M−H]$^-$, 100%); **HRMS** (ES$^+$): calcd. for $C_{18}H_{17}F_3NO$, 320.1184; found, 320.1257.

b) *trans* isomer – **^{1}H NMR** (400 MHz, $CDCl_3$) 7.68 (2H, m, F_3C-ArH_{ortho}), 7.60 (2H, m, F_3C-ArH_{meta}), 7.42 (1H, d, *J* = 7.6 Hz), 7.16 (1H, m), 6.85 (1H, m), 6.65 (1H, m), 4.62 (1H, d, *J* = 5.1 Hz, OC*H*), 4.05 (1H, td, *J* = 8.4, 6.1 Hz, OCH_2), 3.88 (1H, d, *J* = 11.3 Hz, NC*H*), 3.85-3.60 (1H, m, OCH_2), 2.50-2.43 (1H, m, NCC*H*), 2.08-1.99 (1H, m, CH_2), 1.72-1.66 (1H, m, CH_2); **LRMS** (ESI$^-$) 318 ([M−H]$^-$, 100%).

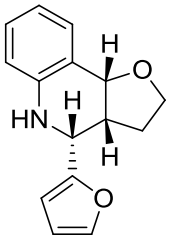
4-(Tert-butyl)-2,3,3a,4,5,9b-hexahydrofuro[3,2-c]quinoline 128



Trimethylacetaldehyde (0.62 g, 3.0 mmol) and aniline (0.30 g, 3.0 mmol) were subjected to general general procedure 5.5. Purification of the crude *via* flash column chromatography (silica, 8:2 petroleum ether/EtOAc) afforded the pure product *cis*-**128** (0.61 g, 88%) as a white solid. **Mp** 113-116 ºC; **^{1}H NMR** (400 MHz, $CDCl_3$) 7.31 (1H, d, *J* = 7.6 Hz, N-ArH_{meta}), 7.06 (1H, t, *J* = 7.6 Hz, N-ArH_{meta}), 6.75 (1H, t, *J* = 7.5 Hz, N-ArH_{para}), 6.56 (1H, d,

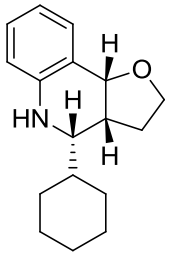
J = 8.1 Hz), 5.19 (1H, d, *J* = 7.5 Hz, OC*H*), 3.89-3.73 (2H, m, OCH_2), 3.63 (1H, s, N*H*), 3.23 (1H, d, *J* = 2.9 Hz, OC*H*), 2.75-2.60 (1H, m, NCC*H*), 2.13-2.03(1H, m, CH_2), 1.88 (1H, dtd, *J* = 12.1, 8.1, 4.0 Hz, CH_2), 1.06 (9H, s, C(CH_3)$_3$); **^{13}C NMR** ($CDCl_3$) 145.5, 129.6, 128.0, 122.5, 118.4, 114.4, 77.5, 66.9, 61.3, 39.7, 33.6, 27.2, 24.4; $\boldsymbol{\nu_{max}}$ (thin film)/cm^{-1} 3350, 2965, 2850, 1620, 1513, 1085; **LRMS** (ESI$^+$) 232 ([M+H]$^+$); **HRMS** (ES$^+$): calcd. for $C_{15}H_{22}NO$, 232.1623; found, 232.1696.

(3a*R*,4*R*,9b*R*)-4-(Furan-2-yl)-2,3,3a,4,5,9b-hexahydrofuro[3,2-c]quinoline 129



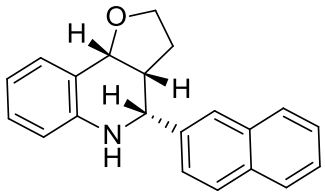
Furfural (0.56 g, 6.0 mmol) and aniline (0.58 g, 6.0 mmol) were subjected to general general procedure 5.5. Purification of the crude *via* flash column chromatography (silica, 8:2 petroleum ether/EtOAc) afforded the pure product *cis*-**129** (1.09 g, 75%) as a yellow solid. Data were consistent with those in the literature.[17] **Mp** 62-63 ºC, (lit[17] 63-66 ºC); **^{1}H NMR** (400 MHz, $CDCl_3$) 7.41 (1H, s, OC*H*), 7.35 (1H, d, *J* = 7.6 Hz, N-ArH_{meta}), 7.08 (1H, t, *J* = 7.7 Hz, N-ArH_{meta}), 6.81 (1H, t, *J* = 7.4 Hz, , N-ArH_{para}), 6.60 (1H, d, *J* = 8.0 Hz, N-ArH_{ortho}), 6.38 (1H, s, furan-*H*), 6.30 (1H, s, furan-*H*), 5.24 (1H, d, *J* = 7.8 Hz), 4.72 (1H, br. s, N*H*), 3.83-3.73 (2H, m, OCH_2), 3.01-2.95 (1H, m, NCC*H*), 2.27-2.17 (1H, m, CH_2), 1.89-1.81 (1H, m, CH_2); **LRMS** (ESI$^+$) 264 ([M+Na]$^+$).

(3a*R*,4*S*,9b*R*)-4-Cyclohexyl-2,3,3a,4,5,9b-hexahydrofuro[3,2-c]quinoline 130



Cyclohexanaldehyde (0.67 g, 6.0 mmol) and aniline (0.58 g, 6.0 mmol) were subjected to general general procedure 5.5. Purification of the crude *via* flash column chromatography (silica, petroleum ether/EtOAc) afforded the pure product *cis*-**130** (0.66 g, 43%) as a white solid. Data were consistent with those in the literature.[18] **Mp** 149 ºC, (lit[18] 148-151 ºC); **^{1}H NMR** (400 MHz, $CDCl_3$) 7.30 (1H, d, *J* = 7.6 Hz, N-ArH_{meta}), 7.05 (1H, t, *J* = 7.6 Hz, N-ArH_{meta}), 6.76 (1H, t, *J* = 7.5 Hz, N-ArH_{para}), 6.54 (1H, d, *J* = 8.1 Hz), 5.13 (1H, d, *J* = 8.1 Hz, OC*H*), 3.82-3.70 (2H, m, OCH_2), 3.13 (1H, d, *J* = 2.8 Hz, NC*H*), 2.76 (1H, dd, *J* = 10.4, 2.7 Hz, NCC*H*), 2.06-1.93 (2H, m, CH_2), 1.90-1.00 (10H, s, cyclohexyl-*H*); **LRMS** (ESI^+) 280 ($[M+Na]^+$).

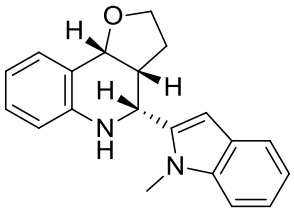
(3a*R*,9b*R*)-4-(Naphthalen-2-yl)-2,3,3a,4,5,9b-hexahydrofuro[3,2-c]quinoline 131



2-Naphthaldehyde (0.94 g, 6.0 mmol) and aniline (0.58 g, 6.0 mmol) were subjected to general general procedure 5.5. Purification of the crude *via* flash column chromatography (silica, petroleum ether/EtOAc) afforded the pure product *cis*-**131** (1.17 g, 75%) as a colourless oil. **^{1}H NMR** (400 MHz, $CDCl_3$) 7.96 (1H, s), 7.91-7.86 (4H, m), 7.58-7.51 (3H, m), 7.42 (1H, m), 7.13 (1H, m), 6.86 (1H, t, *J* = 7.5 Hz), 6.67 (1H, m), 5.34 (1H, d, *J* = 8.0

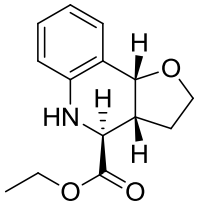
Hz, OC*H*), 4.87 (1H, d, *J* = 2.8 Hz, NC*H*), 3.89-3.70 (2H, m, OCH_2), 2.91 (1H, dtd, *J* = 10.6, 8.0, 3.0 Hz, NCC*H*), 2.33-2.22 (1H, m, CH_2), 1.55-1.48 (1H, m, CH_2); **^{13}C NMR** ($CDCl_3$) 131.3, 129.0, 128.4, 127.9, 127.7, 126.3, 126.0, 124.9, 119.3, 115.0, 76.2, 66.8, 57.9, 45.7, 28.9; ν_{max} (thin film)/cm^{-1} 3417, 1617, 1496, 1352; **LRMS** (ESI$^-$) 300 ([M−H]$^-$, 100%); **HRMS** (ES$^+$): calcd. for $C_{21}H_{20}NO$, 302.1467; found, 302.1539.

(3a*R*,4*R*,9b*R*)-4-(1-Methyl-1H-indol-2-yl)-2,3,3a,4,5,9b-hexahydrofuro[3,2-c]quinoline 132



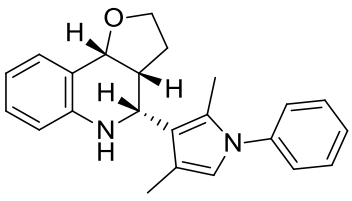
Indol-2-carboxyaldehyde (0.87 g 6.0 mmol) and aniline (0.58 g, 6.0 mmol) were subjected to general general procedure 5.5. Purification of the crude *via* flash column chromatography (silica, petroleum ether/EtOAc) afforded the pure product *cis*-**132** (1.22 g, 59%) as a red oil. **^{1}H NMR** (400 MHz, $CDCl_3$) 7.71 (1H, d, *J* = 8.0 Hz), 7.41-7.35 (3H, m), 7.31-7.27 (2H, m), 7.19-7.09 (4H, m), 6.61 (1H, d, *J* = 8.1 Hz), 5.33 (1H, d, *J* = 8.1 Hz, OC*H*), 5.06 (1H, d, *J* = 2.9 Hz, NC*H*), 3.87-3.84 (1H, m, OCH_2), 3.82 (3H, s, NCH_3), 3.78-3.71 (1H, m, OCH_2), 3.05-2.99 (1H, m, NCC*H*), 2.30 (1H, dd, *J* = 12.1, 9.9 Hz, CH_2), 1.71-1.66 (1H, m, CH_2); **^{13}C NMR** ($CDCl_3$) 145.6, 137.0, 130.3, 129.3, 128.3, 126.2, 125.9, 124.5, 123.1, 122.0, 119.2, 119.1, 119.0, 116.0, 115.1, 114.9, 109.5, 75.9, 66.8, 50.6, 44.8, 30.2, 28.7, 25.7; ν_{max} (thin film)/cm^{-1} 3340, 2970, 2850, 1615, 1030; **LRMS** (ES$^+$) 305 ([M+Na]$^+$); **HRMS** (ES$^+$): calcd. for $C_{20}H_{21}N_2O$, 305.1576; found, 305.1494.

(3a*R*,4*S*,9b*R*)-Ethyl 2,3,3a,4,5,9b-hexahydrofuro[3,2-c]quinoline-4-carboxylate 133



Ethyl glyoxylate (0.61 g 6.0 mmol) and aniline (0.58 g, 6.0 mmol) were subjected to general general procedure 5.5. Purification of the crude *via* flash column chromatography (silica, petroleum ether/EtOAc) afforded the pure product *cis*-**133** (0.61 g, 41%) as an orange oil. Data were consistent with those in the literature.[19] **^{1}H NMR** (400 MHz, $CDCl_3$) 7.31 (1H, d, *J* = 7.5 Hz, N-ArH_{meta}), 7.24 (1H, t, *J* = 7.6 Hz, N-ArH_{meta}), 7.07 (1H, t, *J* = 7.5 Hz, N-ArH_{para}), 6.10 (1H, d, *J* = 8.1 Hz), 5.22 (1H, d, *J* = 7.5 Hz, OC*H*), 5.16 (1H, s, N*H*), 4.35-4.23 (2H, m, CO_2CH_2), 4.21 (1H, d, *J* = 3.2 Hz, NC*H*), 3.85-3.72 (2H, m, OCH_2), 3.12 (1H, qd, *J* = 8.8, 3.2 Hz, NCC*H*), 2.06-1.95(1H, m, CH_2), 1.94-1.90 (1H, CH_2), 1.35 (3H, t, *J* = 7.2 Hz, CH_3); **LRMS** (ESI^-) 246 ($[M-H]^-$, 100%);

(3a*R*,4*S*,9b*R*)-4-(2,4-Dimethyl-1-phenyl-1H-pyrrol-3-yl)-2,3,3a,4,5,9bhexahydrofuro[3,2-c]quinolone 134

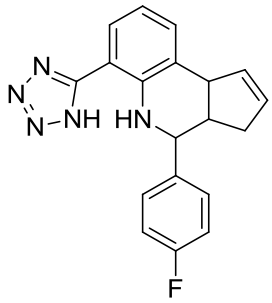


3,5-Dimethyl-1-phenyl pyrazole-4-carboxaldehyde (1.20 g 6.0 mmol) and aniline (0.58 g, 6.0 mmol) were subjected to general general procedure 5.5. Purification of the crude *via* flash column chromatography (silica, petroleum ether/EtOAc) afforded the pure product *trans*-**134** (0.61 g, 66%) as orange oil. **^{1}H NMR** (400 MHz, $CDCl_3$) 7.50-7.37 (7H, m, Ar*H*), 7.16-7.12

(1H, m, Ar*H*), 6.84-6.79 (1H, m, Ar*H*), 6.66 (1H, d, *J*=8.1 Hz, Ar*H*), 4.65 (1H, d, *J*=4.8 Hz, OC*H*), 4.08-4.03 (1H, m, OCH_2), 3.93 (1H, d, *J*=11.2 Hz, NC*H*), 3.92-3.87 (1H, m, OCH_2), 2.67 (1H, t, *J*=5.6 Hz, NCC*H*), 2.39 (3H, s, CH_3), 2.35 (3H, s, CH_3), 2.18-2.13 (1H, m, CH_2), 1.76-1.70 (1H, m, CH_2); **^{13}C NMR** ($CDCl_3$) 148.6, 146.2, 140.1, 138.3, 131.8, 129.5, 129.4, 126.1, 125.5, 120.4, 118.7, 115.2, 77.0, 67.7, 65.6, 49.3, 46.1, 41.6, 29.6, 13.5, 11.9; **LRMS** (ESI^-) 343 ($[M-H]^-$, 100%); **HRMS** (ES^+): calcd. for $C_{23}H_{25}N_2O$, 345.1889; found, 345.1884.

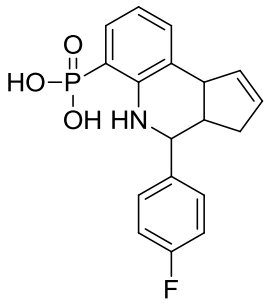
5.3.3 Synthesis of Carboxylic Acid Bioisosteres

4-(4-Fluorophenyl)-6-(1H-tetrazol-5-yl)-3a,4,5,9b-tetrahydro-3H-cyclopenta[c]quinolone 146



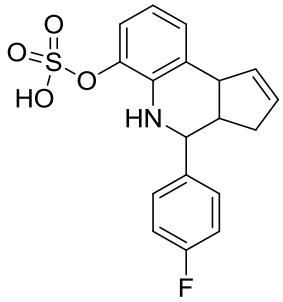
Ammonium chloride (0.22 g, 4.10 mmol) and sodium azide (0.27 g, 4.15 mmol) were added to a solution of 4-(4-fluorophenyl)-3a,4,5,9b-tetrahydro-3H-cyclopenta[c]quinoline-6-carbonitrile (0.40 g, 1.38 mmol) in dry DMF (14 mL) and the mixture was heated at 80 ºC for 24 h. Upon cooling, the reaction was quenched with saturated aqueous $NaHCO_3$ (100 mL) and the aqueous layer was washed with EtOAc. The aqueous phase was acidified to pH < 1 with HCl and the product was extracted with $CHCl_3$ (3 x 50 mL). The combined organic layers were dried and concentrated *in vacuo*. The crude product was purified by flash chromatography (silica gel, pet. ether/EtOAc 8:2) to afford the pure compound (0.46, 78%) as green crystals. **Mp** 223-224 °C; **^{1}H NMR** (400 MHz, $(CD_3)_2SO$) 7.48 (2H, dd, *J* = 8.6, 5.7 Hz, Ar*H*), 7.34 (2H, dd, *J* = 6.8, 5.6 Hz), 7.23 (2H, t, *J* = 7.6 Hz), 5.95-5.91 (1H, m, *H*C=C), 5.61 (1H, d, *J* = 5.2 Hz, C=C*H*), 5.53 (1H, s), 4.68 (1H, d, *J* = 3.2 Hz), 4.07-4.00 (1H, m), 2.97-2.89 (1H, m), 2.38-2.31 (1H, m);); ν_{max} (film) 3330, 2921, 2852, 2214, 1602, 1222, 751; **^{13}C NMR** ($CDCl_3$) 31.2 (*C*H_2), 45.1 (CH_2*C*H), 46.3 (*C*C=C), 59.1 (*C*NH), 115.7, 119.4, 122.6, 124.1, 128.7, 130.2, 131.0, 131.9, 134.6, 137.7, 145.5, 157.3, 163.1; **HRMS** (FI^+): calcd. for $C_{19}H_{16}FN_5$, 333.1390; found, 333.1387.

(4-(4-Fluorophenyl)-3a,4,5,9b-tetrahydro-3H-cyclopenta[c]quinolin-6-yl)phosphonic acid 164



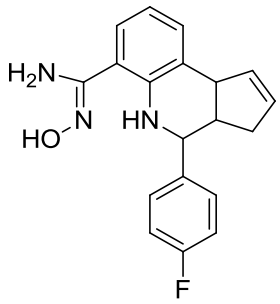
$Pd(PPh_3)_4$ (51 mg, 0.04 mmol, 5 mol%), Cs_2CO_3 (0.36 g, 1.10 mmol) and aryl halide (0.35 g, 1.01 mmol) were placed in microwave tubes , sealed and filled with N_2. THF (4 mL) and dibenzyl phosphonate (0.24 g, 0.91 mmol) was introduced and the reaction mixture was heated in a microwave reactor at 120 ºC for 30 min. The solids were filtered off after cooling down and washed with CH_2Cl_2. The filtrate was concentrated *in vacuo* and the crude was purified by flash chromatography (silica gel, petroleum ether/EtOAc 8:2) to afford title compound as pale yellow oil (0.28 g, 57%). **^{1}H NMR** (400 MHz, $CDCl_3$) 7.45-7.43 (2H, m), 7.28-7.26 (1H, m), 7.13-7.07 (2H, m), 7.02 (1H, d, *J* = 7.6 Hz), 6.64 (1H, t, *J* = 7.7 Hz, NCArH_{para}), 5.84-5.82 (1H, m, *H*C=C), 5.68-5.67 (1H, m, C=C*H*), 4.65 (1H, d, *J* = 3.2 Hz, NC*H*), 4.41 (1H, br. s, N*H*), 4.16-4.11 (1H, m, *H*CC=C), 3.00 (1H, qd, *J* = 9.0, 3.0 Hz), 2.59 (1H, ddq, *J* = 16.3, 9.4, 2.3 Hz), 1.82 (1H, dd, *J* = 16.2, 8.7 Hz, CH_2); ν_{max} (film) 3364, 3053, 2927, 2848, 1896, 1598, 1508, 1476, 1220, 756; **^{1}HRMS** (FI^+): calcd. for $C_{18}H_{17}FNO_3P$, 345.0930; found, 345.0927.

4-(4-Fluorophenyl)-3a,4,5,9b-tetrahydro-3H-cyclopenta[c]quinolin-6-ylhydrogen sulphate 167



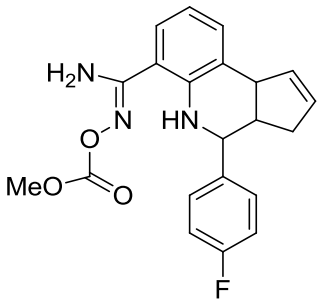
A solution of pyridine-sulfur trioxide complex (0.74 g, 4.62 mmol) and **194** (0.12 g, 0.43 mmol) in DMF/pyridine (1:1, 15 mL) was stirred under an atmosphere of nitrogen for 20 h at room temperature. Solvent was removed *in vacuo* and the crude was purified by flash chromatography (silica gel, MeOH) to afford title compound (0.15 g, 100%) as green crystals. **^{1}H NMR** (400 MHz, $(CD_3)_2SO$) 7.51-7.47 (2H, m, FArH_{meta}), 7.22-7.16 (2H, m, FArH_{ortho}), 6.86-6.83 (1H, m, OAr*H*), 6.59-6.51 (2H, m, OAr*H*), 5.83 (1H, m, *H*C=C), 5.59-5.56 (1H, m, C=C*H*), 4.51 (1H, br. s, NC*H*), 4.01 (1H, d, *J* = 7.8 Hz, *H*CC=C), 2.92 (1H, dd, *J* = 8.9, 3.5 Hz, CH_2), 2.46-2.37 (1H, d, m, CH_2); **^{13}C NMR** ($(CD_3)_2SO$) 31.7 (CH_2), 45.9 (CH_2CH), 46.8 (*C*C=C), 59.3 (*C*NH), 115.6, 118.5, 122.6, 123.5, 124.9, 128.9, 129.7, 133.7, 137.8, 139.2, 145.5, 162.8; ν_{max} (film) 3465, 3016, 2970, 2359, 1739, 1366, 1217, 999, 769; **LRMS** (ES^-): 360.0 (MH^-); **HRMS** (FI^+): calcd. for $C_{18}H_{16}FNO_4S$, 361.0784; found, 361.0784.

(*Z*)-4-(4-Fluorophenyl)-N'-hydroxy-3a,4,5,9b-tetrahydro-3H-cyclopenta[c]quinoline-6-carboximidamide 155



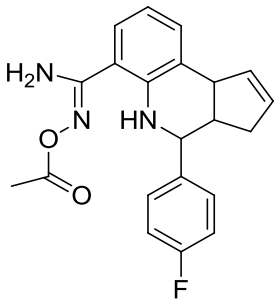
Hydroxylamine hydrochloride (0.21 g, 6.43 mmol) was added to a solution of **146** (0.30 g, 1.03 mmol) in DMF (9 mL), followed by Na_2CO_3 (0.61 g, 5.71 mmol) in water (3.2 mL) over a 5 min period and the reaction was stirred for 12 h at 70 ºC. The mixture was cooled to 0 ºC and was poured into ice-water (100 mL). The compound was filtered and washed with water and hexane. The crude compound was dried and purified by flash chromatography (silica gel, pet. ether/EtOAc 7:3) to afford title compound as orange powder (0.30 g, 91%). **^{1}H NMR** (400 MHz, $CDCl_3$) 7.35 (2H, dd, *J* = 8.6, 5.4 Hz), 7.22 (1H, d, *J* = 7.8 Hz), 7.09 (1H, d, *J* = 7.8 Hz), 7.02-6.96 (2H, m), 6.74 (1H, t, *J* = 7.6 Hz, NCArH_{para}), 5.82-5.79 (1H, m, *H*C=C), 5.65-5.64 (1H, m, C=C*H*), 4.91 (1H, br. s, N*H*), 4.53 (1H, d, *J* = 3.3 Hz, NC*H*), 4.15 (1H, d, *J* = 8.6 Hz, *H*CC=C), 3.00-2.93 (1H, m), 2.90-2.53 (1H, m, CH_2), 1.80-1.74 (1H, m, CH_2); **^{13}C NMR** ($CDCl_3$) 31.7 (*C*H_2), 45.6 (CH_2*C*H), 46.6 (*C*C=C), 56.8 (*C*NH), 115.0, 115.2, 116.1, 117.5, 124.8, 126.9, 127.7, 127.8, 130.4, 130.5, 134.1, 144.7, 153.0; ν_{max} (film) 3600, 3063, 3016, 2970, 2946, 1739, 1366, 1216; **HRMS** (FI^+): calcd. for $C_{19}H_{18}FN_3O$, 323.1434; found, 323.1435.

(Z)-4-(4-Fluorophenyl)-N'-((methoxycarbonyl)oxy)-3a,4,5,9b-tetrahydro-3H-cyclopenta[c]quinoline-6-carboximidamide 158



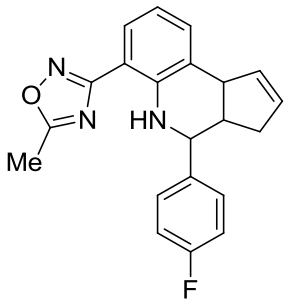
To a solution of **184** (0.50 g, 1.55 mmol) in DMF (17 mL) was added NEt_3 (0.46g, 4.53 mmol) at room temperature and the reaction was stirred for 10 min. The solution was cooled to 0 ºC and methyl chloroformate (0.42 g, 4.46 mmol) was added. The mixture was stirred at room temperature for 12 h before being poured over crushed ice (500 mL). Product was filtered and washed with water and petroleum ether. Purification by flash chromatography (silica gel, petroleum ether/EtOAc 9:1) afforded title compound (0.54 g, 92%) as light brown crystals. ν_{max} (film) 3470, 3385, 3287, 3047, 2960, 2916, 2850, 1775, 1242, 904, 748; **^{1}H NMR** (400 MHz, $CDCl_3$) 7.48 (2H, dd, *J* = 8.6, 5.4 Hz, FArH_{meta}), 7.21-7.18 (1H, m, Ar*H*), 7.14-7.07 (3H, m), 6.89 (1H, s, N*H*), 6.73 (1H, t, *J* = 7.6 Hz, NCArH_{para}), 5.79-5.77 (1H, m, *H*C=C), 5.64 (1H, m, C=C*H*), 4.68 (1H, d, *J* = 3.3 Hz, NC*H*), 4.16 (1H, d, *J* = 9.0 Hz, *H*CC=C), 3.80 (3H, s, OCH_3), 3.09-3.01 (1H, m), 2.59-2.51 (1H, m, CH_2), 1.81 (1H, dd, *J* = 16.0, 8.9 Hz, CH_2); **^{13}C NMR** ($CDCl_3$) 31.8 (*C*H_2), 45.6 (CH_2*C*H), 46.5 (*C*C=C), 55.2 (O*C*H_3), 56.5 (*C*NH), 114.2, 115.1, 115.3, 117.3, 125.1, 127.3, 127.9, 130.6, 131.5, 134.0, 137.9, 145.3, 156.2, 162.9; **HRMS** (FI^+): calcd. for $C_{21}H_{20}FN_3O_3$, 381.1489; found, 381.1491.

(Z)-N'-Acetoxy-4-(4-fluorophenyl)-3a,4,5,9b-tetrahydro-3H-cyclopenta[c]quinoline-6-carboximidamide 156



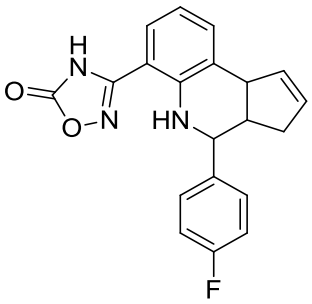
Acetic anhydride (0.32 g, 3.09 mmol) and triethylamine (0.37 g, 3.71 mmol) was added to a solution of **184** (0.50 g, 1.55 mmol) in DMSO (17 mL) and stirred at room temperature for 12 h. The reaction mixture was poured over crushed ice (500 mL) and product was filtered and washed with water and hexane. Purification by flash chromatography (silica gel, petroleum ether/EtOAc 9:1) afforded title compound (0.51 g, 90%) as beige powder. **^{1}H NMR** (400 MHz, $CDCl_3$) 7.49-7.45 (2H, m), 7.21 (1H, dd, *J* = 7.8, 1.4 Hz, Ar*H*), 7.14-7.06 (3H, m), 7.01 (1H, s, N*H*), 6.73 (1H, t, *J* = 7.6 Hz, NCArH_{para}), 5.79-5.75 (1H, m, *H*C=C), 5.64-5.62 (1H, m, C=C*H*), 5.05 (1H, br. s, N*H*), 4.67 (1H, d, *J* = 3.3 Hz, NC*H*), 4.17 (1H, d, *J* = 8.7 Hz, *H*CC=C), 3.09-3.02 (1H, m), 2.62-2.52 (1H, m, CH_2), 2.17 (3H, s, CH_3), 1.85-1.78 (1H, m); **^{13}C NMR** ($CDCl_3$) 19.8 (*C*H_3), 31.8 (*C*H_2), 45.6 (CH_2*C*H), 46.6 (*C*C=C), 56.6 (*C*NH), 115.1, 115.3, 117.3, 125.0, 127.8, 127.9, 130.6, 131.4, 134.0, 145.4, 156.0, 162.9, 167.5 (C=O); ν_{max} (film) 3671, 3624, 3483, 3460, 3336, 3061, 2938, 2869, 2190, 1272, 1222, 748; **HRMS** (FI^+): calcd. for $C_{21}H_{20}FN_3O_2$, 365.1540; found, 365.1543.

3-(4-(4-Fluorophenyl)-3a,4,5,9b-tetrahydro-3H-cyclopenta[c]quinolin-6-yl)-5-methyl-1,2,4-oxadiazole 157



Compound **192** was stirred in DMSO (5 mL) for 15 min and acetic acid (0.52 g, 4.01 mmol) was added and the mixture was stirred at 85 ºC for 24 h. The reaction mixture was cooled to rt and poured over crushed ice (100 g) and once ice melted the product was filtered and washed thoroughly with water and hexane and dried under vacuum. Purification by flash chromatography (silica gel, petroleum ether/EtOAc 94:6) afforded title compound (0.14 g, 50%) as orange oil. **^{1}H NMR** (400 MHz, $CDCl_3$) 7.93 (1H, dd, *J* = 7.9, 1.5 Hz, Ar*H*), 7.51-7.47 (2H, m), 7.19 (1H, d, *J* = 7.5 Hz), 7.13-7.09 (2H, m), 6.82 (1H, t, *J* = 7.6 Hz, NCArH_{para}), 5.88-5.84 (1H, m, *H*C=C), 5.67-5.66 (1H, m, C=C*H*), 4.78 (1H, d, *J* = 3.4 Hz, NC*H*), 4.21 (1H, d, *J* = 8.8 Hz, *H*CC=C), 3.10-3.03 (1H, m), 2.63 (3H, s CH_3), 2.62-2.56 (1H, m, CH_2), 1.87-1.81 (1H, m); $\boldsymbol{\nu_{max}}$ (film) 3752, 3670, 3659, 3326, 2922, 1717, 1586, 1499, 1219, 748; **^{13}C NMR** ($CDCl_3$) 12.2 (*C*H_3), 31.7 (*C*H_2), 45.6 (CH_2*C*H), 46.2 (*C*C=C), 56.6 (*C*NH), 110.7, 115.3, 115.5, 117.5, 126.6, 127.6, 127.7, 127.8, 130.5, 131.8, 134.2, 138.1, 138.2, 145.5, 160.7, 163.2 (C=O), 168.4 (N*C*N), 174.6 (N*C*O); **HRMS** (FI^+): calcd. for $C_{21}H_{18}FN_3O$, 347.1434; found, 347.1437.

3-(4-(4-Fluorophenyl)-3a,4,5,9b-tetrahydro-3H-cyclopenta[c]quinolin-6-yl)-1,2,4-oxadiazol-5(4H)-one 159



Compound **191** was stirred at reflux in xylene (5 mL) for 24 h. The reaction mixture was cooled to rt and poured over crushed ice (100 g) and once ice melted the product was filtered off to yield the title product (0.17 g, 64%) as beige powder. **^{1}H NMR** (400 MHz, $CDCl_3$) 7.29-7.26 (2H, dd, *J* = 8.1, 5.6 Hz, Ar*H*), 7.10-6.99 (4H, m, Ar*H*), 6.85 (1H, d, *J* = 7.1 Hz, Ar*H*), 6.07-6.04 (1H, m, *H*C=C), 5.50 (1H, d, *J* = 5.7 Hz, NC*H*), 5.44-5.41 (1H, m, C=C*H*), 4.14 (1H, d, *J* = 7.1 Hz), 3.23 (1H, quin, *J* = 6.8 Hz, *H*CCC=C), 2.39-2.33 (1H, m, CH_2), 2.18-2.12 (1H, m, CH_2); **^{13}C NMR** ($CDCl_3$) 38.1 (*C*H_2), 45.2 (CH_2*C*H), 46.4 (*C*C=C), 56.7 (*C*NH), 110.4, 111.1, 118.7, 124.3, 124.7, 125.6, 127.6, 130.5, 135.2, 135.5, 139.3, 145.1, 157.7, 160.7, 163.6, 205.7; ν_{max} (film) 3458, 3306, 3055, 2970, 1739, 1535, 1218, 742; **HRMS** (FI^+): calcd. for $C_{20}H_{16}FN_3O_2$, 349.1227; found, 349.1226.

5.4 Experimental for Chapter 4

5.4.1 Synthesis of Methyl Jasmonate

GENERAL PROCEDURE 5.6: Tandem conjugate addition/alkylation

n-BuLi (3.50 mmol, 2.5 M in THF) was added dropwise *via* syringe to a stirred suspension of dimethyl malonate (3.58 mmol) and flame-dried powdered 4Å molecular sieves (0.5 g) in THF (2 mL) at -78 ºC and the mixture was stirred for 1h. A solution of cyclopentenone (2.39 mmol) in THF (0.8 mL) was added dropwise and the temperature of the reaction was allowed to reach -40 ºC. The reaction mixture was stirred for 12h before a solution of alkyl halide (2.63 mmol) in THF (2 mL) was added. The reaction mixture was warmed to rt over 12 hours, before being diluted with Et_2O (20 mL) and saturated aqueous NH_4Cl. The organic layer was separated and the aqueous layer was extracted with Et_2O (3 x 30 mL). The combined organic extracts were washed with brine, dried (Na_2SO_4) and concentrated *in vacuo*. The crude product was purified by flash column chromatography.

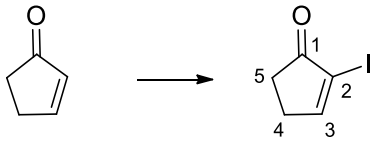
GENERAL PROCEDURE 5.7: Reduction of cyclic iodo-enones

$CeCl_3 \cdot 7H_2O$ (0.1 eq.) was added to a solution of 2-iodocyclopent-2-enone **300** (1.0 eq.) in MeOH at 0 ºC. The reaction was stirred for 5 minutes before $NaBH_4$ (0.8 eq.) was added in ten portions over 40 min. The resultant mixture was allowed to warm to rt over 1h and the solvent was removed *in vacuo*. The residue was partitioned between H_2O (50 mL) and Et_2O (40 mL) and the solution was acidified with 1M HCl to pH 3. The aqueous layer was extracted with Et_2O (3 x 50 mL) and the combined organic layers were washed with water and brine, dried (Na_2SO_4) and concentrated *in vacuo*. The crude product was purified by flash column chromatography.

GENERAL PROCEDURE 5.8: Protection of Enols as Silyl Ethers

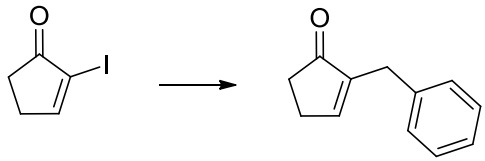
To a mixture of enol (1.0 eq.) and imidazole (2.50 eq.) in dry CH_2Cl_2 was added DMAP (0.3 eq.) and *tert*-butylchlorodimethylsilane (1M in THF, 1.20 eq.). The mixture was stirred for 18h at room temperature. The crude mixture was partitioned between H_2O (50 mL) and CH_2Cl_2 (50 mL) and the aqueous phase was extracted twice more with CH_2Cl_2. The combined organic extracts were washed with brine, dried (Na_2SO_4) and concentrated *in vacuo*. The crude product was purified by flash column chromatography.

2-Iodocyclopent-2-enone 300



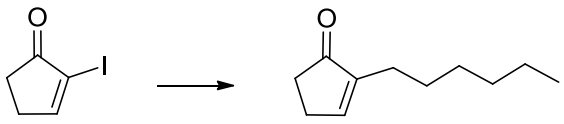
To a solution of 2-cyclopent-1-one (1.0 g, 12.18 mmol) in 1:1 THF/H_2O (60 mL) were added potassium carbonate (2.02 g, 14.62 mmol), iodine (4.64 g, 18.28 mmol) and DMAP (300 mg, 2.44 mmol) successively. The resulting solution was stirred for 1h at room temperature. The reaction mixture was diluted with EtOAc (100 mL) and the organic layer was washed with saturated solution of $Na_2S_2O_3$ (200 mL), followed by 0.1 M HCl (200 mL). The mixture was extracted with EtOAc (3 x 50 mL) and the combined organic extracts were dried with Na_2SO_4 and concentrated *in vacuo*. The crude product was purified by crystallisation from EtOAc to give 2-iodocyclopent-2-enone **300** (2.51 g, 99%). Data were consistent with those in the literature.[20] **^{1}H NMR** (400 MHz, $CDCl_3$) 8.02 (1H, t, *J* = 2.9 Hz, C=C*H*), 2.80-2.76 (2H, m, C(5)H_2), 2.53-2.49 (2H, m, C(4)H_2); **LRMS** (ESI^+) 231 ($[M+Na]^+$).

2-Benzylcyclopent-2-enone 299



A solution of freshly distilled 1,2-dibromoethane (13 μL, 0.15 mmol) in THF (1 mL) was added to a dry flask charged with Zn dust (0.25 g, 3.80 mmol) in THF (1 mL) and was heated at reflux for 10 minutes. A solution of benzyl bromide (0.53 g, 3.10 mmol) in THF (6 mL) was added dropwise to the suspension at 0 ºC and was stirred for 3 h. The reaction mixture was transferred *via* a cannula to a solution of 2-iodo-2-cyclopenten-1-one (0.50 g, 2.40 mmol) and $Pd(PPh_3)_2Cl_2$ (80 mg, 114 μmol) in DMF (10 mL) at 0 ºC. The mixture was allowed to reach room temperature and was stirred for a further 2 hours before quenching with saturated aqueous NH_4Cl (20 mL). The mixture was extracted with Et_2O (3 x 15 mL). The combined organic extracts were washed with brine, dried (Na_2SO_4) and concentrated *in vacuo*. Purification was achieved by flash column chromatography (silica, 85:15 petroleum ether/EtOAc) to yield the pure product **299** (0.37 g, 90%) as a light yellow oil. Data were consistent with those in the literature.[20] **^{1}H NMR** (400 MHz, $CDCl_3$) 7.10-7.25 (6H, m, Ar*H*, C=C*H*), 3.44 (2H, s, PhCH_2), 2.51-2.48 (2H, m, C(5)H_2), 2.40-2.38 (2H, m, C(4)H_2); **HRMS** (FI^+): calcd. for $C_{12}H_1O$, 172.0888; found, 172.0891.

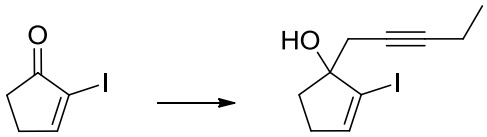
2-Hexylcyclopent-2-enone 304



A solution of *n*-hexylmagnesium bromide (1.56 mL, 2.0 M in Et_2O) was added to dried $ZnBr_2$ (0.38 g, 1.68 mmol) in THF (3 mL) under an atmosphere of argon at -78 ºC. The reaction temperature was allowed to warm up to 0 ºC. A solution of 2-iodo-2-cyclopenten-1-one (0.50

g, 2.40 mmol), $Pd(PPh_3)_2Cl_2$ (80 mg, 114 μmol) in DMF (10 mL) was added *via* cannula. The solution was stirred at 0 ºC for 3h before quenching with saturated aqueous NH_4Cl (40 mL). Upon warming to rt, the product was extracted with Et_2O (3 x 30 mL). The combined organic extracts were washed with brine (30 mL), dried (Na_2SO_4) and concentrated *in vacuo*. Purification *via* flash column chromatography (silica, 85:15 petroleum ether/EtOAc) furnished the pure product **304** (0.32 g, 79%) as a light yellow oil. Data were consistent with those in the literature.[20] **^{1}H NMR** (400 MHz, $CDCl_3$) 7.32-7.30 (1H, m, C=C*H*), 2.58-2.55 (2H, m, C(5)*H*), 2.41-2.39 (2H, m, C(4)*H*), 2.16 (2H, t, *J* = 6.5 Hz, C=CCH_2), 1.62-1.22 (8H, m, hexyl-CH_2), 0.88 (3H, t, *J* = 6.4 Hz, CH_3); **HRMS** (FI^+): calcd. for $C_{11}H_{18}O$, 166.1358; found, 166.1360.

2-Iodo-1-(pent-2-yn-1-yl)cyclopent-2-enol 313



Method A

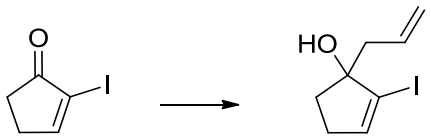
A solution of freshly distilled 1,2-dibromoethane (13 μL, 0.15 mmol) in THF (1 mL) was added to a dry flask charged with Zn dust (0.25 g, 3.80 mmol) in THF (1 mL) and was heated at reflux for 10 minutes. TMSCl (5 μL, 0.35 mmol) was added to the resulting suspension at 0 ºC and the reaction mixture was stirred at 0 ºC for 20 minutes. A solution of 1-Bromo-2-pentyne (0.46 g, 3.10 mmol) in THF (6 mL) was added dropwise and the resulting solution was stirred at room temperature for 1h. The reaction mixture was transferred *via* a cannula to a solution of 2-iodo-2-cyclopenten-1-one (0.50 g, 2.40 mmol) and $Pd(PPh_3)_2Cl_2$ (80 mg, 114 μmol) in DMF (10 mL) at 0 ºC. The reaction mixture was allowed to warm up to room temperature and was stirred for further 2 hours before quenching with saturated aqueous NH_4Cl (20 mL). The product was extracted with Et_2O (3 x 15 mL) and was washed with

brine, dried (Na_2SO_4) and concentrated *in vacuo*. Purification was achieved by flash column chromatography (silica, 9:1 petroleum ether/EtOAc) to afford the pure product **313** (0.49 g, 60%) as a colourless oil.

Method B

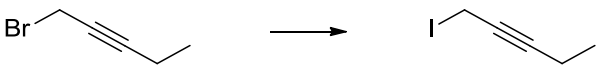
A solution of 1-bromo-2-pentyne (0.46 g, 3.10 mmol) in THF (5 mL) was added to a suspension of flame-dried $ZnBr_2$ (0.38 g, 1.68 mmol), Mg (71 mg, 5.92 mmol) and I_2 (8 mg, 0.03 μmol) in THF (1 mL). The resulting mixture was stirred at room temperature for 3h. A solution of 2-Iodo-2-cyclopentenone (0.50 g, 2.40 mmol) and $Pd(PPh_3)_2Cl_2$ (80 mg, 114 μmol) in DMF (10 mL) was added *via* cannula and was stirred at room temperature overnight. The reaction was quenched by the addition of saturated aqueous NH_4Cl (20 mL) and extracted with Et_2O (3 x 15 mL). The combined organic extracts were washed with brine, dried (Na_2SO_4) and concentrated *in vacuo*. Purification *via* flash column chromatography (silica, 9:1 petroleum ether/EtOAc) afforded the pure product **313** (0.58 g, 71%) as a colourless oil. **^{1}H NMR** (400 MHz, $CDCl_3$) 6.28 (1H, m, C=C*H*), 2.54-2.32 (5H, m), 2.20-2.16 (2H, m, CH_3CH_2), 2.05-1.99 (1H, m, CH_2), 1.13 (3H, t, *J* = 7.5 Hz, CH_3); **^{13}C NMR** ($CDCl_3$) 142.4 (H*C*=C), 104.7 (*C*I), 85.7 (*C*OH), 84.4 (C≡C), 74.1 (C≡C), 34.0, 32.9, 31.2, 14.1 (CH_3), 12.4 (CH_3CH_2); $\boldsymbol{\nu_{max}}$ (thin film)/cm^{-1} 3402, 2976, 2935, 2360, 1704, 1412, 1221; **HRMS** (FI$^+$): calcd. for $C_{10}H_{13}IO$, 276.0011; found, 276.0042.

1-Allyl-2-iodocyclopent-2-enol 311



A solution of freshly distilled 1,2-dibromoethane (13 μL, 0.15 mmol) in THF (1 mL) was added to a dry flask charged with Zn dust (0.25 g, 3.80 mmol) in THF (1 mL) and was heated at reflux for 10 min. A solution of allyl bromide (0.38 g, 3.10 mmol) in THF (6 mL) was added dropwise to the suspension at 0 ºC and was stirred for 3 h. The reaction mixture was transferred *via* a cannula to a solution of 2-iodo-2-cyclopenten-1-one (0.50 g, 2.40 mmol) and $Pd(PPh_3)_2Cl_2$ (80 mg, 114 μmol) in DMF (10 mL) at 0 ºC. The mixture was allowed to reach room temperature and was stirred for a further 2 hours before quenching with saturated aqueous NH_4Cl (20 mL). The mixture was extracted with Et_2O (3 x 15 mL). The combined organic extracts were washed with brine, dried (Na_2SO_4) and concentrated *in vacuo*. Purification was achieved by flash column chromatography (silica, 85:15 petroleum ether/EtOAc) to yield the pure product **311** (0.46 g, 76%) as pale yellow oil. Data were consistent with those in the literature.[20] **^{1}H NMR** (400 MHz, $CDCl_3$) 6.25 (1H, t, *J* = 2.4 Hz, C=C*H*), 5.87-5.62 (1H, m, *H*C=CH_2), 5.35-5.05 (2H, m, HC=CH_2), 2.54-2.14 (5H, m), 2.23-1.79 (2H, m); **HRMS** (FI^+): calcd. for $C_8H_{11}IO$, 249.9855; found, 249.9858.

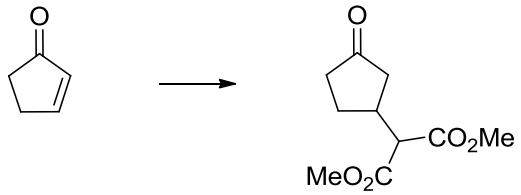
1-Iodopent-2-yne 225



Sodium iodide (5.28 g, 35.22 mmol) was added to a solution of 1-bromopent-2-yne (2.88 g, 19.56 mmol) in absolute acetone (12 mL) and the reaction mixture was heated at reflux for 5 h. Upon cooling, the mixture was diluted with water (30 mL) and the product was extracted with Et_2O (3 x 30 mL). The combined organic layers were washed with saturated aqueous $NaHSO_3$ (50 mL) and brine, dried (Na_2SO_4) and concentrated *in vacuo*. Purification was

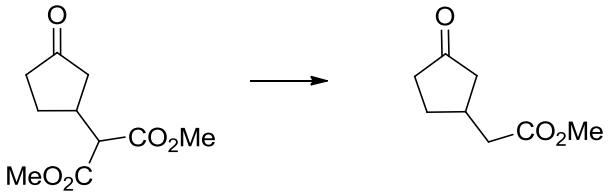
achieved by flash column chromatography (silica, 8:2 petroleum ether/EtOAc) to yield the pure product **225** (2.98 g, 79%) as a colourless liquid. Data were consistent with those in the literature.[21] **^{1}H NMR** (400 MHz, $CDCl_3$) 3.71 (2H, t, *J* = 2.4 Hz, IC*H*$_2$), 2.22 (2H, qt, *J* = 7.5, 2.4 Hz, CH_3CH_2), 1.12 (3H, t, *J* = 7.6 Hz, C*H*$_3$); **LRMS** (ESI^+): 194 ($[M+H]^+$).

3-(Bis-carbomethoxymethyl)-1-cyclopentanone 236



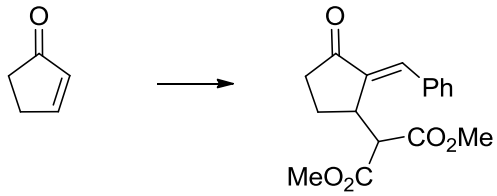
A solution of sodium methoxide (0.95 g, 17.61 mmol) in MeOH (5 mL) was slowly added to dimethyl malonate (2.37 g, 17.91 mmol) and the mixture was stirred at room temperature for 1 hr. Cyclopentenone (0.98 g, 11.94 mmol) was added dropwise and the reaction was stirred for 18 hr at room temperature. The reaction was quenched with brine (20 mL) and the solvent was removed *in vacuo*. The remaining residue was partitioned between water (30 mL) and Et_2O (40 mL). The organic phase was separated and the aqueous phase was extracted with Et_2O (3 x 30 mL). The combined organic layers were washed with brine, dried (Na_2SO_4) and concentrated *in vacuo*. Purification was achieved by flash column chromatography (silica, 8:2 petroleum ether/EtOAc) to yield the pure product **236** (2.36 g, 92%) as a colourless oil. Data were consistent with those in the literature.[22] **^{1}H NMR** (400 MHz, $CDCl_3$) 3.77 (3H, s, OC*H*$_3$), 3.75 (3H, s, OC*H*$_3$), 3.38 (1H, d, *J* = 9.3 Hz, C*H*CO_2Me), 2.88-2.83 (1H, m, C(3)*H*), 2.51 (1H, dd, *J* = 18.4, 7.5 Hz), 2.38-2.30 (1H, m), 2.26-2.18 (2H, m), 2.02 (1H, dd, *J* = 18.1, 10.1 Hz), 1.71-1.63 (1H, m); **HRMS** (FI^+): calcd. for $C_{10}H_{14}O_5$, 214.0841; found, 214.0840.

Methyl 2-(3-oxocyclopentyl)-acetate 296



A mixture of ester **236** (0.23 g, 1.35 mmol), H_2O (24 mg, 1.35 mmol) and NMP (1.35 mL) were heated in a microwave reactor at 202 ºC for 1.2 hr. Purification *via* flash column chromatography (silica, 7:3 petroleum ether/EtOAc) afforded the pure product **296** (0.21 g, 100%) as a colourless oil. Data were consistent with those in the literature.[23] **^{1}H NMR** (400 MHz, $CDCl_3$) 3.70 (3H, s, OC*H*$_3$), 2.65-2.58 (1H, m, C(3)*H*), 2.52-2.46 (3H, m), 2.35-2.15 (3H, m), 1.89 (1H, ddd, *J* = 18.3, 10.0, 1.3 Hz, C(4)*H*), 1.62-1.56 (1H, m, C(4)*H*); **HRMS** (FI^+): calcd. for $C_8H_{12}O_3$, 156.0786; found, 156.0799.

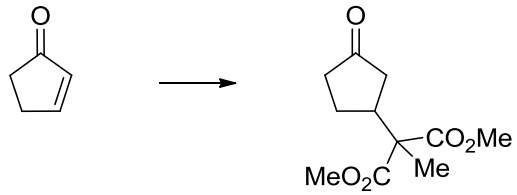
Dimethyl 2-(2-benzylidene-3-oxocyclopentyl)-malonate 293



TFA (40 mg, 0.36 mmol) was added dropwise to a solution of pyrrolidine (55 mg, 0.36 mmol) in MeOH (0.35 mL) and the reaction was stirred for 5 min at room temperature. A solution of cyclopentenone (98 mg, 1.19 mmol), dimethyl malonate (0.31 g, 2.38 mmol) and benzaldehyde (0.13 g, 1.19 mmol) in MeOH (2.2 mL) was added to the mixture and the solution was stirred for a further 48 hr. The solution was concentrated *in vacuo* and the crude was purified *via* column chromatography (silica, 84:16 petroleum ether/EtOAc) to afford the pure product **293** (50 mg, 14%) as a colourless oil. **^{1}H NMR** (400 MHz, $CDCl_3$) 7.52-7.50 (2H, m, Ar*H*), 7.46-7.44 (1H, m, Ar*H*), 7.43 (1H, s, C=C*H*), 7.42-7.39 (2H, m, Ar*H*), 3.78 (3H, s, OC*H*$_3$), 3.77 (3H, s, OC*H*$_3$), 3.50 (1H, d, *J* = 8.8 Hz, C*H*CO_2Me), 3.34-3.28 (1H, m),

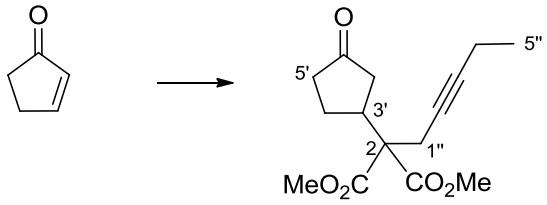
3.00-2.93 (1H, m, C(5)*H*), 2.78-2.73 (1H, m, C(5)*H*), 2.68 (1H, dd, *J* = 18.1, 8.0 Hz, C(4)*H*), 2.32 (1H, dd, *J* = 18.1, 9.9 Hz, C(4)*H*); **^{13}C NMR** ($CDCl_3$) 205.0 (*C*=O), 187.9 (*C*O_2Me), 186.4 (*C*O_2Me), 141.0 (C=*C*H), 134.6 (*C*=CH), 133.2 (Ar*C*), 130.6 (Ar*C*), 129.6 (2 Ar*C*), 128.8 (2 Ar*C*), 56.1 (*C*HCO_2Me), 52.7 (O*C*H_3), 42.1 (*C*(5)), 33.7 (*C*(3)), 33.6 (*C*(4)); $\boldsymbol{\nu_{max}}$ (thin film)/cm^{-1} 2920, 1749, 1630, 1493, 1316, 1145, 753, 691; **HRMS** (FI$^+$): calcd. for $C_{17}H_{18}O_5$, 302.1154; found, 302.1330.

Dimethyl 2-methyl-2-(3-oxocyclopentyl)-malonate 239



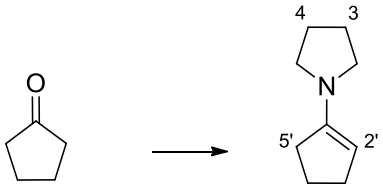
Iodomethane (0.37 g, 2.63 mmol) was subjected to General Procedure **A**. The crude product was purified *via* flash column chromatography (silica, 82:18 petroleum ether/EtOAc) to afford the pure product **239** (0.35 g, 65%) as a colourless oil. **^{1}H NMR** (400 MHz, $CDCl_3$) 3.75 (3H, s, OCH_3), 3.73 (3H, s, OCH_3), 2.86 (1H, tdd, *J* = 11.5, 7.7, 6.4 Hz, C(3)*H*), 2.44-2.20 (2H, m, C(2)*H*, C(5)*H*), 2.25-2.08 (3H, m, C(2)*H*, C(4)*H*, C(5)*H*), 1.77-1.67 (1H, ddd, *J* = 22.1, 10.7, 7.8 Hz, C(4)*H*), 1.46 (3H, s, CH_3); **^{13}C NMR** ($CDCl_3$) 217.4 (*C*=O), 171.7 (*C*O_2Me), 171.6 (*C*O_2Me), 55.5 (*C*CH_3), 52.6 (O*C*H_3), 52.5 (O*C*H_3), 41.6, 40.7, 38.4, 24.6, 17.9 (*C*H_3); $\boldsymbol{\nu_{max}}$ (thin film)/cm^{-1} 2956, 1726, 1435, 1243, 1121, 1091, 980, 883; **HRMS** (FI$^+$): calcd. for $C_{11}H_{16}O_5$, 228.0998; found, 228.0997.

Dimethyl 2-(3-oxocyclopentyl)-2-(pent-2-yn-1-yl)malonate 240



Bromo-2-pentyne (0.39 g, 2.63 mmol) was subjected to General Procedure **A**. The crude product was purified *via* flash column chromatography (silica, 82:18 petroleum ether/EtOAc) afforded the pure product **240** as a colourless oil (0.33 g, 49%). **^{1}H NMR** (400 MHz, $CDCl_3$) 3.75 (6H, s, OC*H*$_3$), 3.05 (1H, dq, *J* = 11.8, 7.5, 5.9 Hz, C(3')*H*), 2.90-2.77 (2H, m, C(1")*H*), 2.57 (1H, dd, *J* = 18.4, 7.8 Hz, C(5')*H*), 2.36-2.18 (4H, m), 2.12 (2H, qt, *J* = 7.5, 2.4 Hz, C*H*$_2$CH$_3$), 1.70-1.65 (1H, m, C(4')*H*), 1.08 (3H, t, *J* = 7.5 Hz, CH_3); **^{13}C NMR** ($CDCl_3$) 217.6 (*C*=O), 170.1 (*C*O$_2$Me), 170.0 (*C*O$_2$Me), 85.5 (C≡C), 73.3 (C≡C), 59.5 (*C*(2)), 52.6 (O*C*H$_3$), 41.2, 40.0 (*C*(3')), 38.5 (*C*(5')), 25.0 (*C*(1")), 24.0 (*C*(4')), 14.0 (*C*H$_3$), 12.3 (*C*(4")); **ν_{max}** (thin film)/cm^{-1} 3459, 2970, 1739, 1436, 1366, 1288, 1217, 1095; **HRMS** (FI^{+}): calcd. for $C_{15}H_{20}O_5$, 280.1311; found, 280.1315.

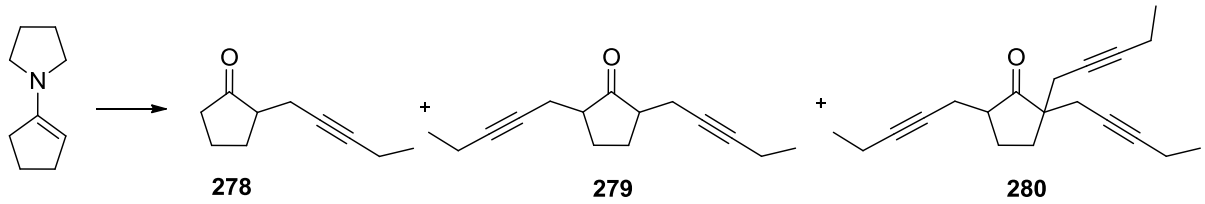
1-(Cyclopent-1-en-1-yl)pyrrolidine 283



Magnesium sulphate (21.4 g) was added in one portion to a solution of cyclopentanone (3.0 g, 35.67 mmol) in cyclohexane (45 mL), under an atmosphere of nitrogen. Pyrrolidine (12.68 g, 0.17 mol) was added dropwise to the resulting suspension at 0 ºC and stirring was continued for 30 minutes at 0 ºC and a further 12 hours at room temperature. The reaction mixture was filtered and the filtrate was washed with cyclohexane (3 x 50 mL) and concentrated *in vacuo*. Purification was achieved *via* distillation under reduced pressure (42 ºC / 1 mmHg) to afford

the pure product **283** (4.81 g, 98%) as a colourless oil. Data were consistent with those in the literature.[24] **^{1}H NMR** (400 MHz, $CDCl_3$) 4.05 (1H, br. s, C=C*H*), 3.8-2.98 (4H, m, NCH_2), 2.48-2.41 (2H, m, CH_2), 2.38-2.30 (2H, m, CH_2), 1.87-1.75 (6H, m, C(3)*H*, C(4)*H*, C(4')*H*); **HRMS** (FI^+): calcd. for $C_9H_{15}N$, 137.1204; found, 137.1207.

Pentynylcyclopentanone



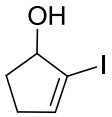
To a stirred solution of enamine **283** (0.2 g, 1.46 mmol) and 1-bromo-2-pentyne (0.19 g, 1.32 mmol) in ethanol (3.5 mL) was added anhydrous NaI (6 mg, 40 μmol) and the reaction was heated at reflux for 5 h. The solvent was removed *in vacuo* and the resulting suspension was diluted with H_2O (40 mL) and the product was extracted with CH_2Cl_2 (3 x 30 mL). The combined organic layers were washed with water and brine, dried (Na_2SO_4) and concentrated *in vacuo*. A mixture of mono- di- and tri-alkylated crude was afforded, which was purified *via* flash column chromatography (silica, 88:2 petroleum ether/EtOAc) to yield the pure products 2-(pent-2-yn-1-yl)cyclopentenone **278** (62 mg, 31%), 2,5-di(pent-2-yn-1-yl)cyclopentanone **279** (55 mg, 19%) and 2,2,5-tri(pent-2-yn-1-yl)cyclopentenone **280** (40 mg, 1%).

2-(Pent-2-yn-1-yl)cyclopentanone. **^{1}H NMR** (400 MHz, $CDCl_3$) 2.54-2.48 (1H, m), 2.33-1.78 (10H, m), 1.10 (3H, t, *J* = 7.5 Hz, CH_3); **^{13}C NMR** ($CDCl_3$) 12.3 (CH_3), 14.0, 24.0, 25.0, 38.5, 40.0, 41.2, 52.6 (OCH_3), 59.5, 73.3, 85.5, 170.0 (CO_2Me), 170.1 (CO_2Me), 217.6 (*C*=O); **HRMS** (FI^+): calcd. for $C_{10}H_{14}O$, 150.1045; found, 150.1043.

2,5-Di(pent-2-yn-1-yl)cyclopentanone. **^{1}H NMR** (400 MHz, $CDCl_3$) 2.55-2.10 (13H, m), 1.80-1.69 (1H, m), 1.13-1.08 (6H, m, CH_3); **^{13}C NMR** ($CDCl_3$) 12.4 (*C*H_3), 14.2, 14.3, 19.0, 19.1, 25.9, 26.4, 47.4, 48.6, 76.3, 82.7, 83.1, 218.5 (*C*=O); **ν_{max}** (KBr disk)/cm^{-1} 2975, 2212, 1736, 1675, 1427, 1319, 1229, 1159, 1064; **HRMS** (FI^+): calcd. for $C_{15}H_{20}O$, 216.1514; found, 216.1515.

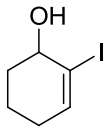
2,2,5-Tri(pent-2-yn-1-yl)cyclopentanone. **^{1}H NMR** (400 MHz, $CDCl_3$) 2.54-2.09 (17H, m), 1.91-1.83 (1H, m), 1.13-1.07 (9H, m, CH_3); **^{13}C NMR** ($CDCl_3$) 12.3 (*C*H_3), 12.4, 14.1, 14.2, 14.3, 18.7, 24.8, 2.9, 25.9, 29.4, 49.1, 51.7, 75.0, 75.6, 82.9, 84.1, 84.2, 219.5 (*C*=O); **ν_{max}** (KBr disk)/cm^{-1} 2976, 2361, 2212, 1709, 1673, 1419, 1360, 1228 1165, 1080, 802; **HRMS** (FI^+): calcd. for $C_{20}H_{26}O$, 282.1984; found, 282.2189.

2-Iodocyclopent-2-enol 319



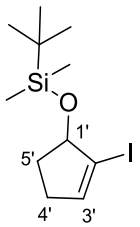
2-Iodocyclopent-2-enone **300** (18.6 g, 89.42 mmol) in MeOH (518 mL) was subjected to General Procedure **B**. The crude product was purified *via* flash column chromatography (silica, 9:1 petroleum ether/EtOAc) to furnish the pure compound **319** (10.25 g, 67%) as a white solid. **Mp** 61-63 ºC; **^{1}H NMR** (400 MHz, $CDCl_3$) 6.31-6.29 (1H, m, C=C*H*), 4.71-468 (1H, m, *H*CO), 2.53-2.46 (1H, m, C(5)*H*), 2.38-2.29 (2H, m, C(4)*H*, C(5)*H*), 1.91-1.84 (1H, m, C(4)*H*);); **^{13}C NMR** ($CDCl_3$) 142.6 (*C*=CI), 100.2 (*C*I), 82.2 (*C*OH), 32.8 (*C*(5)), 31.5 (*C*(4)); **ν_{max}** (thin film)/cm^{-1} 3370, 3028, 1625, 1426, 1161, 1078; **HRMS** (FI^+): calcd. for C_5H_7IO, 209.9542; found, 209.9544.

2-Iodocyclohex-2-enol 325



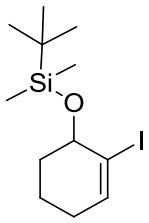
2-Iodocyclohex-2-enone (7.15 g, 32.20 mmol) in MeOH (170 mL) was subjected to General Procedure **B**. The crude product was purified *via* flash column chromatography (silica, 9:1 petroleum ether/EtOAc) to furnish the pure compound **325** (4.96 g, 86%) as a pale yellow oil. Data were consistent with those in the literature.[25] **^{1}H NMR** (400 MHz, $CDCl_3$) 6.51 (1H, t, *J* = 4.1 Hz, C=C*H*), 4.20 (1H, q, *J* = 4.8 Hz, *H*CO), 2.16-1.95 (3H, m, CH_2), 1.90-1.84 (1H, m, CH_2), 1.81-1.63 (2H, m, CH_2); **HRMS** (FI^+): calcd. for C_6H_9IO, 223.9698; found, 223.9701.

tert-Butyl((2-iodocyclopent-2-en-1-yl)oxy)dimethylsilane 320



2-Iodocyclopent-2-enol **319** (2.0 g, 9.52 mmol) in dry CH_2Cl_2 (76 mL) was subjected to General Procedure **C**. The crude product was purified *via* flash column chromatography (silica, hexane) to yield the pure product **320** (2.82 g, 91%) as a pale yellow oil. **^{1}H NMR** (400 MHz, $CDCl_3$) 6.22 (1H, m, C=C*H*), 4.71 (1H, m, *H*COSi), 2.49-2.43 (1H, m, C(5')*H*), 2.28-2.19 (2H, m, C(4')*H*), 1.82-1.75 (1H, m, C(5')*H*), 0.92 (9H, s, SiC(CH_3)$_3$), 0.16 (3H, s, SiCH_3), 0.12 (3H, s, SiCH_3); **^{13}C NMR** (CDCl3) 141.6 (*C*=CI), 101.3 (*C*I), 82.3 (SiO*C*), 32.7 (*C*(5')), 32.6 (*C*(4')), 25.9 (SiC(*C*H_3)$_3$), 18.3 (Si*C*), -4.4 (Si*C*H_3), -4.5 (Si*C*H_3); $\boldsymbol{\nu}_{\mathbf{max}}$ (thin film)/cm^{-1} 2928, 2855, 1739, 1471, 1362, 1250, 1157, 1104, 935, 774, 670; **HRMS** (FI^+): calcd. for $C_{11}H_{21}IOSi$, 324.0406; found, 324.0408.

Tert-butyl((2-iodocyclohex-2-en-1-yl)oxy)dimethylsilane 326

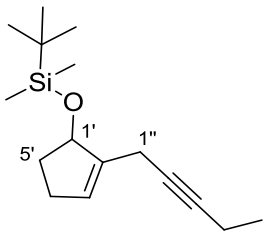


2-Iodocyclohex-2-enol **325** (4.15 g, 18.52 mmol) in dry CH_2Cl_2 (152 mL) was subjected to General Procedure **C**. The crude product was purified *via* flash column chromatography (silica, hexane) to yield the pure product **326** (5.41 g, 84%) as a colourless oil. **^{1}H NMR** (400 MHz, $CDCl_3$) 6.47 (1H, t, *J* = 4.0 Hz, C=C*H*), 4.21 (1H, t, *J* = 4.7 Hz, *H*COSi), 2.15-1.98 (2H, m, CH_2), 1.92-1.86 (1H, m, CH_2), 1.83-1.75 (2H, m, CH_2), 1.66-1.59 (1H, m, CH_2), 0.95 (9H, s, SiC(CH_3)$_3$), 0.22 (3H, s, SiCH_3), 0.12 (3H, s, SiCH_3); **^{13}C NMR** ($CDCl_3$) 140.4 (*C*=CI), 101.6 (*C*I), 72.7 (SiO*C*), 33.6 (*C*H_2), 29.4 (*C*H_2), 25.9 (SiC(*C*H_3)$_3$), 18.2, 17.5 (Si*C*), -4.2 (Si*C*H_3), -4.4 (Si*C*H_3); $\boldsymbol{\nu_{max}}$ (thin film)/cm^{-1} 2929, 2856, 1471, 1360, 1251, 1163, 1061, 892, 773, 667; **HRMS** (FI$^+$): calcd. for $C_{12}H_{23}IOSi$, 338.0563; found, 338.0568.

General Procedure D: α-Alkylation of Silyl-Protected Enols

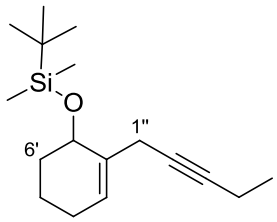
To a stirred solution of the silyl-protected enol (1.0 eq.) in THF at -78 ºC was added *n*-BuLi (1.6M in THF, 1.10 eq.) dropwise. The solution was stirred at -78 ºC for 15 min before alkyl bromide (1.30 eq.) was added and the reaction temperature was allowed to reach -30 ºC over 4 hr. The reaction mixture was diluted with Et_2O (50 mL) and saturated aqueous NH_4Cl. The organic layer was separated and the aqueous layer was extracted with Et_2O (3 x 40 mL). The combined organic extracts were washed with brine, dried (Na_2SO_4) and concentrated *in vacuo*. The crude product was purified *via* flash column chromatography.

Tert-butyldimethyl((2-(pent-2-yn-1-yl)cyclopent-2-en-1-yl)oxy)silane 321



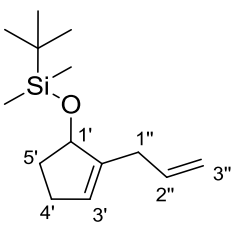
Compound **320** (1.64 g, 5.06 mmol) and 1-bromopent-2-yne (0.97 g, 6.57 mmol) in THF (50.6 mL) were subjected to General Procedure **D**. The crude product was purified *via* flash column chromatography (silica, hexane) to yield the pure product **321** (1.16 g, 88%) as a colourless oil. **^{1}H NMR** (400 MHz, $CDCl_3$) 6.01-5.99 (1H, m, C=C*H*), 4.75-4.72 (1H, m, *H*COSi), 2.49-2.41 (1H, m, C(5')*H*), 2.36-2.15 (6H, m), 1.82 (1H, ddd, *J* = 13.4, 8.9, 4.8 Hz, C(5')*H*), 1.13 (3H, t, *J* = 7.5 Hz, CH_2CH_3), 0.93 (9H, s, $SiC(CH_3)_3$), 0.16 (3H, s, $SiCH_3$), 0.13 (3H, s, $SiCH_3$); **^{13}C NMR** ($CDCl_3$) 133.3 (H*C*=C), 125.6 (HC=*C*), 82.5 (*C*≡C), 79.6 (C≡*C*), 78.1 (SiO*C*), 33.1 (*C*(5')), 30.2 (*C*(4')), 25.8 ($SiC(CH_3)_3$), 19.4 (*C*(1")), 18.3 ($SiC(CH_3)_3$), 14.2 (CH_3), 12.4 (CCH_3), -4.6 ($SiCH_3$), -4.7 ($SiCH_3$); $\boldsymbol{\nu_{max}}$ (thin film)/cm^{-1} 2928, 2856, 2360, 1463, 1254, 1060, 940, 837, 776; **HRMS** (FI^+): calcd. for $C_{16}H_{28}OSi$, 264.1909; found, 264.1912.

Tert-butyldimethyl((2-(pent-2-yn-1-yl)cyclohex-2-en-1-yl)oxy)silane 327



Compound **326** (2.65 g, 7.84 mmol) and 1-bromopent-2-yne (1.50 g, 10.19 mmol) in THF (78.4 mL) were subjected to General Procedure **D**. The crude product was purified *via* flash column chromatography (silica, hexane) to yield the pure product **327** (1.81 g, 83%) as an orange oil. **^{1}H NMR** (400 MHz, $CDCl_3$) 5.77- 5.73 (1H, m, C=C*H*), 4.24 (1H, br. s, *H*COSi), 2.34-2.32 (2H, m, C(1")*H*), 2.17 (2H, q, *J* = 7.5 Hz, CH_2CH$_3$), 2.05-1.75 (3H, m), 1.60-1.52 (3H, m), 1.13 (3H, t, *J* = 7.5 Hz, CH_3), 0.91 (9H, s, SiC(CH_3)$_3$), 0.09 (3H, s, SiCH_3), 0.08 (3H, s, SiCH_3); **^{13}C NMR** ($CDCl_3$) 131.2 (HC=*C*), 129.0 (H*C*=C), 82.5 (*C*≡C), 78.1 (C≡*C*), 66.7 (SiO*C*), 32.5 (*C*(6')), 25.9 (SiC(*C*H$_3$)$_3$), 24.9, 19.7 (*C*(1")), 19.4, 18.3 (Si*C*(CH$_3$)$_3$), 14.2 (*C*H$_3$), 12.4 (*C*H$_2$CH$_3$), -4.6 (Si*C*H$_3$),) -4.7 (Si*C*H$_3$); ν_{max} (thin film)/cm^{-1} 2928, 2855, 1739, 1471, 1362, 1250, 1217, 1157, 1103, 835, 774; **HRMS** (EI/FI): calcd. for $C_{17}H_{30}OSi$, 278.2066; found, 278.2067.

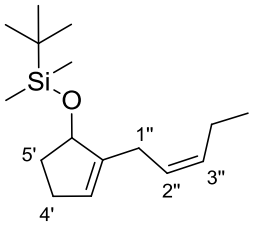
((2-Allylcyclopent-2-en-1-yl)oxy)(tert-butyl)dimethylsilane 330



Compound **320** (500 mg, 1.54 mmol) and allyl bromide (0.24 g, 2.01 mmol) in THF (15.4 mL) were subjected to General Procedure **D**. The crude product was purified *via* flash column

chromatography (silica, hexane) to yield the pure product **330** (0.27 g, 73%) as a colourless oil. **^{1}H NMR** (400 MHz, $CDCl_3$) 6.03-6.01 (1H, m, C(3')*H*), 5.92-5.85 (1H, m, C(2")*H*), 5.09-5.03 (2H, m, C(3")*H*), 4.75-4.72 (1H, m, *H*COSi), 2.49-2.41 (1H, m, C(5')*H*), 2.36-2.18 (6H, m), 1.83 (1H, ddd, *J* = 17.9, 9.5, 4.6 Hz, C(5')*H*), 0.93 (9H, s, SiC(CH_3)$_3$), 0.16 (3H, s, SiCH_3), 0.14 (3H, s, SiCH_3); **^{13}C NMR** ($CDCl_3$) 133.3 (*C*(3')H), 125.6 (*C*(2')), 118.0 (*C*(2")H), 116.4 (*C*(3")H), 79.6 (SiO*C*), 33.1 (*C*(5')), 31.6 (*C*(1")), 30.2 (*C*(4')), 25.8 (SiC(CH_3)$_3$), 18.3 (Si*C*(CH_3)$_3$), -4.6 (SiCH_3), -4.7 (SiCH_3); $\boldsymbol{\nu_{max}}$ (thin film)/cm^{-1} 2361, 1650, 1265, 1222; **HRMS** (FI^+): calcd. for $C_{14}H_{26}OSi$, 238.1753; found, 238.1743.

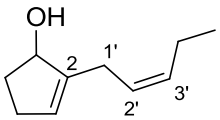
(*Z*)-Tert-butyldimethyl((2-(pent-2-en-1-yl)cyclopent-2-en-1-yl)oxy)silane 332



Compound **320** (1.00 g, 3.08 mmol) and (*Z*)-1-bromopent-2-ene (600 mg, 4.00 mmol) in THF (30.8 mL) were subjected to General Procedure **D**. The crude product was purified *via* flash column chromatography (silica, hexane) to yield the pure product **332** (630 mg, 78%) as a colourless oil. **^{1}H NMR** (400 MHz, $CDCl_3$) 5.48-5.45 (3H, m, C(3')*H*, C(2")*H*, C(3")*H*), 4.72 (1H, t, *J* = 5.6 Hz, *H*COSi), 2.91 (1H, d, *J* = 14.4 Hz, C(1")*H*), 2.71 (1H, d, *J* = 14.6 Hz, C(1")*H*), 2.42-2.36 (1H, m, C(4')*H*), 2.29-2.22 (1H, m, C(5')*H*), 2.19-2.12 (1H, m, C(4')*H*), 2.06 (2H, quintet, *J* = 7.5 Hz, C$H_2$$CH_3$), 1.73-1.65 (1H, m, C(5')*H*), 0.97 (3H, t, *J* = 7.5 Hz, CH_2CH_3), 0.92 (9H, s, SiC(CH_3)$_3$), 0.11 (3H, s, SiCH_3), 0.10 (3H, s, SiCH_3); **^{13}C NMR** ($CDCl_3$) 145.3 (*C*(2')), 132.5 (*C*(3')), 126.0 (*C*(3")), 125.9 (*C*(2")), 79.2 (SiO*C*), 34.3 (*C*(5')), 29.6 (*C*(4')), 26.3 (*C*(1")), 25.9 (SiC(*C*H_3)$_3$), 20.4 (*C*$H_2$$CH_3$), 18.2 Si*C*($CH_3$)$_3$), 14.3 (*C*$H_3$),

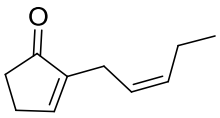
-4.4 (Si*C*H$_3$), -4.8 (Si*C*H$_3$); ν_{max} (thin film)/cm^{-1} 2958, 2930, 2856, 1462, 1360, 1250, 1080, 833, 773, 670; **HRMS** (FI$^+$): calcd. for $C_{16}H_{30}OSi$, 266.2066; found, 266.2184.

(*Z*)-2-(Pent-2-en-1-yl)cyclopent-2-enol 333



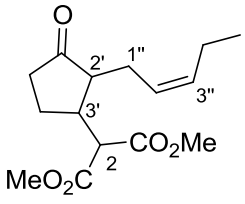
TBAF (2.00 mL, 1.0M in THF) was added dropwise to a suspension of silyl ether **332** (500 mg, 1.88 mmol) and flame-dried powdered 4Å molecular sieves in THF (4.5 mL) at 0 ºC. The reaction mixture was allowed to warm up to room temperature and was stirred for a further 2h. The reaction was quenched by the addition of saturated aqueous NH_4Cl (30 mL) and the product was extracted with Et_2O (3 x 50 mL). The combined organic layers were washed with brine, dried (Na_2SO_4) and concentrated *in vacuo*. Purification *via* flash column chromatography (silica, petroleum ether/Et_2O 85:15) afforded the pure product **333** (220 mg, 79%) as a colourless oil. **^{1}H NMR** (400 MHz, $CDCl_3$) 5.56 (1H, m, C(3)*H*), 5.53-4.42 (2H, m, C(2')*H*, C(3')*H*), 4.66 (1H, m, *H*CO), 2.97-2.82 (2H, m, C(1')*H*), 2.47-2.39 (1H, m, C(4)*H*), 2.35-2.26 (1H, m, C(5)*H*), 2.24-2.17 (1H, m, C(4)*H*), 2.09 (2H, quintet, *J* = 7.5 Hz, C*H*$_2$CH$_3$), 1.72 (1H, ddd, *J* = 17.5, 8.6, 4.0 Hz, C(5)*H*), 1.48 (1H, br. s, O*H*), 0.98 (3H, t, *J* = 7.6 Hz, C*H*$_3$); **^{13}C NMR** ($CDCl_3$) 144.9 (*C*(2)), 133.0 (*C*(3)), 127.7 (*C*(3')), 125.8 (*C*(2')), 79.0 (SiO*C*), 34.0 (*C*(5)), 29.7 (*C*(4)), 26.1 (*C*(1')), 20.4 (*C*H$_2$CH$_3$), 14.3 (*C*H$_3$); ν_{max} (thin film)/cm^{-1} 3303, 3011, 2962, 2854, 1456, 1310, 1043; **HRMS** (FI$^+$): calcd. for $C_{10}H_{16}O$, 152.1201; found, 152.1196.

(*Z*)-2-(Pent-2-en-1-yl)cyclopent-2-enone 334



To a stirred solution of enol **333** (135 mg, 8.87 mmol) in CH_2Cl_2 (9.3 mL) was added Dess-Martin periodinate (410 mg, 9.66 mmol) at rt. The reaction was stirred for 30 min before being filtered through a Celite pad. The filtrate was concentrated *in vacuo* and purified *via* flash column chromatography (silica, petroleum ether/Et_2O 9:1) to afford the pure product **334** (130 mg, 100%) as a colourless oil. **^{1}H NMR** (400 MHz, $CDCl_3$) 7.30 (1H, m, C(3)*H*), 5.53 (1H, m, C(3')*H*), 5.42 (1H, m, C(2')*H*), 2.91 (2H, dt, *J* = 7.2, 1.5 Hz, C(1')*H*), 2.57 (2H, ddd, *J* = 9.5, 4.8, 2.4 Hz, C(4)*H*), 2.43-2.41 (2H, m, C(5)*H*), 2.07 (2H, quintet, *J* = 7.5 Hz, C*H*$_2$CH$_3$), 0.97 (3H, t, *J* = 7.6 Hz, C*H*$_3$); **^{13}C NMR** ($CDCl_3$) 209.6 (C=O), 157.6 (*C*(2)), 145.3 (*C*(3)), 133.7 (*C*(3')), 124.4 (*C*(2')), 34.6 (*C*(5)), 26.5 (*C*(4)), 22.8 (*C*(1')), 20.5 (*C*H$_2$CH$_3$),14.2 (*C*H$_3$); $\boldsymbol{\nu_{max}}$ (thin film)/cm^{-1} 1705, 1633, 792, 733; **HRMS** (FI$^+$): calcd. for $C_{10}H_{14}O$, 150.1045; found, 150.1040.

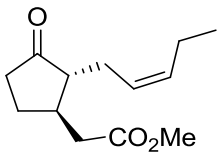
(Z)-Dimethyl 2-(3-oxo-2-(pent-2-en-1-yl)cyclopent-1-en-1-yl)malonate 337



To a suspension of sodium methoxide (30 mg, 0.49 mmol) in anhydrous MeOH (0.2 mL) was added dimethyl malonate (70 mg, 0.50 mmol) dropwise at room temperature. After stirring the reaction mixture for 1 h, enone **334** (50 mg, 0.33 mmol) in MeOH (50 μL) was added very dropwise. The reaction was stirred at room temperature for 18 h before being quenched with

brine. The solvent was removed *in vacuo*. The residue was diluted with water (30 mL) and the product was extracted with Et_2O (3 x 20 mL). The combined organic layers were washed with brine, dried (Na_2SO_4) and concentrated under reduced pressure. Purification was achieved *via* flash column chromatography (silica, petroleum ether/Et_2O 9:1) to furnish the pure product **337** (70 mg, 74%) as a colourless oil. **^{1}H NMR** (400 MHz, $CDCl_3$) 5.48 (1H, dtt, *J* = 10.7, 7.3, 1.5 Hz, C(3")*H*), 5.25 (1H, dtt, *J* = 10.7, 7.5, 1.5 Hz, C(2")*H*), 3.76 (6H, s, OCH_3), 3.63 (1H, d, *J* = 6.4 Hz, C*H*($CO_2Me)_2$), 2.64 (1H, tt, *J* = 9.9, 6.4 Hz, C(3')*H*), 2.41-2.01 (8H, m), 1.84-1.74 (1H, m, C(4')*H*), 0.96 (3H, t, *J* = 7.5 Hz, CH_3); **^{13}C NMR** ($CDCl_3$) 218.3 (C=O), 168.4 (*C*O_2Me), 134.5 (*C*(3")), 124.4 (*C*(2")), 53.7 (*C*(2)), 52.6 (O*C*H_3), 52.5 (O*C*H_3), 51.6 (*C*(2')), 40.2 (*C*(3')), 37.4 (*C*(5')), 26.0 (*C*(1")), 24.1 (*C*(4')), 20.6 (*C*H_2CH$_3$),14.1 (*C*H_3); **ν_{max}** (thin film)/cm^{-1} 2958, 1732, 1435, 1230, 1151, 1024; **HRMS** (FI$^+$): calcd. for $C_{15}H_{22}O_5$, 282.1467; found, 282.1466.

(±) - Methyl Jasmonate 388



A mixture of ester **337** (50 mg, 0.18 mmol), H_2O (3 μL, 0.18mmol) and NMP (0.18 mL) was heated in a microwave reactor at 202 ºC for 1.5 hr. The reaction mixture was cooled to room temperature and the crude was purified *via* flash column chromatography (silica, petroleum ether/Et_2O 8:2) to afford (±)-methyl jasmonate **388** (33mg, 82%) as a scented colourless oil. Data were consistent with those in the literature for racemic methyl jasmonate.[26,27] **^{1}H NMR** (400 MHz, $CDCl_3$) 5.46 (1H, dtt, *J* = 10.9, 7.2, 1.5 Hz, C(10)*H*), 5.26 (1H, dtt, *J* = 10.7, 7.3, 1.5 Hz, C(9)*H*), 3.70 (3H, s, CO_2CH_3), 2.75-2.68 (1H, m, C(2)*H*), 2.40-2.35 (3H, m, C(5)*H*,

C(8)*H*), 2.34-2.30 (2H, m, C(3)*H*), 2.26-2.22 (1H, m, C(4)*H*), 2.16-2.12 (1H, m, C(5)*H*), 2.05 (2H, ddq, *J* = 7.8, 7.3, 1.5 Hz, C(11)*H*), 1.90 (1H, ddt, 10.6, 5.9, 1.5 Hz, C(7)*H*), 1.50 (1H, m, C(4)*H*), 0.96 (3H, t, *J* = 7.6 Hz, CH_3); **^{13}C NMR** ($CDCl_3$) 218.9 (C=O), 172.4 (*C*O_2Me), 134.1 (*C*(10)), 124.9 (*C*(9)), 53.9 (*C*(7)), 51.6 (O*C*H_3), 38.8 (*C*(2)), 38.0 (*C*(3)), 37.7 (*C*(5)), 27.2 (*C*(4)), 25.5 (*C*(8)), 20.6 (*C*$H_2$$CH_3$), 14.1 (*C*$H_3$); **HRMS** (EI/FI): calcd. for $C_{13}H_{20}O_3$, 224.1413; found, 224.1409.

5.5 References

1. Gopinath, R.; Haque, S. J.; Patel, B. K. *J. Org. Chem.* **2002**, *67*, 5842-5845.

2. Parry, P. R.; Bryce, M. R.; Tarbit, B. *Org. Biomol. Chem.* **2003**, *1*, 1447-1449.

3. Feuerstein, M.; Doucet, H.; Santelli, M. *J. Organomet. Chem.* **2003**, *687*, 327-336.

4. Katritzky, A. R.; Tala, S. R.; Lu, H.; Vakulenko, A. V.; Chen, Q. Y.; Sivapackiam, J.; Pandya, K.; Jiang, S. B.; Debnath, A. K. *J. Med. Chem.* **2009**, *52*, 7631-7639.

5. Korolev, D. N.; Bumagin, N. A. *Tetrahedron Lett.* **2006**, *47*, 4225-4229.

6. Hosoya, T.; Aoyama, H.; Ikemoto, T.; Kihara, Y.; Hiramatsu, T.; Endo, M.; Suzuki, M. *Biorg. Med. Chem.* **2003**, *11*, 663-673.

7. Korolev, D. N.; Bumagin, N. A. *Tetrahedron Lett.* **2005**, *46*, 5751-5754.

8. Rajamaki, S.; Innitzer, A.; Falciani, C.; Tintori, C.; Christ, F.; Witvrouw, M.; Debyser, Z.; Massa, S.; Botta, M. *Bioorg. Med. Chem. Lett.* **2009**, *19*, 3615-3618.

9. Kumar, R. S.; Nagarajan, R.; Perumal, P. T. *Synthesis* **2004**, 949-959.

10. Kumar, D.; Narayanam, M. K.; Chang, K.-H.; Shah, K. *Chem. Biol. Drug Des.* **2011**, *77*, 182-188.

11. Ma, Y.; Qian, C. T.; Xie, M. H.; Sun, J. *J. Org. Chem.* **1999**, *64*, 6462-6467.

12. Sabitha, G.; Reddy, M. S. K.; Arundhathi, K.; Yadav, J. S. *ARKIVOC* **2006**, 153-160.

13. Yadav, J. S.; Reddy, B. V. S.; Reddy, J. S. S.; Rao, R. S. *Tetrahedron* **2003**, *59*, 1599-1604.

14. Ma, Y.; Qian, C. T.; Xie, M. H.; Sun, J. *J. Org. Chem.* **1999**, *64*, 6462-6467.

15. Maiti, G.; Kundu, P. *Tetrahedron Lett.* **2006**, *47*, 5733-5736.

16. Yadav, J. S.; Reddy, B. V. S.; Madhuri, C. R.; Sabitha, G. *Synthesis* **2001**, 1065-1068.

17. More, S. V.; Sastry, M. N. V.; Yao, C. F. *Synlett* **2006**, 1399-1403.

18. Katritzky, A. R.; Qiu, G. F.; Yang, B. Z. *J. Org. Chem.* **1997**, *62*, 8210-8214.

19. Boglio, C.; Lemiere, G.; Hasenknopf, B.; Thorimbert, S.; Lacote, E.; Malacria, M. *Angew. Chem. Int. Ed.* **2006**, *45*, 3324-3327.

20. Negishi, E.; Tan, Z.; Liou, S. Y.; Liao, B. Q. *Tetrahedron* **2000**, *56*, 10197-10207.

21. Harre, M.; Trabandt, J.; Westermann, J. *Liebigs Ann. Chem.* **1989**, *1989*, 1081-1083.

22. Reddy, S. H. K.; Chiba, K.; Sun, Y. M.; Moeller, K. D. *Tetrahedron* **2001**, *57*, 5183-5197.

23. Mase, N.; Fukasawa, M.; Kitagawa, N.; Shibagaki, F.; Noshiro, N.; Takabe, K. *Synlett* **2010**, 2340-2344.

24. Zhao, X. H.; Liu, D. L.; Xie, F.; Zhang, W. B. *Tetrahedron* **2009**, *65*, 512-517.

25. Sha, C. K.; Huang, S. J.; Zhan, Z. P. *J. Org. Chem.* **2002**, *67*, 831-836.

26. dos Santos, A. A.; Clososki, G. C.; Simonelli, F.; de Oliveira, A. R. M.; Marques, F. D.; Zarbin, P. H. G. *J. Braz. Chem. Soc.* **2001**, *12*, 673-679.

27. Chapuis, C.; Buchi, G. H.; Wuest, H. *Helv. Chim. Acta* **2005**, *88*, 3069-3088.